Chemical Constituents from the Broth Extract of Cultivated *Fomitopsis* meliae and the Leaves of *Gyrinops vidalii* (P. H. Ho)

Siriwan Srisit

A Thesis Submitted in Partial Fulfillment of Requirements for
degree of Master of Science in Chemistry
April 2025

สารองค์ประกอบทางเคมีจากสารสกัดน้ำเลี้ยงเชื้อของ *Fomitopsis* meliae ที่เพาะเลี้ยงและใบของกฤษณาน้อย (*Gyrinops vidalii* (P. H. Ho))

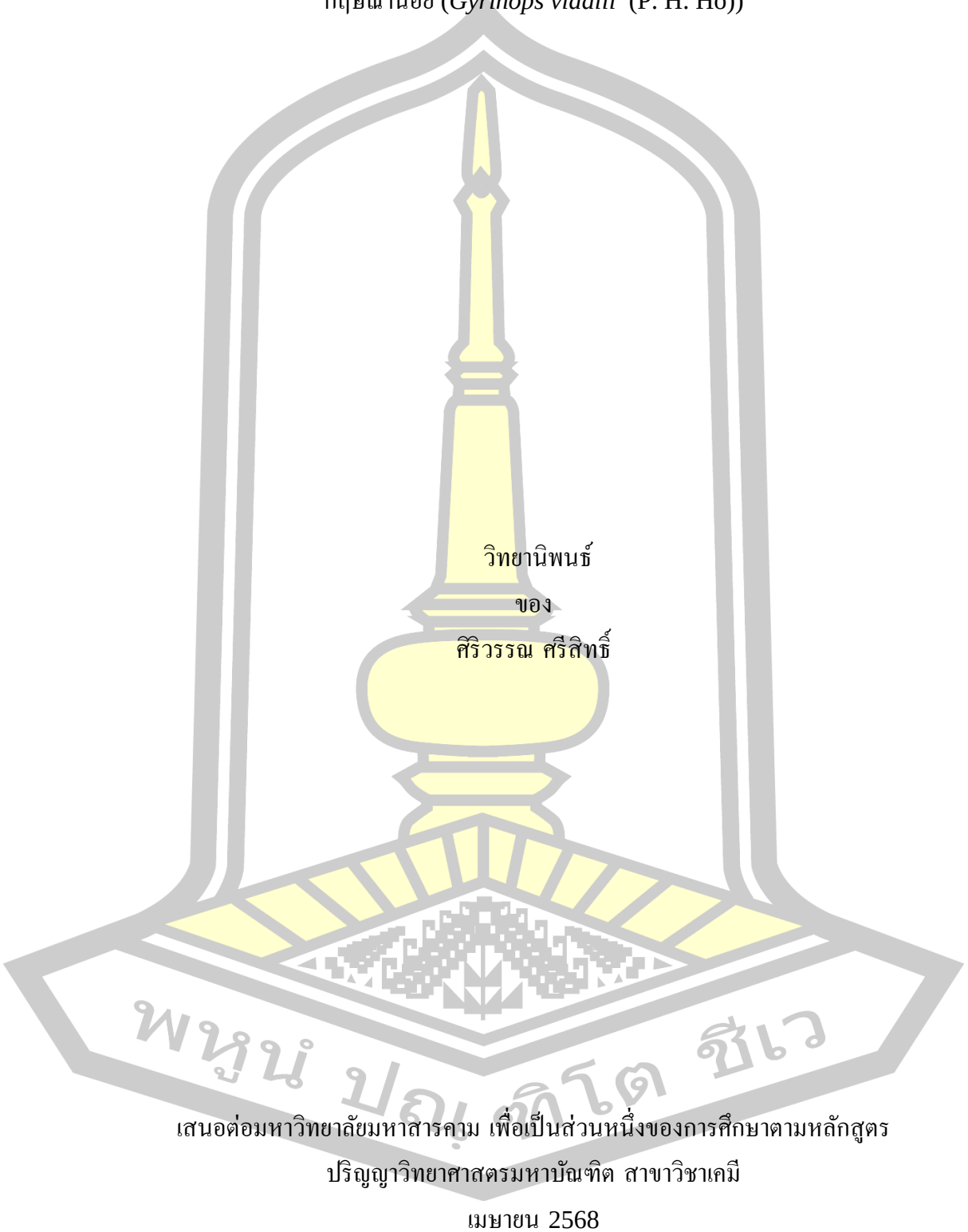

วิทยานิพนธ์

ของ

ศิริวรรณ ศรีสิทธิ์

เสนอต่อมหาวิทยาลัยมหาสารคาม เพื่อเป็นส่วนหนึ่งของการศึกษาตามหลักสูตร

ปริญญาวิทยาศาสตรมหาบัณฑิต สาขาวิชาเคมี

เมษายน 2568

Chemical Constituents from the Broth Extract of Cultivated *Fomitopsis* meliae and the Leaves of *Gyrinops vidalii* (P. H. Ho)

Siriwan Srisit

A Thesis Submitted in Partial Fulfillment of Requirements

for Master of Science (Chemistry)

April 2025

The examining committee has unanimously approved this Thesis, submitted by Miss Siriwan Srisit , as a partial fulfillment of the requirements for the Master of Science Chemistry at Mahasarakham University

Examining Committee

.....Chairman
(Assoc. Prof. Panawan Moosophon , Ph.D.)

.....Advisor
(Assoc. Prof. Prapairat Seephonkai , Ph.D.)

.....Committee
(Assoc. Prof. Chatthai Kaewtong , Ph.D.)

.....Committee
(Asst. Prof. Pakin Noppawan , Ph.D.)

Mahasarakham University has granted approval to accept this Thesis as a partial fulfillment of the requirements for the Master of Science Chemistry

.....	.....
(Prof. Pairot Pramual , Ph.D.)	(Prof. Anongrit Kangrang , Ph.D.)
Dean of The Faculty of Science	Acting Dean of Graduate School

TITLE Chemical Constituents from the Broth Extract of Cultivated *Fomitopsis* meliae and the Leaves of *Gyrinops vidalii* (P. H. Ho)

AUTHOR Siriwan Srisit

ADVISORS Associate Professor Prapairat Seephonkai , Ph.D.

DEGREE Master of Science **MAJOR** Chemistry

UNIVERSITY Mahasarakham University **YEAR** 2025

ABSTRACT

PART I: Chemical Constituents from the Broth Extract of Cultivated *Fomitopsis meliae*

This study aimed to identify antibacterial compounds from the broth extract of *Fomitopsis meliae* (Mahasarakham University Culture Collection; MSUCC009). From small-scale fermentation, the broth extract of *F. meliae* showed antibacterial activity. Therefore, the fermentation of this fungal strain was scaled up and the broth extract was chemically investigated. Purification of the broth extract led to the isolation of two 5-hydroxymethylfuran metabolites, 5-hydroxymethyl-2-furoic acid methyl ester (94) and 5-hydroxymethyl-2-furancarboxylic acid (HMFCA; 95), together with a pyrimidine base, uracil (96). This is the first isolation report of 5-hydroxymethylfuran derivatives from the genus *Fomitopsis*. The structures of isolated compounds (94–96) were elucidated based on nuclear magnetic resonance (NMR) and mass spectrometry (MS) spectroscopic methods, and comparison with previous reports. Compound 95 exhibited antibacterial activity against methicillin-susceptible *Staphylococcus aureus* (MSSA) with MIC and MBC values of > 0.25 mg/mL. Compounds 94 and 95, were also tested against human lung adenocarcinoma (A549) cell lines. These two compounds were inactive in this cytotoxicity assay.

PART II: Chemical Constituents from the Leaves of *Gyrinops vidalii* (P. H. Ho)

Plants in the genus *Gyrinops* are widely distributed in Southeast Asia; however, *Gyrinops vidalii* is the only species found specifically in Thailand and Laos. In our present study, the ethyl acetate (EtOAc) extract from the leaves of *G. vidalii* collected from northeastern Thailand exhibited antioxidant activity toward 2,2-diphenyl-1-picrylhydrazyl (DPPH) radical, with an SC_{50} value of 47.23 ± 3.84 µg/mL. This EtOAc extract was chemically investigated for the first time, leading to the isolation of a *C*-glycosylxanthone, mangiferin (18), two benzophenoneglycosides, aquilarinenside E (40) and iriflophenone 2-*O*-α-L-rhamnoside (41), a terpenoid, blumenol A or vomifoliol (42), a flavonoid, 5,7,4′-trimethoxyflavone (43), and a phenolic compound, 4-methoxybenzoic acid (44), together with three unknown

compounds, A–C. The structures of 18, 40–44, were identified based on NMR and mass spectroscopic data, and confirmed by comparison with the previous reported data in literatures. Iriflophenone (40a) was obtained from acid hydrolysis of compound 40. The structures of A–C are currently under elucidation.

Keyword : Fomitopsis meliae, 5-Hydroxymethylfuran, HMFCA, 5-Hydroxymethyl-2-furan carboxylic acid, Medicinal mushrooms, Gyrinops vidalii, C-Glycosylxanthone, Benzophenoneglycoside, Terpenoid, Flavonoid, Phenolic compound

ACKNOWLEDGEMENTS

I would like to express profound appreciation to my advisor, Assoc. Prof. Prapairat Seephonkai, for her assistance and support throughout the research, encompassing guidance, encouragement, and exceptional attention to the students.

I would like to thank Assoc. Prof. Aphidech Sangdee for the antibacterial activity test, Asst. Prof. Ruchilak Rattarom for the cytotoxic activity assay, Asst. Prof. Pasakorn Bunchalee for species plant identification, and Asst. Prof. Worrawat Promden for the DPPH radical scavenging activity and α-glucosidase inhibitory activity assay.

Thank you for the financial support from Mahasarakham University (Postgraduate), the National Research Council of Thailand, and Center of Excellence for Innovation in Chemistry (PERCH-CIC).

Finally, I would like to express my gratitude to my family for their encouragement and support in everything. I also want to thank my friends for their encouragement, especially the Natural Product Research Group (NPRG) for their exceptional assistance.

Siriwan Srisit

TABLE OF CONTENTS

Page

LIST OF TABLES

Page

LIST OF FIGURES

Page

LIST OF FLOW CHARTS

Flow chart **Page**

LIST OF ABBREVIATIONS

ATCC	American Type Culture Collection
CO_2	Carbon dioxide
^{13}C NMR	Carbon-13 nuclear magnetic resonance spectroscopy
PERCH-CIC	Center of Excellence for Innovation in Chemistry
δ	Chemical shift
$CHCl_3$	Chloroform
CFU	Colony-forming unit
CC	Column chromatography
COSY	Correlation spectroscopy
J	Coupling constants
^oC	Deegree Celsius
DNA	Deoxyribonucleic acid
DMST	Department of Medical Sciences Thailand
Acetone-d_6	Deuterated acetone
$CDCl_3$	Deuterated chloroform
DMSO-d_6	Deuterated dimethyl sulfoxide
CD_3OD	Deuterated methanol
CH_2Cl_2	Dichloromethane
MTT	3-(4,5-Dimethylthiazol-2-yl)-2,5-diphenyltetrazolium bromide
DEPT	Distortionless enhancement by polarization transfer

d	Doublet (spectral multiplicity)
EtOAc	Ethyl acetate
EtOH	Ethyl alcohol
Fr.	Fraction
g	Gram
g/mol	Gram per mole
HSV-1	Herpes simplex virus type 1
Hz	Hertz
HMBC	Heteronuclear multiple bond correlation
HSQC	Heteronuclear single quantum coherence
HRESIMS	High-resolution electrospray ionization mass
HCT116	Human colorectal carcinoma
MRC-5	Human fetal lung fibroblast
BGC-823	Human gastric cancer
HepG2	Human hepatocellula carcinoma
H460	Human large-cell lung cancer
HL-60	Human leukemia
A549	Human lung adenocarcinoma
^{1}H NMR	Hydrogen-1 nuclear magnetic resonance spectroscopy
HMFCA	5-Hydroxymethyl-2-furancarboxylic acid
IC_{50}	Inhibitory concentration at 50%
ITS	Internal transcribed spacer
LPS	Lipopolysaccharide

L	Liter
RAW 264.7	Macrophage cell line
MSUCC	Mahasarakham University Culture Collection
MSUT	Mahasarakham University Thailand
MEB	Malt extract broth
MS	Mass spectrometry
MHz	Megahertz
MeOH	Methanol
MRSA	Methicillin-resistant *Staphylococcus aureus*
MSSA	Methicillin-susceptible *Staphylococcus aureus*
µg/mL	Micrograms per milliliter
µL	Microliter
µM	Micromolar
mg/mL	Milligrams per milliliter
mL	Milliliter
mm	Millimeters
MBC	Minimum bactericidal concentration
MIC	Minimum inhibitory concentration
MHA	Mueller Hinton agar
MHB	Mueller Hinton broth
multi.	Multiplicity
nm	Nanometer
NCBI	National Center for Biotechnology Information

NRCT	National Research Council of Thailand
NPRG	Natural Product Research Group
NJ	Neighbor-Joining
NO	Nitric oxide
NMR	Nuclear magnetic resonance
NOESY	Nuclear overhauser effect spectroscopy
ppm	Parts per million
%	Percent
PCR	Polymerase chain reaction
PDA	Potato dextrose agar
PDB	Potato dextrose broth
rpm	Revolutions per minute
RNA	Ribonucleic acid
s	Singlet (spectral multiplicity)
TLC	Thin-layer chromatography
2D NMR	Two-dimensional nuclear magnetic resonance spectroscopy
v/*v*	Volume per volume
H_2O	water

CHAPTER 1

INTRODUCTION

1.1. Background

Thailand, situated in central southeastern Asia, is part of the Indo-Burmese Region, a global hotspot for biodiversity (Van WELZEN et al., 2011). Thailand is an ecologically rich nation, endowed with significant variety, featuring a flora of vascular plants exceeding 11,000 species. The patterns of biodiversity vary throughout various regions of the country (Maxwell, 2004). There are approximately 15,000 known animal a8especies and approximately 10,000 identified microorganism species (Thailand Country Study on Biodiversity, 1992). This vast diversity of organisms has historically been and remains a crucial resource for human survival (Baimai, 2010).

Fungi are eukaryotic microorganisms that serve essential ecological functions as decomposers and mutualists of plants and animals, facilitating carbon cycling in forest ecosystems, mediating mineral nutrition for plants, and alleviating carbon constraints for other soil species (Tedersoo et al., 2014). Approximately 69,000 fungal species have been identified, whereas over 1,500,000 species are anticipated to exist (Hawksworth, 1991). Fungi are heterotrophic eukaryotes that lack chlorophyll, possess uninucleate or multinucleate cells, and utilize chitinous cell walls for nutrient assimilation (Alexopolous et al., 1996). The three significant categories of fungus are molds, yeasts, and mushrooms (Bueno and Silva, 2014). Fungi encompass unicellular yeasts that reproduce via budding to be molds that generate multicellular filaments

(hyphae), typically formed in specialized spore-producing structures known as fruiting bodies (Walker and McGinnis, 2014).

Mushrooms are classified under the Basidiomycetes and some to the Ascomycetes, contributing as a globally prevalent food source. Since ancient times, people have consumed mushrooms for their nutritional benefits and medicinal value. (Blair et al., 2015). In numerous nations, mushrooms are regarded as components of gourmet cuisine, primarily due to their unique flavor, and are valued by individuals as a culinary enhancement. Mushrooms contain nutrients such as easily digestible proteins, carbs, vitamins, fiber, minerals, and antioxidants (Pinky et al., 2019). Mushrooms secrete diverse secondary metabolites, including terpenoids and phenolics, to safeguard the fruiting body against detrimental organisms such as viruses, bacteria, and insects, utilizing these compounds as chemical defenses with antiviral, antioxidant, and other biological properties (El-Maradny et al., 2021). Medicinal mushrooms contain bioactive compounds with a wide range of therapeutic effects, including anti-inflammatory, antioxidant, and immune-boosting properties (Wasser, 2002).

The genus *Fomitopsis* stands out due to its significant medicinal potential (Bishop, 2020; Janardhanan et al., 2020). The various species of *Fomitopsis* are known for producing a variety of bioactive compounds, particularly lanostane triterpenoids (Han et al., 2016; Isaka et al., 2017; Liu et al., 2022; Naranmandakh et al., 2018; Sofrenić et al., 2021; Zhao et al., 2018), which exhibit diverse biological activities such as anti-cancer, anti-inflammatory, and immunomodulatory effects (Bishop, 2020; Gao et al., 2018; Janardhanan et al., 2020). These mushrooms have been traditionally used

to promote health and treat diseases, and recent scientific investigations have supported their therapeutic potential, however; has been studied to a much lesser extent than *Ganoderma lucidum* or *Inonotus obliquus* (Gründemann et al., 2020; Janardhanan et al., 2020; Naranmandakh et al., 2018). In the previous report, the broth extract of *Fomitopsis meliae* exhibited good antibacterial activity (Kumar and Prasher, 2022). There are very few reports about an investigation of the chemical constituents of *F. meliae*. Therefore, *F. meliae* (Mahasarakham University Culture Collection; MSUCC009) was selected for large scale fermentation and the broth extract of this fungal strain was chemically investigated in this study.

1.2. Research objective

This research aims to investigate the chemical constituents from the culture broth extract of *Fomitopsis meliae* and evaluate the biological activities of the isolated compounds from this species.

1.3. Expected result

The expected results of this research are information on chemical constituents from the culture broth extract of *Fomitopsis meliae* and the biological activities of the isolated compounds.

1.4. Scope of research

Extraction of the culture fermentation of *Fomitopsis meliae*, purification of the broth extract, structure elucidation of the isolated pure compounds, and biological

activity assays of the extracts and isolated pure compounds are in the scope of this research.

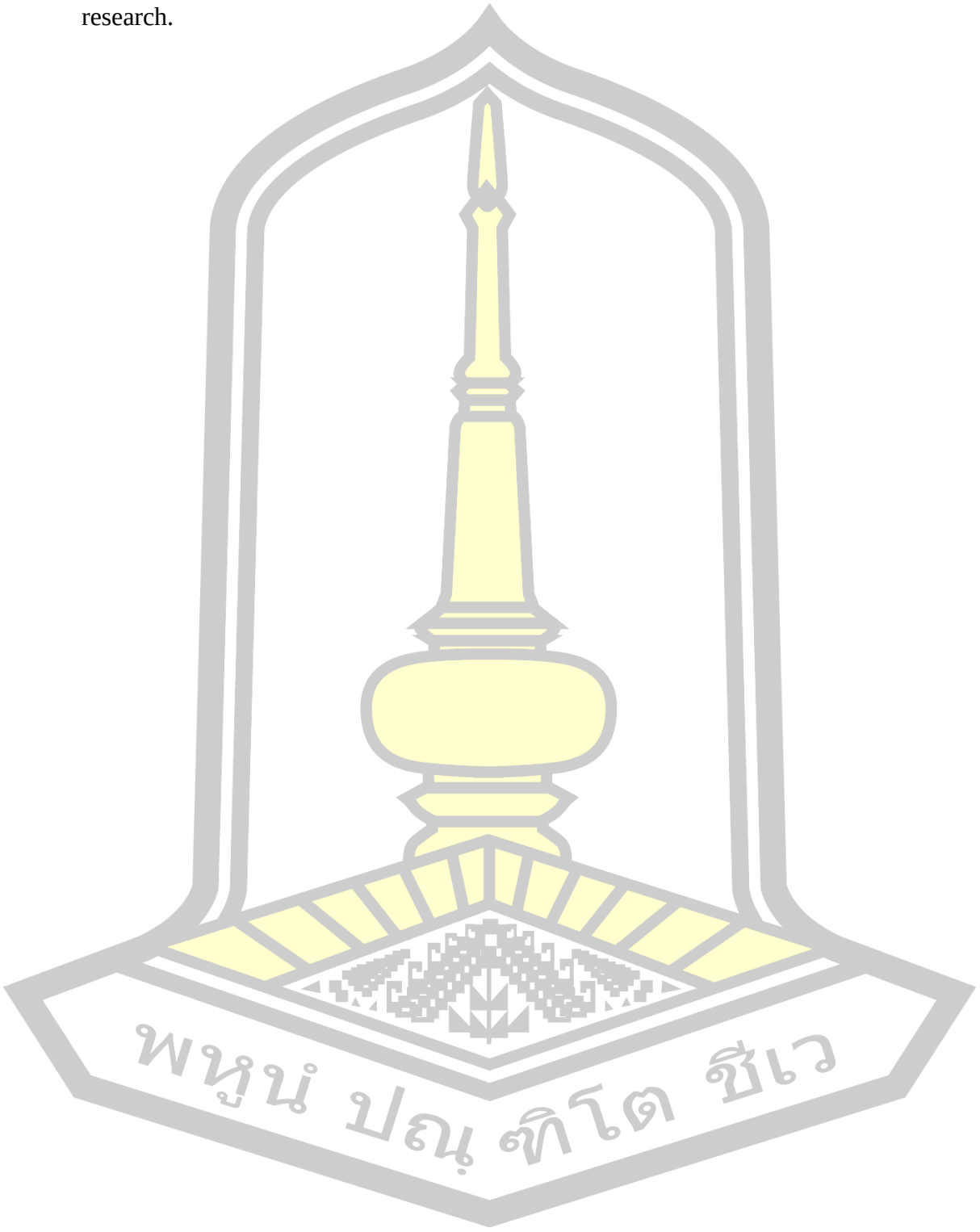

CHAPTER 2

LITERATURE REVIEW

2.1. *Fomitopsis meliae*

The genus *Fomitopsis* stands out due to its significant medicinal potential (Bishop, 2020; Janardhanan et al., 2020). *Fomitopsis meliae* (Underw.) Gilb. was identified in 1981 (Gilbertson, 1981) and regarded as a synonym of *Fomes meliae* (Underw.) Murrill (Murrill, 1903) and *Polyporus meliae* Underw. (Underwood, 1897). In the previous report, the broth extract of *F. meliae* exhibited good antibacterial activity (Kumar and Prasher, 2022). There are very few reports about an investigation of the chemical constituents of *F. meliae*.

As part of our research for bioactive compounds and extract with medicinal potential from mushroom sources in northeastern Thailand (Samchai et al., 2011; Seephonkai et al., 2011; Seephonkai et al., 2024), natural fruiting bodies of mushrooms were collected and isolated for living cultures. These fungal strains were subjected to small-scale fermentation. the broth and mycelial extracts from small-scale fermentation were screened for their antibacterial activity. Among them, the broth extract of *F. meliae* (Underw) Gilb. (Fomitopsidaceae, Agaricomycetes) (MSUCC009) showed antibacterial activities against methicillin-resistant *Staphylococcus aureus* (MRSA), methicillin-susceptible *Staphylococcus aureus* (MSSA), and *Bacillus cereus*. Therefore, *Fomitopsis meliae* (MSUCC009) was selected for large scale fermentation and the broth extract of this fungal strain was chemically investigated in this research.

There are numbers of reports on chemical constituents of the genus *Fomitopsis*. Herein, chemical constituents of *Fomitopsis* which were reported in 2016–2022 were summarized.

2.2. Isolated compounds from *F. pinicola*

Thirteen previously new lanostane triterpenoids, nor-pinicolic acid A (**1**), nor-pinicolic acid B (**2**), nor-pinicolic acid C (**3**), nor-pinicolic acid D (**4**), nor-pinicolic acid E (**5**), nor-pinicolic acid F (**6**), pinicopsic acid A (**7**), pinicopsic acid B (**8**), pinicopsic acid C (**9**), pinicopsic acid D (**10**), pinicopsic acid E (**11**), pinicopsic acid F (**12**), and pinicopsic acid G (**13**), along with eleven lanostane triterpenoids, 16α-hydroxy-3-oxolanosta-7,9(11),24-trien-21-oic acid (**14**), 3β-hydroxylanosta-7,9(11),24-trien-21-oic acid (**15**), 3β,16α-dihydroxylanosta-7,9(11),24-trien-21-oic acid (**16**), 3-oxolanosta-7,9(11),24-trien-21-oic acid (**17**), 3β-hydroxylanosta-8,24-dien-21-oic acid (**18**), boscartene D (**19**), pinicolic acid A (**20**), ganosinoside A (**21**), pinicolic acid B (**22**), pinicolic acid C (**23**), and pinicolic acid D (**24**) (**Figure 1**), were isolated from ethyl acetate (EtOAc) extract of the fruiting bodies of *F.* pinicola (Liu et al., 2022). The fruiting bodies of *F. pinicola* were collected from the Altai Mountains at Xinjiang, People's Republic of China on August 2015. Pinicopsic acid F (**12**) and 16α-hydroxy-3-oxolanosta-7,9(11),24-trien-21-oic acid (**14**), showed moderate inhibitory activities against lipopolysaccharide (LPS)-induced nitric oxide (NO) production in macrophage cell lines (RAW 264.7), with inhibitory concentration (IC_{50}) values of 24.5 and 25.7 μM, respectively.

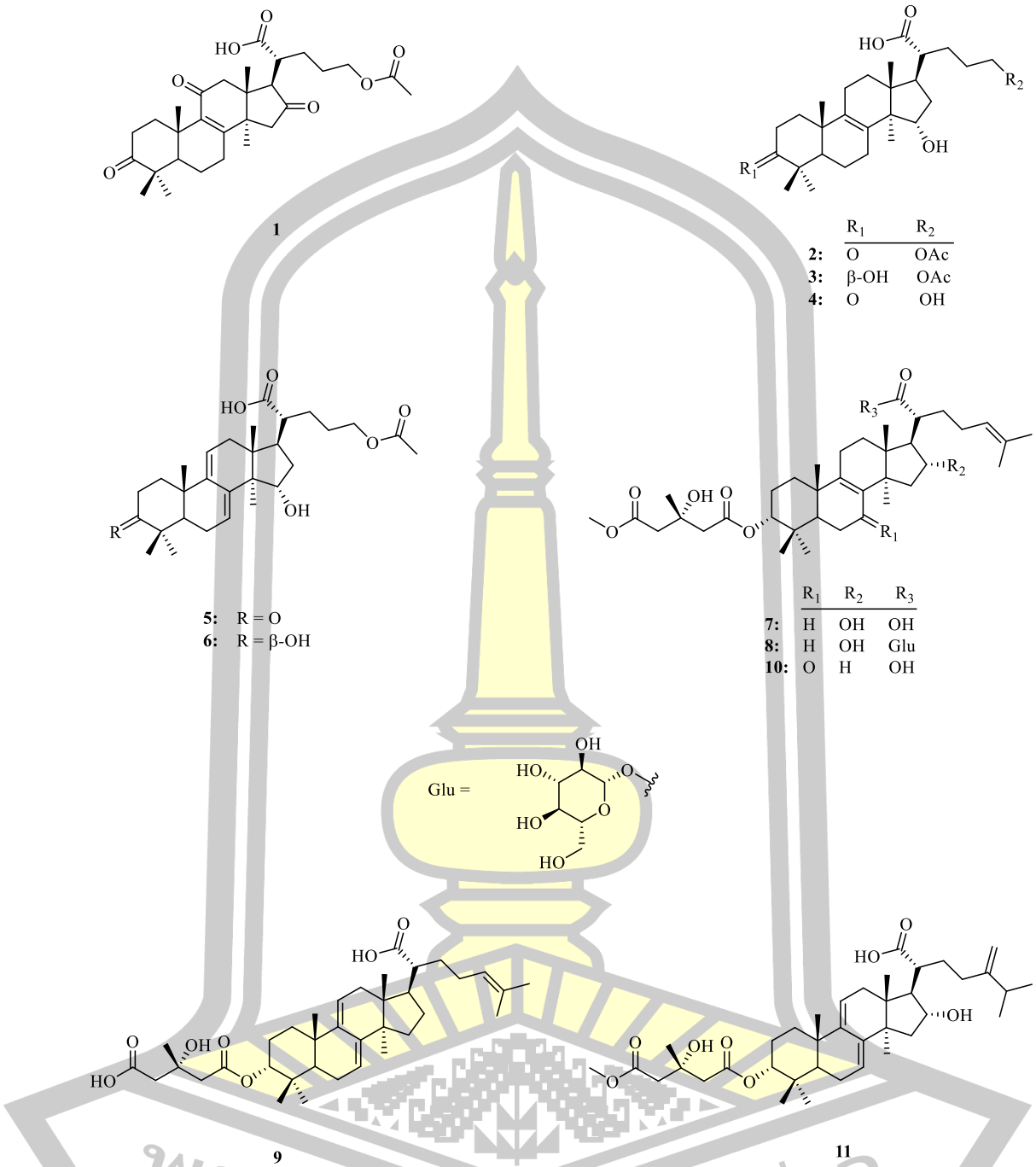

Figure 1. Structures of compounds **1**–**24**.

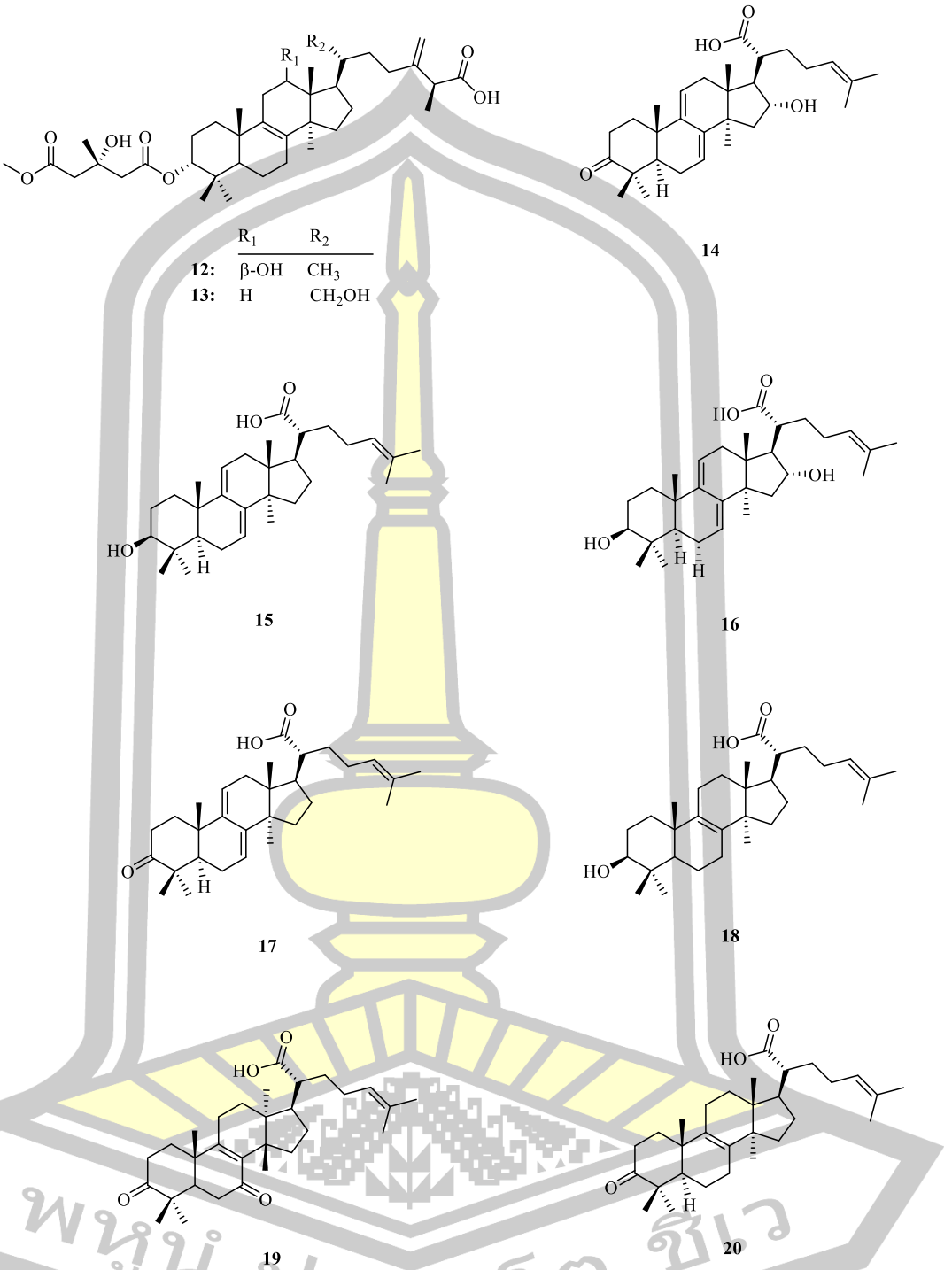

Figure 1 (continued)**.** Structures of compounds **1**–**24**.

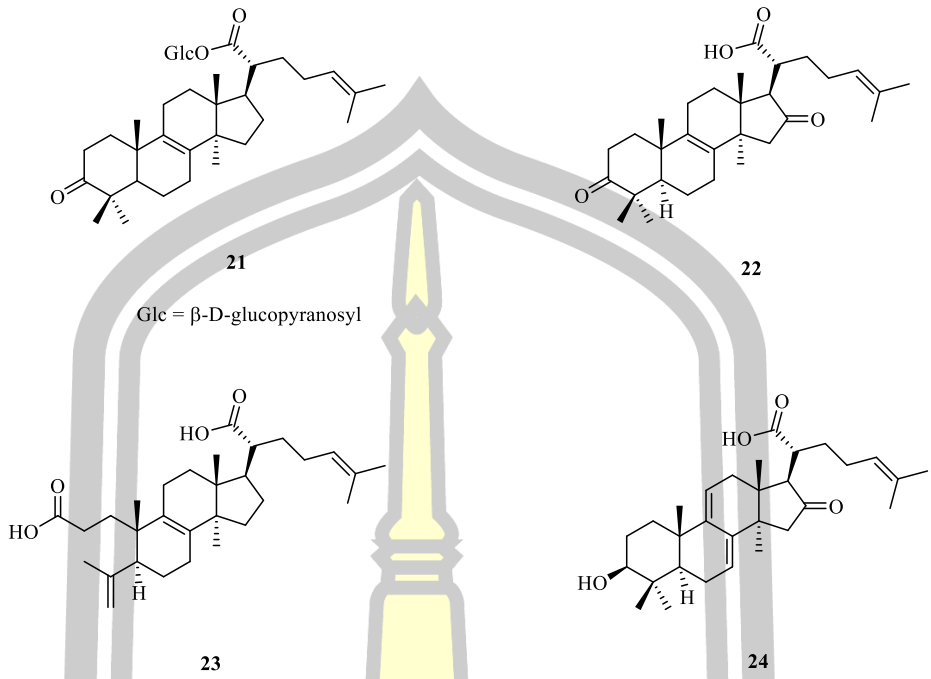

Figure 1 (continued)**.** Structures of compounds **1**–**24**.

2.3. Isolated compounds from *F. betulina*

Thirteen new compounds 24-methylene lanostane triterpenoids, polyporenic acid E (**25**), polyporenic acid F (**26**), polyporenic acid G (**27**), polyporenic acid H (**28**), polyporenic acid I (**29**), polyporenic acid J (**30**), polyporenic acid K (**31**), polyporenic acid L (**32**), fomitoside L (**33**), fomitoside M (**34**), fomitoside N (**35**), polyporenic acid M (**36**), fomitoside O (**37**), together with seventeen known analogues, palustrisoic acid F (**38**), dehydropachymic acid (**39**), pachymic acid (**40**), 3*α*-(acetyloxy)-16*α*-hydroxy-24-methylene-lanost-8-en-21-oic acid (**41**), poricoic acid H (**42**), fomitoside J (**43**), cerevisterol (**44**), 3-epi-dehydropachymic acid (**45**), dehydrotumulosic acid (**46**), 3-epi-dehydrotumulosic acid (**47**), 16*α*-hydroxyeburiconic acid (**48**), polyporenic acid C (**49**), polyporenic acid A (**50**), piptolinic acid B (**51**), 3*α*-[4-carboxy-3-hydroxy-3-methyl-1-oxobutoxy]-12*α*-hydroxy-24-methylene-lanost-8-en-26-oic acid (**52**),

12α-hydroxy-3α-(3′-hydroxy-4′-methoxycarbonyl-3′-methylbutyryloxy)-24-methyllanosta-8,24(31)-dien-26-oic acid (**53**), and betulin (**54**) (**Figure 2**), were isolated from EtOAc extract of the fruiting bodies of *F. betulina* (Sofrenić et al., 2021). The fruiting bodies of *F. betulina* were collected in village Ogladjenovac, near Valjevo at the geographic coordinate in November 2016. Two new compounds, fomitoside L (**33**) and fomitoside N (**35**), showed cytotoxicity against human leukemia (HL-60) cells, with IC_{50} values of 15.8 and 23.7 µM, respectively. The known compounds, dehydropachymic acid (**39**), pachymic acid (**40**), fomitoside J (**43**), dehydrotumulosic acid (**46**), and 12α-hydroxy-3α-(3′-hydroxy-4′-methoxycarbonyl-3′-methylbutyryloxy)-24-methyllanosta-8,24(31)-dien-26-oic acid (**53**), exhibited considerable activity against HL-60 cells and selectivity with respect to human fetal lung fibroblast (MRC-5)cells were noticed for with IC_{50} values of 10.9, 11.0, 19.6, 19.9, and 19.2 µM and 8.6, 9.8, 1.8, 5.8, and 2.2 respectively.

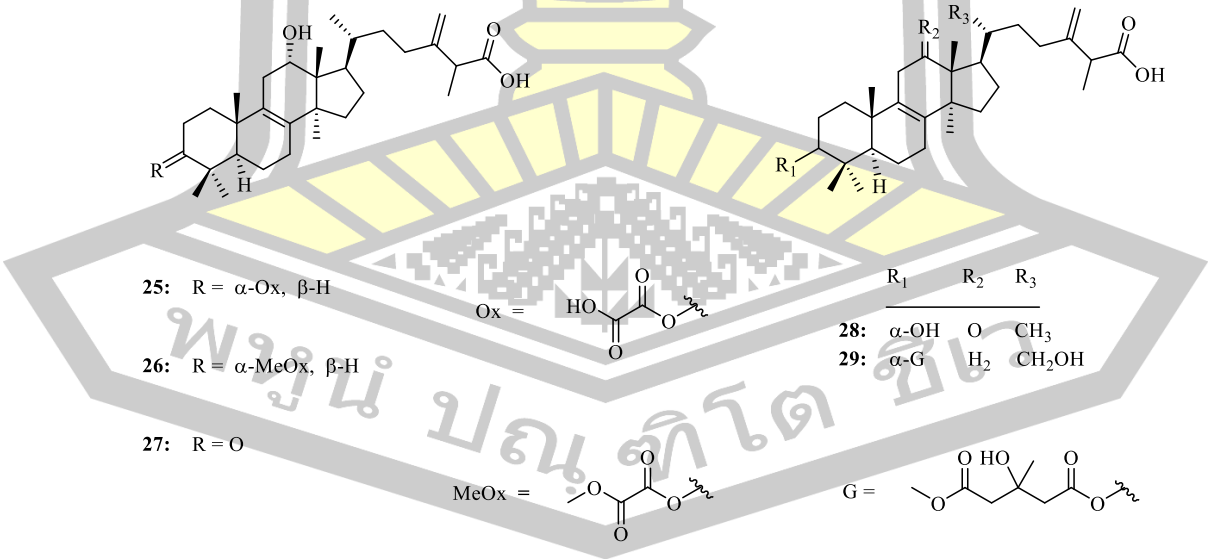

Figure 2. Structures of compounds **25**–**54**.

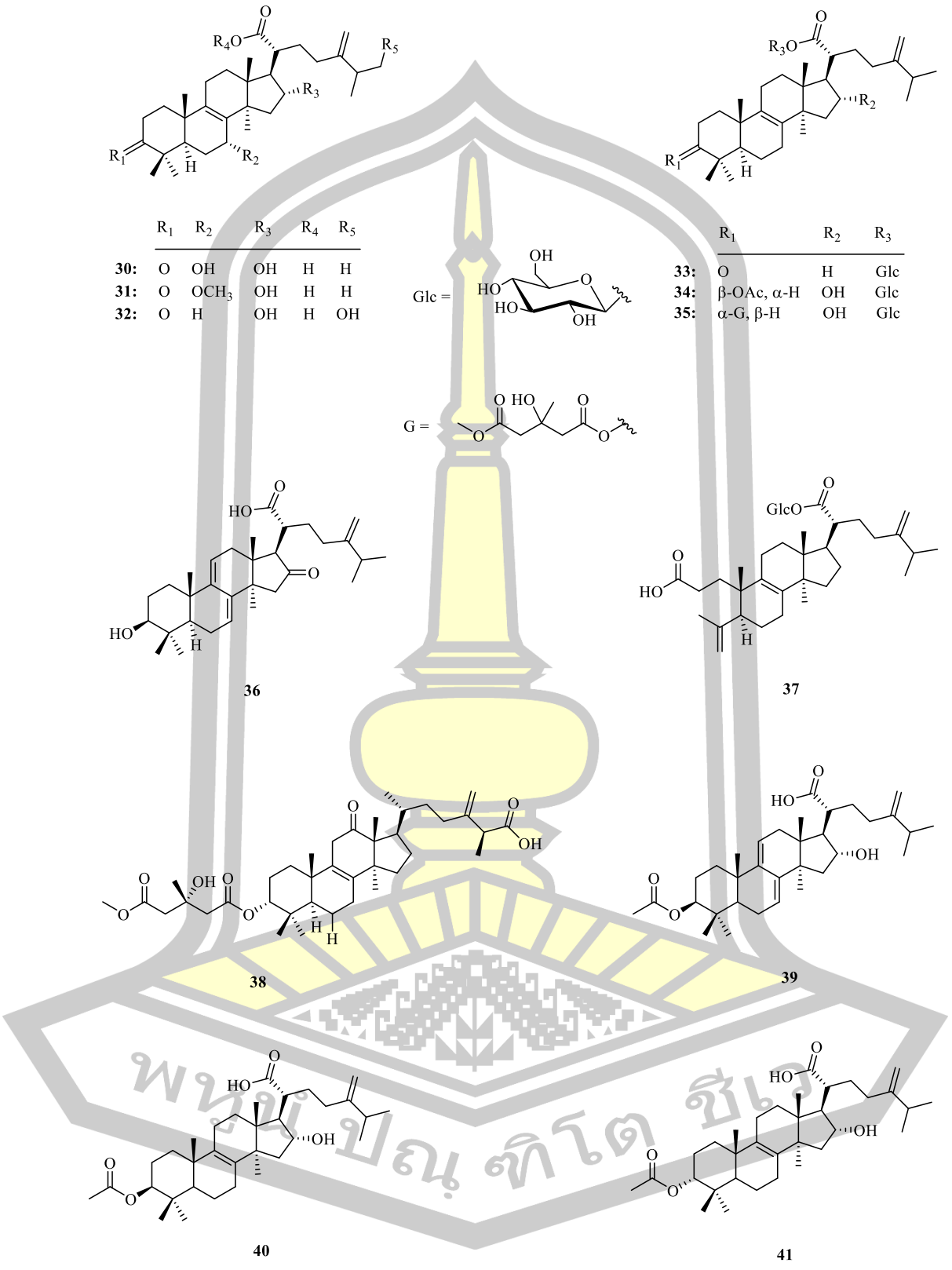

Figure 2 (continued)**.** Structures of compounds **25**–**54**.

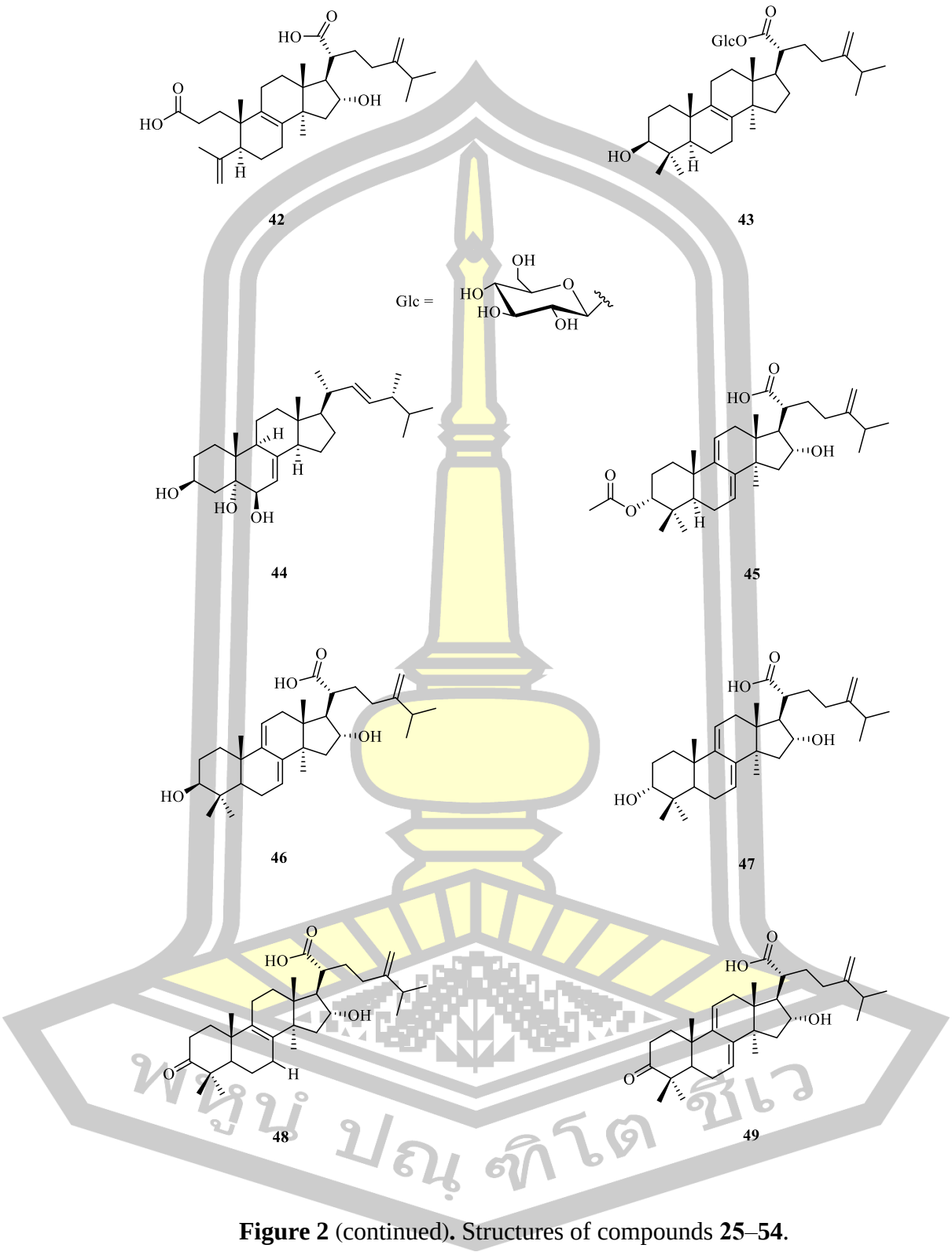

Figure 2 (continued)**.** Structures of compounds **25**–**54**.

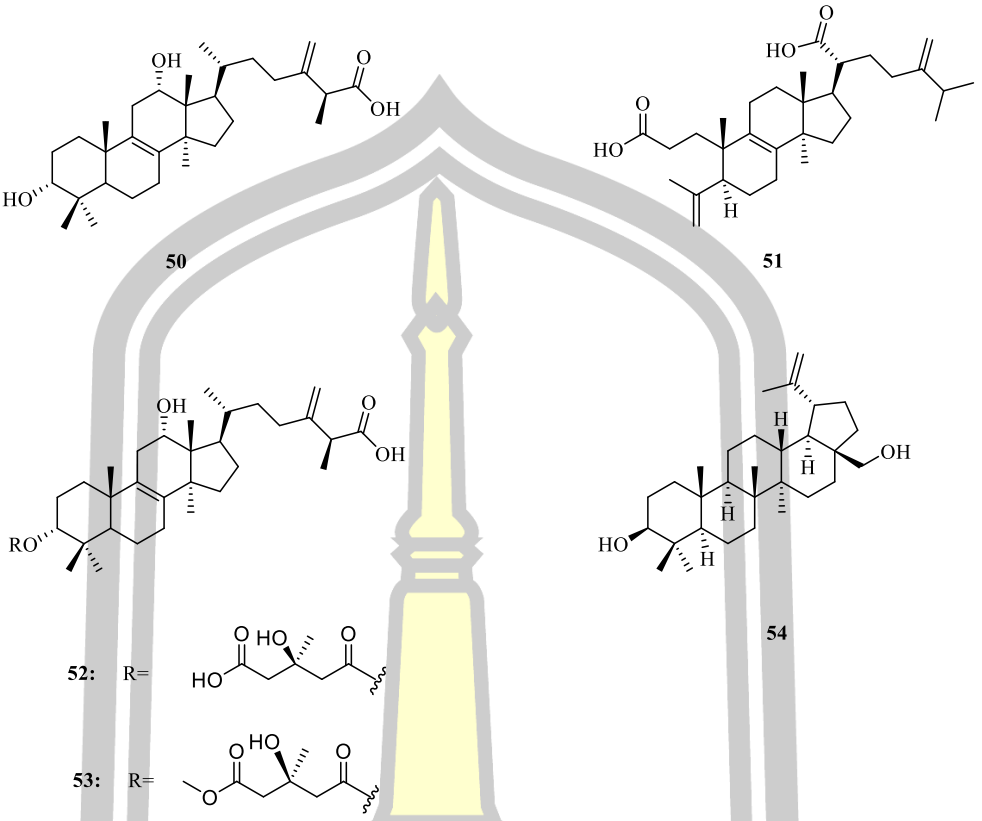

Figure 2 (continued)**.** Structures of compounds **25**–**54**.

2.4. Isolated compounds from *F. palustris*

Fifteen new lanostane-type C_{31} triterpenoid derivatives, palustrisoic acid A (**55**), palustrisoic acid B (**56**), palustrisoic acid C (**57**), palustrisoic acid D (**58**), palustrisoic acid E (**59**), palustrisoic acid G (**60**), palustrisoic acid H (**61**), palustrisolide A (**62**), palustrisolide B (**63**), palustrisolide C (**64**), palustrisolide D (**65**), palustrisolide E (**66**), palustrisolide F (**67**), and palustrisolide G (**68**) (**Figure 3**), palustrisoic acid F (**38**) (**Figure 2**), as well as five known lanostane-type C_{31} triterpenoid derivatives, (25*S*,3′*S*)-(+)-12*α*-hydroxy-3*α*-[3′-hydroxy-3′-methylglutaryloxy]-24-methyllanosta-8,24(31)-dien-26-oic acid (**52**), (25*S*,3′*S*)-(+)-12*α*-hydroxy-3*α*-[3′-hydroxy-4′-methoxycarbonyl-

3′-methylbutyryloxy]-24-methyllanosta-8,24(31)-dien-26-oic acid (**53**) (**Figure 2**), 3α-acetylpolyporenic acid (**69**), polyporenic acid B (**70**) (**Figure 3**), and pachymic acid (**40**) (**Figure 2**), were isolated from the aqueous ethyl alcohol (EtOH) extract of the fruiting bodies of cultivated *F. palustris* (Zhao et al., 2018). The fruiting body of *F. palustris* was collected from a tree in Chebaling natural reserve, Shixing County, Guangdong Province, People's Republic of China. Polyporenic acid B (**70**) showed strong cytotoxicity against the human colorectal carcinoma (HCT116) cell line, the human lung carcinoma (A549) cell lines, and the human hepatocellular carcinoma (HepG2) cell lines with IC_{50} values of 8.4, 12.1, and 12.2 µM respectively. Palustrisolide A (**62**), palustrisolide C (**64**), and palustrisolide G (**68**), demonstrated weak cytotoxicity against three cell lines.

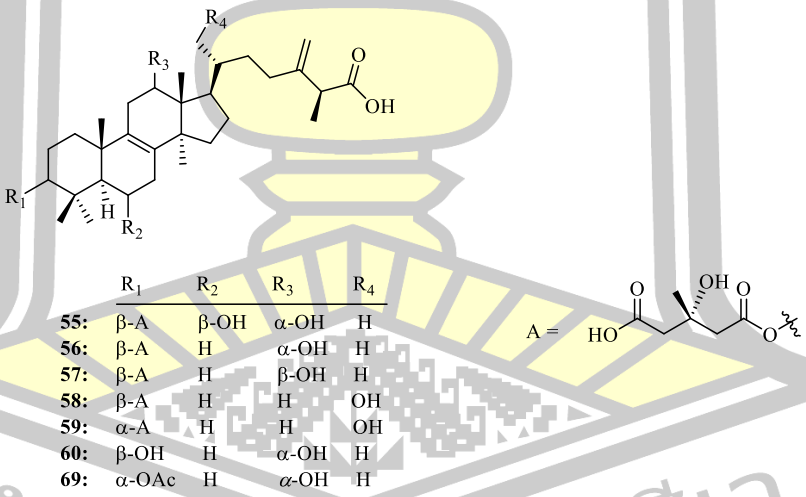

	R_1	R_2	R_3	R_4
55:	β-A	β-OH	α-OH	H
56:	β-A	H	α-OH	H
57:	β-A	H	β-OH	H
58:	β-A	H	H	OH
59:	α-A	H	H	OH
60:	β-OH	H	α-OH	H
69:	α-OAc	H	α-OH	H

Figure 3. Structures of compounds **55**–**70**.

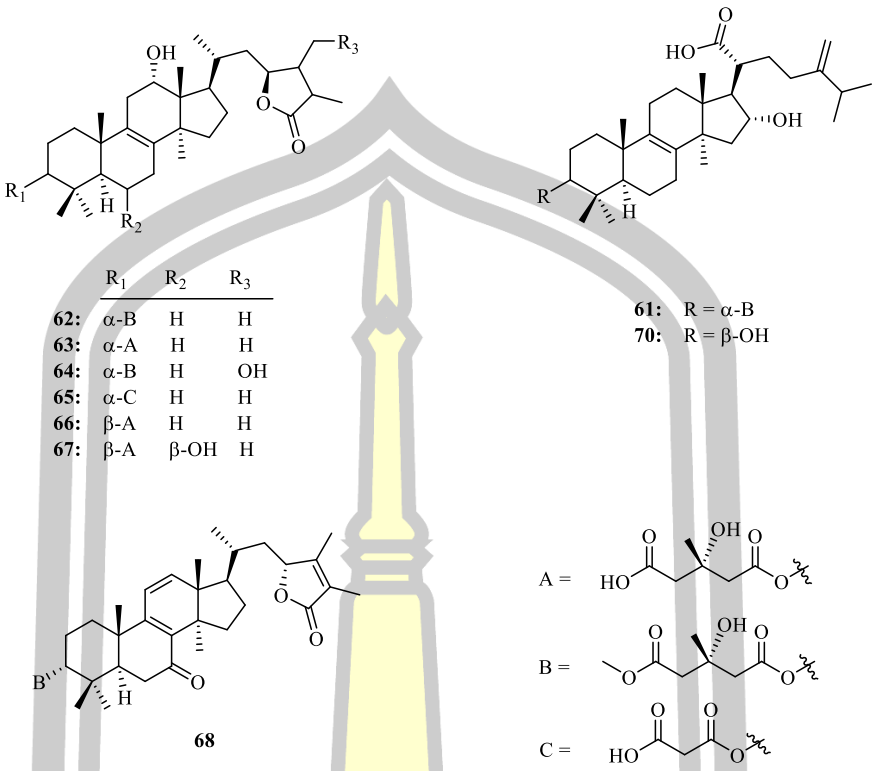

Figure 3 (continued)**.** Structures of compounds **55**–**70**.

2.5. Isolated compounds from *F. officinalis*

Four new lanostane triterpenoids, fomitopsin G (**71**), fomitopsin H (**72**), demalonyl fomitopsin H (**73**), and fomitopsin D ethyl ester (**74**), together with four known triterpenoids, fomitopsin F (**75**), (25*S*)-(+)-12*α*-hydroxy-3*α*-malonyloxy-24-methyllanosta-8,24(31)-dien-26-oic acid (**76**), fomefficinic acid G (**77**), and 15*α*-hydroxy-3-oxo-24-methylenelanosta-7,9(11)-dien-21-oic acid (**78**) (**Figure 4**), were isolated from chloroform ($CHCl_3$) extract of the fruiting bodies of *F. officinalis* (Naranmandakh et al., 2018). The fruiting bodies of *F. officinalis* were collected at Khoninnuga, Mandal Soum, Selenge Province, Mongolia in April 2015. Compounds

7 2–**7 5** and **78** , exhibited moderate inhibition activities against *Trypanosoma congolense* with IC_{50} values ranging from 7.0–27.1 μM.

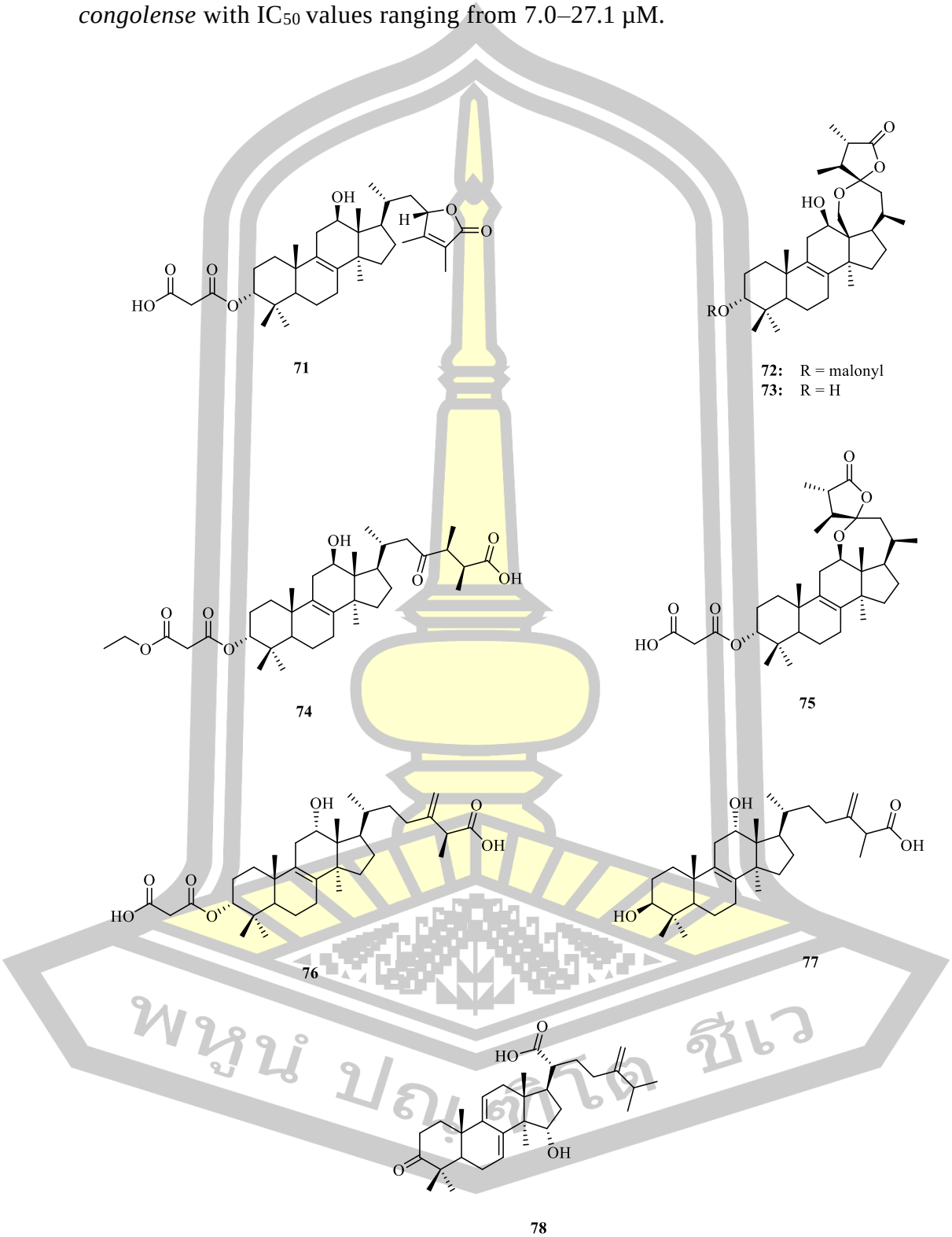

Figure 4. Structures of compounds **71**–**78**.

Eight 24-methyl-lanostane triterpenes named officimalonic acid A (**79**), officimalonic acid B (**80**), officimalonic acid C (**81**), officimalonic acid D (**82**), officimalonic acid E (**83**), officimalonic acid F (**84**), officimalonic acid G (**85**), and officimalonic acid H (**86**), as well as one known lanostane triterpene, fomitopsin A (**87**) (**Figure 5**), were isolated from EtOAc extract of the fruiting bodies of *Fomes officinalis* (Han et al., 2016). Fruiting bodies of *F. officinalis* were bought from Xinjiang Uyghur Medicine Hospital (Xinjiang, China). Compounds **82**, **83**, **85**, **86** and **87**, showed potent inhibitory effects on NO production LPS-induced RAW 264.7 cells, with IC_{50} values in the range of 5.1–8.9 μM. Compounds **83**, **85**, and **86**, exhibited moderate cytotoxicity against three human cancer cell lines, human large-cell lung cancer (H460) cell line, HepG2, and human gastric cancer (BGC-823) cell line with IC_{50} values in the range of 20–70 μM.

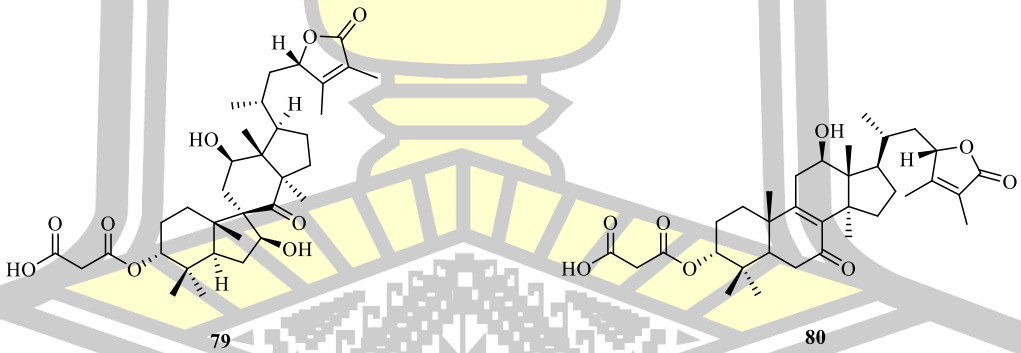

Figure 5. Structures of compounds **79**–**87**.

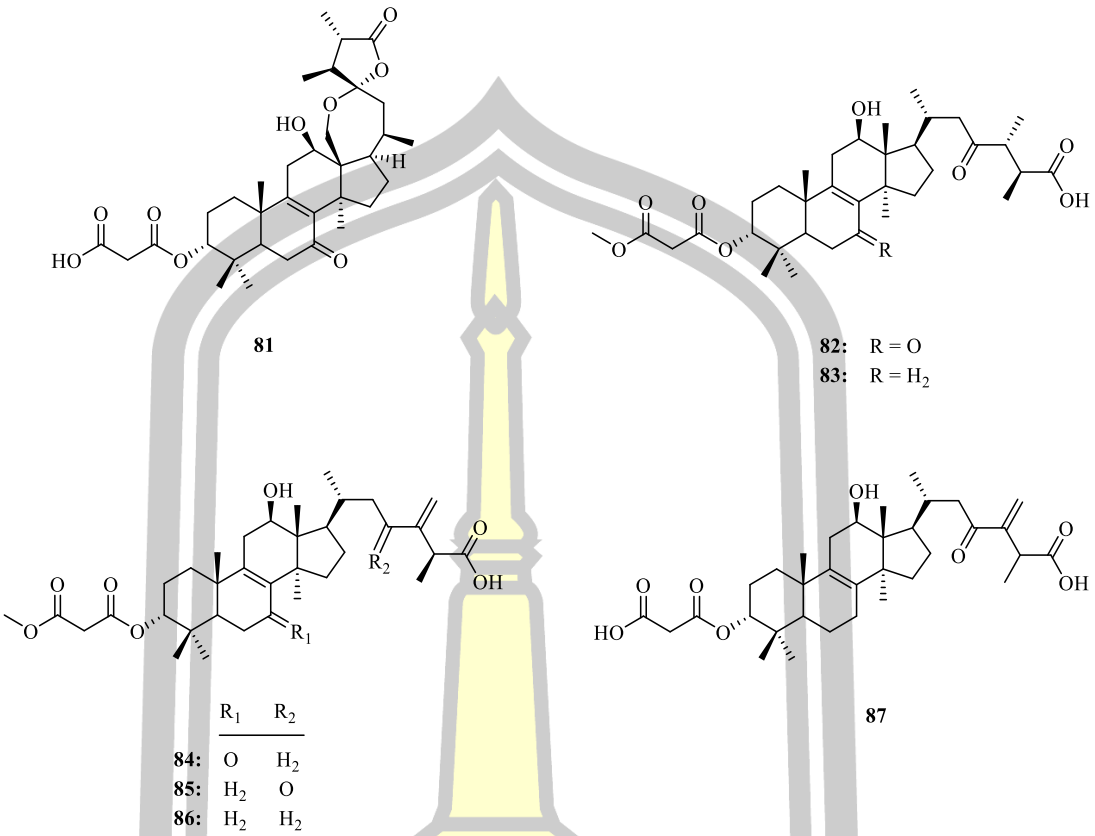

Figure 5 (continued)**.** Structures of compounds **79**–**87**.

2.6. Isolated compounds from *F. feei*

Three 24-methyl-lanostane triterpenoids, fomitopsin D (**88**), fomitopsin E (**89**) (**Figure 6**), and fomitopsin F (**75**) (**Figure 4**), along with four known compounds, carboxyacetylquercinic acid (**90**), 3α-carboxyacetoxy-24-methylene-23-oxolanost-8-en-26-oic acid (**91**), daedalol C (**92**), and quercinic acid B (**93**) (**Figure 6**), were isolated from dichloromethane (CH_2Cl_2) extract from fruiting bodies of the basidiomycete *F. feei* (Isaka et al., 2017). The mushroom specimens were collected on a dead wood (unidentified) in Thai Mueang district, Pang-Nga province, Thailand, on June 14, 2015. Fomitopsin D (**88**) exhibited activity against herpes simplex virus type 1 (HSV-1) with an IC_{50} value of 17 µg/mL. Fomitopsins E (**89**) and F (**75**), showed

activity against *B. cereus* with minimum inhibitory concentration (MIC) values of 6.25 µg/mL.

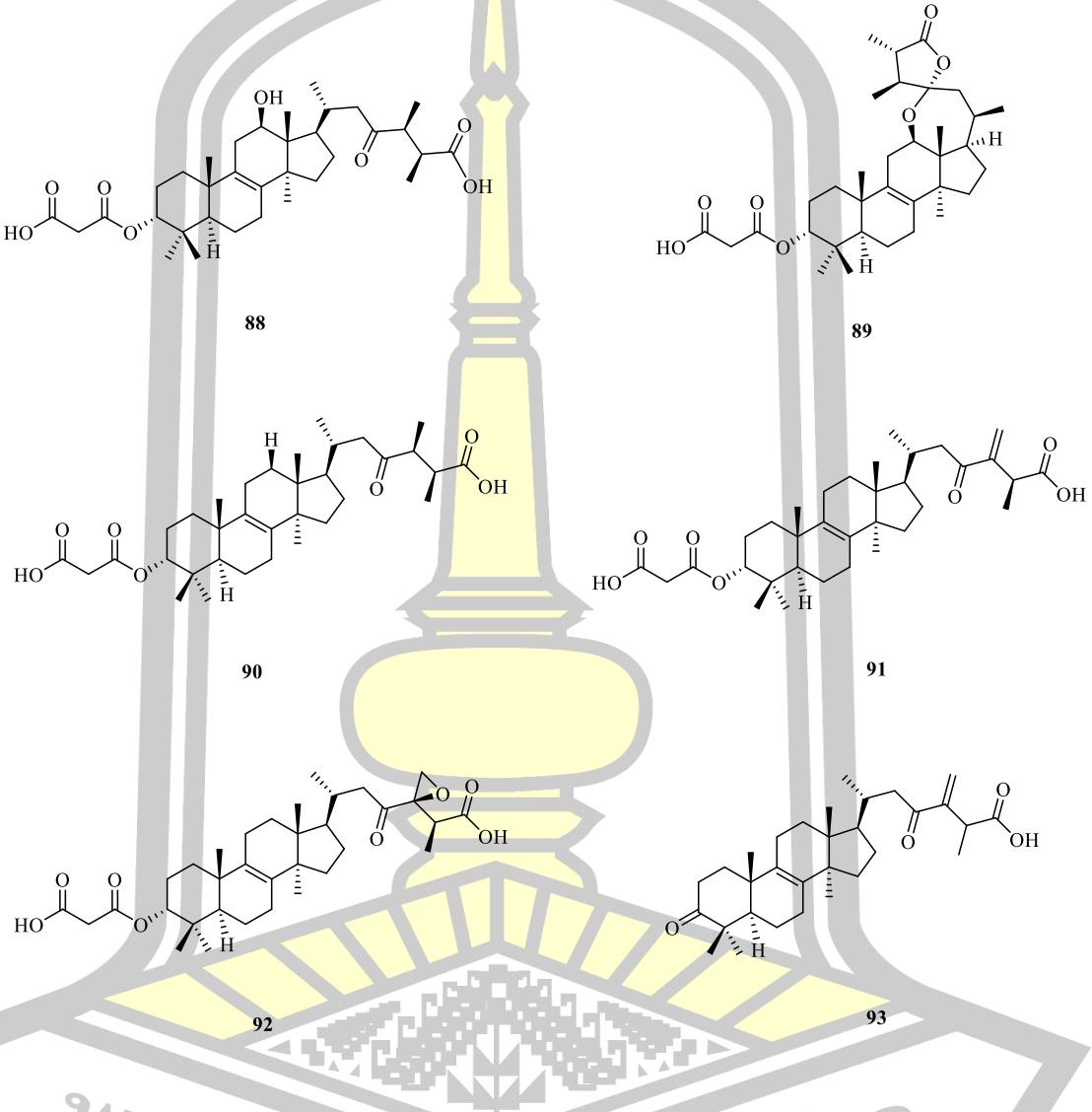

Figure 6. Structures of compounds **88**–**93**.

CHAPTER 3

MATERIALS AND METHODS

3.1. General experimental procedure

Nuclear magnetic resonance (NMR) spectra (^{1}H NMR 400 MHz, ^{13}C NMR 100 MHz) were recorded on a Bruker Ascend-400 (Prodigy unit) with deuterated solvents; deuterated chloroform ($CDCl_3$) (δ_H 7.26/δ_C 77.0 ppm) (ZEOtope, Zeochem AG, Rüti, Switzerland), deuterated acetone (acetone-d_6) (δ_H 2.05/δ_C 29.8 ppm) (Merck, Darmstadt, Germany), and deuterated methanol (CD_3OD) (δ_H 3.31/δ_C 49.0 ppm) (Eurisotop, France, Switzerland). High-resolution electrospray ionization mass (HREESIMS) spectra were measured with a Bruker micrOTOF mass spectrometer (Bruker Daltonik, Bremen, Germany) and an Agilent TOF/Q-TOF mass spectrometer (Agilent Technologies, CA, USA). Column chromatography (CC) was performed using silica gel 60 (Merck, Darmstadt, Germany), silica gel 60H (Merck, Darmstadt, Germany), and Sephadex LH-20 (Sigma Aldrich, St. Louis, MO, USA). Pre-coated silica gel 60 F_{254} on Aluminium sheets (Merck, Darmstadt, Germany) were used for analytical thin-layer chromatography (TLC).

3.2. Fungal material

The mushroom specimens were collected from Maha Sarakham Province, northeastern Thailand, on May 24, 2022. The voucher collection (Mahasarakham University Thailand; MSUT-7902) was deposited at the Medicinal Mushroom Museum, Faculty of Science, Mahasarakham University, and the living culture

(MSUCC009) is preserved at the Department of Biology, Faculty of Science, Mahasarakham University.

3.3. Fungal culture and DNA extraction

A pure culture of the fungal isolate *F. meliae* (MSUCC009) was grown in potato dextrose broth (PDB) medium at room temperature for 7 days. After incubation, the fungal mycelium was harvested, and its genomic deoxyribonucleic acid (DNA) was extracted using the GF-1 Plant DNA Extraction Kit (Vivantis, Malaysia). The quality and quantity of the extracted genomic DNA were measured with a NanoDrop™ Lite spectrophotometer (Thermo Fisher Scientific). The genomic DNA was then stored at -20 °C for future experimental use.

3.4. Molecular identification of the *F. meliae* MSUCC009

The Internal transcribed spacer (ITS) region was amplified using the primers ITS1 (5′-TCCGTAGG TGAACCTGCG G-3′) and ITS4 (5′-TCCTCCGCTTATTGA TATGC-3′) (White et al., 1990). Polymerase chain reaction (PCR) was conducted for the ITS gene (Sangdee et al., 2015). The resulting PCR products were purified using the Gel/PCR DNA Fragments Extraction Kit (Vivantis, Malaysia). Sequencing was carried out by Macrogen Inc. (Korea). The partial ITS sequence data were compared with those in the National Center for Biotechnology Information (NCBI) database using the nucleotide BLAST program (www.ncbi.nih.gov/blast). The novel partial sequence was deposited in the GenBank nucleotide sequence database. Reference sequences from related species were downloaded and aligned using ClustalW (www.genome.jp/tools/clustalw/). Phylogenetic analysis of the ITS region was

performed using MEGA program (Tamura et al., 2013), and a neighbor-joining (NJ) tree was constructed with 1000 bootstrap replicates using the Kimura 2-parameter method for pairwise deletion at uniform rates.

3.5. Large scale fermentation

The fungal strain was maintained on potato dextrose agar (PDA). The agar was cut into small plugs, 3 plugs were placed and inoculated into 24 × 250 mL Erlenmeyer flasks containing 25 mL of malt extract broth (MEB) and incubated at room temperature for 19 days. The primary culture of 25 mL MEB was transferred into 24 × 1000 mL Erlenmeyer flask containing 250 mL MEB and incubated under static conditions.

3.6. Extraction

The grown mycelium (residue) was separated from the broth (filtrate) by filtration. The broth was extracted with EtOAc (9 L), and the EtOAc layer was concentrated to yield a broth extract (3.49 g). The wet mycelium were macerated in methanol (MeOH) (1.5 L) for 5 days, filtered, and concentrated. The concentrate residue was suspended in 50 mL water (H_2O) and partitioned with EtOAc (3 × 300 mL). The collected EtOAc layer was then concentrated to obtain a mycelium extract (1.25 g) (**Flow chart 1**).

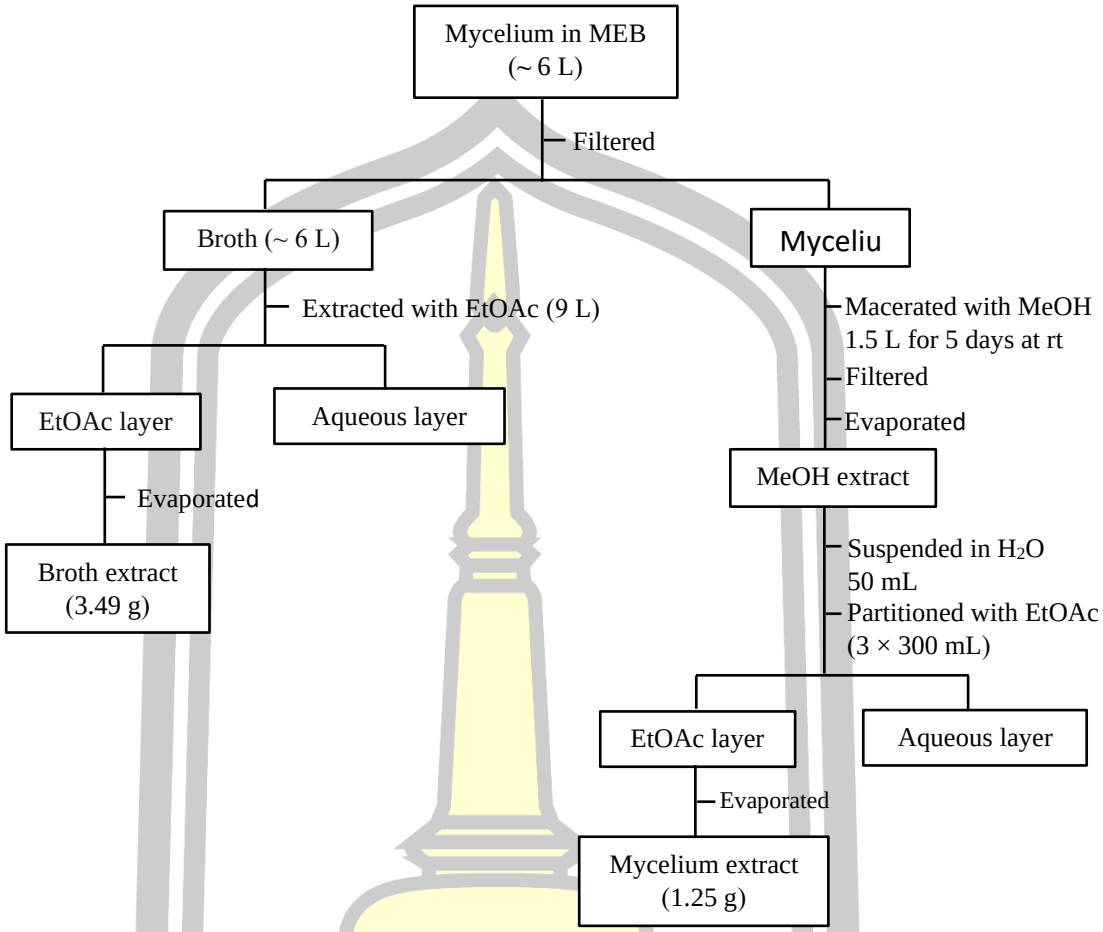

Flow chart 1. Extraction of the mycelium of *F. meliae*.

3.7. Isolation

The broth extract was fractionated by silica gel column chromatography (Merck KGaA) (4.0 × 28 cm, hexane–EtOAc 80:20 to 0:100, and then with EtOAc–MeOH 100:0 to 30:70) (**Figure 7**) to obtain twelve fractions (Fr. 1 to Fr. 12). Fraction (Fr.) 7 (530 mg) was further purified by silica gel (3.0 × 22 cm) and a subsequent silica gel CC (1.5 × 16 cm) eluted with step gradient elution as the same manner described above to yield **94** (light-brown solid; 7.9 mg). Fr. 8 (294.7 mg) was separated over silica gel column (2.0 × 19 cm, hexane–EtOAc 80:20 to 0:100, and then with EtOAc–MeOH 100:0 to 0:100) into three fractions (Fr. 8A to Fr. 8C). Compound **95** (light-brown

crystal; 79.4 mg) was obtained from Fr. 8A (145.9 mg) by Sephadex LH-20 column (1.5 × 20 cm; MeOH) (Merck KGaA) CC purification. A combined fraction of Fr. 10 and Fr. 11 (314 mg) was fractionated over a Sephadex LH-20 column (3.5 × 19 cm, MeOH) followed by a silica gel column (1.5 × 17 cm, hexane–EtOAc 80:20 to 0:100, and then with EtOAc–MeOH 100:0 to 0:100) to give **96** (white colorless solid; 3.3 mg) (**Flow chart 2**).

Figure 7. Isolation of the broth extract of *F. meliae*.

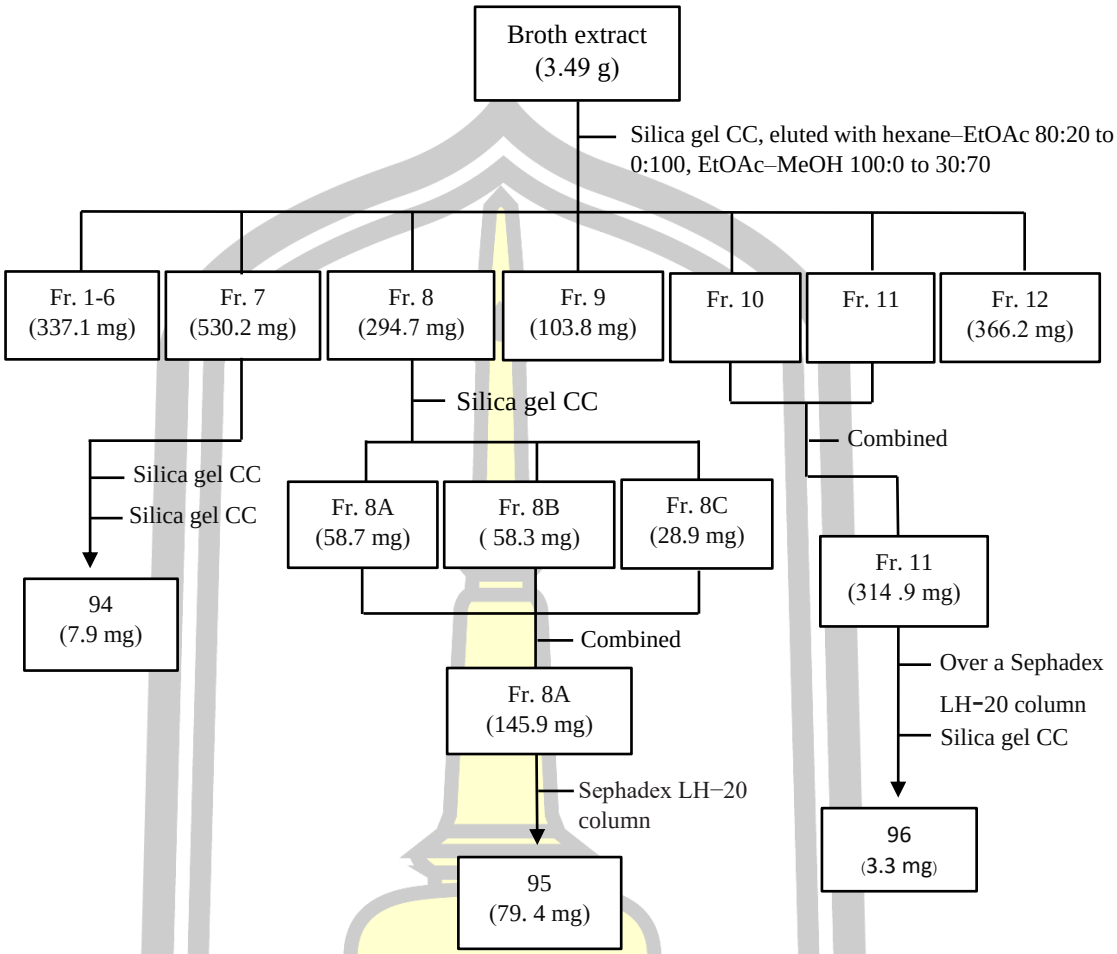

Flow chart 2. Isolation of the broth extract of *F. meliae*.

3.8. Antibacterial activity assay

3.8.1. Agar well diffusion assay

The antibacterial activities were tested using the agar well diffusion method (Sangdee et al., 2016). The Gram-positive pathogenic bacteria methicillin-susceptible *S. aureus* (MSSA) DMST 2933, methicillin-resistant *S. aureus* (MRSA) DMST 20651 and *Bacillus cereus* ATCC 11778 were cultured on Mueller Hinton agar (MHA) at 37 °C for 16–18 h. A single colony of each bacterium (*S. aureus* (MSSA and MRSA), and *B. cereus*) was inoculated into Mueller Hinton broth

(MHB) and incubated at 37 °C for 4 h with shaking at 250 rpm, then adjusted to a 0.5 McFarland standard. A sterile cotton swab was dipped into the standardized bacterial suspension and swabbed in four directions over the entire surface of the MHA plates. The plates were then cut using a 7 mm sterile cork borer. The extract solutions (50 mg/mL) were added to each well at 0.1 mL per well. The plates were incubated at 37 °C for 16–18 h, after which the zones of inhibition surrounding each well were measured. The negative control of 10% (*v/v*) MeOH was used, while tetracycline (250 µg/mL) was used as a positive control. The potential pure compounds (1.0 mg/mL) were then evaluated for antibacterial activity against suspected pathogens as described above.

3.8.2. MIC and MBC assay

The potential pure compounds were then evaluated for their MIC and minimum bactericidal concentration (MBC) using some modified the microdilution method (Wiegand et al., 2008). One colony of the pathogenic bacteria was inoculated into MHB medium, and the inoculated tubes were then incubated at 37 °C with shaking at 250 rpm for 4 h. The bacterial suspension was standardized to 4–5 × 10^6 CFU/mL, followed by the addition of 10 µL of the standardized inoculum to the wells of a 96-well polystyrene tray. Subsequently, 90 µL of each diluted mycelium extract (0.25, 0.125, and 0.0625 mg/mL) in MHB was separately added. An uninoculated control well and a control growth well were included in each plate. Tetracycline (250 µg/mL) was used as the reference standard.

3.9. Cytotoxicity assay

The cytotoxic activity against human lung adenocarcinoma (A549) cell lines was assayed using the previously described method with some modifications (Min et al., 2023; Su et al., 2009). Briefly, cell suspensions in culture medium (100 µL per well) were seeded into 96-well plates and incubated at 37 °C in a humidified 5% carbon dioxide (CO_2) atmosphere. After 24 h, 100 µL of culture medium containing the test sample was added to each well, followed by an additional 72 h incubation. Half of the medium was removed then added 10 µL of 5 mg/mL 3-(4,5-dimethyl- thiazol-2-yl)-2,5-diphenyl tetrazolium bromide (MTT) (Invitrogen®, Life Technologies Corporation, Oregon, USA) in phosphate buffer saline (Gibco®, Life Technologies Limited, Paisley, UK), and the cells were incubated for 4 h at 37 °C. Afterward, the medium was removed, deuterated dimethyl sulfoxide (DMSO) (50 µL per well) was added, and absorbance was measured at 570 nm on a microplate reader (SPECTROstar Nano, BMG LABTECH, Ortenberg, Germany). The absorbance values were used to calculate cell viability relative to the control. All assays were performed in duplicate, and results were expressed as %cytotoxicity compared to the control group.

CHAPTER 4

RESULTS AND DISCUSSION

4.1. Molecular identification of the fungal isolate MSUCC009

From the DNA sequence, the ITS region, comprising 636 nucleotides, was submitted to GenBank with the accession number PP724744. A BLAST search on NCBI (www.ncbi.nih.gov/blast) revealed that the ITS sequence had the highest similarity to *Fomitopsis* cf. *meliae* WS3JB14 (KT844682) and *F. serialis* isolate 6_2B10_3M (MH541019), with 100.00% and 99.21% homology, respectively. A phylogenetic tree constructed from 13 aligned sequences with similar characteristics placed the fungal isolate MSUCC009 in the same clade as *Fomitopsis* species (**Figure 8**). Based on these data, the fungal isolate MSUCC009 was identified as *F. meliae.*

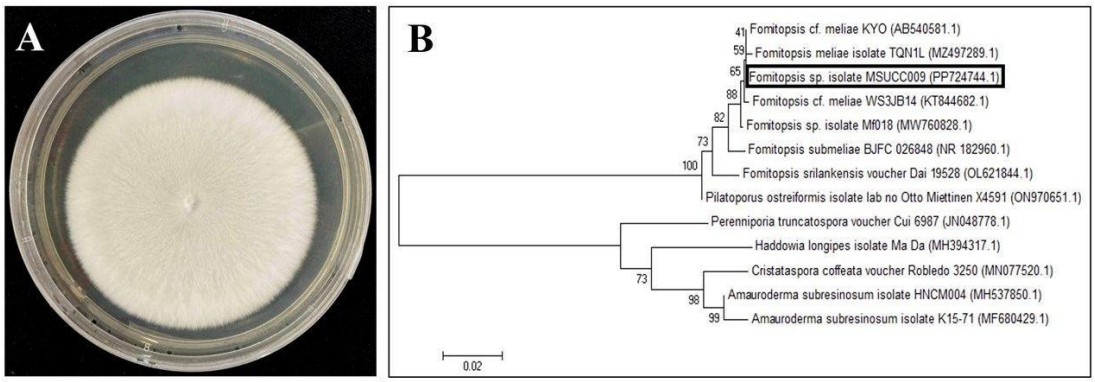

Figure 8. Cotton morphology of 7-days-old of the fungal *F. meliae* (MSUCC009) on PDA medium and NJ tree depicting the fungal isolate *F. meliae* (MSUCC009) alongside related species, constructed from partial ITS Rdna region sequences. The tree was rooted at the midpoint and developed using the GTR + GAMMA model (**A**). Branch lengths indicate the expected number of substitutions per site, and support values above branches represent bootstrap percentages (**B**).

4.2. Large scale fermentation and extraction

From large scale fermentation (24 × 250 mL MEB each flask), the cultures were harvested on day 21 when the white mycelia had grown well, and the color of the filtrate had started to change from light yellow to dark brown. The combined filtrate (~ 6 L) was extracted with EtOAc, yielding 3.49 g of the dark brown gum broth extract (**Figure 9A**). The wet mycelium were initially macerated in MeOH to extract broth polar and non-polar organic substances. The aqueous solution of this MeOH extract was then further partitioned with EtOAc to isolate EtOAc-soluble molecules and remove some non-polar (lipophilic) and polar (hydrophilic) compounds. The mycelium extract (**Figure 9B**), 1.25 g, was obtained from the extraction of combined 24 × 250 mL MEB flask of wet mycelium.

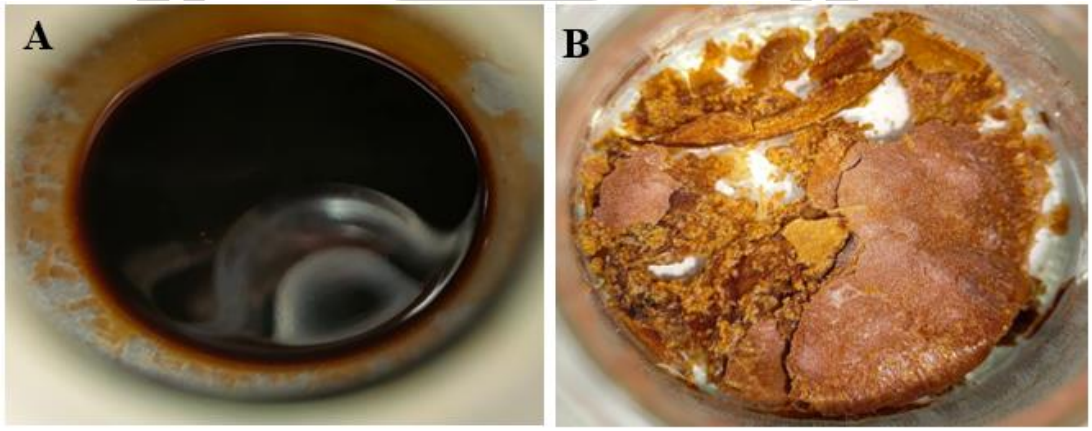

Figure 9. The broth extract (**A**) and mycelium extract (**B**) of *F. meliae*.

4.3. Isolation and identification of compounds

From the isolation, three compounds were isolated from the broth extract of *F. meliae*.

Based on spectroscopy data the isolated compounds were identified as 5-hydroxymethyl-2-furoic acid methyl ester (**94**), 5-hydroxymethyl-2-furancarboxylic acid (HMFCA; **95**), and uracil (**96**) (**Figure 10**).

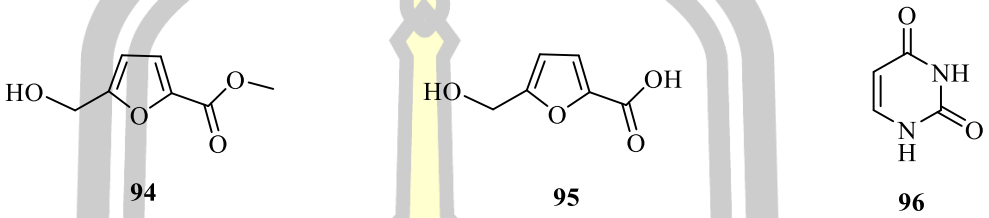

Figure 10. Structures of compounds **94**–**96**.

The isolation of compounds **94**–**96** from *F. meliae* has never been reported. From previous report, compound **94** was first isolated from the broth extract of *Curvularia lunata* (Liu et al., 2009) and is believed to be a phytotoxin responsible for causing *Curvularia* leaf spot on maize. HMFCA (**95**) was initially isolated from the broth and mycelium extracts of *Pyricularia grisea* and exhibited antitumor activity (Munekata and Tamura, 1981). It has been used as an intermediate in the synthesis of an interleukin inhibitor, suggesting its potential as a therapeutic agent for inflammatory diseases (Braisted et al., 2003). Later, the isolation of this compound from the marine fungus *Wardomyces anomalus* and its inhibitory p56lck tyrosine kinase activity have been reported (Abdel-Lateff et al., 2003). In our study, compounds **94** and **95** were also tested for their cytotoxicity against A549 cell lines. Both of them showed inactive results at the tested concentration 20 µg/mL. The isolation of uracil (**96**), one of the four nucleobases in the nucleic acid of ribonucleic acid (RNA), from fungi is a common occurrence documented in various studies (Chapla et al., 2014; Qin et al., 2014; Quiao

and Uy, 2013; Yan et al., 2010). The identification of uracil reinforces the role of fungi as a source of essential biochemical compounds.

4.3.1. 5-Hydroxymethyl-2-furoic acid methyl ester (**94**)

Compound **94** ($C_7H_8O_4$) was isolated as a light-brown solid. Its structure was elucidated based on ^1H and ^{13}C 2D NMR spectroscopic data in $CDCl_3$ and confirmed by comparison with the previous reported data in literature (Brandolese et al., 2018), as shown in **Table 1**. The ^1H, ^{13}C and 2D NMR spectroscopic data of **94** are shown in **Table 2**. The (^1H, ^{13}C and 2D) NMR and mass (MS) spectra of **94** are shown in **Figures A3**–**A14**.

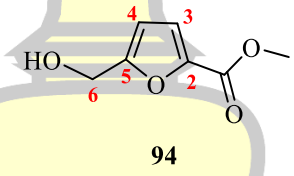

94

Table 1. ^1H and ^{13}C NMR spectroscopic data of **94** in $CDCl_3$ compared with literature.

Position	Compound **94** [a]		5-Hydroxymethyl-2-furoic acid methyl ester [b]	
	δ_H multi. (*J* in Hz)	δ_C	δ_H multi. (*J* in Hz)	δ_C
2	-	144.0	-	144.5
3	7.13, d (3.4)	118.9	7.14, d (3.4)	119.2
4	6.41, d (3.4)	109.4	6.42, d (3.4)	109.8
5	-	158.4	-	158.6
6	4.67, s	57.5	4.68, d (3.4)	57.9
2-COO<u>C</u>H$_3$	3.89, s	52.0	3.89, s	52.3
2-<u>C</u>OOCH$_3$	-	159.2	-	159.5

[a] Calibration of solvent $CDCl_3$ δ_H 7.26/δc 77.0 ppm, [b] (Brandolese et al. 2018).

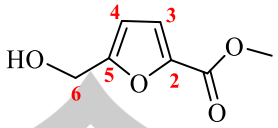

94

Table 2. ^{1}H, ^{13}C and 2D NMR spectroscopic data of **94** in $CDCl_3$.

Position	δ_H multi. (J in Hz)	δ_C	COSY	NOESY	HMBC
2	-	144.0	-	-	-
3	7.13, d (3.4)	118.9	4	4, 6	5, 2, 4
4	6.41, d (3.4)	109.4	3	3	5, 2, 3
5	-	158.4	-	-	-
6	4.67, s	57.5	3, 4	-	5, 2, 3, 4
2-COO$\underline{C}H_3$	3.89, s	52.0	-	-	2-$\underline{C}OOCH_3$, 2
2-$\underline{C}OOCH_3$	-	159.0	-	-	-

Calibration of $CDCl_3$ δ_H 7.26/δc 77.0 ppm.

4.3.2. 5-Hydroxymethyl-2-furancarboxylic acid (HMFCA; **95**)

Compound **95** ($C_6H_6O_4$) was isolated as a light-brown crystal. Its structure was elucidated based on ^{1}H and ^{13}C NMR spectroscopic data in acetone-d_6 and confirmed by comparison with the previous reported data in literature (Brandolese et al., 2018), as shown in **Table 3**. The ^{1}H, ^{13}C NMR and MS spectra of **95** are shown in **Figures A15–A17**.

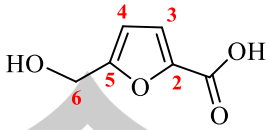

95

Table 3. ^{1}H and ^{13}C NMR spectroscopic data of **95** in acetone-d_6 compared with literature.

Position	Compound **95** [a]		HMFCA[b]	
	δ_H multi. (*J* in Hz)	δ_C	δ_H multi. (*J* in Hz)	δ_C
2	-	144.9	-	144.8
3	7.15, d (3.4)	119.5	7.14	118.7
4	6.46, d (3.4)	109.6	6.46, d (3.4)	108.9
5	-	159.5	-	159.1
6	4.59, s	57.3	4.58, s	56.8
2-COOH	-	160.1	-	160.2

[a] Calibration of acetone-d_6 δ_H 2.05/δ_C 29.8 ppm, [b] (Brandolese et al., 2018).

4.3.3. Uracil (**96**)

Compound **96** ($C_4H_4N_2O_2$) was isolated as a white colorless solid. Its structure was elucidated based on ^{1}H NMR spectroscopic data in CD_3OD and confirmed by comparison with the previous reported data in literature (Quiao and Uy, 2013), as shown in **Table 4**. The ^{1}H NMR spectrum of **96** is shown in **Figure A18**.

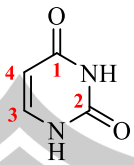

96

Table 4. ^{1}H NMR spectroscopic data of **96** in CD_3OD compared with literature.

Position	Compound **96** [a]	Uracil [b]
	δ_H multi. (*J* in Hz)	δ_H multi. (*J* in Hz)
1	-	-
2	-	-
3	7.40, d (7.7)	7.38, d (8.0)
4	5.61, d (7.7)	5.60, d (8.0)

[a] Calibration of CD_3OD δ_H 3.31ppm, [b] (Quiao and Uy 2013).

4.4. Antibacterial activity

The antibacterial activity screening of the broth and mycelial extracts of *F. meliae* against *S. aureus* (MRSA and MSSA) and *B. cereus* is shown in **Table 5**. The broth extract showed antibacterial activities against all the tested bacteria (**Table 5**). The broth extract was then determined for MIC and MBC. This extract exhibited the antibacterial activities with the same MIC and MBC values of 3.0 mg/mL against the tested bacteria.

For the antibacterial activity of the isolated pure compounds **94** and **95**, only **95** exhibited antibacterial activity against *S. aureus* (MSSA) with MIC and MBC values of > 0.25 mg/mL as shown in **Table 5**.

Table 5. Antibacterial activities of the F. meliae extracts and compounds **94** and **95**.

Sample	Inhibition zone (mm)			MIC/MBC (mg/mL)		
	S. aureus (MSSA)	*S. aureus* (MRSA)	*B. cereus*	*S. aureus* (MSSA)	*S. aureus* (MRSA)	*B. cereus*
Broth extract	33 × 33	32 × 32	31 × 31	3.0/3.0	3.0/3.0	3.0/3.0
Mycelium extract	0	0	10 × 10	-	-	-
Tetracycline	28 × 28	30 × 30	30 × 30	-	-	-
94	-	-	-	ND	ND	ND
95	18 × 18	-	-	> 0.25	ND	ND

Tetracycline was used as a positive control and tested at 250 µg/mL, ND = not detected.

4.5. Cytotoxicity

Compounds **94** and **95** were tested for their cytotoxicity against A549 cell lines. Both of them showed inactive results at the tested concentration 20 µg/mL.

CHAPTER 5

CONCLUSION

Two known 5-hydroxymethylfuran, 5-hydroxymethyl-2-furoic acid methyl ester (**94**) and 5-hydroxymethyl-2-furancarboxylic acid (HMFCA; **95**), together with a pyrimidine base, uracil (**96**), were first isolated from the culture broth extract of *F. meliae* (MSUCC009). 5-Hydroxymethyl-2-furancarboxylic acid exhibited the antibacterial activity against *S. aureus* (MSSA). These discoveries enhance our understanding of fungal chemical ecology and highlight the potential of *F. meliae* as a source of bioactive natural compounds.

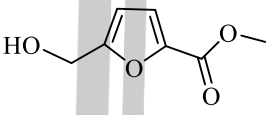

94

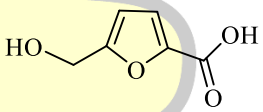

95

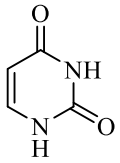

96

REFERENCES

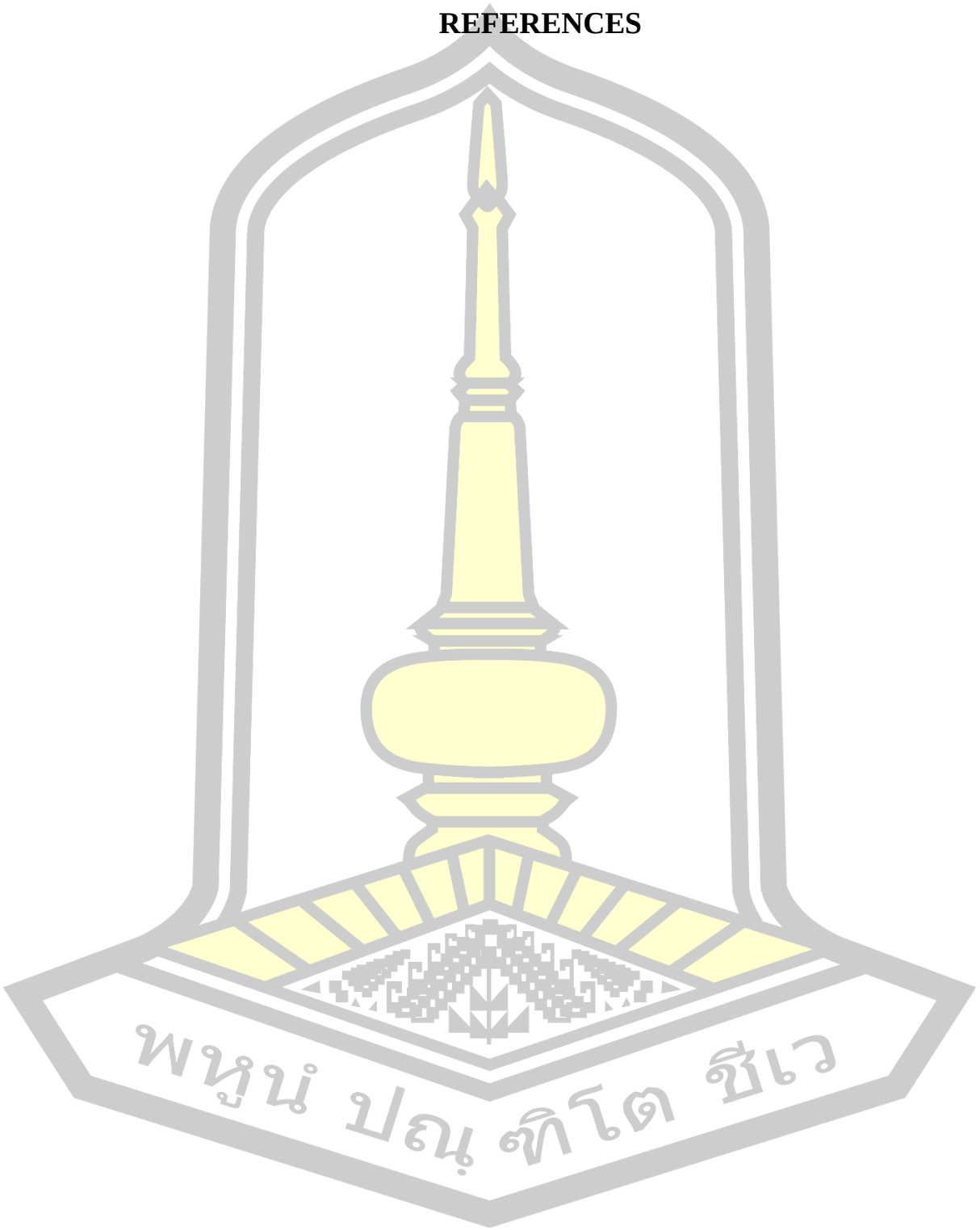

REFERENCES

Abdel-Lateff, A.; Klemke, C.; König, G. M.; Wright, A. D. Two new xanthone derivatives from the algicolous marine fungus *Wardomyces anomalus*. Journal of Natural Products. **2003**; 66(5), 706−708.

Alexopolous, C.; Mims, C.; Blackwell, M. Introductory Mycology John Wiley & Sons. Inc. New York. **1996**.

Baimai, V. Biodiversity in Thailand. The Journal of the Royal Institute of Thailand. **2010**; 2: 107−118.

Bishop, K. S. Characterisation of extracts and anti-cancer activities of *Fomitopsis pinicola*. Nutrients. **2020**; 12(3): 609.

Blair, A.; Ritz, B.; Wesseling, C.; Freeman, L. B. Pesticides and human health. Occupational and Environmental Medicine. **2015**; 72(2) 81−82.

Braisted, A. C.; Oslob, J. D.; Delano, W. L.; Hyde, J.; McDowell, R. S.; Waal, N.; Yu, C.; Arkin, M. R.; Raimundo, B. C. Discovery of a potent small molecule IL-2 inhibitor through fragment assembly. Journal of the American Chemical Society. **2003**; 125(13): 3714−3715.

Brandolese, A.; Ragno, D.; Di Carmine, G.; Bernardi, T.; Bortolini, O.; Giovannini, P. P.; Pandoli, O. G.; Altomare, A.; Massi, A. Aerobic oxidation of 5-hydroxymethylfurfural to 5-hydroxymethyl-2-furancarboxylic acid and its derivatives by heterogeneous NHC-catalysis. Organic & Biomolecular Chemistry. **2018**; 16(46): 8955−8964.

Bueno, D.J.; Silva, J.O. The fungal hypha. Encyclopedia of Food Microbiology (2nd ed). **2014**; pp. 11−19.

Chapla, V. M.; Zeraik, M. L.; Leptokarydis, I. H.; Silva, G. H.; Bolzani, V. S.; Young, M. C. M.; Pfenning, L. H.; Araújo, A. R. Antifungal compounds produced by Colletotrichum gloeosporioides, an endophytic fungus from Michelia champaca. Molecules. **2014**; 19(11): 19243−19252.

El-Maradny, Y. A.; El-Fakharany, E. M.; Abu-Serie, M. M.; Hashish, M. H.; Selim, H. S. Lectins purified from medicinal and edible mushrooms: Insights into their antiviral activity against pathogenic viruses. International journal of biological macromolecules. **2021**; 179: 239−258.

Gao, Y.; Wang, P.; Wang, Y.; Wu, L.; Wang, X.; Zhang, K.; Liu, Q. In vitro and in vivo activity of *Fomitopsis pinicola* (sw. Ex fr.) karst chloroform (fpkc) extract against s180 tumor cells. Cellular Physiology and Biochemistry. **2018**; 44(5): 2042−2056.

Gilbertson, R. L. North American wood-rotting fungi that cause brown rots. Mycotaxon. **1981**; 12: 372−416.

Gründemann, C.; Reinhardt, J. K.; Lindequist, U. European medicinal mushrooms: Do they have potential for modern medicine?–An update. Phytomedicine. **2020**; 66: 153131.

Han, J.; Li, L.; Zhong, J.; Tohtaton, Z.; Ren, Q.; Han, L.; Huang, X.; Yuan, T. Officimalonic acids A− H, lanostane triterpenes from the fruiting bodies of *Fomes officinalis*. Phytochemistry. **2016**; 130, 193−200.

Hawksworth, D. L. The fungal dimension of biodiversity: magnitude, significance, and conservation. Mycological research. **1991**; 95(6): 641−655.

Isaka, M.; Chinthanom, P.; Srichomthong, K.; Thummarukcharoen, T. Lanostane triterpenoids from fruiting bodies of the bracket fungus *Fomitopsis feei*. Tetrahedron Letters. **2017**; 58(18), 1758−1761.

Janardhanan, K. K.; Ravikumar, K. S.; Karuppayil, S. M. Medicinal mushroom bioactives: Potential sources for anti-cancer drug development. International Journal of Applied Pharmaceutics. **2020**; 12(4): 40−45.

Kumar, V.; Prasher, I. B. Antimicrobial potential of endophytic fungi isolated from *Dillenia indica* L. and identification of bioactive molecules produced by *Fomitopsis meliae* (Undrew.) Murril. Natural Product Research. **2022**; 36(23); 6064−6068.

Liu, T.; Liu, L.; Jiang, X.; Huang, X.; Chen, J. A new furanoid toxin produced by *Curvularia lunata*, the causal agent of maize Curvularia leaf spot. Canadian Journal of Plant Pathology. **2009**; 31(1): 22−27.

Liu, Y.; Liu, W.; Li, M.; Yuan, T. Lanostane triterpenoids from the fruiting bodies of *Fomitopsis pinicola* and their anti-inflammatory activities. Phytochemistry. **2022**; 193: 112985.

Maxwell, J. A synopsis of the vegetation of Thailand. Tropical Natural History. **2004**; 4(2), 19−29.

Min, S. J.; Lee, H.; Shin, M.-S.; Lee, J. W. Synthesis and biological properties of pyranocoumarin derivatives as potent anti-inflammatory agents. International Journal of Molecular Sciences. **2023**; 24(12): 10026.

Munekata, M.; Tamura, G. Antitumor activity of 5-hydroxy-methyl-2-furoic acid. Agricultural and Biological Chemistry. **1981**; 45(9): 2149−2150.

Murrill, W. A. The polyporaceae of North America.-III. the genus *Fomes*. Bulletin of the Torrey Botanical Club. **1903**; 30(4): 225−232.

Naranmandakh, S.; Murata, T.; Odonbayar, B.; Suganuma, K.; Batkhuu, J.; Sasaki, K. Lanostane triterpenoids from *Fomitopsis officinalis* and their trypanocidal activity. Journal of natural medicines. **2018**; 72(2): 523−529.

Pinky, N. J.; Islam, S.; Alice, R. S. Edibility detection of mushroom using ensemble methods. International Journal of Image, Graphics and Signal Processing, **2019**; 11(4): 55−62.

Qin, C.; Lin, X.; Ai, W.; Zhong, Z.; Xian, J.; Xu, S.; Liu, Y. Secondary metabolites from mangrove Sonneratia apetala endophytic fungus *Neofusicoccum* sp. SaBA3. Natural Product Research and Development. **2014**; 26(8): 1212−1215.

Quiao, M. A. D.; Uy, M. M. Pyrimidines from the Philippine marine sponge *Aaptos suberitoides*. International journal of scientific and engineering research. **2013**; 4(1): 1−4.

Samchai, S.; Seephonkai, P.; Kaewtong, C. Two indole derivatives and phenolic compound isolated from mushroom *Phellinus linteus*. Chinese Journal of Natural Medicines. **2011**; 9(3): 173−175.

Sangdee, K.; Nakbanpote, W.; Sangdee, A. Isolation of the entomopathogenic fungal strain Cod-MK1201 from a cicada nymph and assessment of its antibacterial activities. International journal of Medicinal Mushrooms. **2015**; 17(1): 51−63. .

Sangdee, K.; Seephonkai, P.; Buranrat, B.; Surapong, N.; Sangdee, A. Effects of ethyl acetate extracts from the *Polycephalomyces nipponicus* isolate Cod-MK1201 (Ascomycetes) against human pathogenic bacteria and a breast cancer cell line. International journal of Medicinal Mushrooms. **2016**; 18(8): 733−743.

Seephonkai, P.; Samchai, S.; Thongsom, A.; Sunaart, S.; Kiemsanmuang, B.; Chakuton, K. DPPH radical scavenging activity and total phenolics of *Phellinus* mushroom extracts collected from northeast of Thailand. Chinese Journal of Natural Medicines. **2011**; 9(6): 441−445.

Seephonkai, P.; Theerapong, T.; Jaikhan, S.; Klinhom, U.; Kaewtong, C. Characterisation of indole alkaloids and phenolic acids from wild mushroom Tropicoporus linteus and its chemical profiles compared with other Sanghuang mushrooms. Natural Product Research. **2024**; 38(2): 198−205.

Sofrenić, I.; Anđelković, B.; Todorović, N.; Stanojković, T.; Vujisić, L.; Novaković, M.; Milosavljević, S.; Tešević, V. Cytotoxic triterpenoids and triterpene sugar esters from the medicinal mushroom *Fomitopsis betulina*. Phytochemistry. **2021**; 181: 112580.

Su, C.-R.; Yeh, S. F.; Liu, C. M.; Damu, A. G.; Kuo, T.-H.; Chiang, P.-C.; Bastow, K. F.; Lee, K.-H.; Wu, T.-S. Anti-HBV and cytotoxic activities of pyranocoumarin derivatives. Bioorganic & medicinal chemistry. **2009**; 17(16): 6137−6143.

Tamura, K.; Stecher, G.; Peterson, D.; Filipski, A.; Kumar, S. MEGA6: molecular evolutionary genetics analysis version 6.0. Molecular biology and evolution. **2013**; 30(12): 2725−2729.

Tedersoo, L.; Bahram, M.; Põlme, S.; Kõljalg, U.; Yorou, N. S.; Wijesundera, R.; Ruiz, L. V.; Vasco-Palacios, A. M.; Thu, P. Q.; Suija, A.; Smith, M. E.; Sharp, C.; Saluveer, E.; Saitta, A.; Rosas, M.; Riit, T.; Ratkowsky, D.; Pritsch, K.; Põldmaa, K.; Piepenbring, M.; Phosri, C.; Peterson, M.; Parts, K.; Pärtel, K.; Otsing, E.; Nouhra, E.; Njouonkou, A. L.; Nilsson, R. H.; Morgado, L.N.; Mayor, J.; May, T. W.; Majuakim, L.; Lodge, D.J.; Lee, S.S.; Larsson, K.-H.;

Kohout, P.; Hosaka, K.; Hiiesalu, I.; Henkel, T. W.; Harend, H.; Guo, L.-D.; Greslebin, A.; Grelet, G.; Geml, J.; Gates, G.; Dunstan, W.; Dunk, C.; Drenkhan, R.; Dearnaley, J.; Kesel, A. D.; Dang, T.; Chen, X.; Buegger, F.; Brearley, F.Q.; Bonito, G.; Anslan, S.; Abell, S.; Abarenkov, K. Global diversity and geography of soil fungi. Science. **2014**; 346(6213): 1256688.

Thailand Country Study on Biodiversity. Ministry of Science, Technology and Environment. Bangkok. **1992**.

Underwood, L. M. Some new fungi, chiefly from Alabama. Bulletin of the Torrey Botanical Club. **1897**; 24(2): 81−86.

Van Welzen, P. C.; Madern, A.; Raes, N.; Parnell, J.; Simpson, D.; Byrne, C.; Curtis, T.; Macklin, J.; Trias-Blasi, A.; Prajaksood, A. The current and future status of floristic provinces in Thailand. In Trisurat, Y.; Land use, Shrestha, R. P.; lkemade, R. A (Eds.). Land use, climate change and biodiversity modeling: perspectives and applications. **2011**; pp. 219−247.

Walker, D. H.; McGinnis, M. Diseases caused by fungi. Pathobiology of Human Disease: A Dynamic Encyclopedia of Disease Mechanisms. 2014; pp. 217−221.

Wasser S. P. Medicinal mushrooms as a source of antitumor and immunomodulating polysaccharides. Applied Microbiology and Biotechnol. **2002**; 60(3): 258–274.

White, T.J.; Bruns, T.; Lee, S.; Taylor, J. Amplification and direct sequencing of fungal ribosomal RNA genes for phylogenetics. In PCR-protocols. **1990**; pp. 315−322.

Wiegand, I.; Hilpert, K.; Hancock, R. E. W. Agar and broth dilution methods to determine the minimal inhibitory concentration (MIC) of antimicrobial substances. Nature protocols. **2008**; 3(2): 163−175.

Yan, H.-J.; Gao, S.-S.; Li, C.-S.; Li, X.-M.; Wang, B.-G. Chemical constituents of a marine-derived endophytic fungus *Penicillium commune* G2M. Molecules. **2010**; 15(5): 3270−3275.

Zhao, J.; Yang, Y.; Yu, M.; Yao, K.; Luo, X.; Qi, H.; Zhang, G.; Luo, Y. Lanostane-type C_{31} triterpenoid derivatives from the fruiting bodies of cultivated *Fomitopsis palustris***.** Phytochemistry. **2018**; 152: 10−21.

APPENDIX

LIST OF FIGURES

Figure **Page**

Figure **Page**

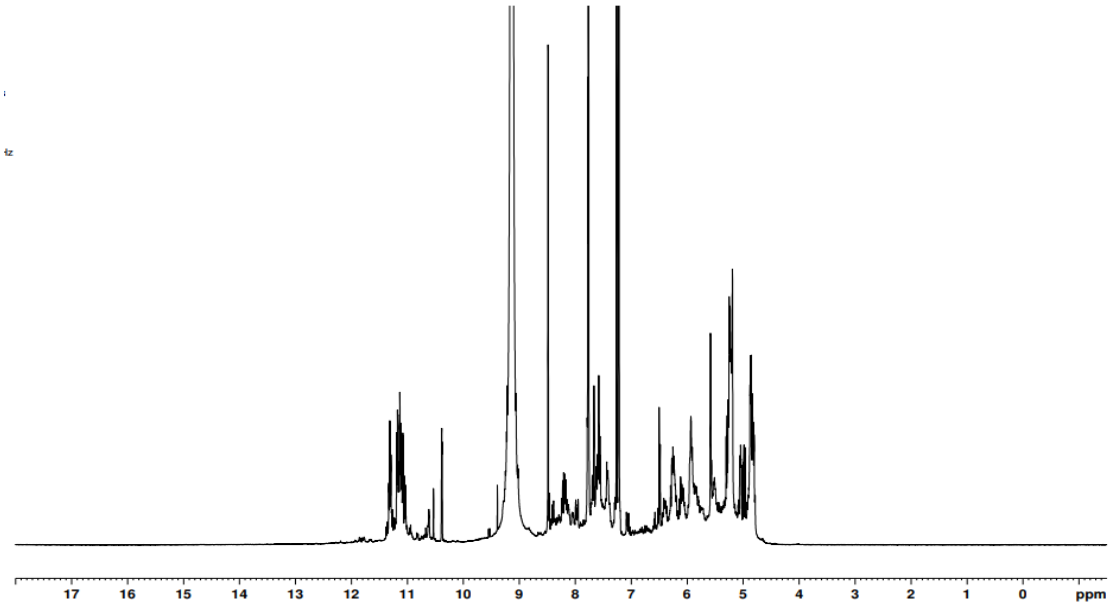

Figure A1. ^{1}H NMR spectrum of the broth extract from *F. meliae* ($CDCl_3$, 400 MHz).

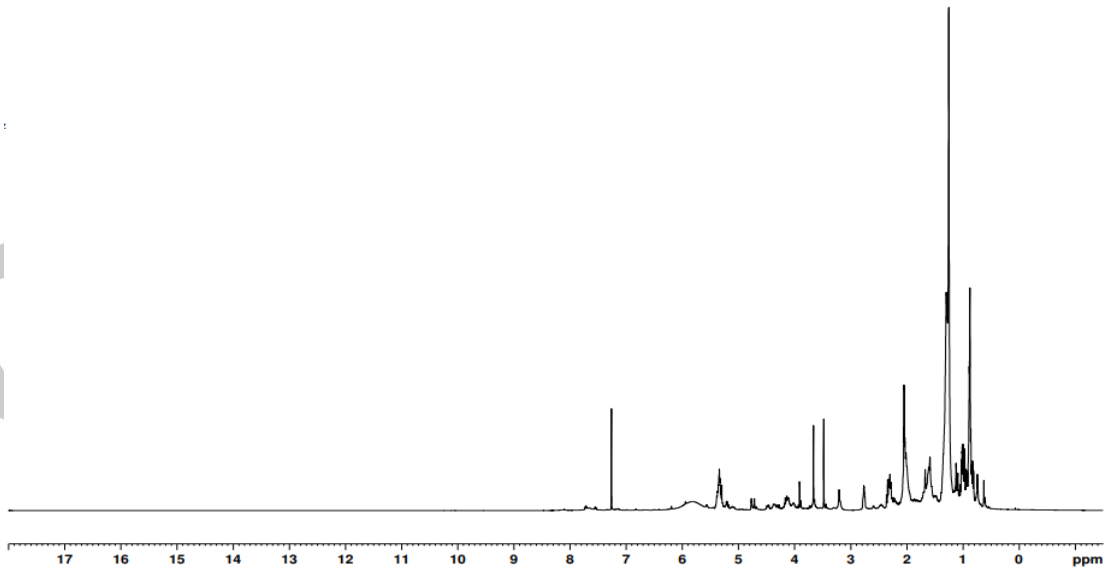

Figure A2. ^{1}H NMR spectrum of the mycelium of *F. meliae* ($CDCl_3$, 400 MHz).

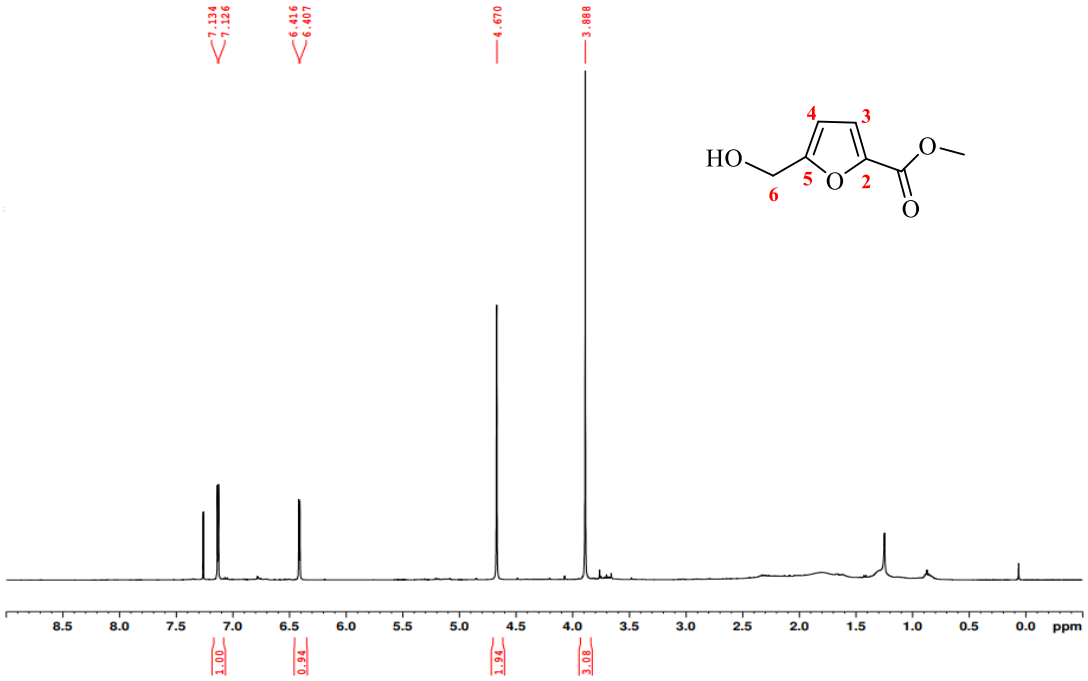

Figure A3. ^{1}H NMR of compound **94** ($CDCl_3$, 400 MHz).

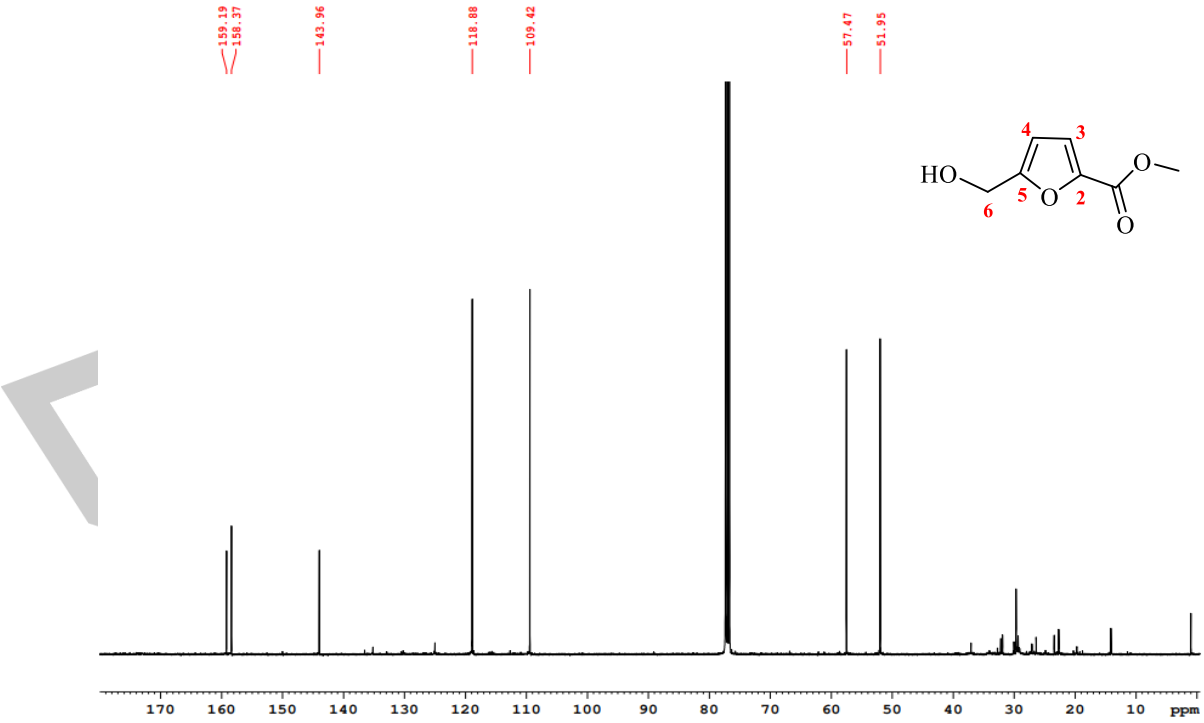

Figure A4. ^{13}C NMR of compound **94** ($CDCl_3$, 100 MHz).

Figure A5. DEPT-135 spectrum of compound **94** in $CDCl_3$.

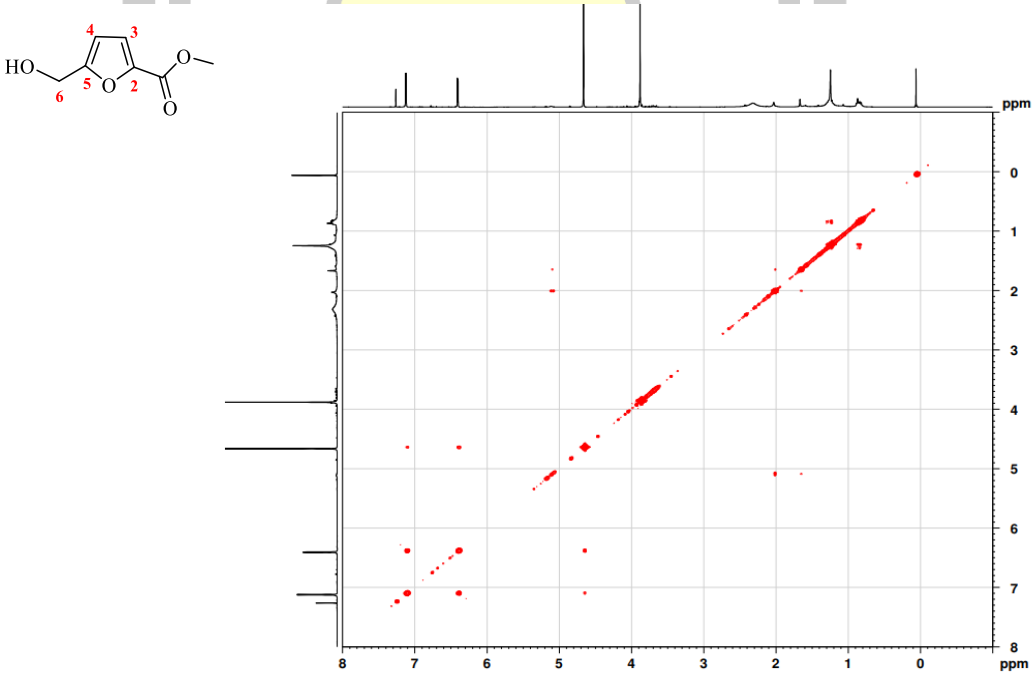

Figure A6. COSY spectrum of compound **94** in $CDCl_3$.

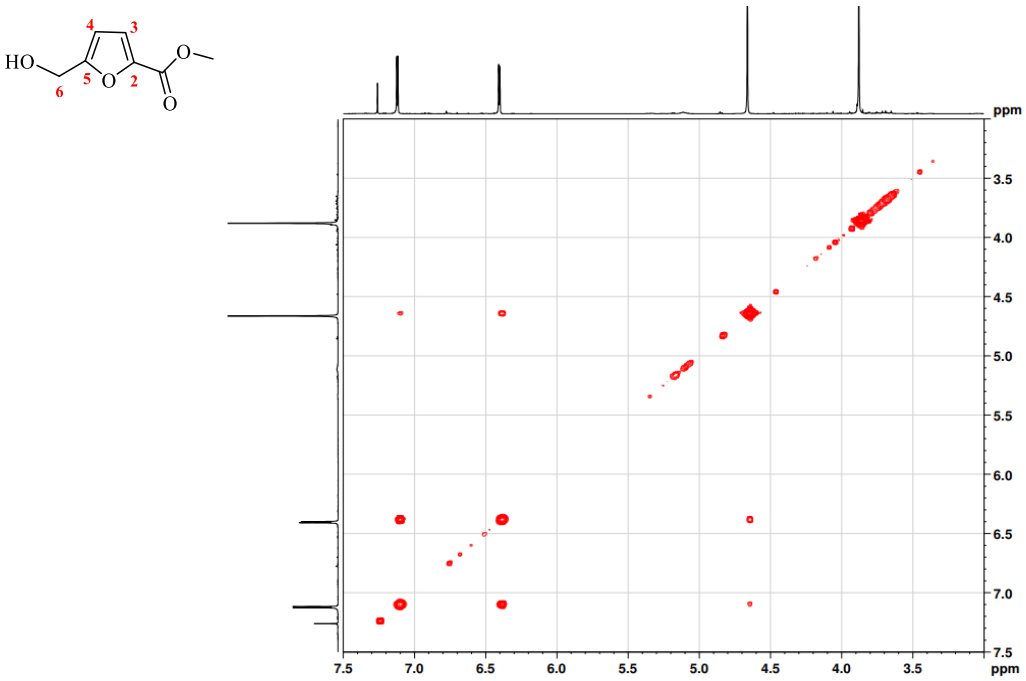

Figure A7. COSY spectrum (expansion 1) of compound **94** in $CDCl_3$.

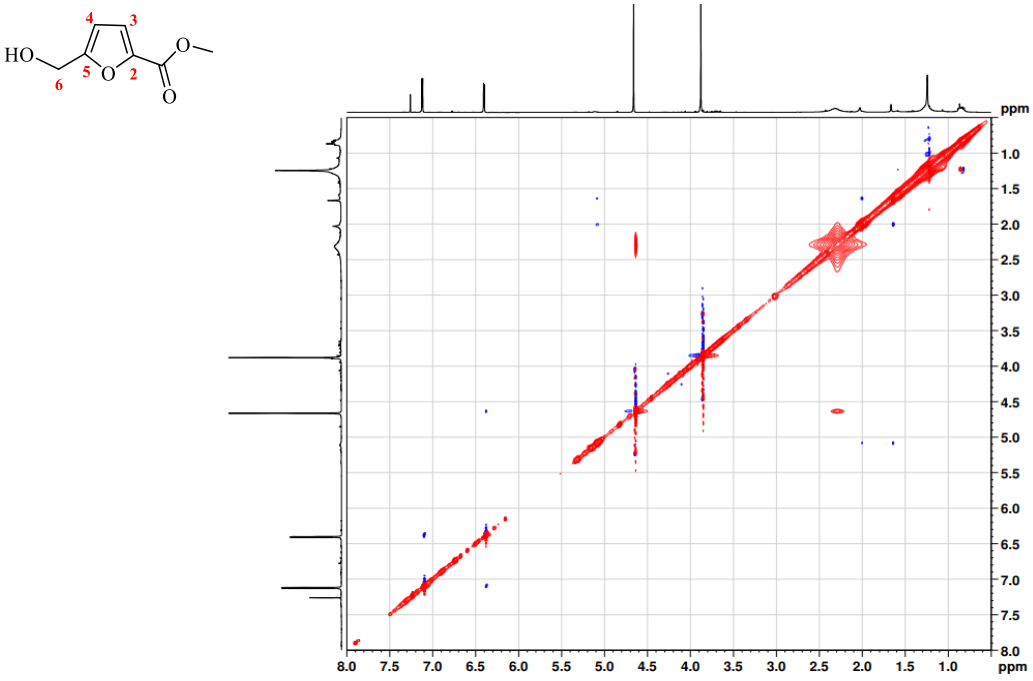

Figure A8. NOESY spectrum of compound **94** in $CDCl_3$.

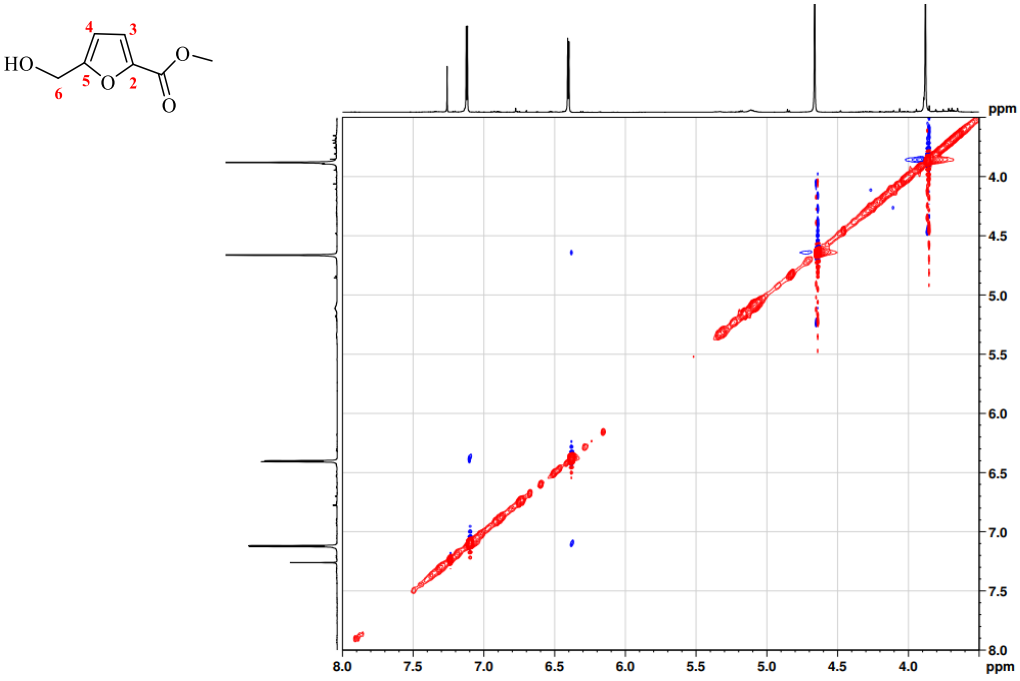

Figure A9. NOESY spectrum (expansion 1) of compound **94** in $CDCl_3$.

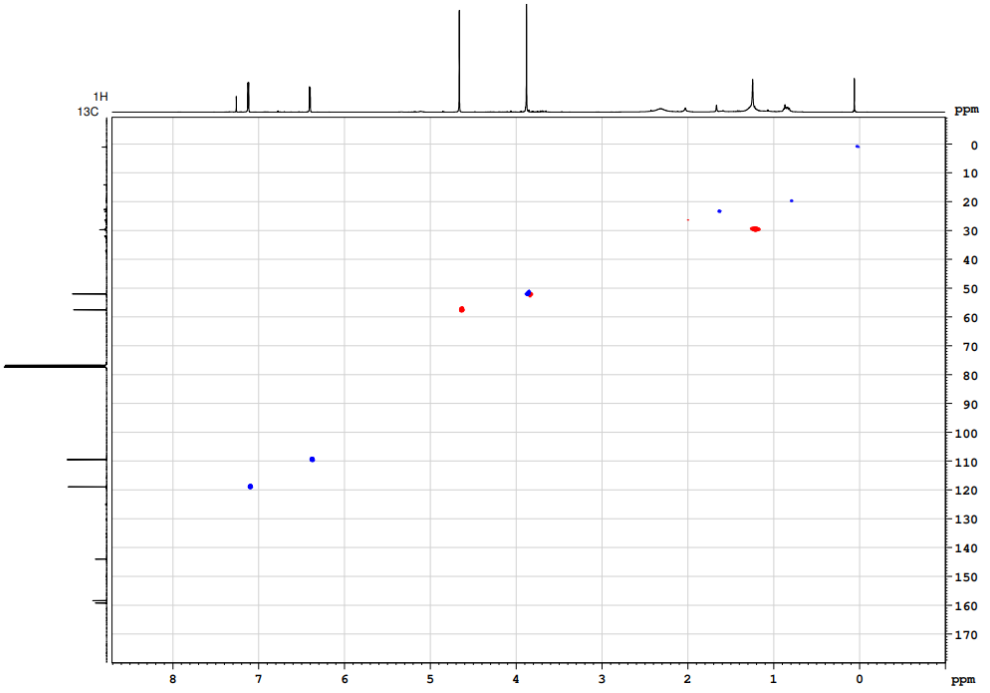

Figure A10. HSQC spectrum of compound **94** in $CDCl_3$.

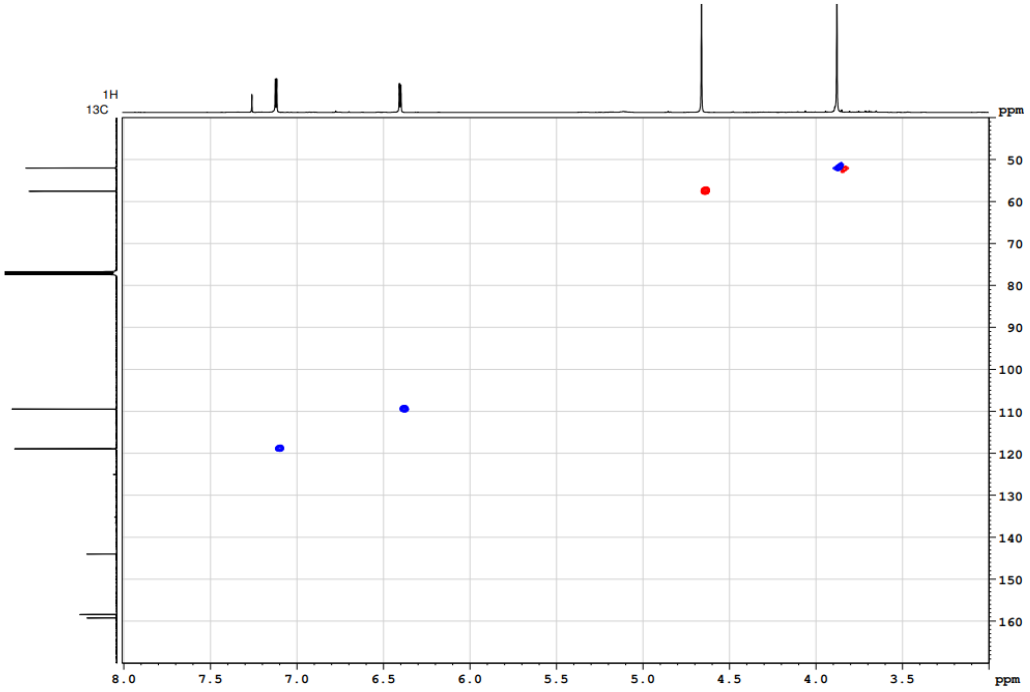

Figure A11. HSQC spectrum (expansion 1) of compound **94** in $CDCl_3$.

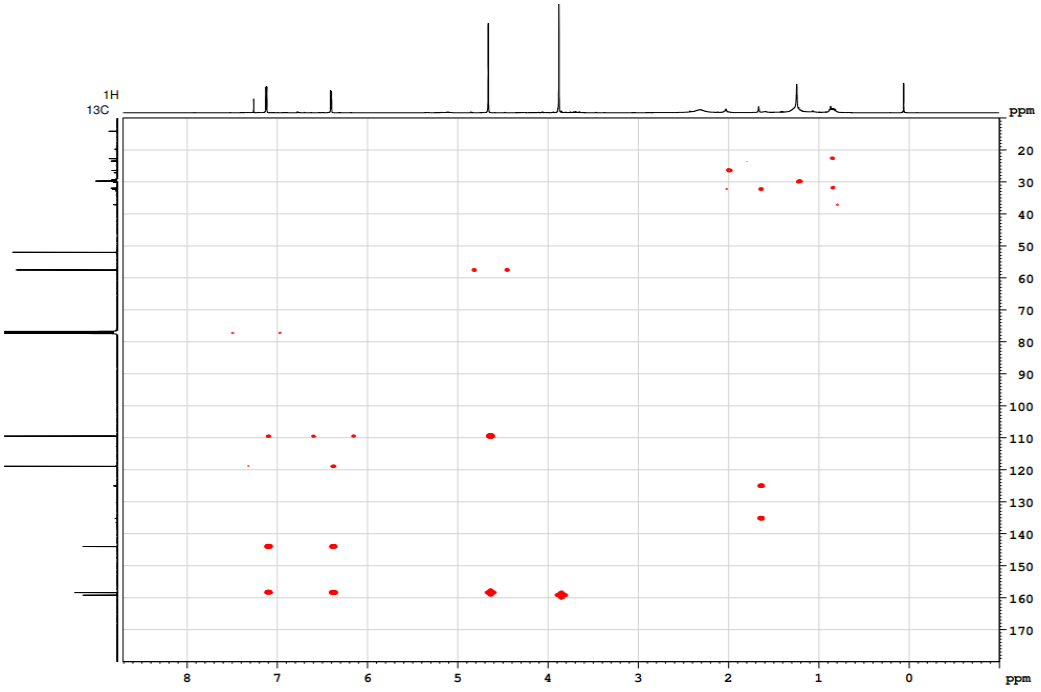

Figure A12. HMBC spectrum of compound **94** in $CDCl_3$.

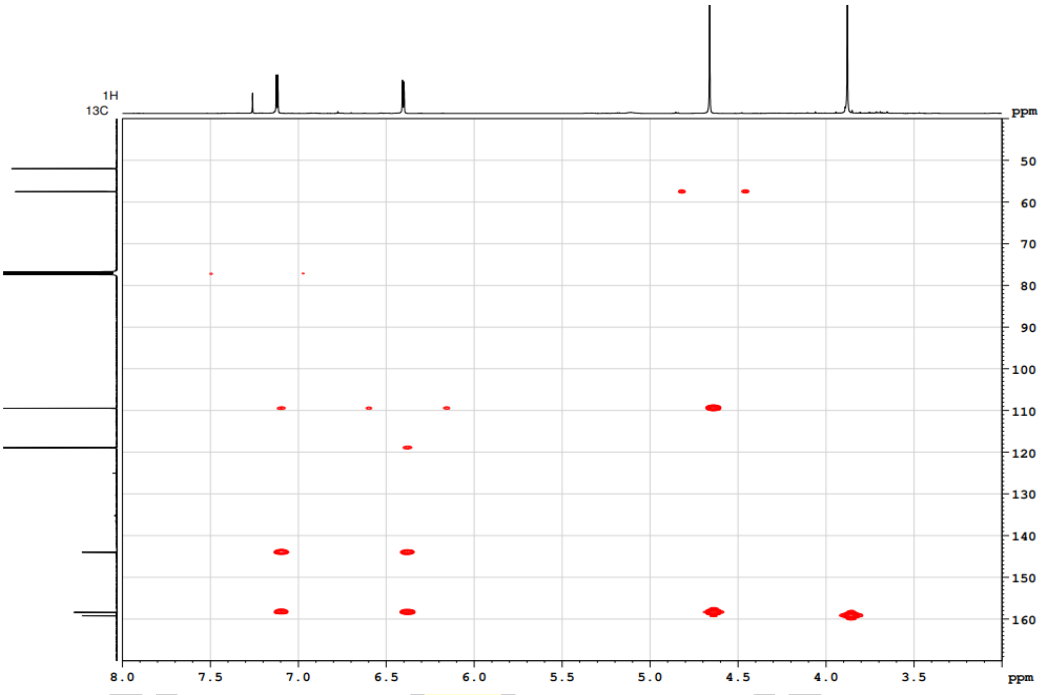

Figure A13. HMBC spectrum (expansion 1) of compound **94** in $CDCl_3$.

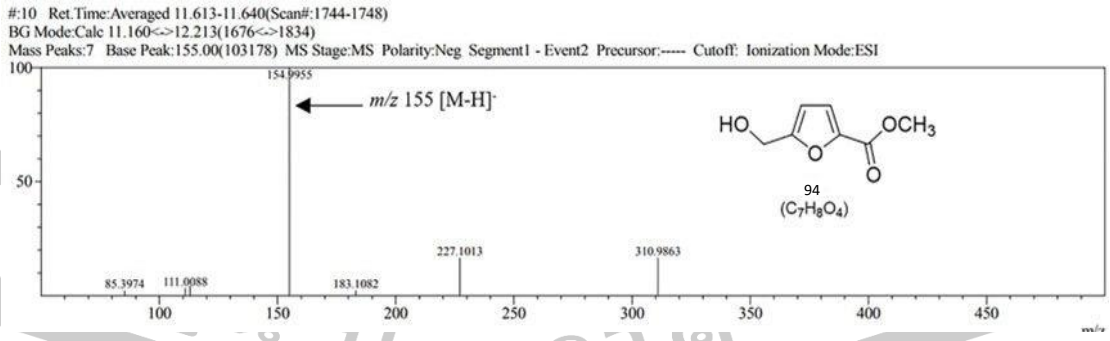

Figure A14. MS spectrum (negative mode) of compound **94**.

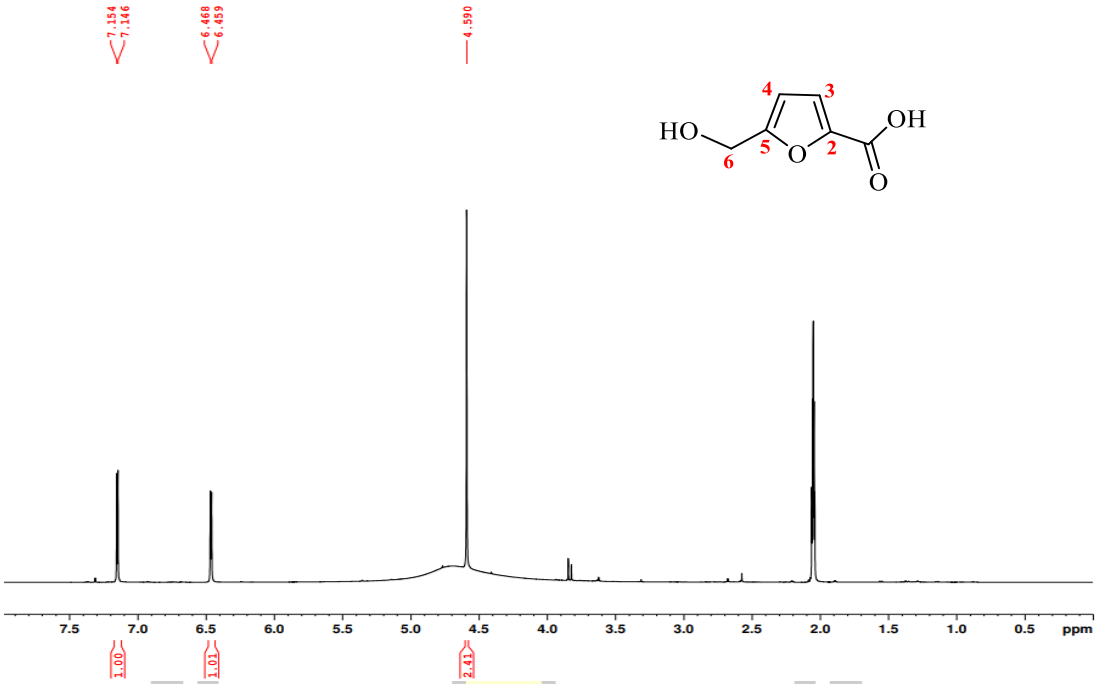

Figure A15. ^{1}H NMR of compound **95** (acetone-d_6, 400 MHz).

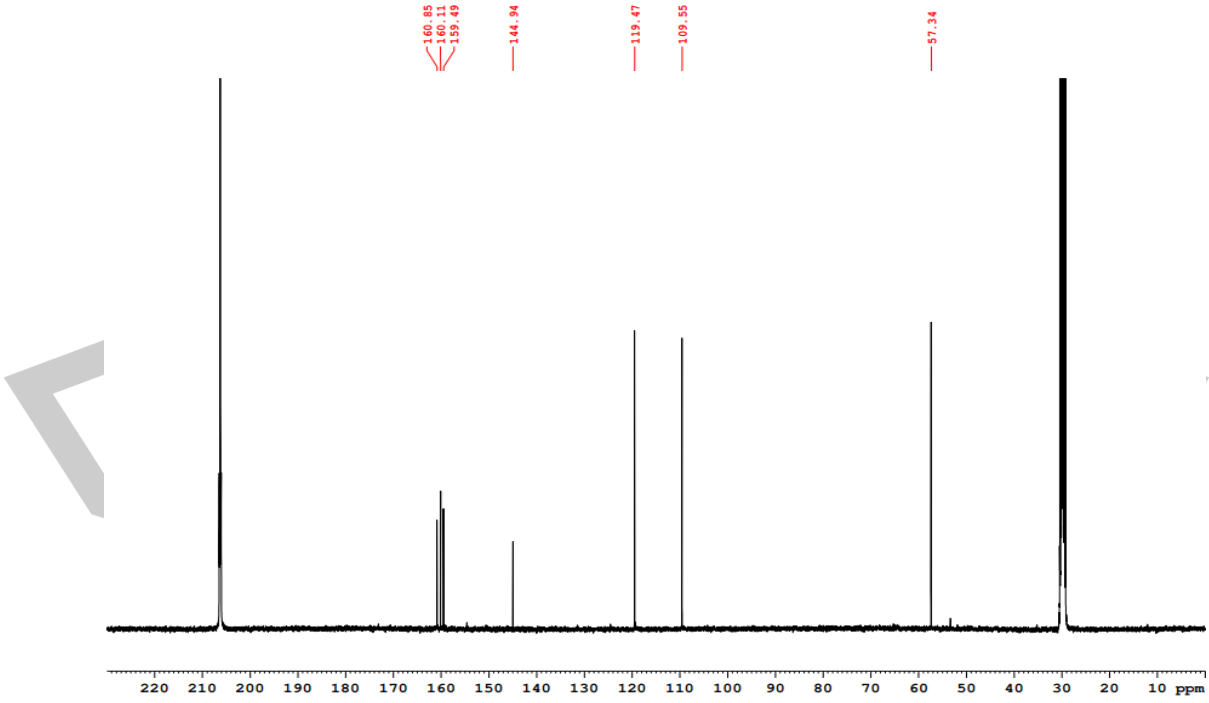

Figure A16. ^{13}C NMR of compound **95** (acetone-d_6, 100 MHz).

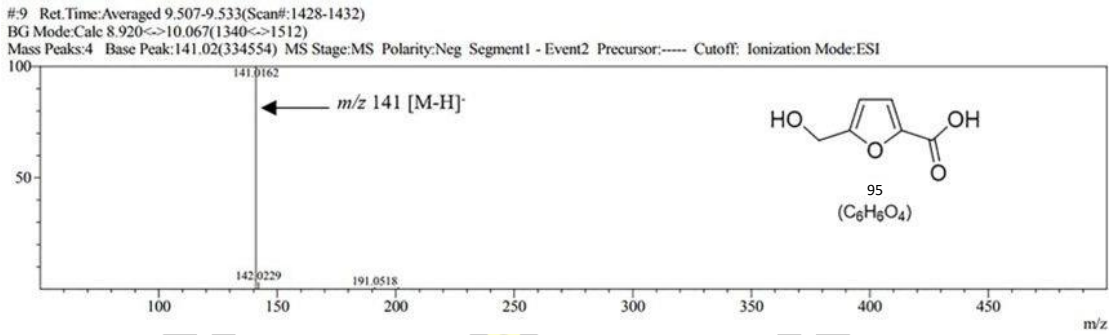

Figure A17. MS spectrum (negative mode) of compound **95**.

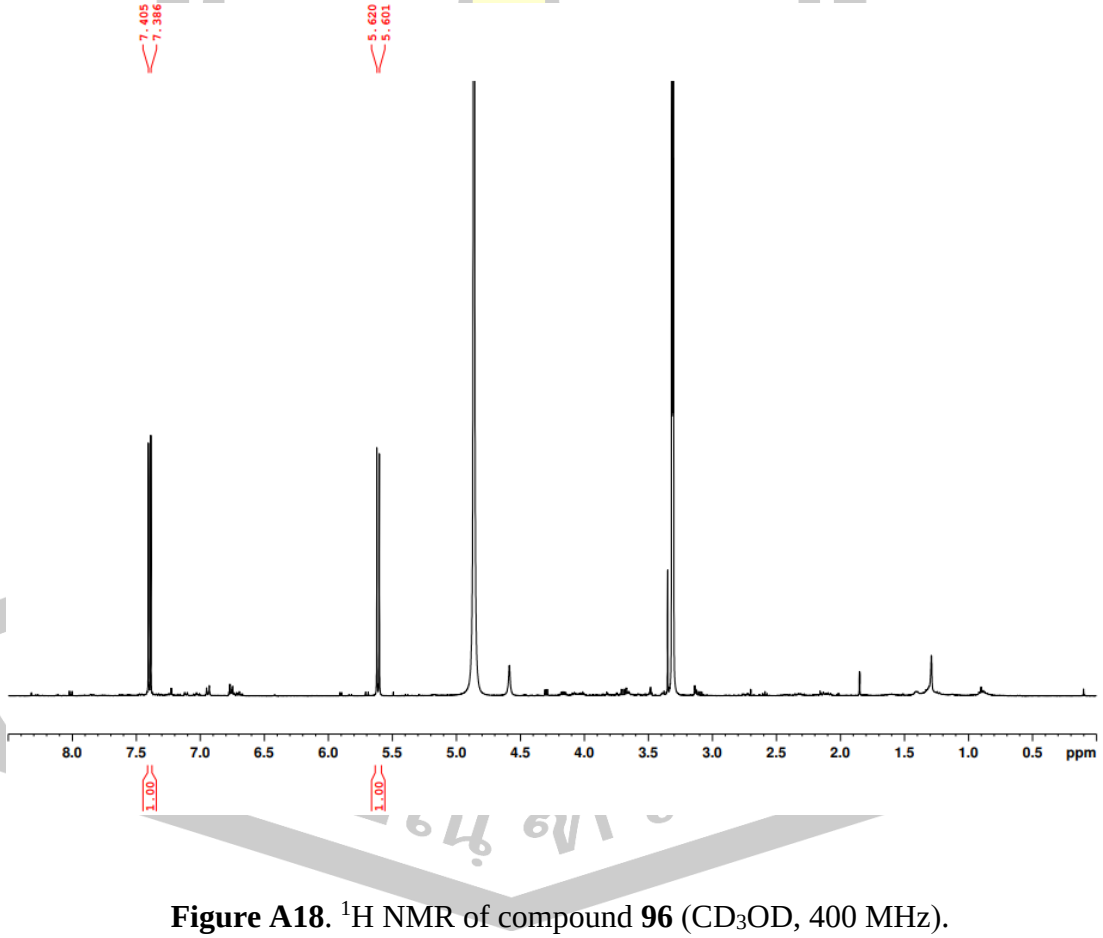

Figure A18. ^{1}H NMR of compound **96** (CD_3OD, 400 MHz).

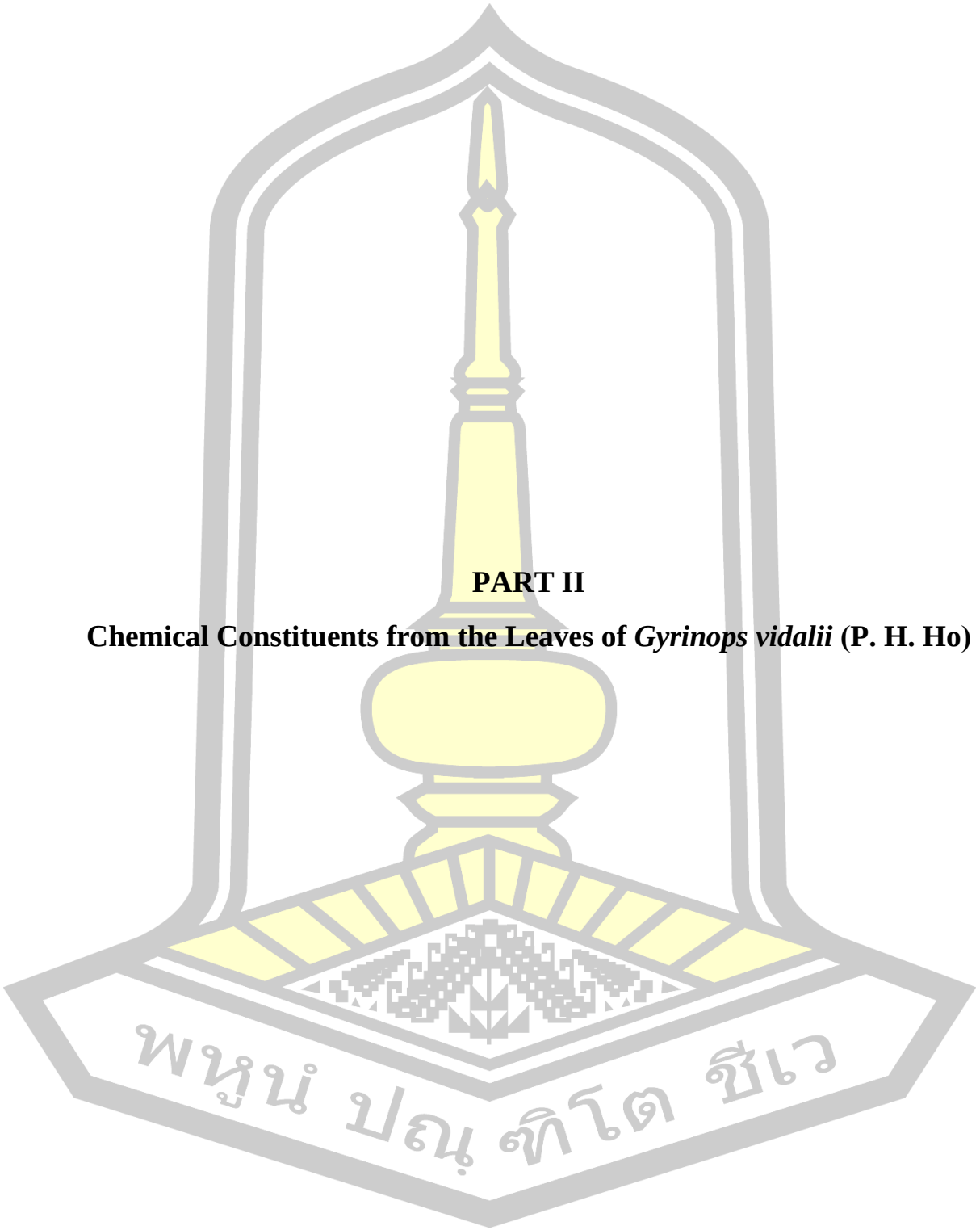

PART II

Chemical Constituents from the Leaves of *Gyrinops vidalii* (P. H. Ho)

TABLE OF CONTENTS

Page

Page

LIST OF TABLES

Table **Page**

LIST OF FIGURES

LIST OF FLOW CHARTS

LIST OF ABBREVIATIONS

A	Absorbance
br	Broad (spectral multiplicity)
brs/bs	Broad singlet (spectral multiplicity)
AChE	Acetylcholinesterase
ATR-FTIR	Attenuated Total Reflectance Fourier Transform Infrared Spectrometer
^{13}C NMR	Carbon-13 nuclear magnetic resonance spectroscopy
cm	Centimeter
δ	Chemical shift
$CHCl_3$	Chloroform
CC	Column chromatography
COSY	Correlation spectroscopy
J	Coupling constants
°C	Deegree Celsius
ATCC	Department of Medical Sciences Thailand
DMST	Department of Medical Sciences Thailand
acetone-d_6	Deuterated acetone
$CDCl_3$	Deuterated chloroform
DMSO-d_6	Deuterated dimethyl sulfoxide
CD_3OD	Deuterated methanol
DMSO	Dimethyl sulfoxide
DPPH	2,2-Diphenyl-1-picrylhydrazyl

DEPT	Distortionless enhancement by polarization transfer
d	Doublet (spectral multiplicity)
dd	Doublet of doublet (spectral multiplicity)
EtOAc	Ethyl acetate
GAE/g	Gallic acid equivalent per gram
SGC-7901	Gastric carcinoma
g	Gram
BEL-7402	Hepatocellular carcinoma
Hz	Hertz
HMBC	Heteronuclear multiple bond correlation
HSQC	Heteronuclear single quantum coherence
HPLC-MS	High-Performance Liquid chromatography-Mass Spectrometry
HRESIMS	High-resolution electrospray ionization mass
K562	Human myeloid leukemia cell line
^{1}H NMR	Hydrogen-1 nuclear magnetic resonance spectroscopy
IC_{50}	Inhibitory concentration at 50%
L	Liter
MSU	Mahasarakham University
MS	Mass
MHz	Megahertz
m	Meter
MeOH	Methanol

MRSA	Methicillin-resistant *S. aureus*
MSSA	Methicillin-susceptible *S. aureus*
MJ	Methyl jasmonate
µg/mL	Microgram/milliliter
µL	Microliter
µM	Micromolar
mg	Milligram
mg/mL	Milligrams per milliliter
mL	Milliliter
mm	Millimeters
mM	Millimolar
min	Minute
MHA	Mueller Hinton agar
MHB	Mueller Hinton broth
m	Multiplet (spectral multiplicity)
multi.	Multiplicity
nm	Nanometer
NMR	Nuclear magnetic resonance
NOESY	Nuclear overhauser effect spectroscopy
ppm	Parts per million
PNPG	*p*-Nitrophenyl-*α*-D-glucopyranoside
%	Percent
PTLC	Preparative thin-layer chromatography

q	Quartet (spectral multiplicity)
QE/g	Quercetin equivalent per gram
RSA	Radical scavenging activity
rpm,	Revolutions per minute
SA	Salicylic acid
SC_{50}	Scavenging concentration at 50%
s	Singlet (spectral multiplicity)
$NaHCO_3$	Sodium bicarbonate
SD	Standard deviation
H_2SO_4	Sulfuric acid
TLC	Thin-layer chromatography
t	Triplet (spectral multiplicity)
2D NMR	Two-dimensional nuclear magnetic resonance spectroscopy
UV-VIS	Ultraviolet-visible
U/mL	Units per milliliter
v/v	Volume per volume
H_2O	Water

CHAPTER 1

INTRODUCTION

1.1. Background

Thailand, situated in central southeastern Asia, is part of the Indo-Burmese Region, a global hotspot for biodiversity (Van Welzen et al., 2011). Thailand is an ecologically rich nation, endowed with significant variety, featuring a flora of vascular plants exceeding 11,000 species. The patterns of biodiversity vary throughout various regions of the country (Maxwell, 2004). There are approximately 15,000 known animal species and approximately 10,000 identified microorganism species (Thailand Country Study on Biodiversity, 1992). This vast diversity of organisms has historically been and remains a crucial resource for human survival (Baimai, 2010).

Plants serve as significant sources of bioactive chemicals, encompassing a vast array of diverse molecules, and have been utilized as natural medicine for ages. Plant-derived molecules are usually referred to as "phytochemicals" or "secondary metabolites." Although these chemicals are not essential for the growth and performance of fundamental life processes, they exhibit several biological features (Kennedy and Wightman, 2011; Newman and Cragg, 2016). Plant bioactive compounds are crucial for human health owing to their diverse biological effects, including antioxidant, anticarcinogenic, antiallergenic, anti-inflammatory, antimutagenic, and antimicrobial activities, which can positively influence various noncommunicable diseases, such as autoimmune, inflammatory, cardiovascular,

cancer, metabolic, and neurodegenerative disorders. Identifying these components and elucidating their advantageous health impacts are highly sought-after pursuits in scientific research. The examination of natural sources for new physiologically active metabolites has been a crucial component of various drug discovery initiatives (Dincheva et al., 2023).

The genus *Gyrinops* is a tropical evergreen tree commonly grown in the lowland forest regions and mainly distributed in Southeast Asia. It is one of the genus of the Thymelaeaceae family which is classified as agarwood-producing genera similar to *Aquilaria* (Compton and Zich, 2002), a closely related genus. Hou (1960) distinguished the two species based on a single morphological trait, the quantity of stamens. *Gyrinops* contains five stamens, whereas *Aquilaria* displays double that number (Eurlings and Gravendeel, 2005). In Chinese medicine, *Aquilaria* and *Gyrinops* have been widely used as sedative, analgesic, and digestive activities (China Pharmacopoeia Editorial Board, 2010) as well as incense for religious ceremonies and perfume material for aromatherapy in southeast Asian countries and middle East (Persoon and Van Beek, 2008; Ito, 2008). Among nine species of *Gyrinops*, *G. vidalii* P. H. Ho (Thai name "Gritsanah Noi") is only species found specifically in Thailand and Lao People's Democratic Republic (Lee and Mohamed, 2016; Lee et al., 2018; Lee et al., 2022; Li et al., 2023). *G. vidalii* was first collected from the area of Nongkhai Province (opposite to Pak Sane, Laos), northeastern Thailand, in 1997 and later identified (Maxwell, 2000). Previous study of chemical constituents from this genus led to the isolation of triterpenoids from *G. walla* (Schun et al., 1986; Munasinghe et al., 2021), sesquiterpenoids and chromones from *G. salicifolia* (Shao et al., 2016a; Shao et al.,

2016b; Dong et al., 2019) which some of them exhibited acetylcholinesterase (AChE) inhibitory and cytotoxic activities.

Phytochemical constituents of *Gyrinops vidalii* have never been reported. Therefore, in our continuing search for bioactive compounds from local plants and their utilizations, phytochemicals from the leaves of *G. vidalii* collected from northeastern Thailand were investigated for the first time.

1.2. Research objective

This research aims to investigate the chemical constituents from the EtOAc extract of the leaves of *Gyrinops vidalii* and to evaluate the biological activities of the leaves extract and the isolated compounds from this species.

1.3. Expected result

This research is expected to provide information on the chemical constituents of *Gyrinops vidalii* leaf extracts and their biological activities.

1.4. Scope of research

The scope of this research includes the extraction of the leaves from *Gyrinops vidalii*, purification of the ethyl acetate (EtOAc) extract, structure elucidation of the isolated pure compounds, and evaluation of the biological activities of the leaf extracts.

CHAPTER 2

LITERATURE REVIEW

2.1. *Gyrinops vidalii* P. H. Ho

Among nine species of *Gyrinops*, *G. vidalii* P. H. Ho (Gritsanah Noi) is only species found specifically in Thailand and Lao People's Democratic Republic (Lee and Mohamed, 2016; Lee et al., 2018; Lee et al., 2022; Li et al., 2023). *G. vidalii* was first collected from the area of Nongkhai Province (opposite to Pak Sane, Laos), northeastern Thailand, in 1997 and later identified (Maxwell, 2000). The morphology of this species is trees, 10–15 m tall. The inner bark is silvery fibrous. Leaves oblong or lanceolate, 4–7.5 cm long, with a long tail–like tip, 1–2 cm long. Many veins are arranged to form a border inside. Petiole is about 5 mm long. Inflorescences are umbel-like, 2–3 flowers per cluster, covered with short, soft hairs. Flower pedicels are about 5 mm long. Calyx cream, scattered with short, soft hairs. Corolla tube is about 1 cm long, divided into 5 lobes, 1.5–2 mm long, and persistent. 5 petals are attached to the mouth of the corolla tube as scale-like appendages, about 0.5 mm in size, covered with short, soft hairs. Stamens 5, opposite to the petals, sessile. Anthers lanceolate, about 1.5 mm long. Ovary 2-locular. Dry fruit, split into 2 halves, spindle-shaped, up to 3 cm long. Peduncle about 2 cm long. (Hou, 1960; Ho, 1992).

Phytochemical constituents of *Gyrinops vidalii* have never been reported. There are only a few publications on the chemical constituents of the genus *Gyrinops* published between 1985–2021.

2.2. Isolated compounds from *G. walla*

Four sesquiterpenes, γ-selinene (**1**), α-guaiene (**2**), β-caryophyllene (**3**), and α-cadinol (**4**) (**Figure 1**), were produced in calli and cell suspensions of *G. wall* (Munasinghe et al., 2021). The calli and cell suspensions were chemical and biological elicited with salicylic acid (SA) and methyl jasmonate (MJ), and the sterilized fungal homogenate (carbohydrate equivalents) of *Fusariym oxysporum*, *Phaeocremonium parasitica*, *Aspergillus niger*, *Trichoderma viride*, *Penicillium commune*, and *Lasidiplodia theobromae* fungal strains, respectively.

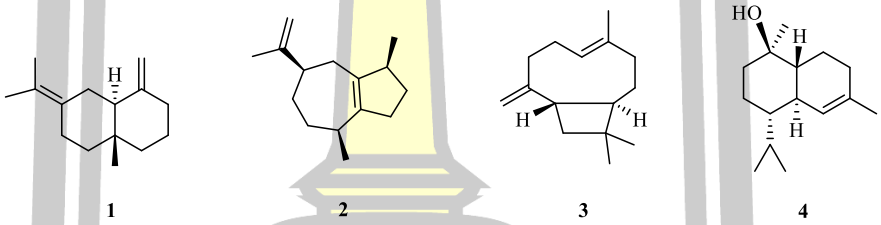

Figure 1. Structures of compounds **1**–**4**.

A new C_{32} tirucallane-type triterpene, wallenone (**5**) (**Figure 2**) was isolated from the chloroform ($CHCl_3$) extract of the leaves of *G. walla* (Schun et al., 1986).

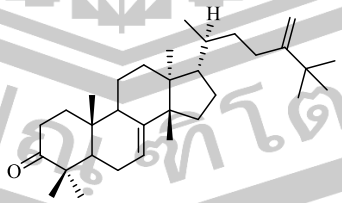

Figure 2. Structure of compound **5**.

2,6-Dimethoxybenzoquinone (**6**), cucurbitacin I (**7**), friedelan-3*β*-yl acetate (**8**), friedelin (**9**), friedelan-3*β*-ol (**10**), apigenin-7,4′-dimethyl ether (**11**), luteolin-7,3′,4′-trimethyl ether (**12**), (+)-syringaresinol (**13**), velutin (**14**), pilloin (**15**) , genkwanin (**16**), and sitoindoside I (**17**), were isolated from the $CHCl_3$ extract, when mangiferin (**18**) (**Figure 3**), a yellow precipitate, was obtained from the methanol (MeOH) extract, which was obtained by standing at room temperature, and further repeated crystallization from the MeOH from twigs and leaves of *G. walla*. The plant was collected from Sri Lanka in August 1981 (Schun and Cordell, 1985). This is the first isolation of cucurbitacin I (**7**), sitoindoside I (**17**), and mangiferin (**18**) from this plant family.

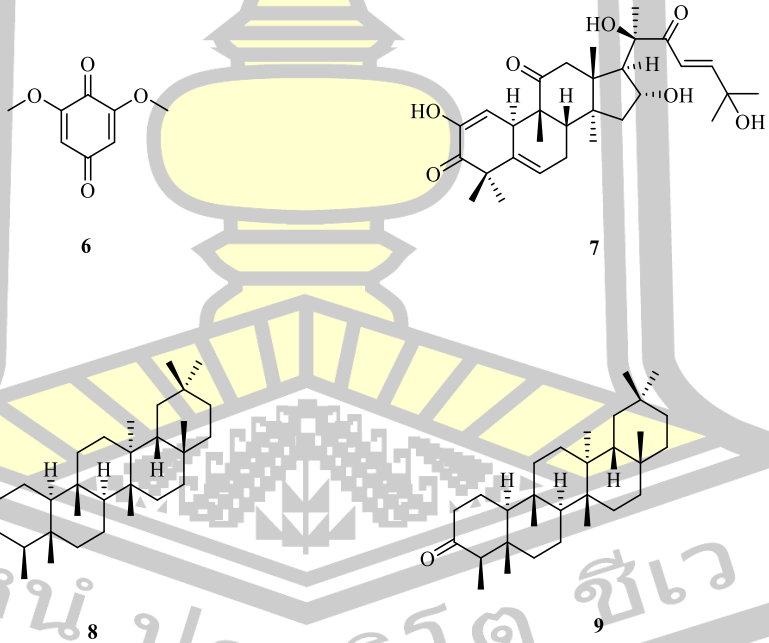

Figure 3. Structures of compounds **6**–**18**.

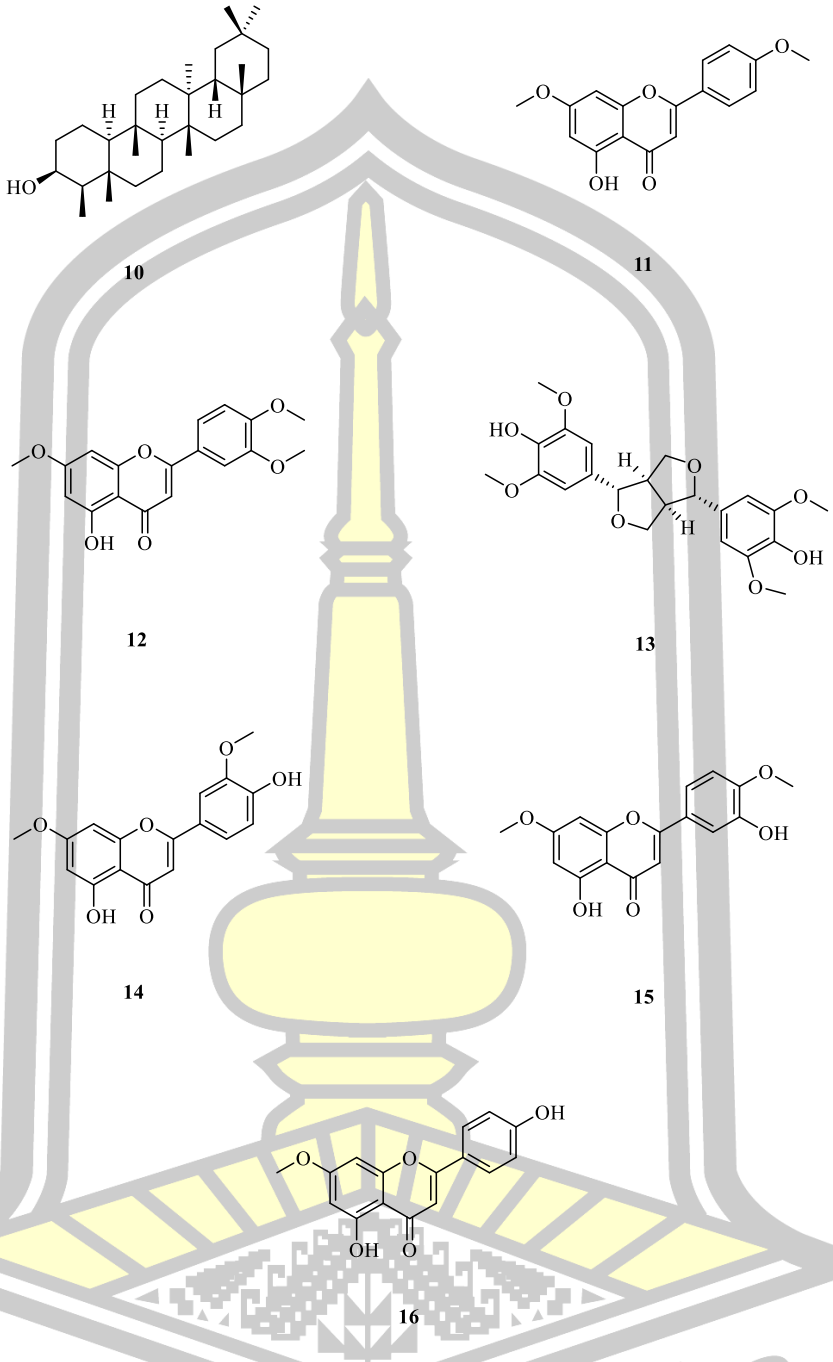

Figure 3 (continued)**.** Structures of compounds **6**–**18**.

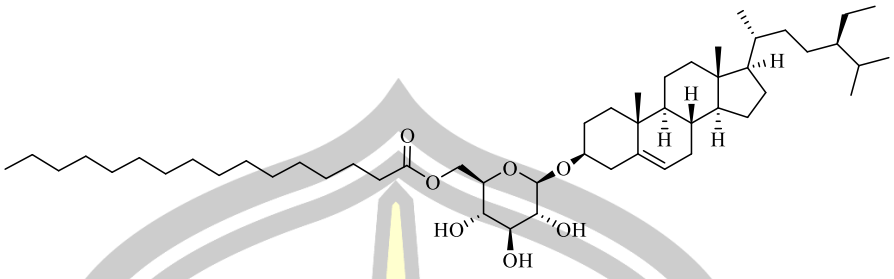

17

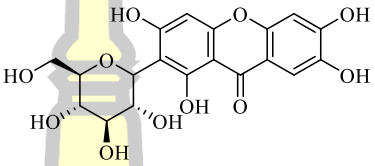

18

Figure 3 (continued)**.** Structures of compounds **6**−**18**.

2.3. Isolated compounds of agarwood from *G. salicifolia*

Two new 2-(2-phenylethyl)chromone derivatives, gyrinone A (**19**), and gyrinone B (**20**), as well as one new 2-(2-phenylethenyl)chromone, 5-hydroxy-2-[2-(3-hydroxy-4-methoxyphenyl)ethenyl]chromone (**21**) (**Figure 4**), were isolated from the ethyl acetate (EtOAc) extract of agarwood originated from *G. salicifolia* (Dong et al., 2019). The agarwood sample was collected in Papua New Guinea, then traded in Macao, one of China's special administrative regions, in December 2014. None of the compounds, showed acetylcholinesterase (AChE) inhibitory activity or cytotoxicity against human myeloid leukemia cell line (K562).

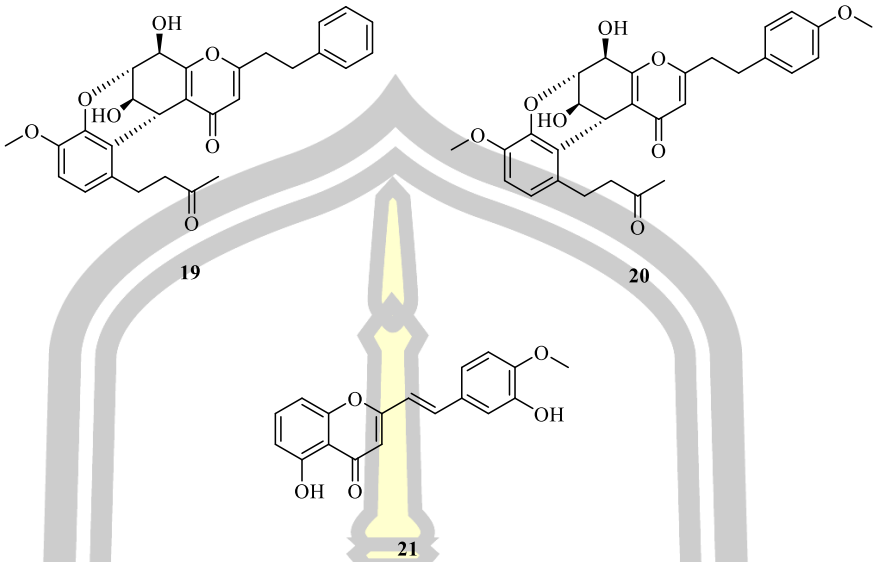

Figure 4. Structures of compounds **19**–**21**.

Three new 2-(2-phenylethyl)chromone derivatives, 6,7-dihydroxy-2-(2-phenylethyl)chromone (**22**), 6-hydroxy-7-methoxy-2-[2-(4-methoxyphenyl)ethyl]chromone (**23**), and 5,8-dihydroxy-2-[2-(3-hydroxy-4-methoxyphenyl)ethyl]chromone (**24**), and a new 2-(2-phenylethenyl)chromone derivative, 5-hydroxy-2-[2-(4-methoxyphenyl)ethenyl]chromone (**25**), together with two known 2-(2-phenylethyl)chromone derivatives, 6,7-dihydroxy-2-chromone (**26**) and 6-hydroxy-2-[2-(4-hydroxyphenyl)ethyl]chromone (**27**) (**Figure 5**), were isolated from the EtOAc extract of agarwood originated from *G. salicifolia* (Shao et al., 2016). The plant material was collected in Papua New Guinea, then traded in Macao, China's special administrative regions, in December 2014. Compounds **22**, **23**, and **26**, showed moderate cytotoxicity against K562, hepatocellular carcinoma (BEL-7402), and gastric carcinoma (SGC-7901) cell lines with IC_{50} values of 5.76 to 20.1 μM.

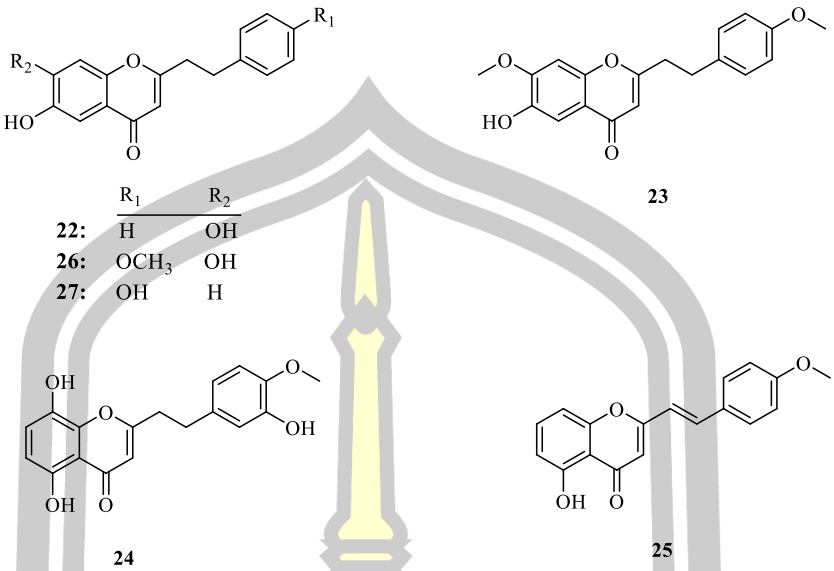

Figure 5. Structures of compounds **22**–**27**.

Six new sesquiterpenoids, 4*β*,7*α*-*H*-eremophil-9(10)-ene-12,13-diol (**28**), 4*β*, 7*α*-*H*-eremophil-9(10)-ene-11,12,13-triol (**29**), 4*β*,7*α*-*H*-eremophil-1(2),9(10)-dien-11,12,13-triol (**30**), 4*β*,7*α*,8*α*-*H*-eremophil-9(10)-ene-8,12-epoxy-11*α*,13-diol (**31**), 4*β*,7*α*-*H*-11,13-dihydroxy-eremophil-1(10)-ene-11-methyl ester (**32**), and 4*β*,5*α*,7*α*,8*α*-*H*-3*β*-hydroxy-1(10)-ene-8,12-epoxy-guaia-12-one (**33**), as well as six known sesquiterpenoids, eremophil-9(10)-ene-11,12-diol (**34**), (+)-trans-nootkatol (**35**), 12,15-dioxo-*α*-selinen (**36**), guaianolide (**37**), (−)-gweicurculactone (**38**), and 2-oxoguaia-1(10),3,5,7(11),8-pentaen-12,8-olide (**39**) (**Figure 6**), were isolated from the EtOAc extract of agarwood originated from *G. salicifolia* (Shao et al., 2016). The plant material was collected in Papua New Guinea, then traded in Macao, China, in December 2014. Compounds **28**, **33**, **38,** and **39**, displayed moderate inhibitory activity against AChE with an inhibition percentage of 33.3%, 35.3%, 46.2%, and 54.2%, respectively (at 50 μg/mL). Compounds **32**, **35**–**37**, showed weak inhibitory activity

against AChE with an inhibition percentage of 11.2%, 20.9%, 11.4%, and 21.1%, respectively. Compounds **29**–**31** and **34** were inactive.

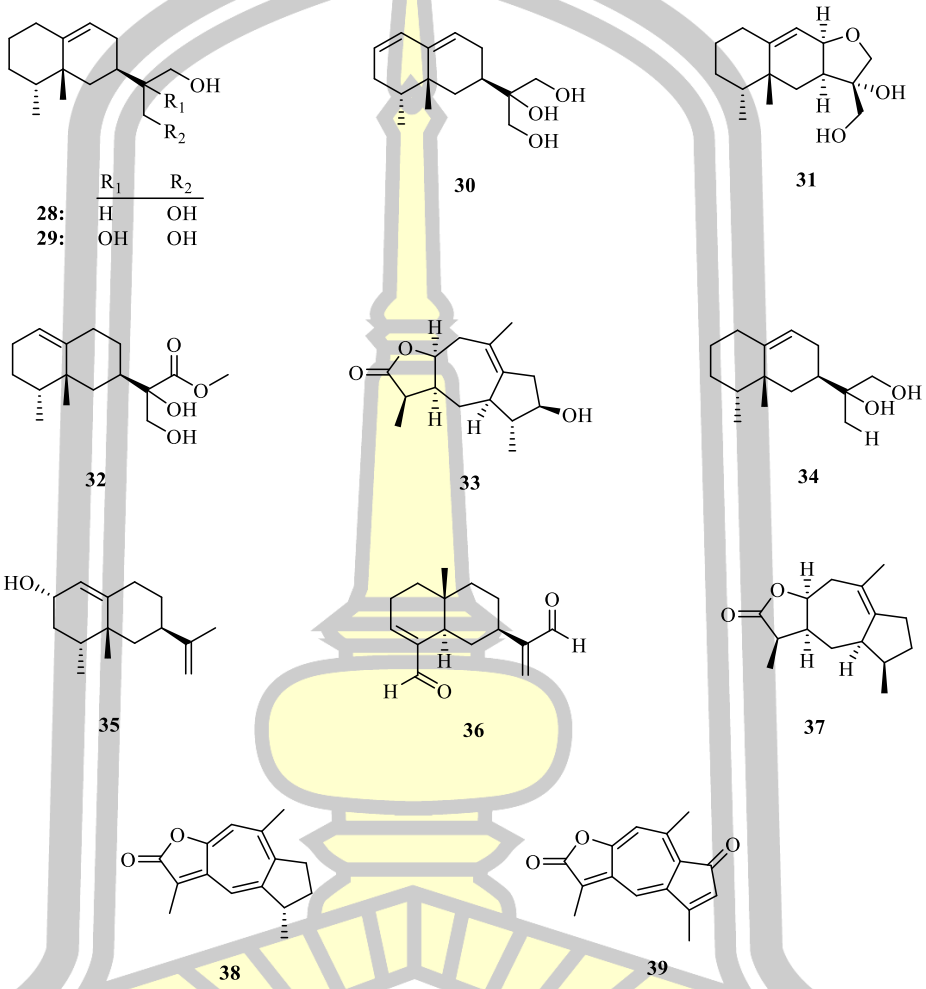

Figure 6. Structures of compounds **28**–**39**.

CHAPTER 3

MATERIALS AND METHODS

3.1. General experimental procedure

Nuclear magnetic resonance (NMR) spectra (^{1}H NMR 400 MHz, ^{13}C NMR 100 MHz) were recorded on a Bruker Ascend-400 (Prodigy unit) with deuterated solvents; deuterated chloroform ($CDCl_3$) (δ_H 7.26/δ_C 77.0 ppm) (ZEOtope, Zeochem AG, Rüti, Switzerland), deuterated acetone (acetone-d_6) (δ_H 2.05/δ_C 29.8 ppm) (Merck, Darmstadt, Germany), deuterated methanol (CD_3OD) (δ_H 3.31/δ_C 49.0 ppm) (Eurisotop, France, Switzerland), and deuterated dimethyl sulfoxide (DMSO-d_6) (δ_H 2.50/δ_C 39.5 ppm) (Cambridge Isotope Laboratories, MA, USA). High-resolution electrospray ionization mass (HRESIMS) spectrum was recorded on a ThermoFinnigan MAT 95 XL spectrometer. The mass (MS) spectrum was recorded on a LC-ESI-QTOF 6540 (Agilent Technologies, Singapore) coupled with an Agilent 1260 infinity Series HPLC system (Agilent, Waldbronn, Germany). Infrared spectra were recorded on an Attenuated Total Reflectance Fourier Transform Infrared Spectrometer (ATR-FTIR) (ATR-FTIR Bruker, INVENIO–S) at the Scientific Instrument Academic Service Unit. Column chromatography (CC) was performed using silica gel 60 (Merck, Darmstadt, Germany), silica gel 60H (Merck, Darmstadt, Germany), and Sephadex LH-20 (Sigma Aldrich, St. Louis, MO, USA). Pre-coated silica gel 60 F_{254} on Aluminium sheets (Merck, Darmstadt, Germany) were used for analytical thin-layer chromatography (TLC).

3.2. Plant material

The leaves of *Gyrinops vidalii* (**Figure 7**) were collected from Bueng Kan Province, northeastern Thailand, on 8 May, 2023. The plant materials were authenticated by Asst. Prof. Pasakorn Bunchalee. A voucher specimen (N.TAESUK 001) was deposited at the Department of Biology, Faculty of Science, Mahasarakham University (MSU).

Figure 7. The collection of the leaves of *G. vidalii* at Bueng Kan Province.

3.3. Extraction

Fresh leaves of *G. vidalii* were roughly cut and dried in the oven at 55 °C and the dried leaves (280 g) were extracted in MeOH (10 L, 2 days, room temperature). Through filtration (cotton sheet), the filtrate was concentrated under reduced pressure until ~1 L remaining and left overnight in a round bottom flask at room temperature. Later, the sediment at the bottom of the flask was separated by filtration (Whatman No. 1). The collected sediment was then triturated in hexane, EtOAc, and then MeOH to obtain compound **18** (pale-yellow powder; 4.68 g). The filtrate was concentrated and the residue was suspended in water (H_2O) (500 mL) and further partitioned with hexane (1 L × 2) and EtOAc (1 L × 3) respectively. The EtOAc layer was evaporated until ~500 mL remaining and standing overnight at the room temperature before filtration to separate between the sediment and EtOAc soluble part. The sediment was triturated in EtOAc (~20 mL) and then MeOH (~20 mL × 2) to get **18** (pale-yellow powder; 323.7 mg) while the collected the hexane and EtOAc layers were concentrated to obtained the hexane (10.30 g) and EtOAc (4.48 g) extracts (**Flow chart 1**).

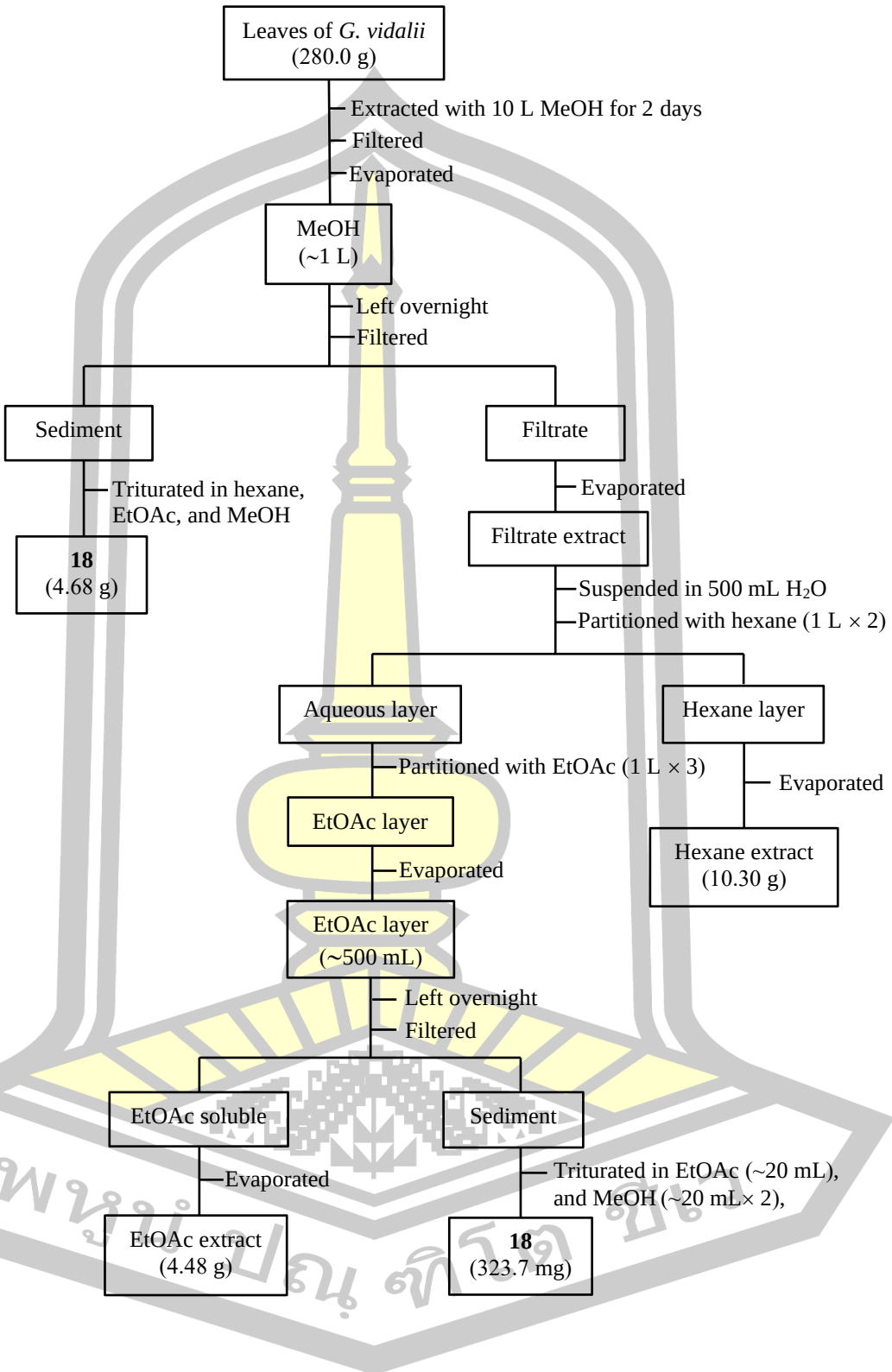

Flow chart 1. The extraction of the leaves of *G. vidalii*.

3.4. Isolation

From the ^{1}H NMR spectrum of the EtOAc extract in CD_3OD (**Figure A2**), signals corresponding to a major compound containing aromatic and sugar moiety protons were observed. The EtOAc extract (4.48 g) was then subjected to purify by silica gel column chromatography (CC) (4.5 × 31 cm) (**Figure 8**) using hexane–EtOAc (8:2 to 0:10) and then EtOAc–MeOH (9:1 to 0:10) as eluent to afford thirteen fractions (Fr.1 to Fr.13).

Fr. 2 (13.1 mg) was separated by Sephadex LH-20 CC (1.5 × 17 cm, 100% MeOH) to yield compounds **44** (green amorphous solid; 6.4 mg) and **43** (yellow amorphous solid; 1.3 mg).

Fr.3 (72.4 mg) was subjected to silica gel CC (1.5 × 18.3 cm, hexane–EtOAc 100:0 to 0:100 followed by EtOAc–MeOH 90:10 to 0:100) and further purified by preparative thin-layer chromatography (PTLC) (6.0 × 20 cm, Hexane–EtOAc 60:40) to afford compound **B** (light-brown powder; 1.0 mg).

Fr.4 (18.5 mg) was subjected to silica gel CC (1.5 × 16 cm, hexane–EtOAc 10:0 to 0:100, and then with EtOAc–MeOH 90:10 to 30:70) to afford Fr.4A and compound **B** (light-brown powder; 1.0 mg). Fr.4A (4.7 mg) was separated by PTLC (6.0 × 20 cm, hexane–EtOAc 40:60) to yield compound **C** (light-yellow oil; 3.1 mg).

Fr.5 (5.3 mg) was purified by PTLC (6.0 × 20 cm, Hexane–Acetone 60:40) to give compound **C** (light-yellow oil; 1.5 mg).

Fr.8 (64.0 mg) was purified by silica gel CC (1.5 × 18.5 cm, hexane–EtOAc 80:20 to 0:100, and then with EtOAc–MeOH 80:20 to 0:100) to obtain Fr.8A (28.8 mg) which was subjected to silica gel CC (1.5 × 19.5 cm, hexane–EtOAc 80:20 to 0:10, and then with EtOAc–MeOH 90:10 to 60:40) to provide two subfractions Fr.8A-1 and Fr.8A-2. Fr. 8A-1 (22.4 mg) was purified by Sephadex LH-20 CC (100% MeOH) to afford compounds **B** (light-brown powder; 3.5 mg) and **42** (light-yellow oil; 4.0 mg). Fr.8A-2 (6.0 mg) was purified by Sephadex LH-20 CC (100% MeOH) to yield compound **B** (light-brown powder; 4.4 mg).

A combined Fr.10 and Fr.11 (216.5 mg) was washed with EtOAc to give compound **40** (light-yellow crystal; 129.2 mg) and a filtrate fraction (Fr.11A). Fr.11A (87.3 mg) was separated by a silica gel CC (1.5 × 19.3 cm, hexane–EtOAc 60:40 to 0:100 followed by EtOAc–MeOH 80:20 to 0:100) to obtain two subfractions Fr.11A-1 and Fr.11A-2. Both two fractions, Fr.11A-1 (13.0 mg) and Fr.11A-2 (37.0 mg), were further purified by silica gel CC eluted with step gradient elution as the same manner described above to afford compound **40** (light-yellow crystal; 1.0 mg) and **40** (light yellow crystal; 16.5 mg), from Fr.11A-1 and Fr.11A-2 respectively.

Fr.12 (2.61 g) was fractionated by silica gel CC (4.5 × 28.5 cm, hexane–EtOAc 60:40 to 0:100, and then with EtOAc–MeOH 80:20 to 0:100) to provide compound **40** (light-yellow crystal; 22.0 mg) and two fractions Fr.12B and Fr.12C. Fr.12B (1.06 g) was purified over a silica gel CC (3.0 × 26.0 cm, hexane–EtOAc 80:20 to 0:100, and then with EtOAc–MeOH 80:20 to 0:100) to obtain two subfractions Fr.12B-1 and Fr.12B-2. Fr.12B-1(38.0 mg) was purified by silica gel CC (1.5 × 16.8 cm,

hexane–EtOAc 60:40 to 0:100, and then with EtOAc–MeOH 90:10 to 0:100) to give compounds **40** (light yellow crystal; 9.6 mg), **41** (light-brown solid; 9.7 mg), compound **41** (light- brown solid; 8.6 mg), and a subfraction Fr.12B-1-3. Fr.12B-1-3 (7.6 mg) was purified by PTLC (7 × 20 cm, hexane-EtOAc 20:80) to afford compound **40** (light-yellow crystal; 1.2 mg).

Fr.12B-2 (770.8 mg) was purified by silica gel CC (3 × 25 cm, hexane-EtOAc 90:10 to 0:100, and then with EtOAc-MeOH 80:10 to 20:80) to provide three subfractions Fr. 12 B-2-1, Fr.12B-2-2 and Fr.12B-2-3. Fr.12B-2-1 (58.6 mg) was purified over silica gel (1.5 × 18.5 cm, hexane-EtOAc 40:60 to 0:100, and then with EtOAc-MeOH 90:10 to 0:100) to afford compounds **40** (light-yellow crystal; 1.8 mg) and **41** (light-brown solid;13.1 mg). Fr.12B-2-2 (623.2 mg) was purified by Sephadex LH-20 CC (100% MeOH) to yield compound **41** (light-brown solid; 505.3 mg). Fr.12B-2-3 (65.9 mg) was purified by silica gel CC (hexane-EtOAc 40:60 to 0:100, and then with EtOAc–MeOH 90:10 to 0:100) to obtain compound **41** (light-brown solid; 11.2 mg) and a subfraction Fr.12B-2-3-2, which was further purified by silica gel CC to yield **41** (light-brown solid; 4.5 mg).

Fr.12C (1.25 g) was purified over silica gel CC (3.5 × 24.5 cm, hexane–EtOAc 20:80 to 0:100, and then with EtOAc–MeOH 95:5 to 0:100) to give compound **41** (light-brown solid; 83.7 mg) and a fraction Fr.12C-2. Fr.12C-2 (765.9 mg) was purified by Sephadex LH-20 CC (100% MeOH) and further purified by silica gel CC (3 × 23.4 cm, hexane−EtOAc 10:10 to 0:10, and then with EtOAc−MeOH 90:10 to 0:10) to obtain three fractions Fr.12C-2-1, Fr.12C-2-2 and Fr.12C-2-3. Fr.12C-2-1 (16.3 mg) was

purified by Sephadex LH-20 CC (100% MeOH) to yield compound **B** (light-brown powder; 3.5 mg). Fr.12C-2-2 (171.1 mg) was subjected to CC silica gel to provide two fractions Fr.12C-2-2-1 and Fr.12C-2-2-2. Fr.12C-2-2-1 (7.2 mg) was purified by PTLC (6.0 × 10 cm, EtOAc–MeOH 90:10) and purified by silica gel CC to afford compound **41** (light-brown solid; 1.9 mg). Fr.12C-2-2-2 (159.7 mg) was purified by Sephadex LH-20 CC to yield compound **A** (dark-orange solid; 15.9 mg). Fr.12C-2-3 (582.2 mg) was purified over silica gel (1.5 × 18.5 cm, hexane–EtOAc 40:60 to 0:100 followed by EtOAc–MeOH 90:10 to 0:100) to obtain two fractions Fr.12C-2-3-1 and Fr.12C-2-3-2. Fr.12C-2-3-1 (103.5 mg) was purified by silica gel CC to give compound **A** (dark-orange solid; 8.1 mg). Fr.12C-2-3-2 (252.6 mg) was purified by silica gel CC to yield compound **A** (dark-orange solid; 10.5 mg) (**Flow chart 2**).

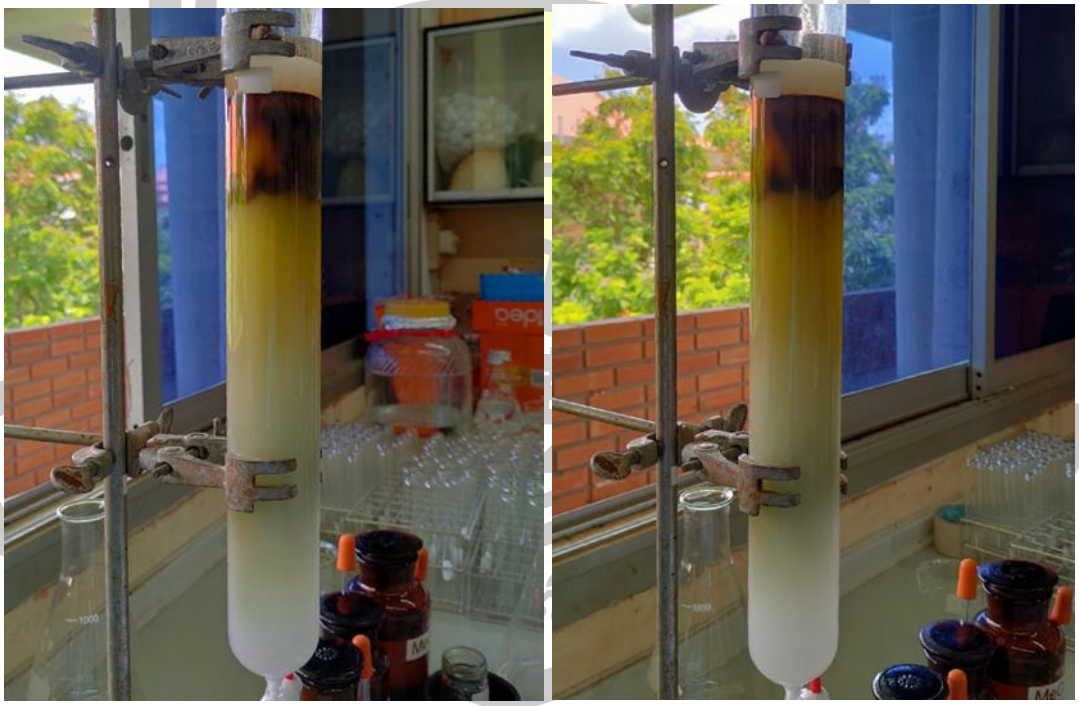

Figure 8. The isolation of the EtOAc extract of *G. vidalii* by column chromatography.

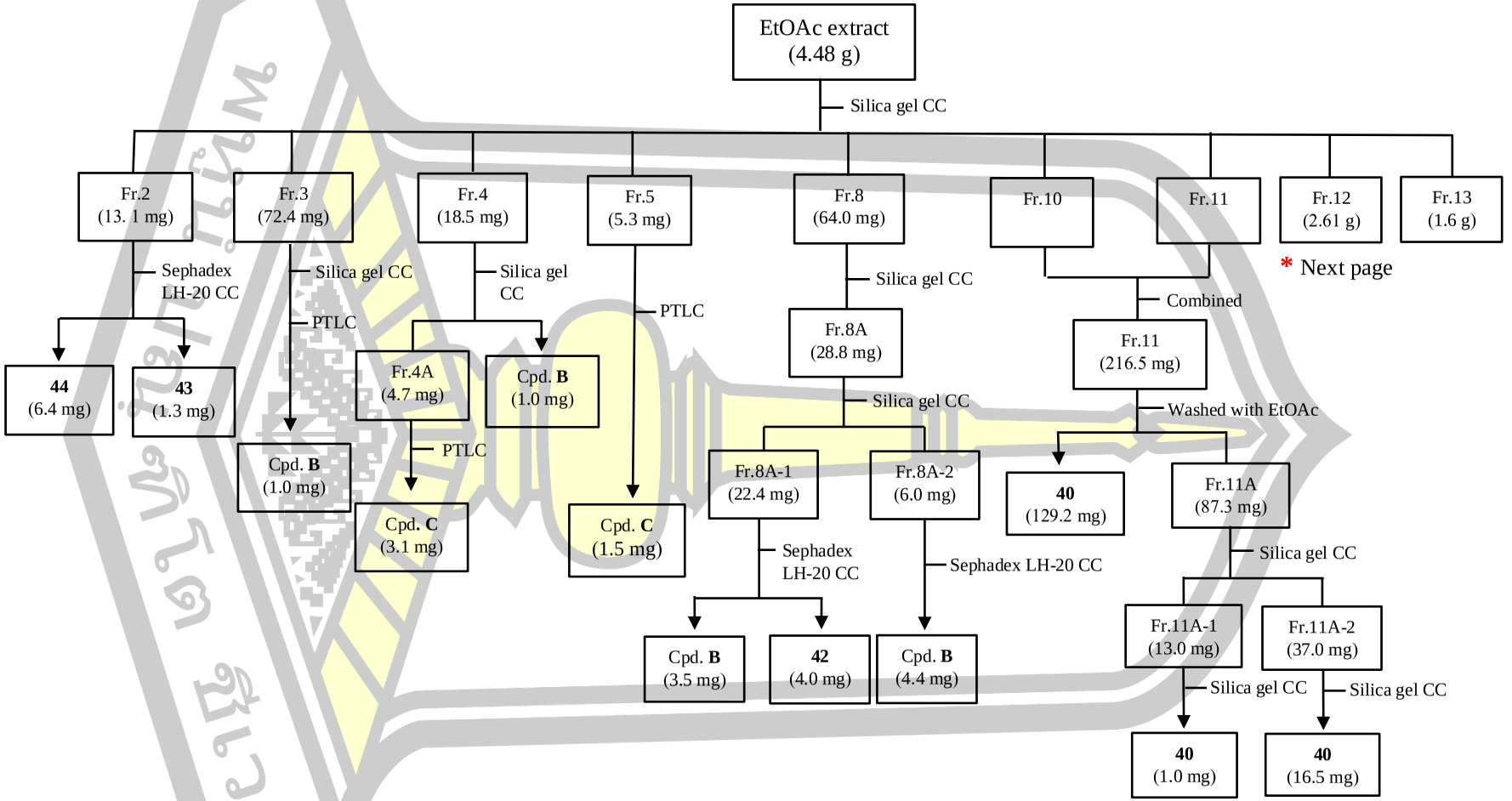

Flow chart 2. The isolation of the EtOAc extract from the leaves of *G. vidalii*.

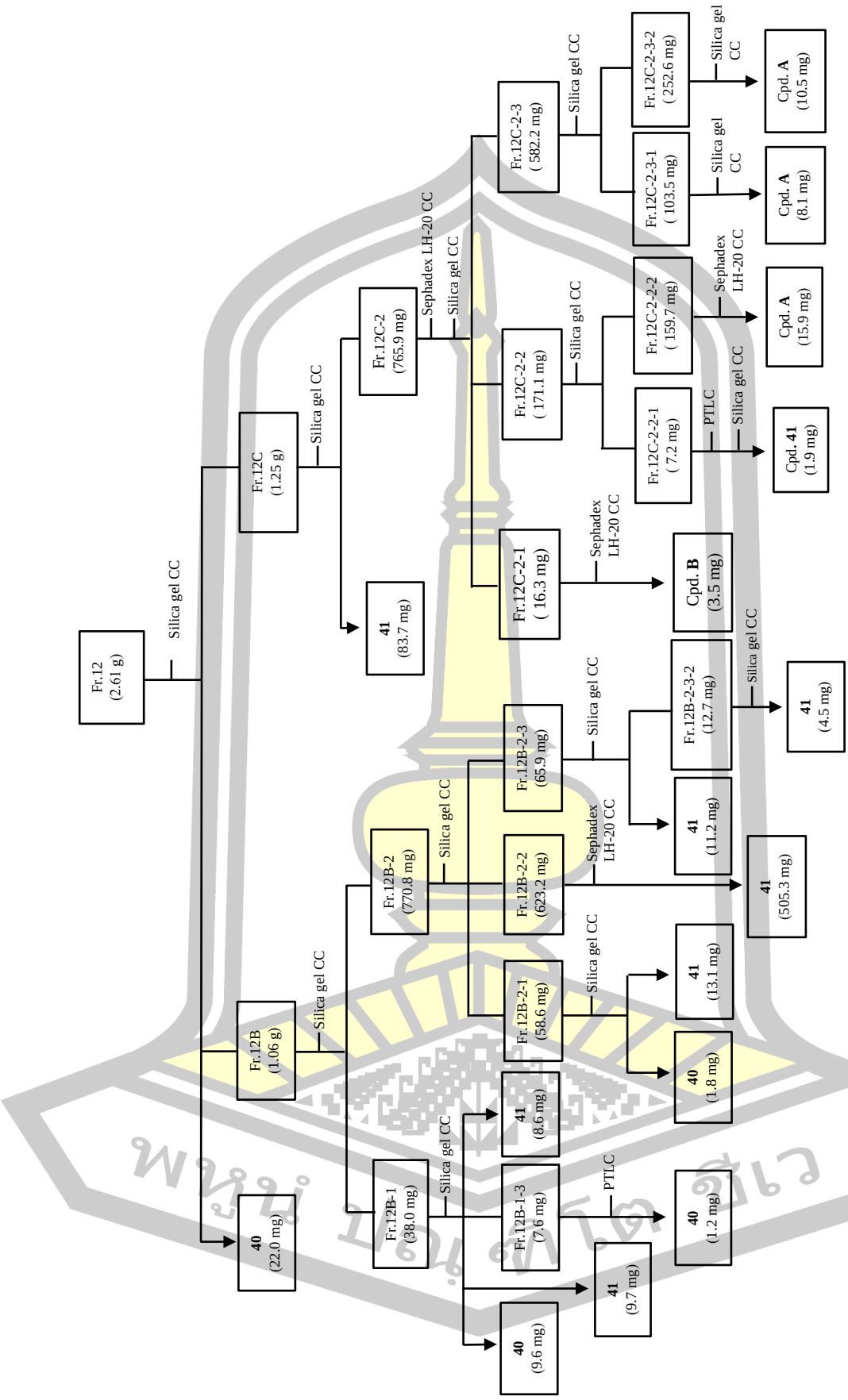

Flow chart 2 (continued). The isolation of the EtOAc extract from the leaves of *G. vidalii*.

3.5. Acid hydrolysis of 40

Compound **40** (7.6 mg) was dissolved in 10% sulfuric acid (H_2SO_4) (1.5 mL) and heated at 95 °C in the oil bath for 1 h. After cooling to room temperature, the reaction was neutralized with sodium bicarbonate ($NaHCO_3$) and extracted with EtOAc (1.0 mL × 3). The organic layer was concentrated to get compound **40a** (5.7 mg; 75%) (**Flow chart 3**).

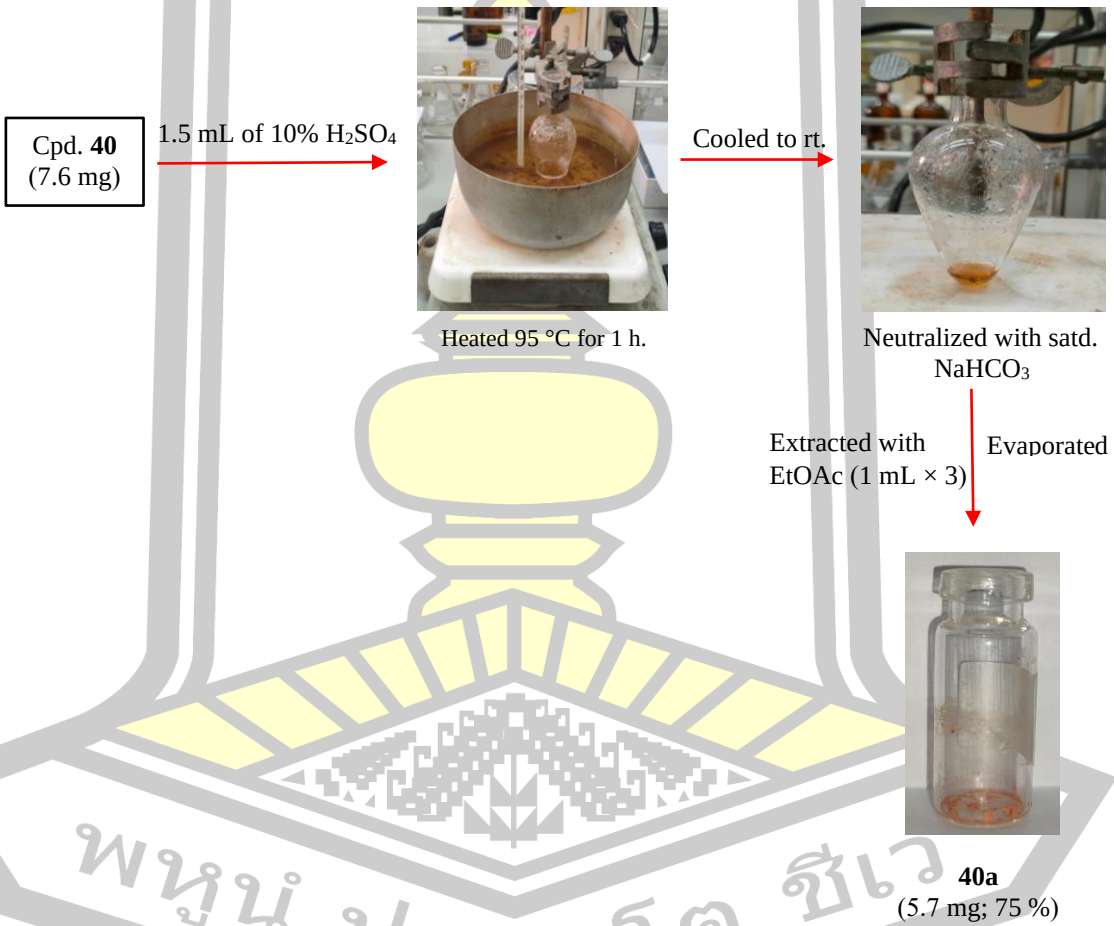

Flow chart 3. Acid hydrolysis of **40**.

3.6. DPPH radical scavenging activity assay

2,2-Diphenyl-1-picrylhydrazyl (DPPH) (Sigma-Aldrich) radical scavenging activity assay was performed as previously described by Promden et al. (Promden et al., 2024). Briefly, 20 µL of each sample solution (1 mg/mL in dimethyl sulfoxide; DMSO) was mixed with 180 µL of DPPH solution (100 µM in MeOH) in a 96-well microplate. The mixture was incubated at 37 °C for 30 min in the dark. The absorbance (A) of the samples and control was measured at 515 nm using the FLUOstar® Omega plate reader (BMG LABTECH). The DPPH• radical scavenging activity (RSA)was calculated in term of %RSA. For the active samples, the scavenging concentration at 50% (SC_{50}) was determined using a calibration curve within the linear range, plotting concentrations against %RSA. The experiments were performed in triplicate and reported as average ± standard deviation (SD). Ascorbic acid was used as a standard compound.

$$\%RSA = [(A\ control - A\ sample) = A\ control] \times 100$$

3.7. *α*-Glucosidase inhibitory activity assay

The inhibitory activity toward *α*-glucosidase was assayed using the previously described method with some modifications (Promden et al., 2024). For screening, samples were first dissolved in DMSO to obtain the final concentration 100 µg/mL 2.5% DMSO in buffer. An aliquot of 10 µL was added to each well of a 96-well microplate. Subsequently, 130 µL of 100 mM phosphate buffer (pH 6.8) was added to each well, followed by the introduction of 20 µL of *Saccharpmyces cerevisiae* *α*-glucosidase (0.5 U/mL) (Sigma-Aldrich, St. Louis, MO, USA). The microplate was

then incubated at 37 °C for 10 min. The enzymatic reaction was started by addition of 50 µL of 2.5 mM *p*-nitrophenyl-*α*-D-glucopyranoside (PNPG) (Sigma-Aldrich, St. Louis, MO, USA) as a substrate. The reaction progress was monitored for 10 min, and the absorbance (A) of control and samples were measured at 405, using a (ultraviolet-visible) UV-Vis spectrophotometer microplate reader. In the control reaction, 10 µL of 2.5% DMSO was used instead of the compounds. The percentage inhibition was calculated using the-equation below.

$$\%\text{Inhibition} = [\text{A sample} - \text{A control}) / \text{A control}] \times 100$$

3.8. Antibacterial activity assay

3.8.1. Agar well diffusion assay

The antibacterial activities were tested using the agar well diffusion method (Sangdee et al., 2016). The Gram-positive pathogenic bacteria methicillin-susceptible *S. aureus* (MSSA) DMST 2933, methicillin-resistant *S. aureus* (MRSA) DMST 20651 and *Bacillus cereus* ATCC 11778 were cultured on Mueller Hinton agar (MHA) at 37 °C for 16–18 h. A single colony of each bacterium (*S. aureus* (MSSA and MRSA), and *B. cereus*) was inoculated into Mueller Hinton broth (MHB) and incubated at 37 °C for 4 h with shaking at 250 rpm, then adjusted to a 0.5 McFarland standard. A sterile cotton swab was dipped into the standardized bacterial suspension and swabbed in four directions over the entire surface of the MHA plates. The plates were then cut using a 7 mm sterile cork borer. The extract solutions (50 mg/mL) were added to each well at 0.1 mL per well. The plates were incubated at 37 °C for 16–18 h, after which the zones of inhibition surrounding each

well were measured. The negative control of 10% (*v/v*) MeOH was used, while tetracycline (250 µg/mL) was used as a positive control. The potential pure compounds (1.0 mg/mL) were then evaluated for antibacterial activity against suspected pathogens as described above.

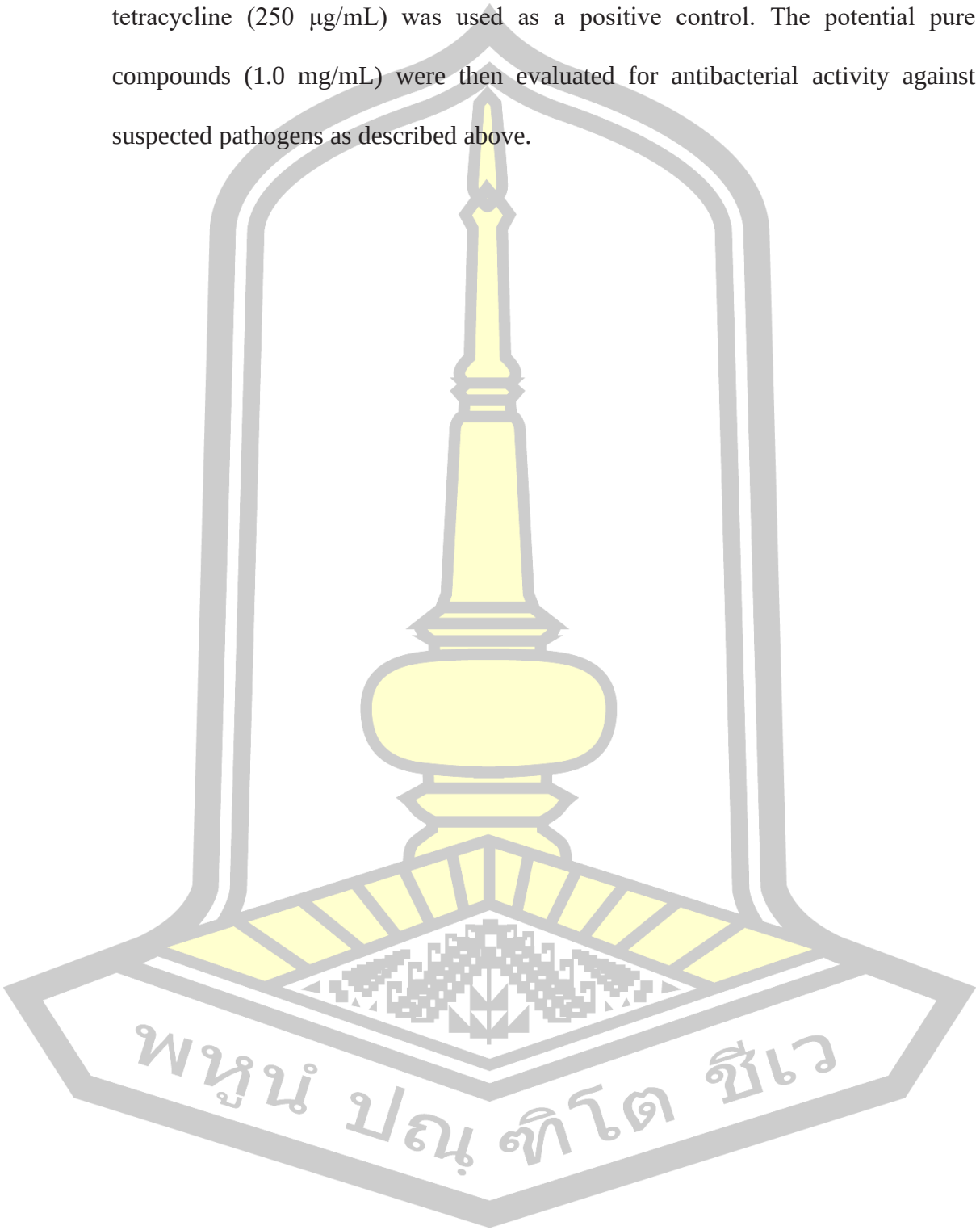

CHAPTER 4

RESULTS AND DISCUSSION

4.1. Extraction

Extraction of *G. vidalii* leaves (280 g) yielded 10.30 g of hexane extract and 4.48 g of EtOAc extract.

4.2. Isolation and identification of compounds

Phytochemical investigation of the EtOAc extract led to the isolation of six compounds. Based on spectroscopy data, the isolated compounds were identified as a *C*-glycosylxanthone, mangiferin (**18**), two benzophenoneglycosides, aquilarinenside E (**40**) and iriflophenone 2-*O*-α-L-rhamnoside (**41**), a terpenoid, blumenol A or vomifoliol (**42**), a flavonoid, 5,7,4´-trimethoxyflavone (**43**), and a phenolic compound, 4-methoxybenzoic acid (**44**) (**Figure 9**). Additionally, compound **40a**, identified as iriflophenone, was obtained from the acid hydrolysis of **40**.

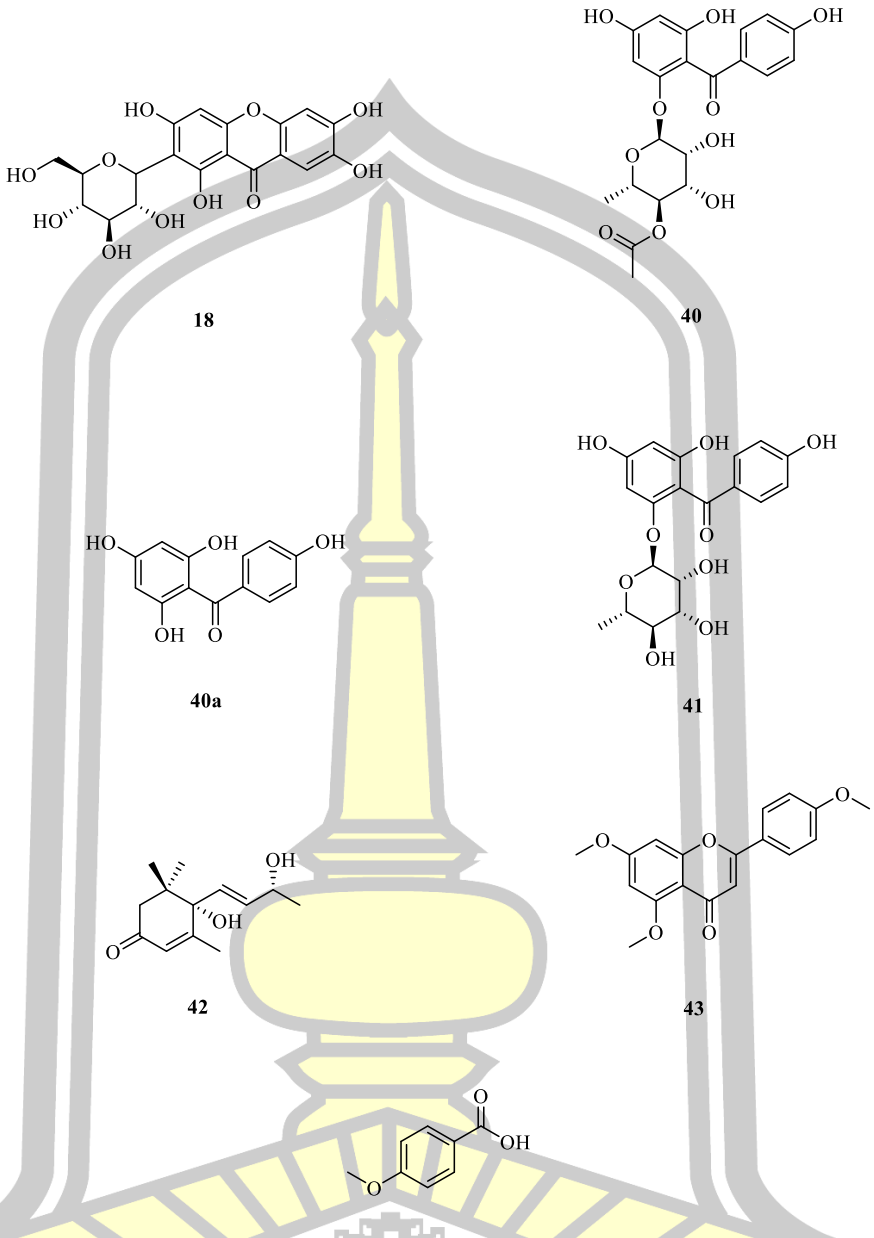

Figure 9. Structure of compounds **18**, **40–44**.

4.2.1. Mangiferin (**18**)

Compound **18** ($C_{19}H_{18}O_{11}$) was isolated as a pale-yellow powder. Its structure was elucidated based on ^{1}H, ^{13}C and 2D NMR spectroscopic data in DMSO-d_6 and confirmed by comparison with the previous reported data in literatures (Djemgou et al., 2010; Shahat et al., 2003), as shown in **Table 1**. The ^{1}H, ^{13}C and 2D NMR spectroscopic data of **18** in DMSO-d_6 are shown in **Table 2**. The ^{1}H, ^{13}C and 2D NMR spectra of **18** are shown in **Figures A4**–**A23**. Mangiferin (**18**) is a *C*-glycosylxanthone primarily isolated from mango, *Mangifera indica* L. (Anacardiaceae). It was also produced in other higher plants (Anacardiacae, Gentianaceae, and Iridaceae) (Sanugul et al., 2005) Recently, the isolation of mangiferin from the leaves of *A. sinensis* (Feng et al., 2011; Qi et al., 2009; Yu et al., 2013) and *A. crassna* (Ito et al., 2012; Ray et al., 2014) has been reported. Various pharmacological activities of mangiferin have been reviewed (Du et al., 2018; Feng et al., 2019; Imran et al., 2017; Kaurav et al., 2023).

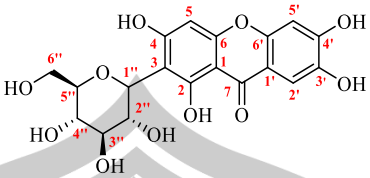

18

Table 1. ^{1}H and ^{13}C NMR spectroscopic data of **18** in DMSO-d_6 compared with literatures.

Position	Compound **18**[a]		Mangiferin[b]		Mangiferin[c]	
	δ_H, multi. (*J* in Hz)	δ_C	δ_H, multi. (*J* in Hz)	δ_C	δ_H, multi. (*J* in Hz)	δ_C
Xanthone moiety						
1	-	101.3	-	101.29	-	101.2
2	-	161.8	-	161.76	-	161.7
3	-	107.6	-	107.56	-	107.5
4	-	163.9	-	163.81	-	163.8
5	6.37, s	93.3	6.35, s	93.31	6.40, s	93.3
6	-	156.2	-	156.21	-	156.2
7	-	179.1	-	179.07	-	179.0
1′	-	111.7	-	111.63	-	111.4
2′	7.37, s	108.0	7.36, s	108.00	7.41, s	107.8
3′	-	143.8	-	143.76	-	143.9
4′	-	150.8	-	154.17	-	150.9
5′	6.86, s	102.6	6.84, s	102.56	6.86, s	102.4
6′	-	154.1	-	150.82	-	154.6
2-OH	13.76, s	-	-	-	13.80, s	-
Glucopyranosyl moiety						
1″	4.59, d (9.8)	73.1	4.58, d (9.8)	73.09	4.60, d (8.3)	73.1
2″	4.04, t (9.0)	70.2	4.03, dd (9.1, 9.0)	70.62	4.03, t (9.5)	70.3
3″	3.25–3.12, m	79.0	3.20, m	79.14	3.16, m	79.0
4″	3.25–3.12, m	70.7	3.14, m	70.26	3.16, m	70.6
5″	3.25–3.12, m	81.6	3.16, m	81.53	3.16, m	81.5
6″	3.40, dd, (11.6, 5.8) 3.69, d (10.8)	61.5	3.40, dd (11.6, 5.5) 3.68, br. d (11.6)	62.78	3.40, dd (11.0, 2.1) 3.60, dd (11.0, 4.6)	61.4

[a] Calibration of DMSO-d_6 δ_H 2.50/δ_C 39.5 ppm, [b] (Shahat *et al.*, 2003), [c] (Djemgou *et al.*, 2010).

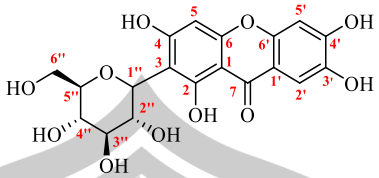

18

Table 2. ^{1}H, ^{13}C and 2D NMR spectroscopic data of **18** in DMSO-d_6.

Position	δ_H multi. (*J* in Hz)	δ_C	COSY	NOESY	HMBC
Xanthone moiety					
1	-	101.3	-	-	-
2	-	161.8	-	-	-
3	-	107.6	-	-	-
4	-	163.9	-	-	-
5	6.37, s	93.3	-	1″, 6″	7, 4, 6, 3, 1, 1″
6	-	156.2	-	-	-
7	-	179.1	-	-	-
1′	-	111.7	-	-	-
2′	7.37, s	108.0	-	1″, 6″	7, 6′, 4′, 3′, 1′, 5′
3′	-	143.8	-	-	-
4′	-	150.8	-	-	-
5′	6.86, s	102.6	-	1″, 6″	7, 6′, 4′, 3′, 1′
6′	-	154.1	-	-	-
2-OH	13.76, s	-		1″, 6″	7, 4, 2, 3,1
Glucopyranosyl Moiety					
1″	4.59, d (9.8)	73.1	2″	2-OH, 2″, 3″, 4″, 5″	5″, 3″, 2″, 4, 2, 3
2″	4.04, t (9.0)	70.2	1″, 3″, 4″, 5″	1″, 6″, 3″, 4″, 5″	3″, 1″
3″	3.25–3.12, m	79.0	2″, 6″	2-OH, 1″, 2″, 6″	4″, 2″
4″	3.25–3.12, m	70.7	2″, 6″	2-OH, 1″, 2″, 6″	5″, 3″, 6″
5″	3.25–3.12, m	81.6	2″, 6″	2-OH, 1″, 2″, 6″	3″
6″	3.40, dd (11.6, 5.8) 3.69, d (10.8)	61.5	6″, 3″, 4″, 5″	6″, 3″, 4″, 5″	5″, 4″

Calibration of DMSO-d_6 δ_H 2.50/δc 39.5 ppm.

4.2.2. Aquilarinenside E (**40**)

Compound **40** ($C_{21}H_{22}O_{10}$) was isolated as a light-yellow crystal. Its structure was elucidated based on FTIR, mass (MS) and (^{1}H, ^{13}C and 2D) NMR spectroscopic data and confirmed by comparison with the previous reported data in literature (Sun et al., 2014), as shown in **Table 3**. The ^{1}H, ^{13}C and 2D NMR spectroscopic data of **40** in CD_3OD and DMSO-d_6, are shown in **Table 4** and **Table 5**, respectively. FTIR, MS and (^{1}H, ^{13}C and 2D) NMR spectra of **40**, are shown in **Figures A24**–**A71**. Aquilarinenside E (**40**) was detected in the leaves of *A. sinensis* using High-Performance Liquid Chromatography-Mass Spectrometry (HPLC-MS) (Yu et al., 2013). Recently, the isolation of this compound from the leaves and flower buds (Sun et al., 2014; Yuan et al., 2017) of *A. sinensis*, and the pericarps of *A. yunnanensis* (Sun et al., 2019) has been reported.

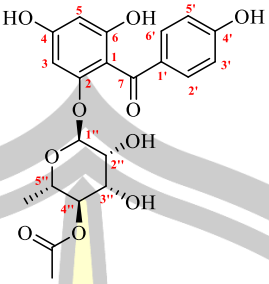

40

Table 3. ^{1}H and ^{13}C NMR spectroscopic data of **40** compared with literature.

Position	Compound **40**[a] (CD_3OD)		Aquilarinenside E[b] (CD_3OD)		Compound **40**[c] (DMSO)	
	δ_H, multi. (*J* in Hz)	δ_C	δ_H, multi. (*J* in Hz)	δ_C	δ_H, multi. (*J* in Hz)	δ_C
Iriflophenone Moiety						
1	-	109.6	-	109.7	-	109.4
2	-	157.8	-	158.0	-	154.8
3	6.24, d (2.1)	94.9	6.25, d (2.0)	95.1	6.10, d (1.9)	93.4
4	-	162.9	-	163.1	-	159.4
5	6.08, d (2.1)	98.0	6.08, d (2.0)	98.1	6.04, d (1.9)	96.7
6	-	160.4	-	160.6	-	156.4
7	-	197.6	-	197.7	-	192.8
1′	-	132.9	-	133.1	-	130.1
2′/6′	7.62, d (8.8)	132.7	7.6, d (8.7)	132.8	7.55, d (8.8)	131.3
3′/5′	6.84, d (8.8)	116.2	6.8, d (8.7)	116.3	6.80, d (8.8)	115.1
4′	-	163.4	-	163.1	-	161.8
4-OH	-	-	-	-	9.65, s	-
6-OH	-	-	-	-	9.57, s	-
4′-OH	-	-	-	-	10.26, s	-
Rhamnopyranosyl Moiety						
1″	5.29, d (1.7)	99.6	5.29, d (1.4)	99.8	5.21, d (1.5)	97.8
2″	3.54−3.50, m	71.5	3.51, m	71.6	3.46−3.41, m	69.8
3″	3.10, dd (9.8, 3.4)	69.7	3.09, m	69.9	3.23−3.15, m	67.5
4″	4.80, t (9.8)	75.0	3.79, m	79.2	4.67, t (9.8)	73.3
5″	3.50−3.44, m	68.7	3.48, m	68.8	3.36 (overlap)*	66.9
2″-OH	-	-	-	-	5.18, d (4.4)	-
3″-OH	-	-	-	-	4.77, d (6.4)	-
4″-OCO$\underline{CH}_3$	2.06, s	21.0	2.0, s	21.1	1.98, s	20.9
4″-O$\underline{C}$OCH$_3$	-	172.6	-	172.7	-	170.0
5″-CH$_3$	1.05, d (6.3)	17.8	1.05, d (6.0)	17.9	0.90, d (6.2)	17.4

[a] Calibration of CD_3OD δ_H 3.31/δ_C 49.0 ppm, [b] (Sun et al., 2014), [c] Calibration of DMSO-d_6 δ_H 2.50/δ_C 39.5 ppm, *overlapped with the solvent peak.

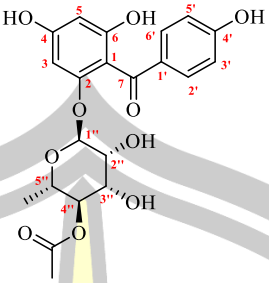

40

Table 4. ^{1}H, ^{13}C and 2D NMR spectroscopic data of **40** in CD_3OD.

Position	δ_H multi. (*J* in Hz)	δ_C	COSY	NOESY	HMBC
Iriflophenone moiety					
1	-	109.6	-	-	-
2	-	157.8	-	-	-
3	6.24, d (2.1)	94.9	5	5, 1″, 5″	7, 4, 2, 1, 5
4	-	162.9	-	-	-
5	6.08, d (2.1)	98.0	3	3	4, 6, 1, 3
6	-	160.4	-	-	-
7	-	197.6	-	-	-
1′	-	132.9	-	-	-
2′/6′	7.62, d (8.8)	132.7	3′/5′	3′/5′, 5″	7, 4′, 2′/6′, 3′/5′
3′/5′	6.84, d (8.8)	116.2	2′/6′	2′/6′	4′, 1′, 3′/5′
4′	-	163.4	-	-	-
Rhamnopyranosyl moiety					
1″	5.29, d (1.7)	99.6	2″	3, 2″	2, 5″
2″	3.54−3.50, m	71.5	3″	1″, 3″	4″, 3″
3″	3.10, dd (9.8, 3.4)	69.7	4″, 5″	4″, 2″	4″
4″	4.80, t (9.8)	75.0	5″, 3″	3″, 5″-CH_3	4″-O<u>C</u>OCH_3, 3″, 5″-CH_3
5″	3.50−3.44, m	68.7	1″, 4″, 5″-CH_3	5″-CH_3	-
4″-OCO<u>*CH*</u>$_3$	2.06, s	21.0	-	-	4″, 4″-O<u>C</u>OCH_3
4″-O<u>C</u>OCH_3	-	172.6	-	-	-
5″-CH_3	1.05, d (6.3)	17.8	5″	4″, 5″	4″, 5″

Calibration of CD_3OD δ_H 3.31/δc 49.0 ppm.

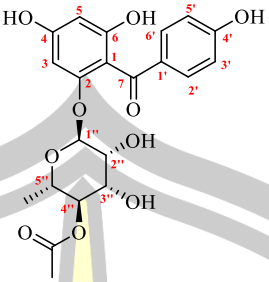

40

Table 5. ^{1}H, ^{13}C and 2D NMR spectroscopic data of **40** in DMSO-d_6.

Position	δ_H multi. (J in Hz)	δ_C	COSY	NOESY	HMBC
Iriflophenone Moiety					
1	-	109.4	-	-	-
2	-	154.8	-	-	-
3	6.10, d (1.9)	93.4	-	-	7, 4, 2, 1, 5
4	-	159.4	-	-	-
5	6.04, d (1.9)	96.7	-	-	7, 4, 6, 1, 3
6	-	156.4	-	-	-
7	-	192.8	-	-	-
1′	-	130.1	-	-	-
2′/6′	7.55, d (8.8)	131.3	3′/5′	3′/5′	7, 4′, 2′/6′, 3′/5′
3′/5′	6.80, d (8.8)	115.1	2′/6′	2′/6′	4′, 1′, 3′/5′
4′	-	161.8	-	-	-
4-OH	9.65, s	-	-	4′-OH, 6-OH, 5″	5, 4, 3
6-OH	9.57, s	-	-	4′-OH, 4-OH, 5″	6, 2, 1, 5
4′-OH	10.26, s	-		6-OH, 4-OH, 5″	3′/5′
Rhamnopyranosyl Moiety					
1″	5.21, d (1.5)	97.8	-	-	2, 2″, 5″
2″	3.46−3.41, m	69.8	2″-OH, 3″	2″-OH, 3″	-
3″	3.23−3.15, m	67.5	3″-OH, 4″, 2″	2″	4″
4″	4.67, t (9.8)	73.3	5″, 3″	-	4″-O$\underline{C}$OCH$_3$, 3″, 5″, 5″-CH$_3$
5″	3.36 (overlap)*	66.9	4″, 5″-CH$_3$	-	4″
2″-OH	5.18, d (4.4)	-	2″	2″, 5″	1″, 2″
3″-OH	4.77, d (6.4)	-	3″	5″, 3″	4″, 2″, 3″
4″-OCO$\underline{CH}_3$	1.98, s	20.9	-	-	-
4″-O$\underline{C}$OCH$_3$	-	170.0	-	-	-
5″-CH$_3$	0.90, d (6.2)	17.4	5″	5″	4″-O$\underline{C}$OCH$_3$, 4″, 5″

Calibration of DMSO-d_6 δ_H 2.50/δc 39.5 ppm, *overlapped solvent peak.

4.2.3. Iriflophenone (**40a**)

Compound **40a** ($C_{13}H_{10}O_5$) was obtained as an orange solid from the acid hydrolysis of compound **40**. Its structure was elucidated based on ^{1}H and ^{13}C NMR spectroscopic data and confirmed by comparison with the previous reported data in literature (Rancon et al., 2001), as shown in **Table 6**. The ^{1}H and ^{13}C NMR spectra of **40a** are shown in **Figures A72**–**A78**. The isolation of Iriflophenone from the leaves of *A. sinensis* (Qi et al., 2009) has been reported.

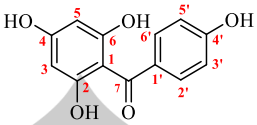

40a

Table 6. ^{1}H and ^{13}C NMR spectroscopic data of **40a** compared with literature.

Position	Compound **40a**[a] (in DMSO-d_6)		Compound **40a**[b] (in acetone-d_6)		Iriflophenone[c] (in acetone-d_6)	
	δ_H, multi. (J in Hz)	δ_C	δ_H, multi. (J in Hz)	δ_C	δ_H, multi. (J in Hz)	δ_C
1	-	99.8	-	105.4	-	106.6
2	-	158.3	-	162.9	-	164.0
3	5.76, s	94.3	5.95, s	95.8	5.99, s	96.9
4	-	158.3	-	164.8	-	164.6
5	5.76, s	94.3	5.95, s	95.8	5.99, s	96.9
6	-	158.3	-	162.9	-	164.0
7	-	194.2	-	197.7	-	198.9
1′	-	130.6	-	133.4	-	134.4
2′/6′	7.51, d (8.7)	131.4	7.60, d, (8.8)	132.3	7.62, d (8.7)	133.4
3′/5′	6.74, d (8.7)	114.7	6.84, d, (8.8)	115.0	6.86, d (8.7)	116.1
4′	-	158.3	-	161.8	-	162.8
2-OH	-	-	-	-	10.22, brs.	-
4-OH	-	-	-	-	9.14, brs.	-
6-OH	-	-	-	-	10.22, brs.	-
4′-OH	-	-	-	-	9.14, brs.	-

[a] Calibration of DMSO-d_6 δ_H 2.50/δc 39.5 ppm, [b] acetone-d_6 δ_H 2.05/δc 29.8 ppm, [c] (Rancon et al., 2001).

4.2.4. Iriflophenone 2-*O*-*α*-L-rhamnoside (**41**)

Compound **41** ($C_{19}H_{20}O_9$) was isolated as a light-brown solid. Its structure was elucidated based on ^{1}H NMR and mass (MS) spectroscopic data and confirmed by comparison with the previous reported data in literatures (Xia et al., 2013; Sun et al., 2020), as shown in **Table 7**. The ^{1}H NMR and mass (MS) spectra of **41** are shown in **Figures A79**–**A83**. The isolation of Iriflophenone 2-*O*-*α*-L-rhamnoside from the agarwood leaves and stems of *A. sinensis* (Hara et al., 2008; Wu et al 2016), and the leaves of *A. crassna* (Ito et al., 2012) has been reported.

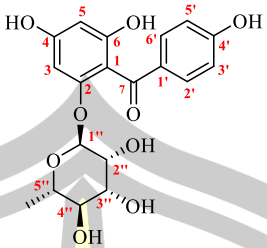

41

Table 7. ^{1}H NMR spectroscopic data of **41** in CD_3OD compared with literatures.

Position	Compound **41**[a]	Iriflophenone 2-*O*-*α*-L-rhamnoside[b]	Iriflophenone 2-*O*-*α*-L-rhamnoside[c]
	δ_H, multi. (*J* in Hz)	δ_H, multi. (*J* in Hz)	δ_H, multi. (*J* in Hz)
Iriflophenone moiety			
1	-	-	-
2	-	-	-
3	6.27, d (2.1)	6.34, d (2.0)	6.29, d (2.0)
4	-	-	-
5	6.04, d (2.1)	6.11, d (2.0)	6.07, d (2.0)
6	-	-	-
7	-	-	-
1′	-	-	-
2′/6′	7.58, d (8.7)	7.65, d (8.5)	7.61, d (8.5)
3′/5′	6.78, d (8.7)	6.85, d (8.5)	6.81, d (8.5)
4′		-	-
Rhamnopyranosyl moiety			
1″	5.19, d (1.6)	5.26, d (1.0)	5.22, d (1.0)
2″	3.39−3.35, m	3.50–3.45, m	3.43, m
3″	3.09, dd (9.5, 3.4)	3.16, dd (9.5, 3.0)	3.12, dd (9.5, 3.5)
4″	3.29–3.21, m	3.32, dd (9.5, 3.0)	3.28, dd (9.5, 3.5)
5″	3.45–3.39, m	3.50–3.45, m	3.40, m
5″-CH_3	1.16, d (6.2)	1.23, d (6.0)	1.19, d (6.0)

[a] Calibration of CD_3OD δ_H 3.31 ppm, [b] (Xia et al., 2013), [c] (Sun et al., 2020).

4.2.5. Blumenol A or Vomifoliol (**42**)

Compound **42** ($C_{13}H_{20}O_3$) was isolated as a light-yellow oil. Its structure was elucidated based on ^1H ,^{13}C and 2D NMR spectroscopic data in CD_3OD and confirmed by comparison with the previous reported data in literatures (Dinh et al., 2020; Huong et al., 2015), as shown in **Table 8**. The ^1H, ^{13}C and 2D NMR spectroscopic data of **42** in CD_3OD are shown in **Table 9**. The ^1H, ^{13}C and 2D NMR spectra of **42** are shown in **Figures A84**–**A105**.

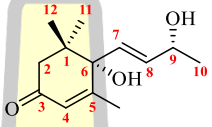

42

Table 8. ^1H and ^{13}C NMR spectroscopic data of **42** in CD_3OD compared with literatures.

Position	Compound **42**		Blumenol A[a]		Vomifoliol[b]	
	δ_H, multi. (J in Hz)	δ_C	δ_H, multi. (J in Hz)	δ_C	δ_H, multi. (J in Hz)	δ_C
1	-	42.4	-	42.42	-	42.4
2	2.16, d (17.0)	50.7	2.18, d (17.0)	50.73	2.18, d (17.0)	50.7
	2.52, d (17.0)	50.7	2.53, d (17.0)	50.73	2.53, d (17.0)	50.7
3	-	201.2	-	201.27	-	201.2
4	5.88, t (1.2)	127.1	5.90, t (1.5)	127.10	5.89, m	127.1
5	-	167.5	-	167.48	-	167.4
6	-	79.9	-	79.95	-	79.9
7	5.79 (overlap)*	130.1	5.81 (overlap)*	130.10	5.80, m	130.1
8	5.79 (overlap)*	136.9	5.82 (overlap)*	136.92	5.83, m	136.9
9	4.36-4.28, m	68.7	4,34, dd (6.5, 4.5)	68.72	4.34, m	68.7
10	1.24, d (6.5)	23.8	1,26 d, (6.5)	23.82	1.26, d (6.5)	23.8
11	1.04, s	23.5	1.06 s	23.46	1.04, s	23.4
12	1.01, s	24.5	1.03 s	24.47	1.06, s	24.5
13	1.92, d (1.3)	19.6	1.94, d (1.5)	19.56	1.94, s	19.5

Calibration of CD_3OD δ_H 3.31/δc 49.0 ppm, [a] (Huong et al., 2015), [b] (Dinh et al 2020), *overlapped signal.

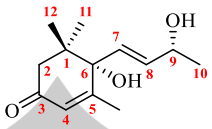

42

Table 9. ^{1}H, ^{13}C and 2D NMR spectroscopic data of **42** in CD_3OD.

Position	δ_H multi. (*J* in Hz)	δ_C	COSY	NOESY	HMBC
1	-	42.4	-	-	-
2	2.16, d (17.0)	50.7	4, 2	2, 12	3, 4, 6, 1, 11
	2.52, d (17.0)	50.7	2, 11	7, 8, 2, 12	3, 6, 1, 11
3	-	201.2	-	-	-
4	5.88, t (1.2)	127.1	2, 13	13	6, 2, 13
5	-	167.5	-	-	-
6	-	79.9	-	-	-
7	5.79 (overlap)*	130.1	9	9, 2, 13, 10, 12	8, 7, 6, 9
8	5.79 (overlap)*	136.9	9	9, 2, 13, 10, 12	8, 7, 6, 9
9	4.36–4.28, m	68.7	7, 8, 10	7, 8, 10	8, 7
10	1.24, d (6.5)	23.8	9	7, 8, 9	8, 9
11	1.04, s	23.5	2	-	6, 2, 1, 12
12	1.01, s	24.5	-	7, 8, 2	3, 6, 2, 1, 11
13	1.92, d (1.3)	19.6	4	4, 7, 8	5, 4, 6

Calibration of CD_3OD δ_H 3.31/δ_c 49.0 ppm, *overlapped signal.

Compound **42** ($C_{13}H_{20}O_3$) was confirmed by ^{1}H NMR spectroscopic data in $CDCl_3$ and confirmed by comparison with the previous reported data in literature (González et al., 1994), as shown in **Table 10**. The ^{1}H NMR spectra of **42** are shown in **Figures A106–A109**. This compound was isolated for the first time from genus *Neolitsea* (Chen et al., 1998).

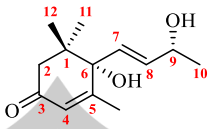

42

Table 10. ^{1}H NMR spectroscopic data of **42** in $CDCl_3$ compared with literature.

Position	Compound **42**[a]	Blumenol A[b]
	δ_H, multi. (*J* in Hz)	δ_H, multi. (*J* in Hz)
1	-	-
2	2.24, d (17.1)	2.25, d (16.8)
	2.45, d (17.1)	2.45, d (16.8)
3	-	-
4	5.90, q (1.2)	5.91, bs
5	-	-
6	-	-
7	5.78, dd (15.6, 0.9)	5.79, d (15.7)
8	5.87, dd (15.6, 5.2)	5.87, dd (15.7, 5.1)
9	4.38-4.44, m	4.42, m
10	1.30, d (6.4)	1.30, d (6.3)
11	1.00, s	1.02 s
12	1.08, s	1.11 s
13	1.90, d (1.4)	1.90, bs

[a] Calibration of $CDCl_3$ δ_H 7.26 ppm, [b] (González et al., 1994).

4.2.6. 5,7,4′-Trimethoxyflavone (**43**)

Compound **43** ($C_{18}H_{16}O_5$) was isolated as a yellow amorphous solid. Its structure was elucidated based on ^{1}H, ^{13}C and 2D NMR spectroscopic data in $CDCl_3$ and confirmed by comparison with the previous reported data in literature (Nadri et al., 2015) as shown in **Table 11**. The ^{1}H, ^{13}C and 2D NMR spectroscopic data of **43** in $CDCl_3$ are shown in **Table 12**. ^{1}H, ^{13}C and 2D NMR spectra of **43** are shown in **Figures A110**–**A127**. The isolation of this compound has been reported from the leaves of *A. sinensis* (Cheng et al., 2013).

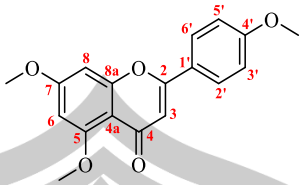

43

Table 11. ^{1}H and ^{13}C NMR spectroscopic data of **43** in $CDCl_3$ compared with literature.

Position	Compound **43**[a]		5,7,4′-Trimethoxyflavone[b]	
	δ_H, multi. (J in Hz)	δ_C	δ_H, multi. (J in Hz)	δ_C
2	-	164.0	-	162.1
3	6.58, s	104.3	6.62, s	107.7
4	-	182.5	-	177.6
4a	-	105.5	-	109.2
5	-	157.7	-	160.9
6	6.49, d (2.3)	92.6	6.56, d (2.4)	92.8
7	-	165.4	-	163.9
8	6.37, d (2.3)	98.0	6.38, d (2.4)	96.1
8a	-	162.2	-	160.7
1′	-	123.6	-	123.9
2′/6′	7.85, d (9.0)	128.0	7.84, d (8.8)	127.6
3′/5′	7.02, d (9.0)	114.5	7.02, d (8.8)	114.4
4′	-	162.6	-	159.8
5-OCH_3	3.49, s	50.9	3.96, s	56.4
7-OCH_3	3.88, s	55.5	3.92, s	55.7
4′-OCH_3	3.90, s	55.8	0.89, s	55.5

[a] Calibration of $CDCl_3$ δ_H 7.26/δ_C 77.0 ppm, [b] (Nadri et al., 2015).

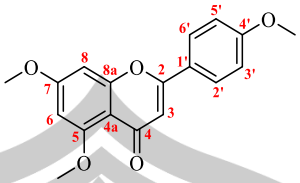

43

Table 12. ^{1}H, ^{13}C and 2D NMR spectroscopic data of **43** in $CDCl_3$.

Position	δ_H multi. (*J* in Hz)	δ_C	COSY	NOESY	HMBC
2	-	164.0	-	-	-
3	6.58, s	104.3	-	2′/6′	4, 2, 1′, 4a
4	-	182.5	-	-	-
4a	-	105.5	-	-	-
5	-	157.7	-	-	-
6	6.49, d (2.3)	92.6	-	7-OCH_3	7, 5, 4a, 8
7	-	165.4	-	-	-
8	6.37, d (2.3)	98.0	-	7-OCH_3, 6	8a, 4a, 6, 7
8a	-	162.2	-	-	-
1'	-	123.6	-	-	-
2'/6'	7.85, d (9.0)	128.0	3′/5′	3′/5′, 3	2, 2′/6′, 4′
3′/5′	7.02, d (9.0)	114.5	2′/6′	2′/6′, 4′-OCH_3	4′, 1′, 3′/5′
4′	-	162.6	-	-	-
5-OCH_3	3.49, s	50.9	-	-	-
7-OCH_3	3.88, s	55.5	-	6, 8	7
4′-OCH_3	3.90, s	55.8	-	3′/5′	4′

Calibration of $CDCl_3$ δ_H 7.26/δ_c 77.0 ppm.

4.2.7. 4-Methoxybenzoic acid (**44**)

Compound **44** ($C_8H_8O_3$) was isolated as a green amorphous solid. Its structure was elucidated based on ^{1}H NMR spectroscopic data in $CDCl_3$ and confirmed by comparison with the previous reported data in literature (Urgoitia et al., 2015), as shown in **Table 13**. The ^{1}H NMR spectra of **44** are shown in **Figures**

A128–**A129**. The isolation of this compound from *A. agallocha* (Naf et al., 1995) and *A. sinensis* (Yang et al., 1989) has been reported.

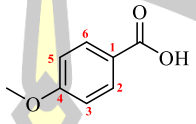

44

Table 13. ^{1}H NMR spectroscopic data of **44** in $CDCl_3$ compared with literature.

Position	Compound **44**[a]	4-methoxybenzoic acid[b]
	δ_H, multi. (*J* in Hz)	δ_H, multi. (*J* in Hz)
2/6	7.95, d (8.8)	8.07, d (8.9)
3/5	6.86, d (8.8)	6.95, d (8.8)
4-OCH_3	3.88, s	3.88, s
COOH	-	-

[a] Calibration of $CDCl_3$ δ_H 7.26 ppm, [b] (Urgoitia, et al 2015).

4.3. Antioxidation activity

Preliminary screening of antioxidation activity of the MeOH, hexane, and EtOAc extracts of *G. vidalii* was evaluated. Among the extracts, the EtOAc extract of *G. vidalii* exhibited the best antioxidant activity with an SC_{50} value of 47.23 ± 3.84 µg/mL (**Table 14**).

Table 14. Antioxidant activity of the extracts from the leaves of *G. vidalii*.

Extract	Antioxidant activity		
	DPPH (SC_{50}, µg/mL)	Total phenolic content (GAE/g extract)	Total flavonoid content (mg QE/g extract)
MeOH	109.53 ± 9.06	76.60 ± 2.97	97.60 ± 4.69
Hexane	>140	16.26 ± 2.03	140.54 ± 10.44
EtOAc	47.23 ± 3.84	192.34 ± 8.39	313.34 ± 2.66

4.4. *α*-Glucosidase inhibitory activity

The *α*-glucosidase inhibitory activity of the MeOH, hexane, and EtOAc extracts of *G. vidalii* was evaluated. The hexane extract of *G. vidalii* exhibited strong *α*-glucosidase inhibition, with an inhibition percentage of 94.49% at a concentration of 100 µg/mL (**Table 15**).

Table 15. *α*-Glucosidase inhibition of the extracts from the leaves of *G. vidalii*.

Extract	*α*-Glucosidase inhibition (%)
	100 µg/mL
MeOH	58.62
Hexane	94.49
EtOAc	19.11

4.5. Antibacterial activity

The antibacterial activity of the MeOH, hexane, and EtOAc extracts of *G. vidalii* against *B. cereus*, *S. aureus* (MRSA), *S. aureus* (MSSA) is shown in **Table 16**. The EtOAc extract showed antibacterial activity against *B. cereus* and *S. aureus* (MRSA) at a concentration of 16.2 mg/mL, while the MeOH extract exhibited antibacterial activity against *B. cereus* at a concentration of 33.8 mg/mL.

Table 16. Antibacterial activity of the extracts from the leaves of *G. vidalii*.

Extract	Concentration (mg/mL)	Inhibition zone (mm)		
		B. cereus	*S. aureus* (MRSA)	*S. aureus* (MSSA)
MeOH	33.8	10 × 10	-	-
Hexane	51.6	-	-	-
EtOAc	16.2	11 × 12	15 × 15	-
Tetracycline	0.25	30 × 29	24 × 23	28 × 28

Tetracycline was used as a positive control.

CHAPTER 5

CONCLUSION

The hexane, EtOAc, and MeOH extracts from the leaves of *Gyrinops vidalii* were evaluated for their antioxidant, α-glucosidase inhibitory, and antibacterial activities. Among the extracts, the hexane extract exhibited strong α-glucosidase inhibitory activity, with the inhibition of 94.49% at a concentration 100 µg/mL. The EtOAc extract showed strong antioxidant activity toward DPPH radical, with an SC_{50} value of 47.23 ± 3.84 µg/mL. Additionally, this extract also showed the antibacterial activity against *B. cereus* and *S. aureus* (MRSA) at the tested concentration of 16.2 mg/mL, while MeOH extract exhibited the antibacterial activity against *B. cereus* at a concentration 33.8 mg/mL.

This EtOAc extract was chemically investigated for the first time, leading to the isolation of mangiferin (**18**), aquilarinenside E (**40**), iriflophenone 2-*O*-α-L-rhamnoside (**41**), blumenol A or vomifoliol (**42**), 5,7,4′-trimethoxyflavone (**43**), and 4-methoxybenzoic acid (**44**), together with three unknown compounds, **A**–**C**. The structures of **18**, **40**–**44**, were identified based on NMR and mass spectroscopic data, and confirmed by comparison with the previous reported data in literatures. Iriflophenone (**40a**) was obtained from acid hydrolysis of compound **40**. The structures of **A**–**C** are currently under elucidation. The biological activity of the isolated compounds will be evaluated.

REFERENCES

Baimai, V. Biodiversity in Thailand. The Journal of the Royal Institute of Thailand. **2010**; *2*, 107−118.

Chen, K-S.; Chang, F-R.; Chia, Y-C.; Wu, T-S.; Wu, Y-C. Chemical constituents of *Neolitsea parvigemma* and *Neolitsea konishii*. Journal of the Chinese Chemical Society. **1988**; 45: 103–110.

Cheng, J. T.; Han, Y. Q.; He, J.; Wu, X. D.; Dong, L. B.; Peng, L. Y.; Li, Y.; Zhao, Q.S. Two new tirucallane triterpenoids from the leaves of *Aquilaria sinensis*. Archives of Pharmacal Research. **2013**; 36: 1084–1089.

China Pharmacopoeia Editorial Board. Pharmacopoeia of the People's Republic of China. China Medical Science and Technology Press. **2010**; pp. 172–173.

Compton, J. G. S.; Zich, F.A. *Gyrinops ledermannii* (Thymalaeaceae), being an agarwood producing species prompts call for further examination of taxonomic implications in the generic delimitation between *Aquilaria* and *Gyrinops*. Flora Malesiana Bulletin. **2002**; 13(1): 61–66.

Dincheva, I.; Badjakov, I.; Galunska, B. New insights into the research of bioactive compounds from plant origins with nutraceutical and pharmaceutical potential. Plants. **2023**; 12(2): 258.

Dinh, N. T.; Thi, H. T.; Thi, H. N.; Thi, H. M. V.; Thi, N. M. N.; Vu, T. K. O. Chemical constituents from ethyl acetate extract of the leaves of *Rourea harmandiana* Pierre. Vietnam Journal of Science, Technology and Engineering. **2020**; 62(2), 30−33.

Djemgou, P. C.; Hussien, T. A.; Hegazy, M.-E. F.; Ngandeu, F.; Neguim, G.; Tane, P.; Abou-El-Hamd, H. M. C-Glucoside xanthone from the stem bark extract of *Bersama engleriana*. Pharmacognosy research. **2010**; *2*(4): 229−232.

Dong, W.-H.; Wang, H.; Guo, F.-J.; Mei, W.-L.; Chen, H.-Q.; Kong, F.-D.; Li, W.; Zhou, K.-B.; Dai, H.-F. Three new 2-(2-phenylethyl) chromone derivatives of agarwood originated from *Gyrinops salicifolia*. Molecules. **2019**; 24(3): 576.

Du, S.; Liu, H.; Lei, T.; Xie, X.; Wang, H.; He, X.; Tong, R.; Wang Y. Mangiferin: An effective therapeutic agent against several disorders (Review). Molecular Medicine Reports. **2018**; 18 (6): 4775–4786.

Eurlings M. C. M.; Gravendeel B. *Trn*L–*trn*F sequence data imply paraphyly of *Aquilaria* and *Gyrinops* (Thymelaeaceae) and provide new perspectives for agarwood identification. Plant Systematics and Evolution. **2005**; 254(1): 1–12.

Feng, J.; Yang, X. W.; Wang, R. F. Bio-assay guided isolation and identification of α-glucosidase inhibitors from the leaves of *Aquilaria sinensis*. Phytochemistry. **2011**; 72 (2−3): 242−247.

Feng, S. T.; Wang, Z. Z.; Yuan, Y. H.; Sun, H. M.; Chen, N. H.; Zhang, Y. Mangiferin: A multipotent natural product preventing neurodegeneration in Alzheimer's and Parkinson's disease models. Pharmacological Research. **2019**; 146: 104336.

González, A. G.; Guillermo, J. A.; Ravelo, A. G.; Jimenez, I. A.; Gupta, M. P. 4, 5-Dihydroblumenol A, a new nor-isoprenoid from *Perrottetia multiflora*. Journal of natural products. **1994**; 57(3): 400−402.

Hara, H.; Ise, Y.; Morimoto, N.; Shimazawa, M.; Ichihashi, K.; Ohyama, M.; Iinuma, M. Laxative effect of agarwood leaves and its mechanism. Bioscience, Biotechnology, and Biochemistry. **2008**; 72(2): 335–345.

Ho, P. H. Thymelaeaceae. Flore du Cambodge du Laos et du Vietnam. **1992**; 26: 38–81.

Hou, D. Thymelaeaceae. In Flora Malesian. **1960**; 6: 1–5.

Huong, P. T. T.; Van Thanh, N.; Diep, C. N.; Thao, N. P.; Cuong, N. X.; Nam, N. H.; Van Minh, C. Antimicrobial compounds from Rhizophora stylosa. Vietnam Journal of Science and Technology. **2015**; 53(2): 205−210.

Imran, M.; Arshad, M. S.; Butt, M. S.; Kwon, J. H.; Arshad, M. U.; Sultan, M. T. Mangiferin: a natural miracle bioactive compound against lifestyle related disorders. Lipids in Health and Disease. **2017**; 16(1): 84.

Ito, T.; Kakino, M.; Hara, H.; Tazawa, S.; Iinuma, M. Identification of phenolic compounds in *Aquilaria crassna* leaves via liquid chromatography-electrospray ionization mass spectroscopy. Food Science and Technology Research. **2012**; 18(2): 259–262.

Kaurav, M.; Kanoujia, J.; Gupta, M.; Goyal, P.; Pant, S.; Rai, S.; Sahu, K. K.; Bhatt, P.; Ghai, R. In-depth analysis of the chemical composition, pharmacological effects, pharmacokinetics, and patent history of mangiferin. Phytomedicine Plus. **2023**; 3(2): 100445.

Kennedy, D. O.; Wightman, E. L. Herbal extracts and phytochemicals: plant secondary metabolites and the enhancement of human brain function. Advances in Nutrition. **2011**; 2(1), 32−50.

Lee, S. Y.; Mohamed, R. The origin and domestication of *Aquilaria*, an important agarwood-producing genus. In: Book: Agarwood. Tropical Forestry, Springer Singapore. **2016**; pp. 1–20.

Lee, S. Y.; Turjaman, M.; Mohamed, R. Phylogenetic relatedness of several agarwood-producing taxa (Thymelaeaceae) from Indonesia. Tropical Life Sciences Research. **2018**.; 29(2): 13–28.

Lee, S. Y.; Turjaman, M.; Chaveerach, A.; Subasinghe, S. M. C. U. P.; Fan, Q.; Liao, W. Phylogenetic relationships of *Aquilaria* and *Gyrinops* (Thymelaeaceae) revisited: evidence from complete plastid genomes. Biological Journal of the Linnean Society. **2022**.; 20(3): 344–359.

Li, T.; Qiu, Z.; Lee, S. Y.; Li, X.; Gao, J.; Jiang, C.; Huang, L.; Liu, J.; Biodiversity and application prospects of fungal endophytes in the agarwood-producing genera, *Aquilaria* and *Gyrinops* (Thymelaeaceae). Arabian journal of chemistry. **2023**.; 16(1), 104435.

Maxwell, J. F. Three more new records for the Thai flora. Nat. Hist. Natural History Bulletin of the Siam Society. **2000**: 48, 225–227.

Maxwell, J. A synopsis of the vegetation of Thailand. Tropical Natural History. **2004**; 4(2): 19−29.

Min, S. J.; Lee, H.; Shin, M. S.; Lee. J. W. Synthesis and biological properties of pyranocoumarin derivatives as potent anti-Inflammatory agents. International Journal of Molecular Sciences. **2023**; 24(12): 10026.

Munasinghe, S.; Somaratne, S.; Weerakoon, S.; Ranasinghe, C. Sustainable utilization of *Gyrinops walla* Gaetner: in vitro production of sesquiterpenes by chemical and biological elicitation. Journal of Genetic Engineering and Biotechnology. **2021**; 19(1): 134.

Nadri, M. H.; Naser, M. A.; Zukifli, R. M.; Muhamad, I. I.; Ahmad, F.; Salleh, W. M. N. H. W.; Sirat, H. M. Antioxidant activity of Piper caninum and

Cyclooxygenase-2 inhibition by methoxylated flavones. African Journal of Traditional, Complementary and Alternative Medicines. **2015**; 12(2): 120−125.

Naf, R.; Velluz, A.; Brauchli, R.; Thommen W. Agarwood oil (*Aquilaria agallocha* Roxb.). Its composition and eight new valencane-, eremophilane- and vetispiranederivatives. Flavour and Fragrance Journal. **1995**; 10(3):147–152.

Newman, D. J.; Cragg, G. M. Natural products as sources of new drugs from 1981 to 2014. Journal of natural products. **2016**; 79(3): 629−661.

Persoon, G. A.; Van Beek, H. H. Growing 'the wood of the gods': Agarwood production in Southeast Asia. In smallholder tree growing for rural development and environmental services. Springer Netherlands. **2008**; pp. 245–262.

Promden, W.; Chanvorachote, P.; Viriyabancha, W.; Sintupachee, S.; De-Eknamkul, W. Maclura cochinchinensis (Lour.) Corner Heartwood Extracts Containing Resveratrol and Oxyresveratrol Inhibit Melanogenesis in B16F10 Melanoma Cells. Molecules. **2024**; 29(11): 2473.

Qi, J.; Lu, J. J.; Liu, J. H.; Yu, B. Y. Flavonoid and a rare benzophenone glycoside from the leaves of *Aquilaria sinensis*. Chemical and Pharmaceutical Bulletin. **2009**: 57(2); 134−137.

Rancon, S.; Chaboud, A.; Darbour, N.; Comte, G.; Bayet, C.; Simon, P.-N.; Raynaud, J.; Di Pietro, A.; Cabalion, P.; Barron, D. Natural and synthetic benzophenones: interaction with the cytosolic binding domain of P-glycoprotein. Phytochemistry. **2001**; 57(4): 553−557.

Ray, G.; Leelamanit, W.; Sithisarn, P.; Jiratchariyakul, W.; Antioxidative compounds from *Aquilaria crassna* leaf. Mahidol University Journal of Pharmaceutical Sciences. **2014**; 41(4): 54−58.

Sangdee, K.; Seephonkai, P.; Buranrat, B.; Surapong, N.; Sangdee, A. Effects of ethyl acetate extracts from the *Polycephalomyces* nipponicus isolate Cod-MK1201 (Ascomycetes) against human pathogenic bacteria and a breast cancer cell line. International journal of Medicinal Mushrooms. **2016**; 18(8): 733−743.

Sanugul, K.; Akao, T.; Li, Y.; Kakiuchi, N.; Nakamura, N.; Hattoti, M. Isolation of a human intestinal bacterium that transforms mangiferin to norathyriol and inducibility of the enzyme that cleaves a *C*-glucosyl bond. Bio. Pharm. Bull. **2005**; 28 (9); 1672–1678.

Schun, Y.; Cordell, G. A. Studies in the Thymelaeaceae III. Constituents of *Gyrinops walla*. Journal of natural products. **1985**; 48(4), 684−685.

Schun, Y.; Cordell, G. A.; Cox, P. J.; Howie, R. A. Wallenone, a C32 triterpenoid from the leaves of *Gyrinops walla*. Phytochemistry. **1986**; 25(3): 753−755.

Shahat, A. A.; Hassan, R. A.; Nazif, N. M.; Van Miert, S.; Pieters, L.; Hammuda, F. M.; Vlietinck, A. J. Isolation of mangiferin from Bombax malabaricum and structure revision of shamimin. Planta medica. **2003**; 69(11): 1068−1070.

Shao, H.; Mei, W.-L.; Dong, W.-H.; Gai, C.-J.; Li, W.; Zhu, G.-P.; Dai, H.-F. 2-(2-phenylethyl) chromone derivatives of agarwood originating from *Gyrinops salicifolia*. Molecules. **2016**; 21(10): 1313.

Shao, H.; Mei, W.-L.; Kong, F.-D.; Dong, W.-H.; Gai, C.-J.; Li, W.; Zhu, G.-P.; Dai, H.-F. Sesquiterpenes of agarwood from *Gyrinops salicifolia*. Fitoterapia. **2016**; 113: 182−187.

Su, C. R.; Yeh, S. F.; Liu, C. M.; Damu, A. G.; Kuo, T. H.; Chiang, P. C; Bastow, K. F.; Lee, K. H; Wu, T. S. Anti-HBV and cytotoxic activities of pyranocoumarin derivatives. Bioorganic & Medicinal Chemistry. **2009**; 17(16): 6137–6143.

Sun, J.; Wang, S.; Xia, F.; Wang, K.-Y.; Chen, J.-M.; Tu, P.-F. Five new benzophenone glycosides from the leaves of *Aquilaria sinensis* (Lour.) Gilg. Chinese Chemical Letters. **2014**; 25(12): 1573−1576.

Sun, H.; Zhang, T-F.; Huo, H.-X.; Guan, P-W.; Wang C. C.; Yao, H-N.; Zhao Y-F.; Tu, P-F.; Li, L. Benzophenone glycosides from the pericarps of Aquilaria yunnanensis S. C. Huang . Natural Product Research. **2019**; 34(14): 2030–2036.

Sun, H.; Zhang, Y.-F.; Huo, H.-X.; Guan, P.-W.; Wang, C.-C.; Yao, H.-N.; Zhao, Y.-F.; Tu, P.-F.; Li, J. Benzophenone glycosides from the pericarps of *Aquilaria yunnanensis* SC Huang. Natural Product Research. **2020**; 34(14): 2030−2036.

Thailand Country Study on Biodiversity. Ministry of Science, Technology and Environment. Bangkok. **1992**.

Urgoitia, G.; SanMartin, R.; Herrero, M. T.; Dominguez, E. An outstanding catalyst for the oxygen-mediated oxidation of arylcarbinols, arylmethylene and aryl acetylene compounds. Chemical Communications. **2015**; 51(23): 4799−4802.

Van Welzen, P. C.; Madern, A.; Raes, N.; Parnell, J.; Simpson, D.; Byrne, C.; Curtis, T.; Macklin, J.; Trias-Blasi, A.; Prajaksood, A. The current and future status of floristic provinces in Thailand. InTrisurat, Y.; Land use, Shrestha, R.P.; lkemade, R. A (Eds.). Land use, climate change and biodiversity modeling: perspectives and applications. **2011**; pp. 219−247.

Wu, Y.; Li, E.; Li, Y.; Wu, Q.; Tian, W.; Liu, K.; Niu, Y.; Wang, D.; Liu, J.-G.; Hu, Y. Iriflophenone glycosides from *Aquilaria sinensis*. Chemistry of Natural Compounds. **2016**; 52: 834-837.

Xia, F; Sun, J; Jiang, Y; Tu, PF. Further chemical investigation of leaves of *Aquilaria Sinensis*. China Journal of Chinese Material Medica. **2013**; 38: 3299–3303.

Yang, J. S.; Wang, Y. L.; Su ,Y. L. Chemical constituents of *Aquilaria sinensis* (Lour.) Gilg. III. Elucidation of the structure of isobaimuxinol and isolation and identification of the constituents of lower boiling point fraction of the volatile oil. Acta Pharmaceutica Sinica B. **1989**; 24(4): 264–268.

Yu, Q.; Qi, J.; Yu, H.; Chen, L.; Kou, J.; Liu, S.; Yu, B. Qualitative and quantitative analysis of phenolic compounds in the leaves of *Aquilaria sinensis* using liquid chromatography-mass spectrometry. Phytochemical Analysis. **2013**; 24(4): 349–356.

Yuan, H.; Zhao, J.; Wang, M.; Khan, S. I.; Zhai, C.; Xu, Q.; Huang, J.; Peng, C.; Xiong, G.; Wang, W. Benzophenone glycosides from the flower buds of Aquilaria sinensis. Fitoterapia. **2017**; 121: 170–174.

APPENDIX

LIST OF FIGURES

Figure **Page**

Figure **Page**

Figure **Page**

Figure **Page**

Figure **Page**

Figure **Page**

Figure **Page**

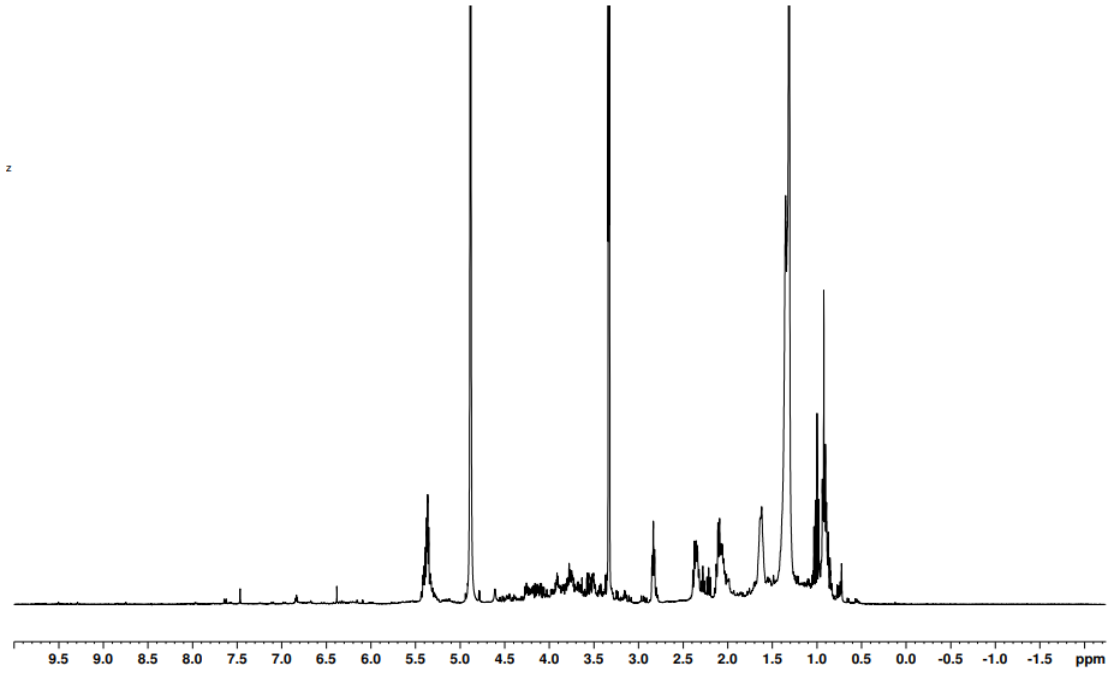

Figure A1. ^{1}H NMR spectrum of the hexane extract of *G. vidalii* (CD_3OD, 400 MHz).

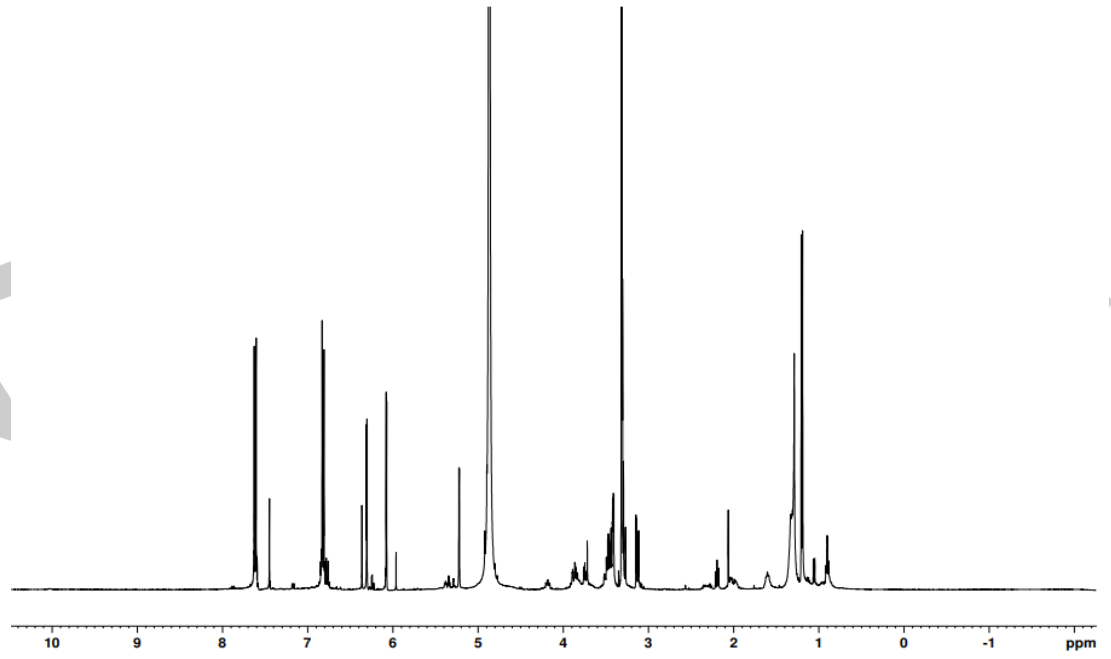

Figure A2. ^{1}H NMR spectrum of the EtOAc extract of *G. vidalii* (CD_3OD, 400 MHz).

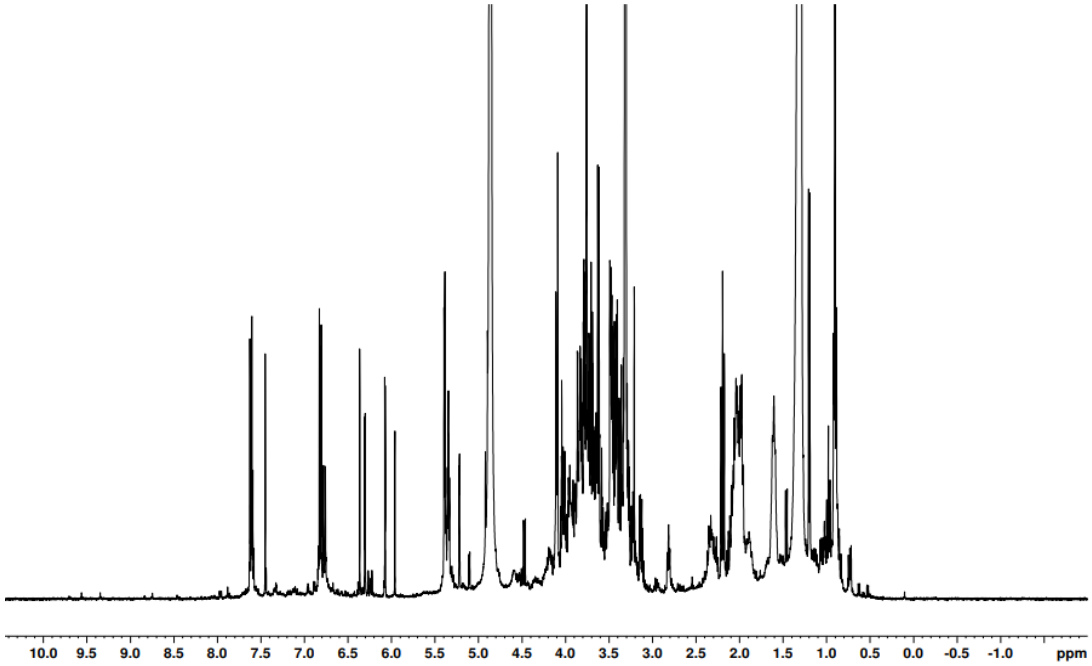

Figure A3. ^{1}H NMR spectrum of the MeOH extract of *G. vidalii* (CD_3OD, 400 MHz).

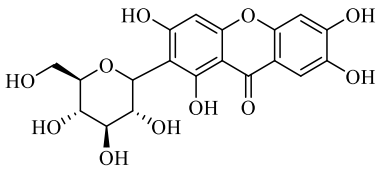

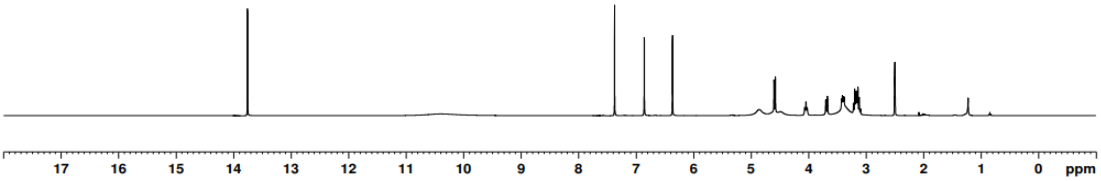

Figure A4. ^{1}H NMR spectrum of **18** (DMSO-d_6, 400 MHz).

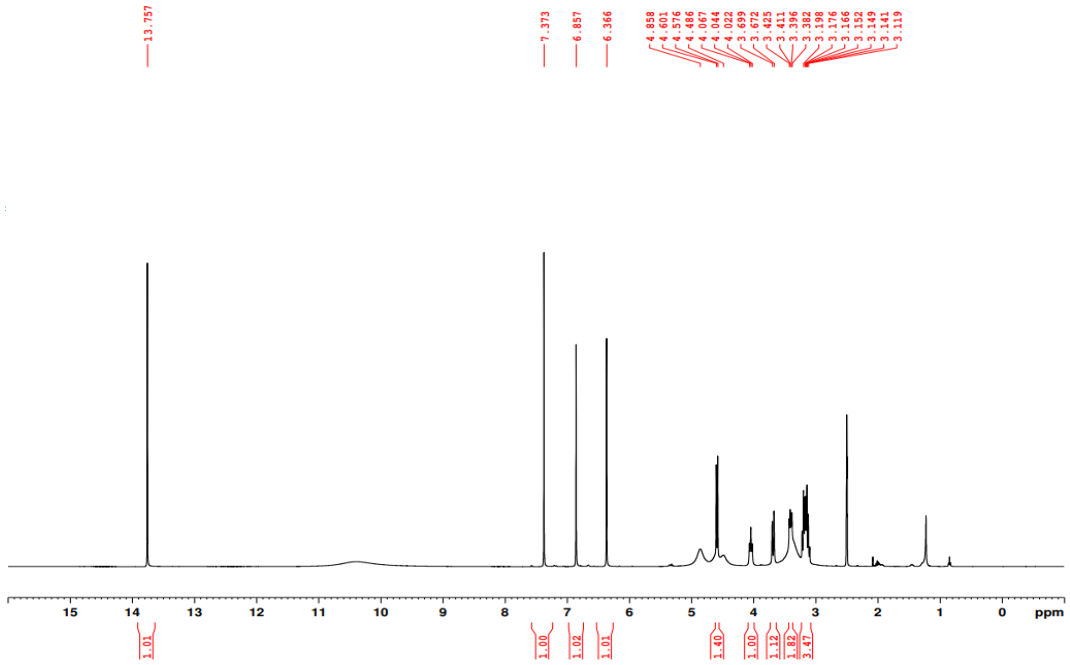

Figure A5. ^{1}H NMR spectrum (expansion 1) of **18** (DMSO-d_6, 400 MHz).

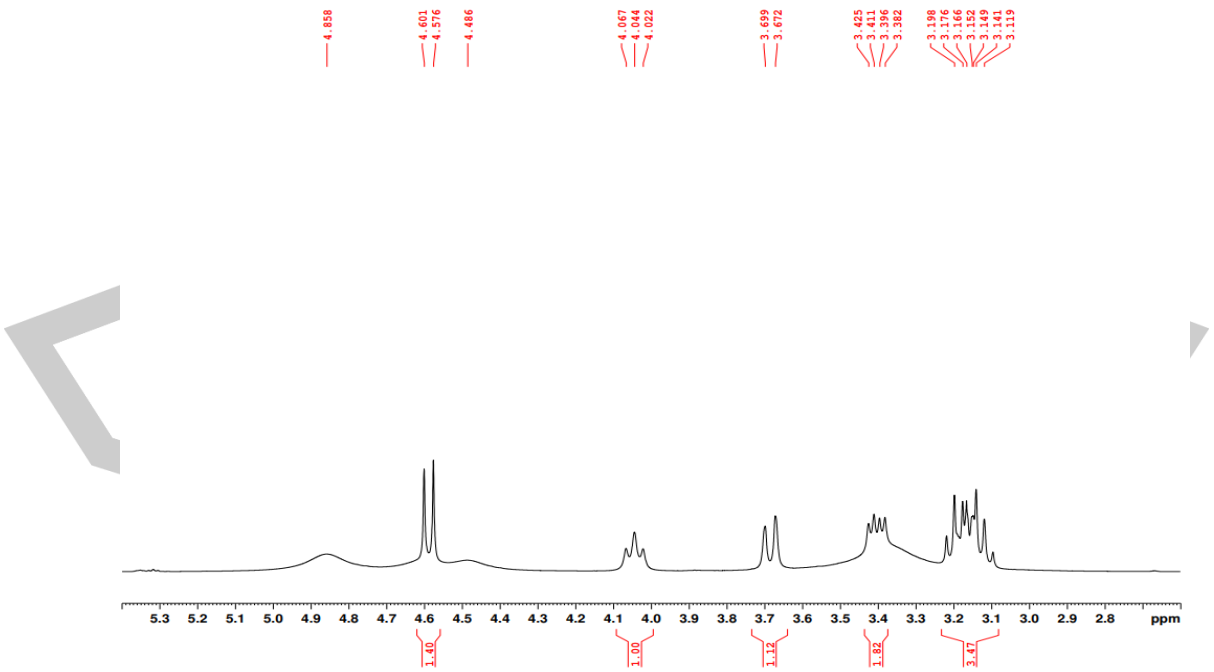

Figure A6. ^{1}H NMR spectrum (expansion 2) of **18** (DMSO-d_6, 400 MHz).

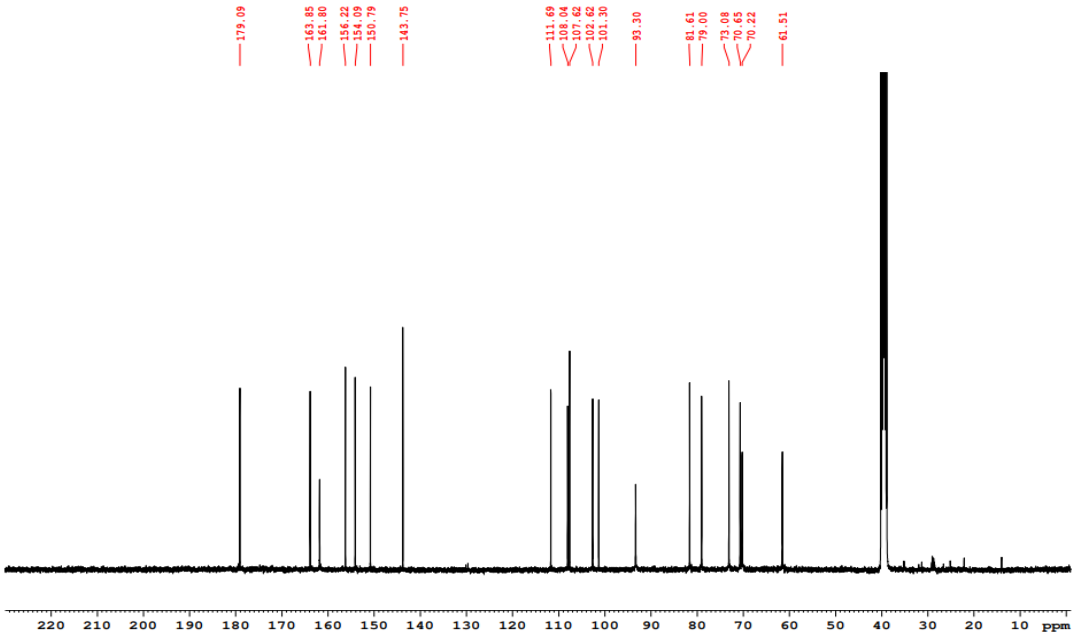

Figure A7. ^{13}C NMR spectrum of **18** (DMSO-d_6, 100 MHz).

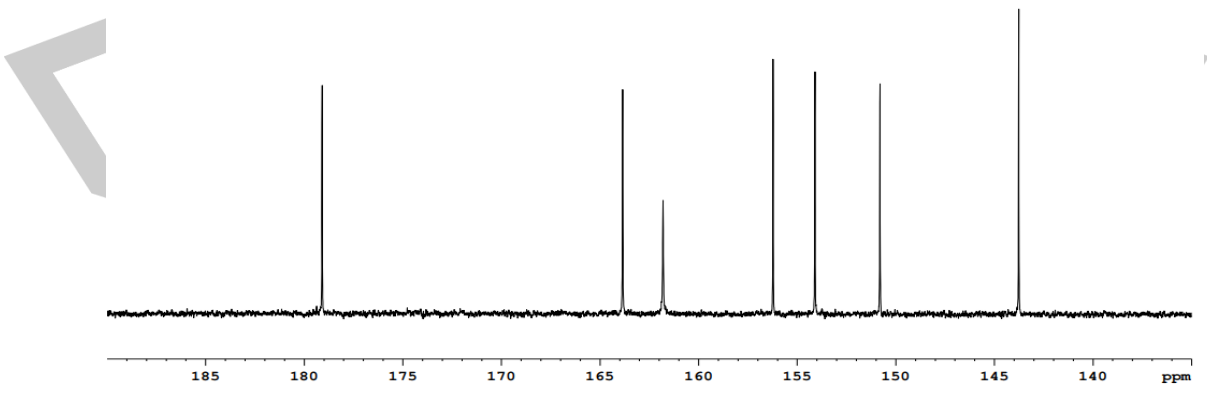

Figure A8. ^{13}C NMR spectrum (expansion 1) of **18** (DMSO-d_6, 100 MHz).

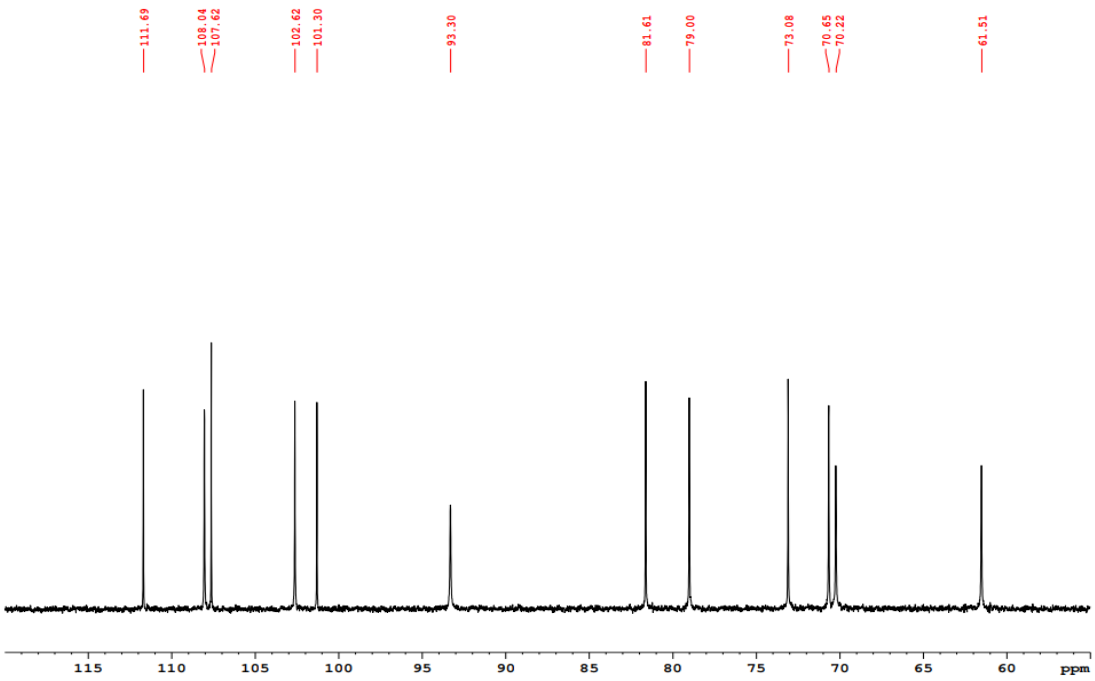

Figure A9. ^{13}C NMR spectrum (expansion 2) of **18** (DMSO-d_6, 100 MHz).

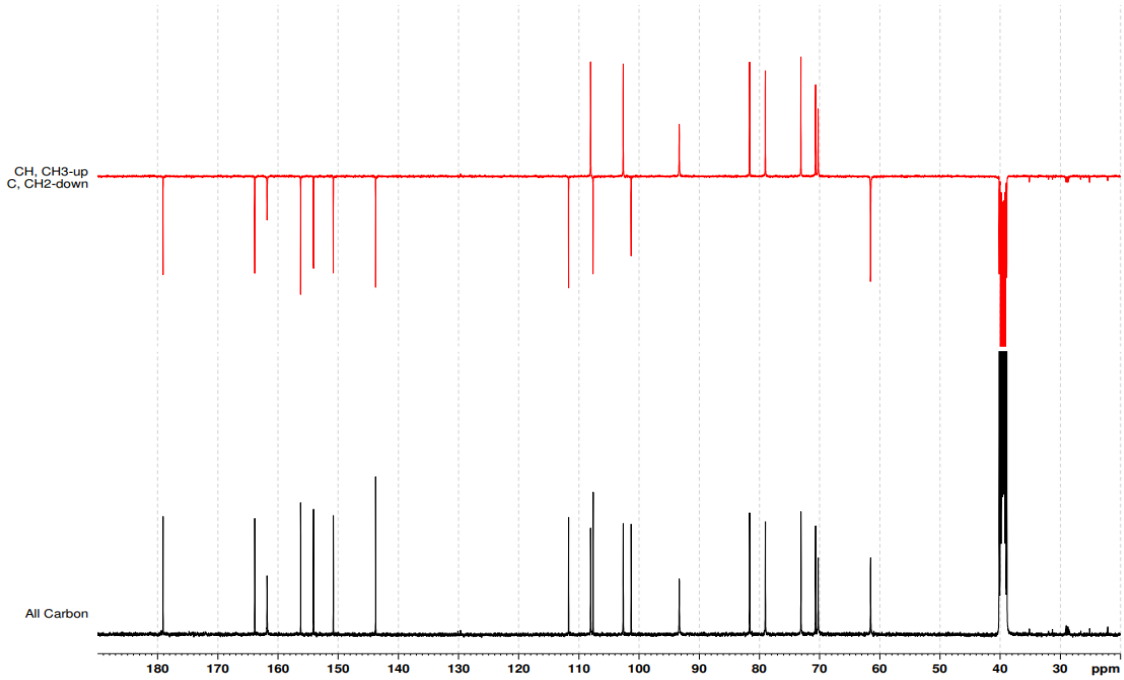

Figure A10. DEPT-135 spectrum of **18** in DMSO-d_6.

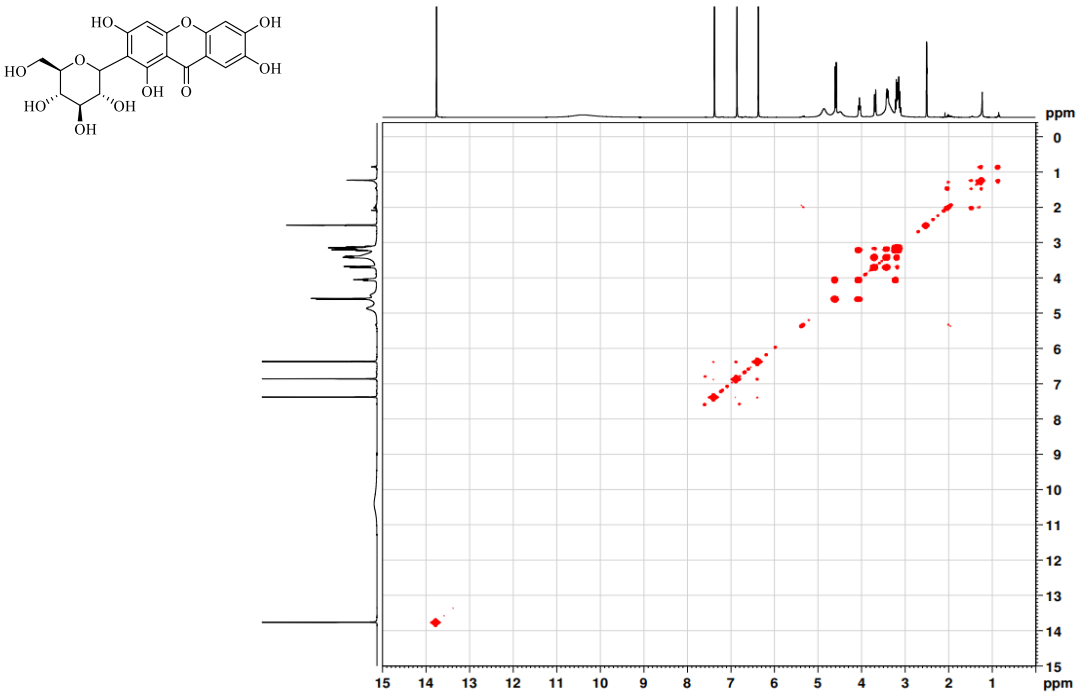

Figure A11. COSY spectrum of **18** in DMSO-d_6.

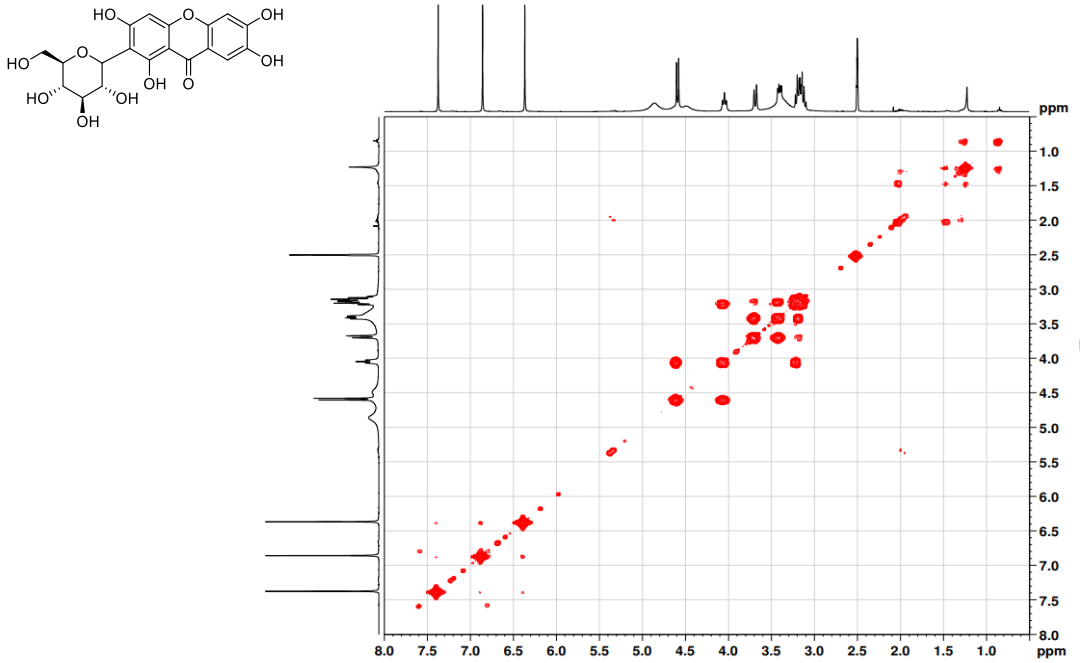

Figure A12. COSY spectrum (expansion1) of **18** in DMSO-d_6.

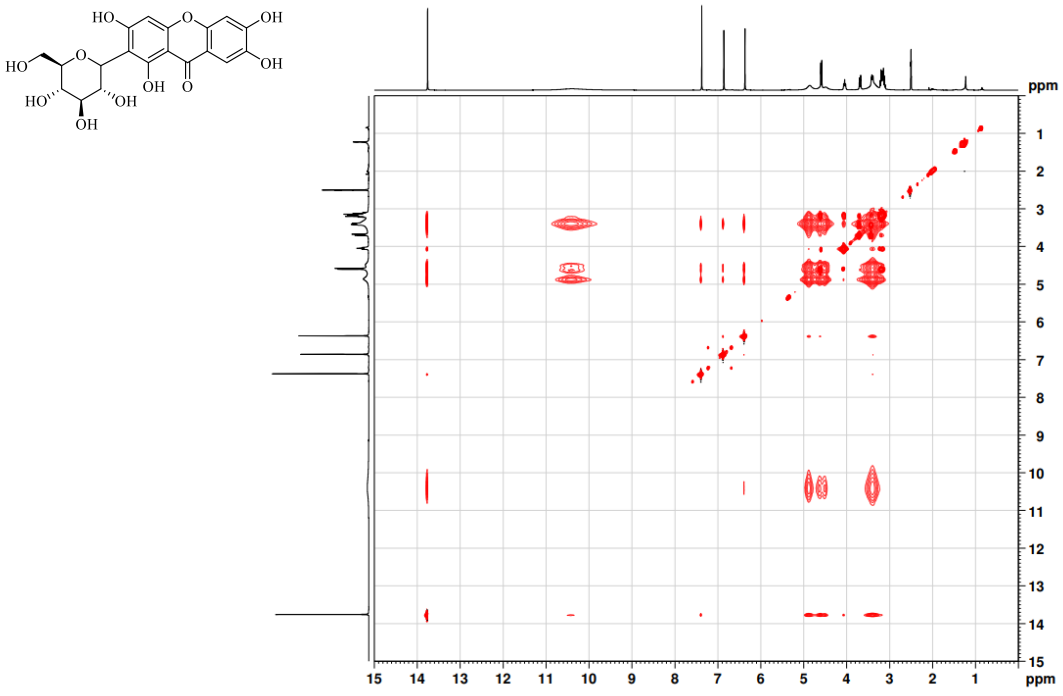

Figure A13. NOESY spectrum of **18** in DMSO-d_6.

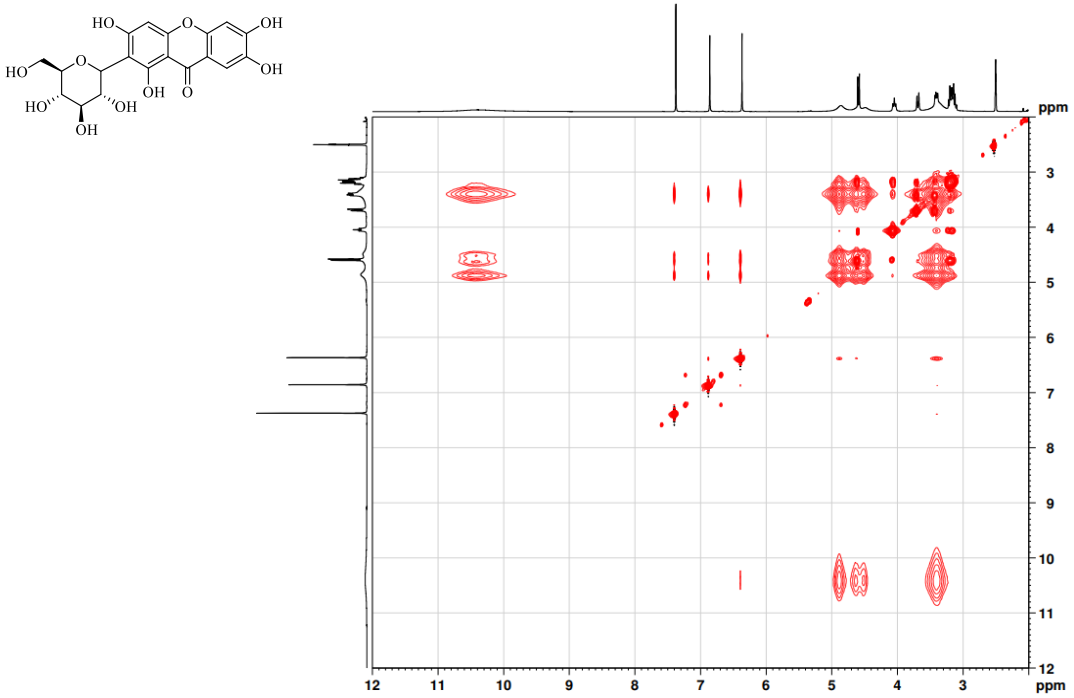

Figure A14. NOESY spectrum (expansion 1) of **18** in DMSO-d_6.

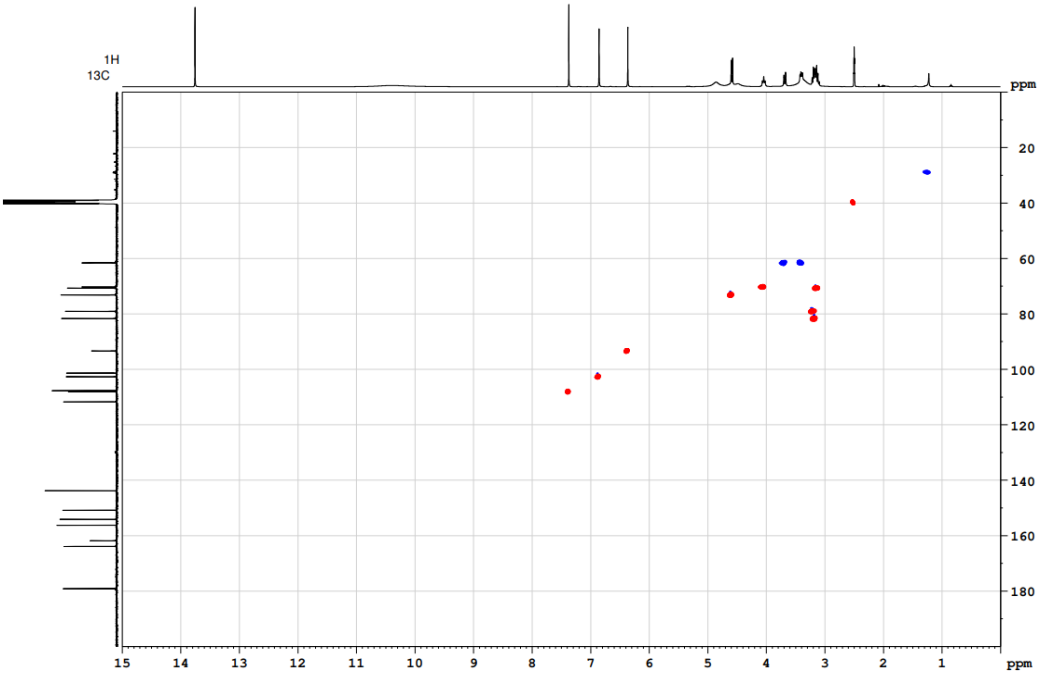

Figure A15. HSQC spectrum of **18** in DMSO-d_6.

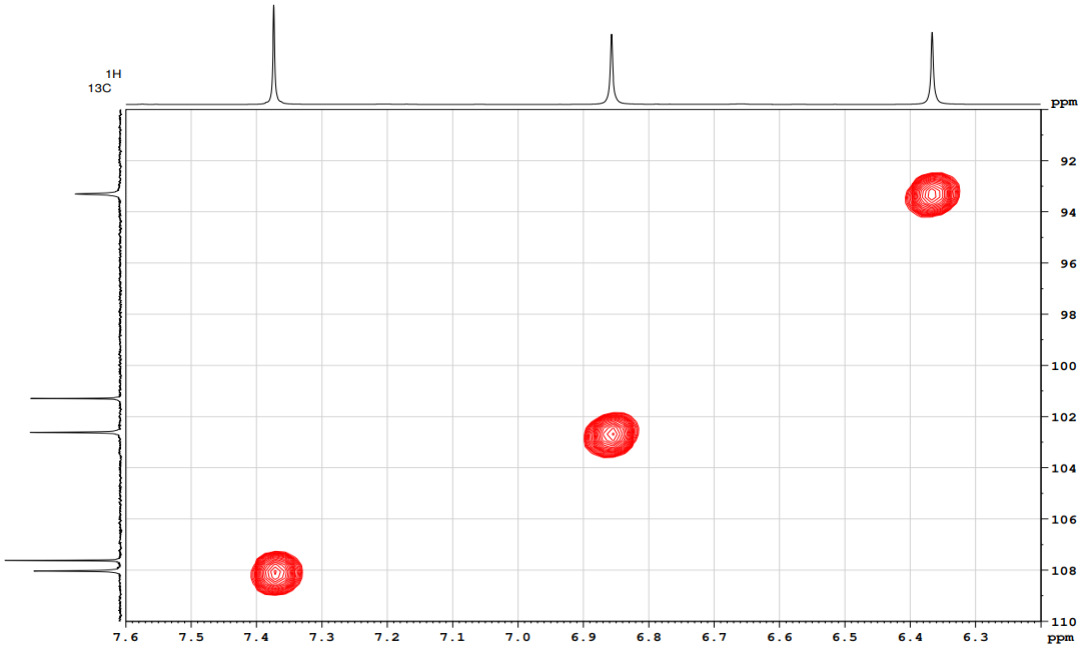

Figure A16. HSQC spectrum (expansion 1) of **18** in DMSO-d_6.

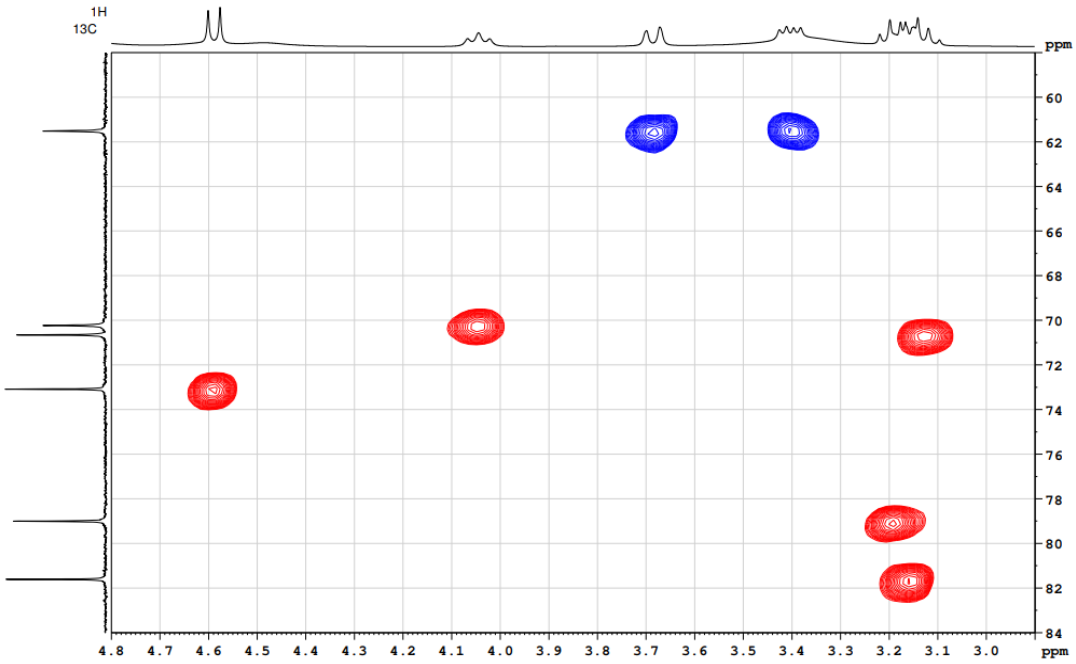

Figure A17. HSQC spectrum (expansion 2) of **18** in DMSO-d_6.

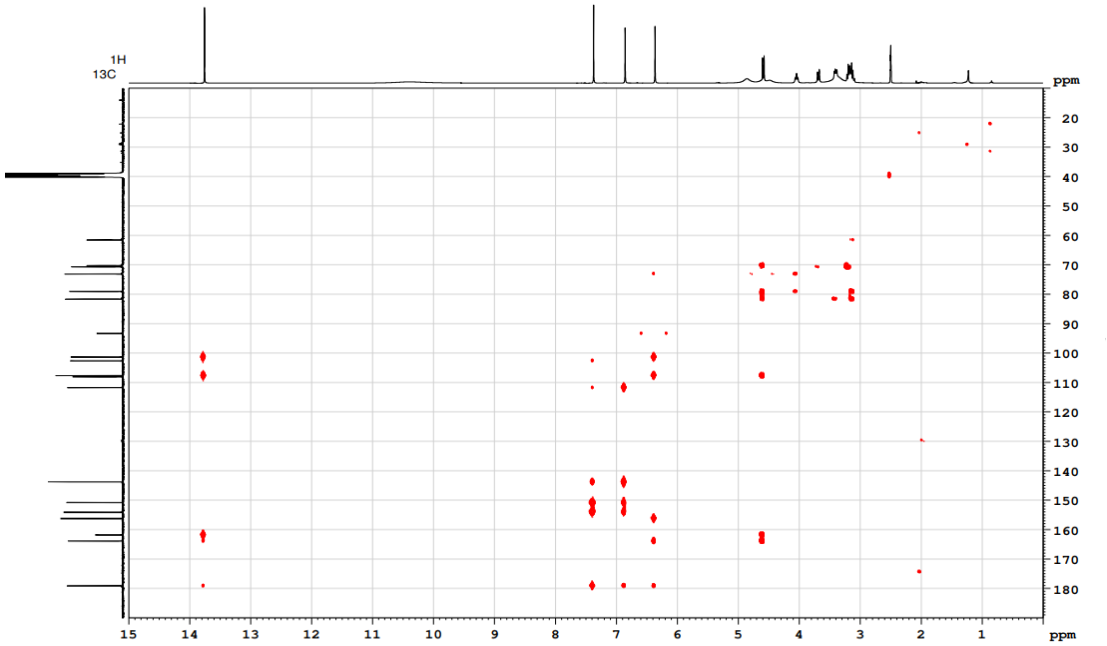

Figure A18. HMBC spectrum of **18** in DMSO-d_6.

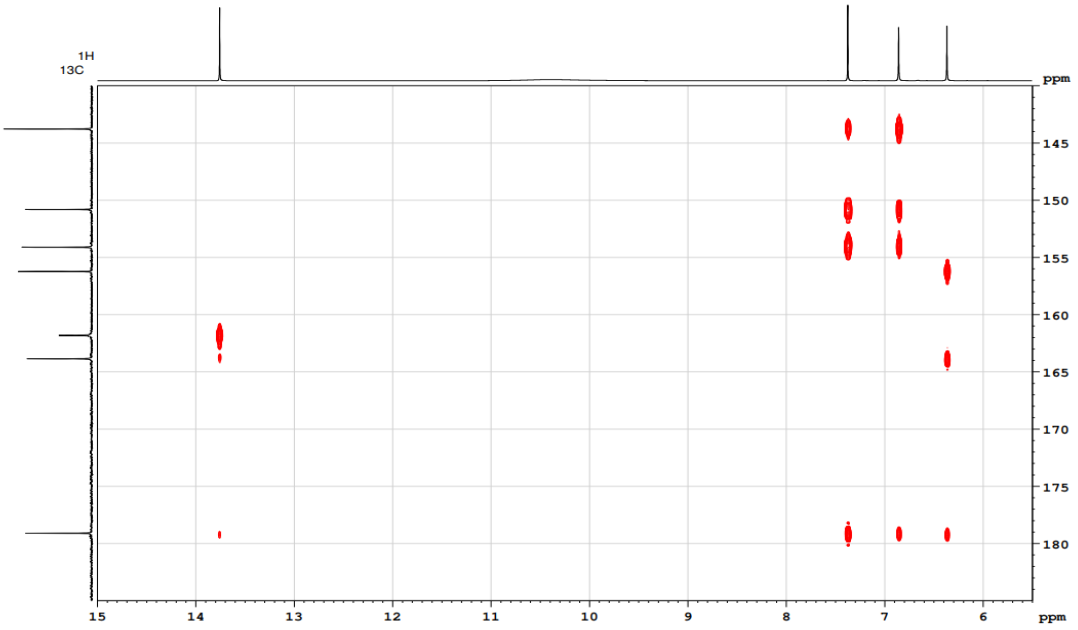

Figure A19. HMBC spectrum (expansion 1) of **18** in DMSO-d_6.

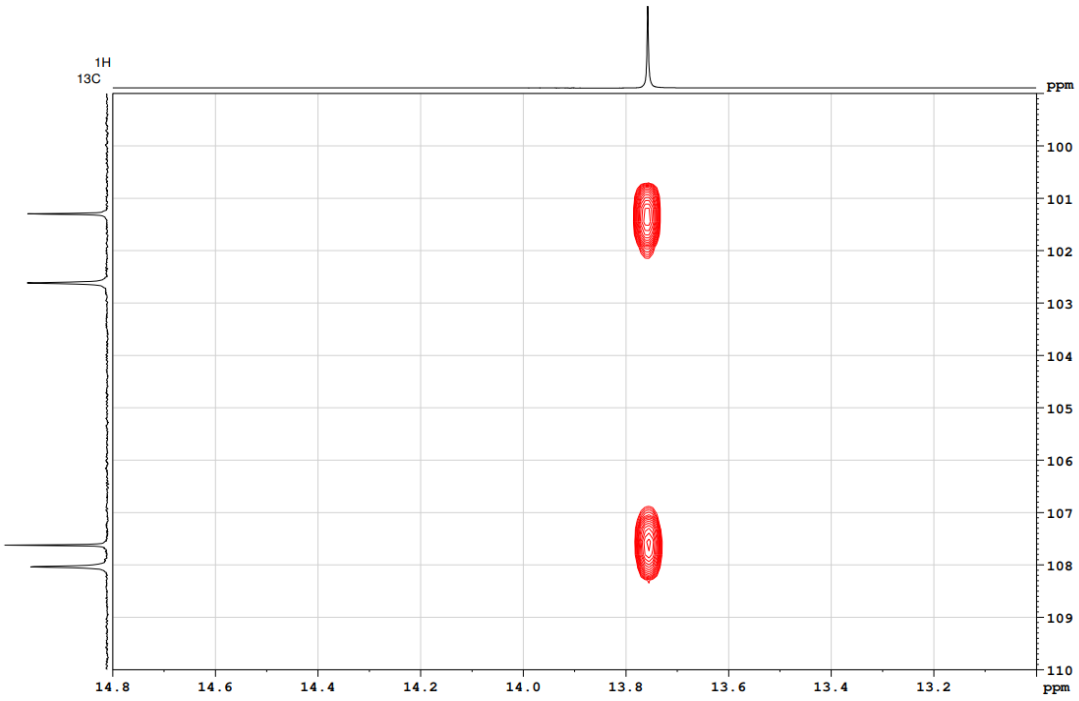

Figure A20. HMBC spectrum (expansion 2) of **18** in DMSO-d_6.

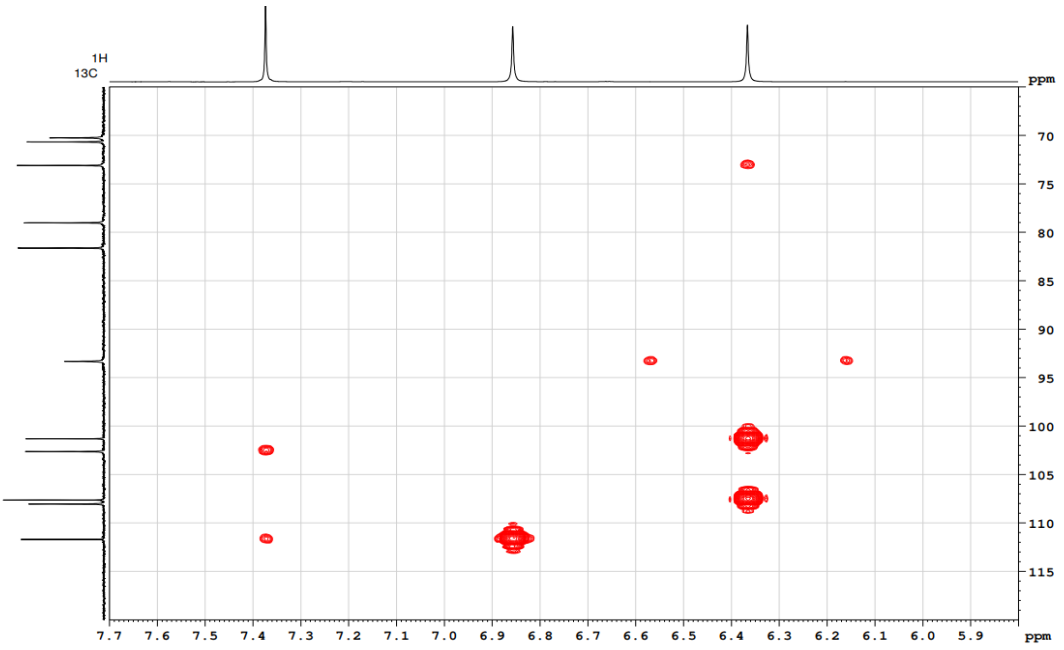

Figure A21. HMBC spectrum (expansion 3) of **18** in DMSO-d_6.

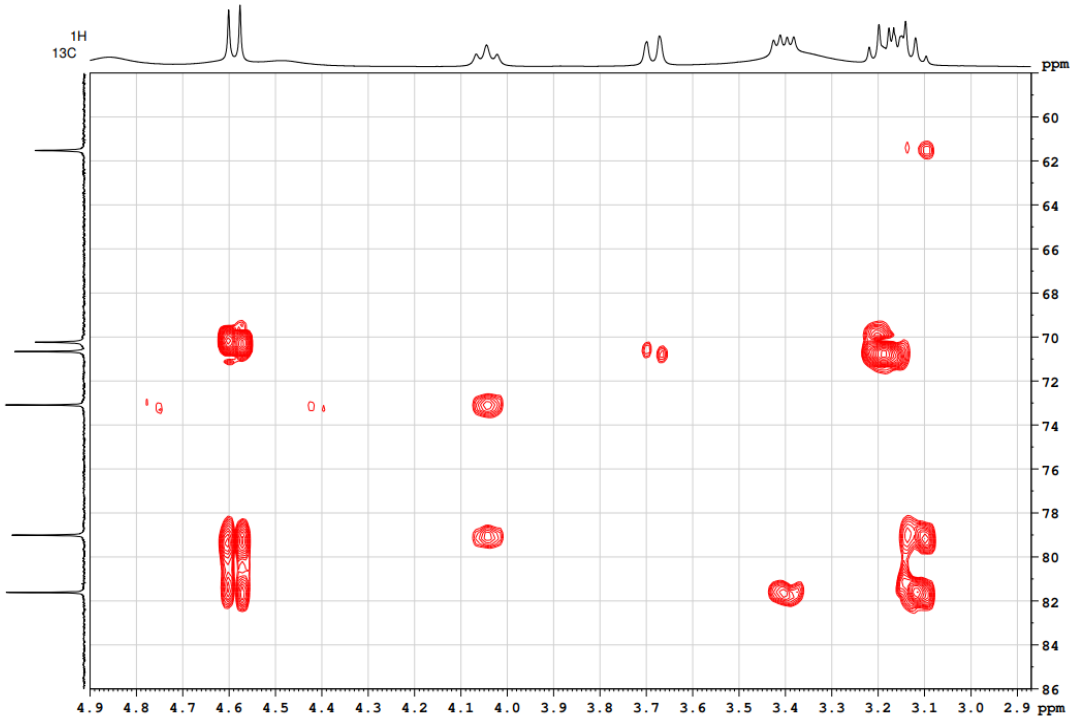

Figure A22. HMBC spectrum (expansion 4) of **18** in DMSO-d_6.

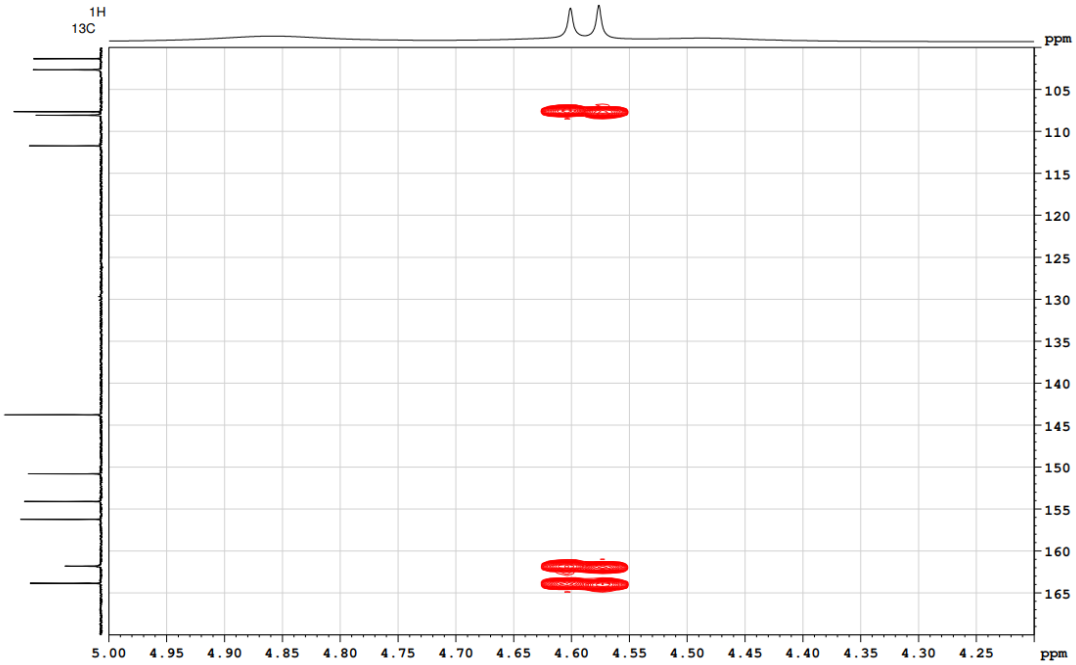

Figure A23. HMBC spectrum (expansion 5) of **18** in DMSO-d_6.

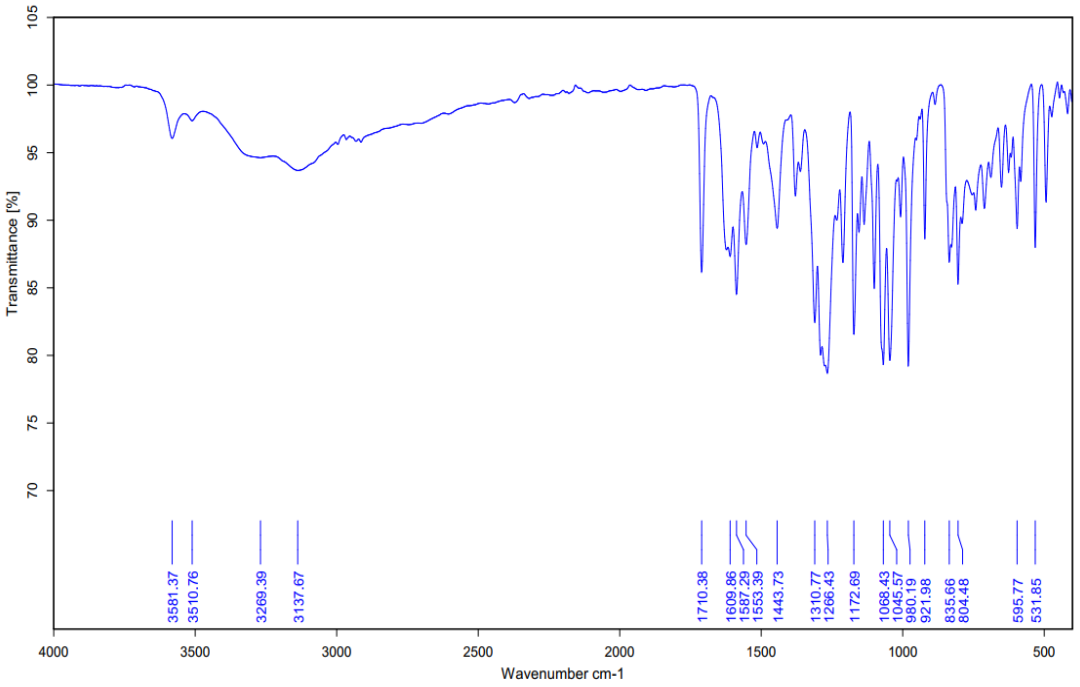

Figure A24. FTIR spectrum of compound **40**.

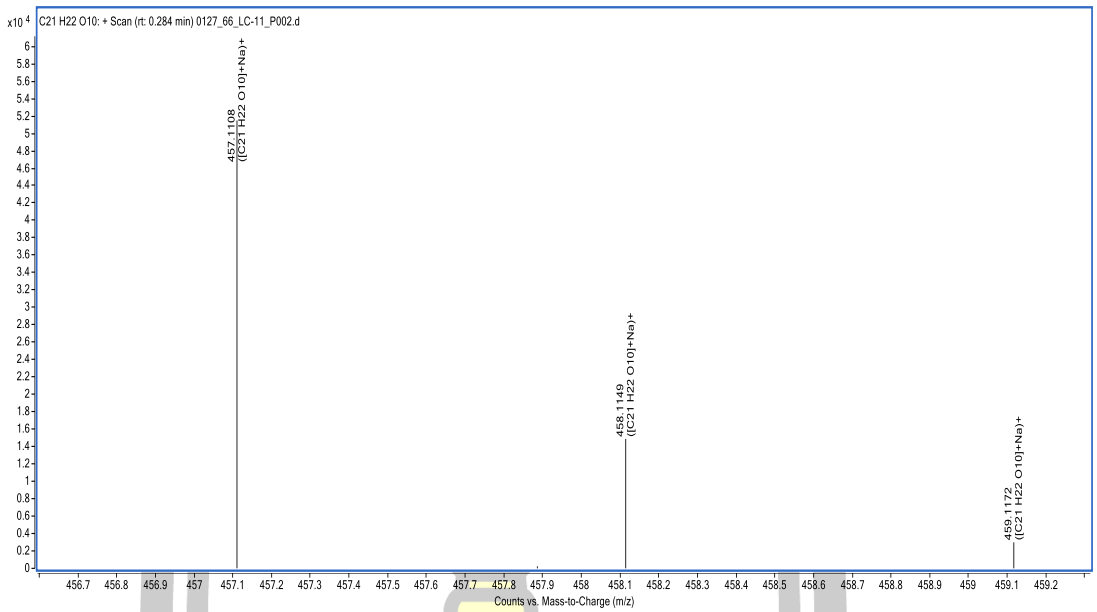

Figure A25. HRESIMS spectrum (positive mode) of compound **40**.

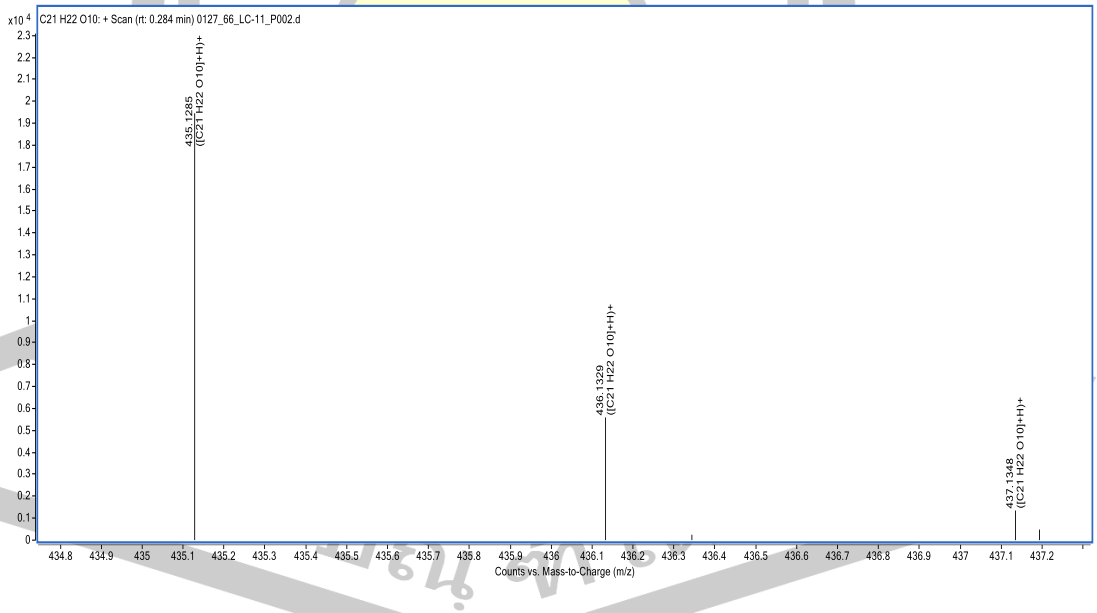

Figure A26. HRESIMS spectrum (positive mode) of compound **40**.

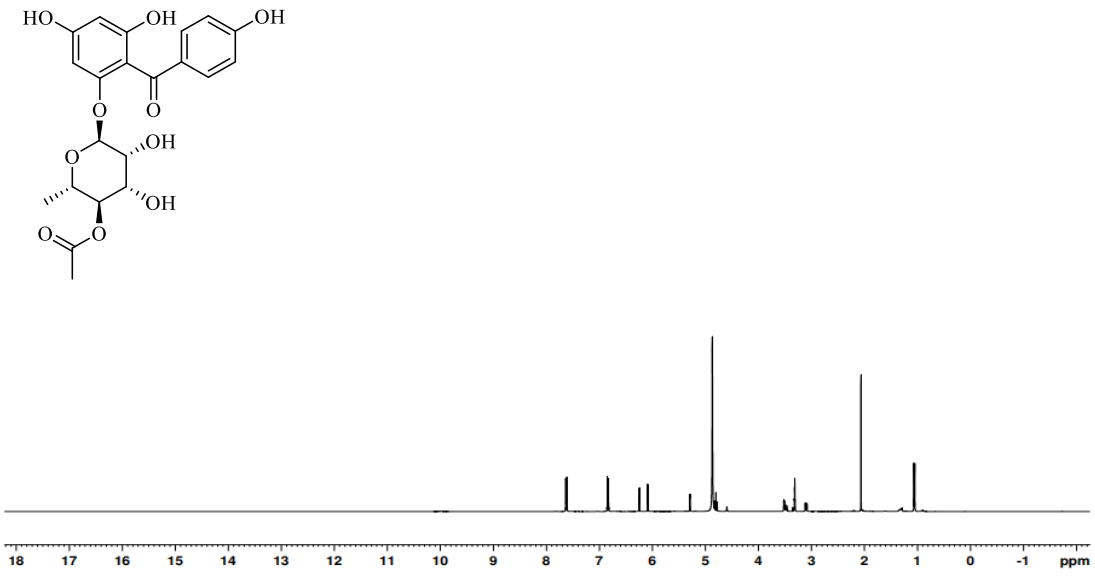

Figure A27. ^{1}H NMR spectrum of **40** (CD_3OD, 400 MHz).

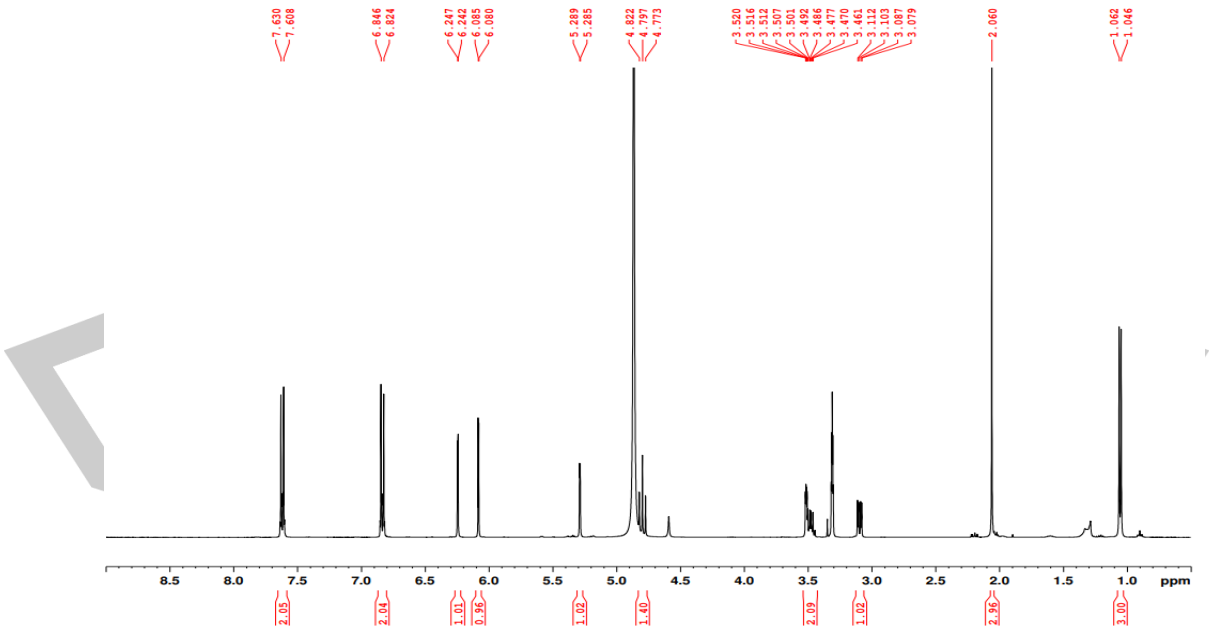

Figure A28. ^{1}H NMR spectrum (expansion 1) of **40** (CD_3OD, 400 MHz).

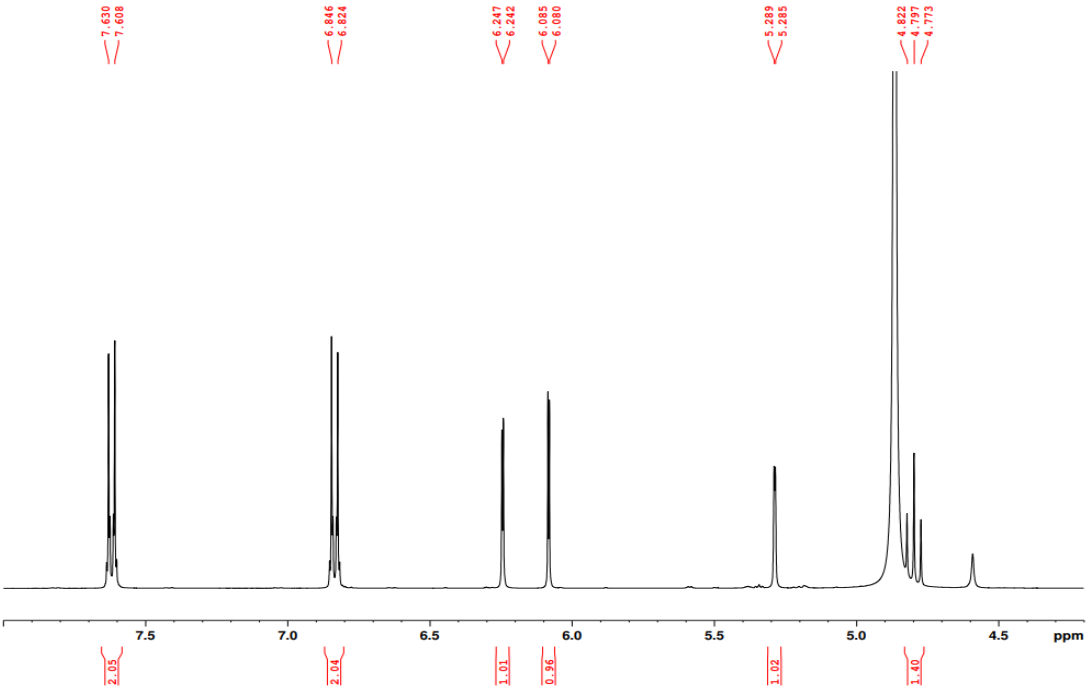

Figure A29. ^{1}H NMR spectrum (expansion 2) of **40** (CD_3OD, 400 MHz).

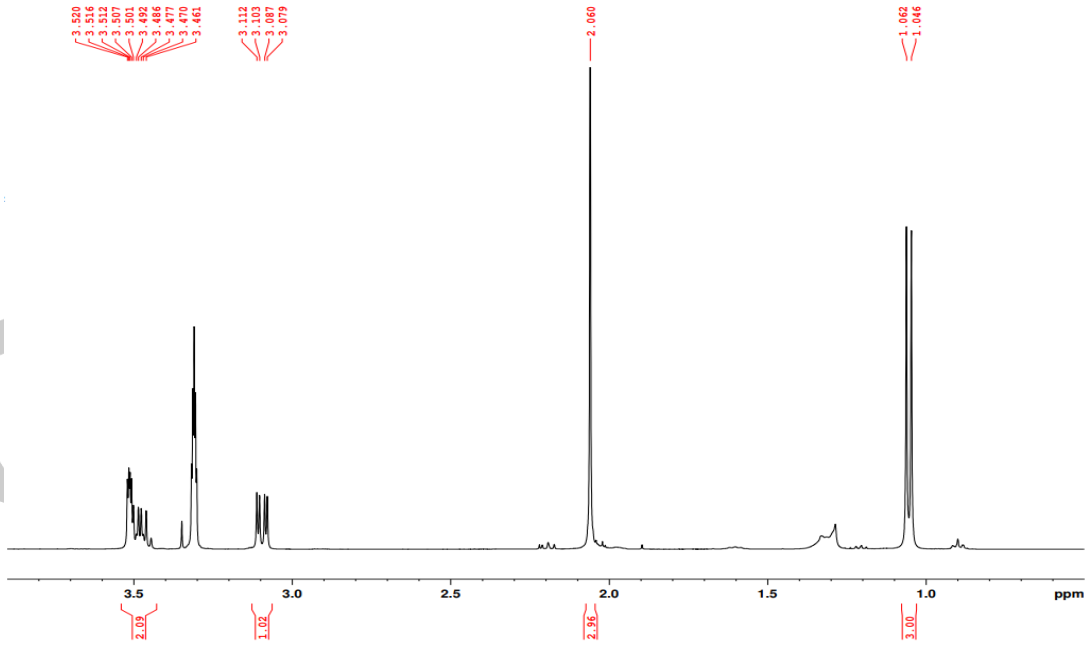

Figure A30. ^{1}H NMR spectrum (expansion 3) of **40** (CD_3OD, 400 MHz).

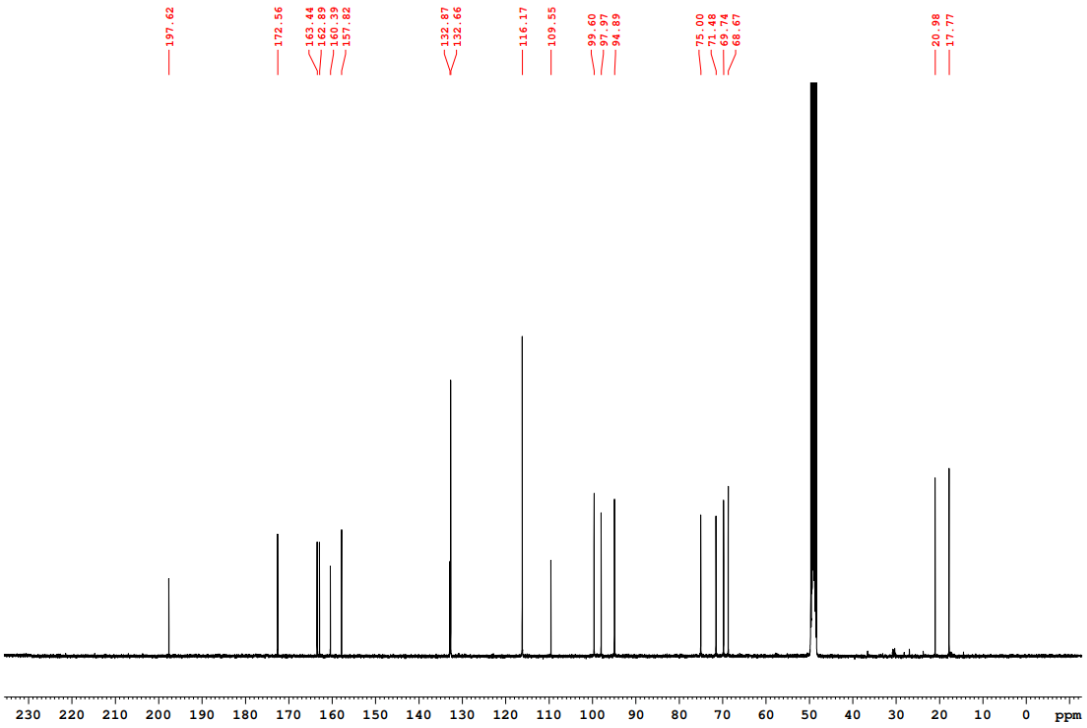

Figure A31. ^{13}C NMR spectrum of **40** (CD_3OD, 100 MHz).

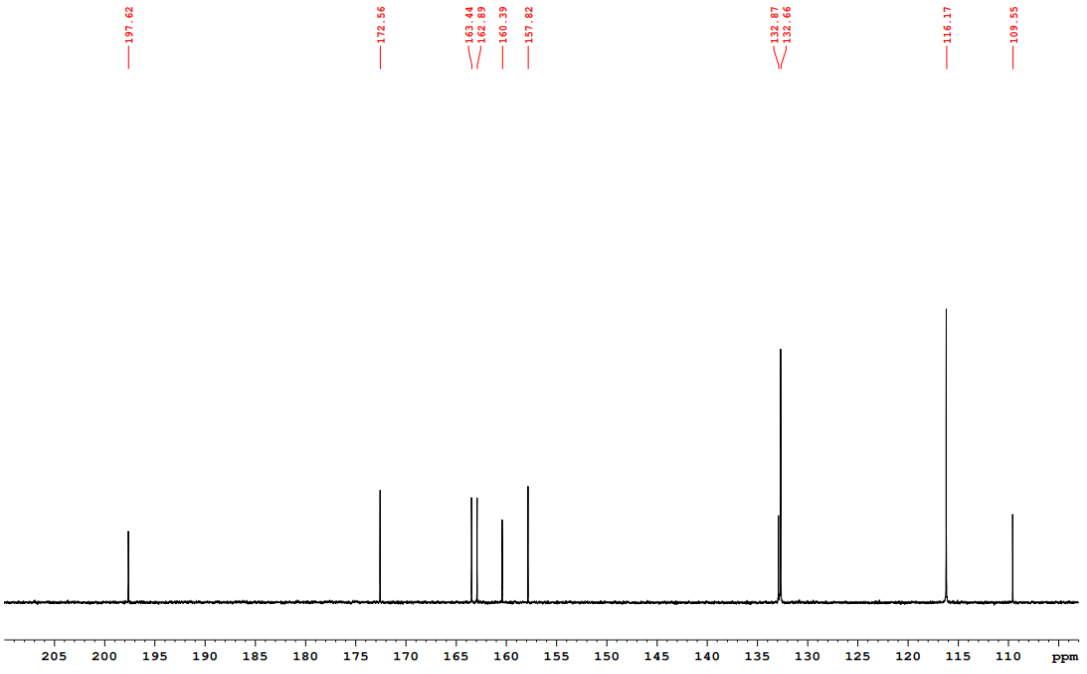

Figure A32. ^{13}C NMR spectrum (expansion 1) of **40** (CD_3OD, 100 MHz)

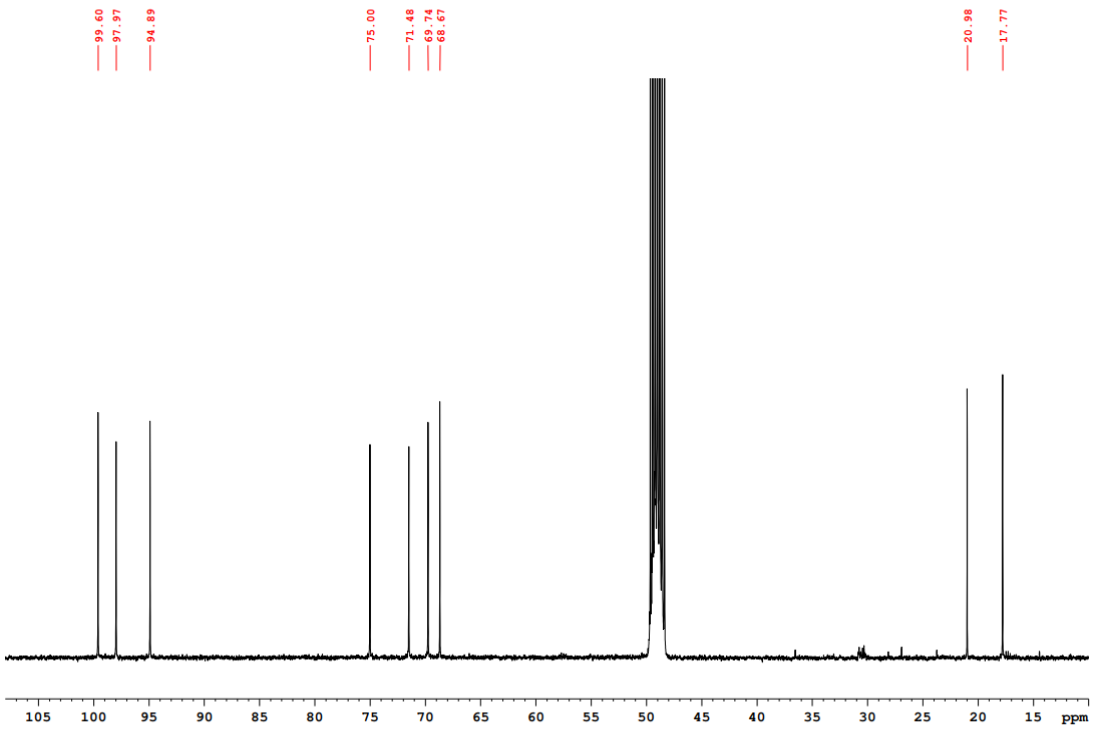

Figure A33. ^{13}C NMR spectrum (expansion 2) of **40** (CD_3OD, 100 MHz).

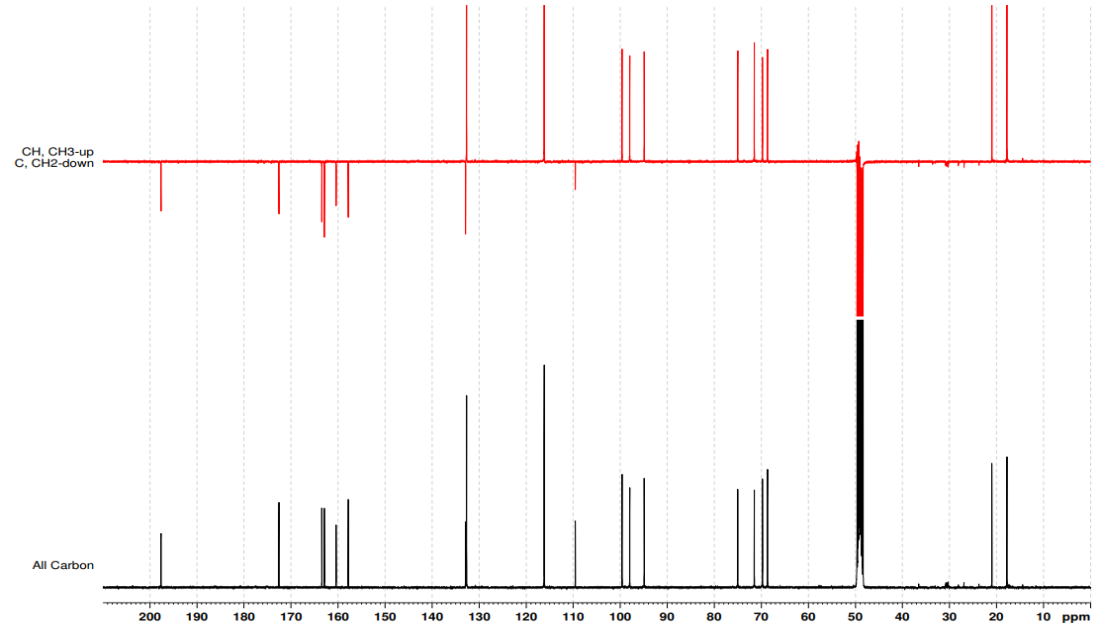

Figure A34. DEPT-135 spectrum of **40** in CD_3OD.

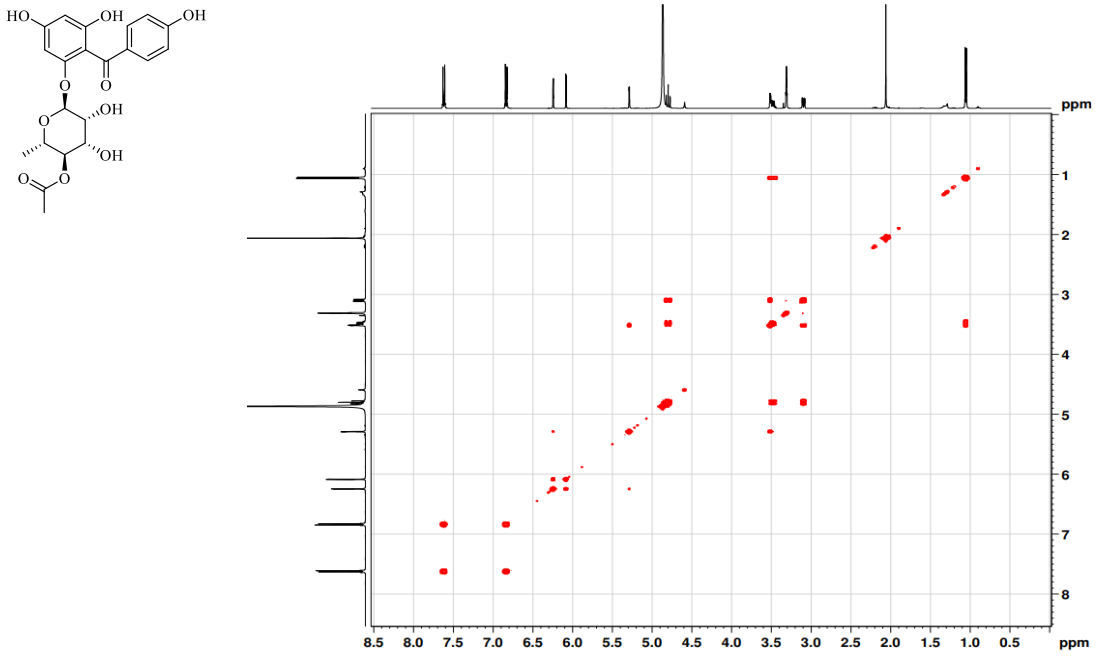

Figure A35. COSY spectrum of **40** in CD_3OD.

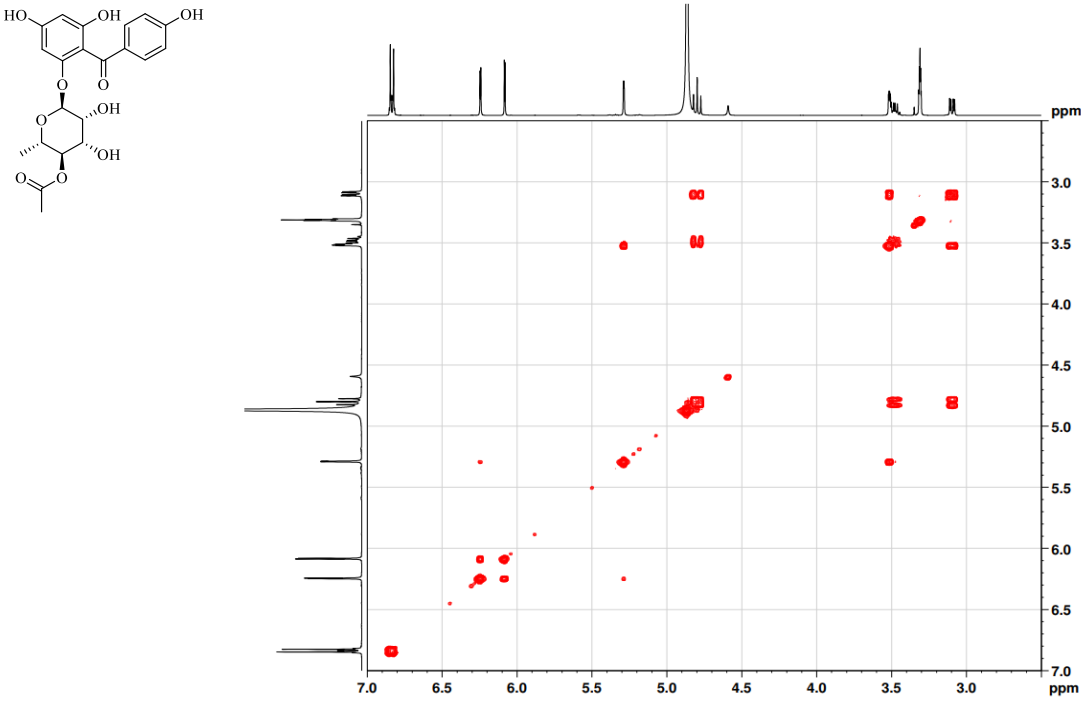

Figure A36. COSY spectrum (expansion 1) of **40** in CD_3OD.

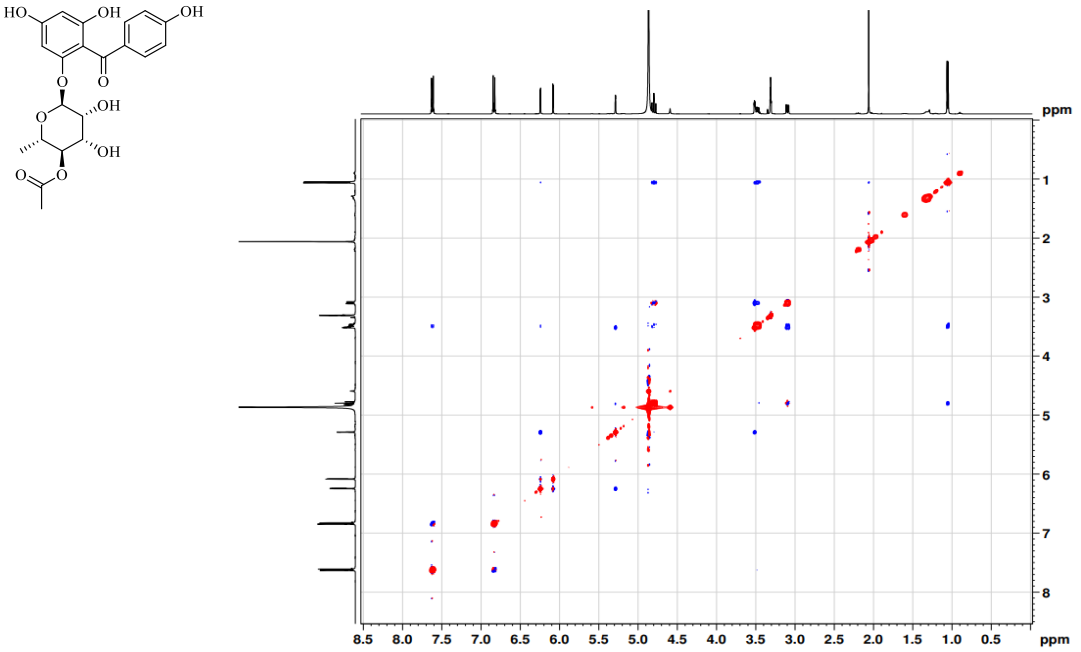

Figure A37. NOESY spectrum of **40** in CD_3OD.

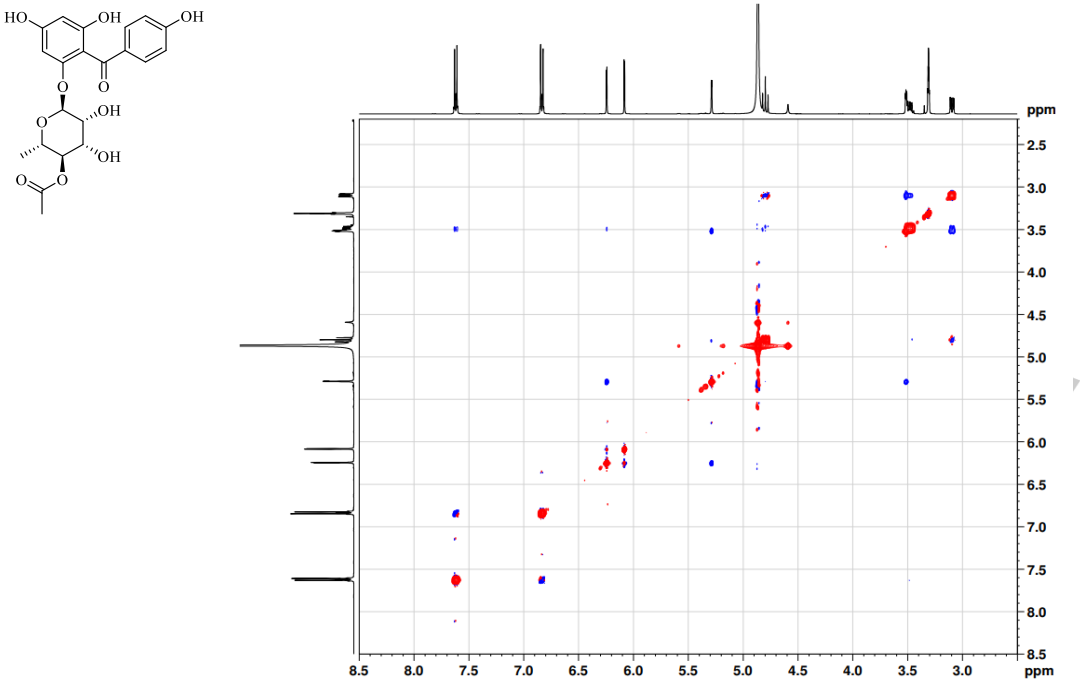

Figure A38. NOESY spectrum (expansion 1) of **40** in CD_3OD.

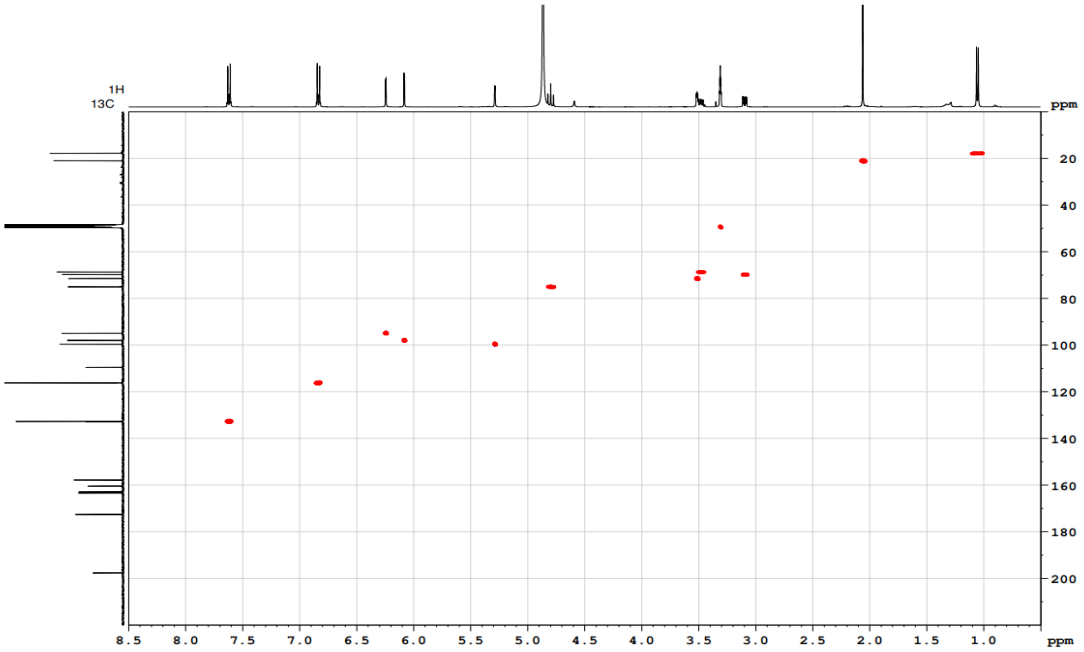

Figure A39. HSQC spectrum of **40** in CD_3OD.

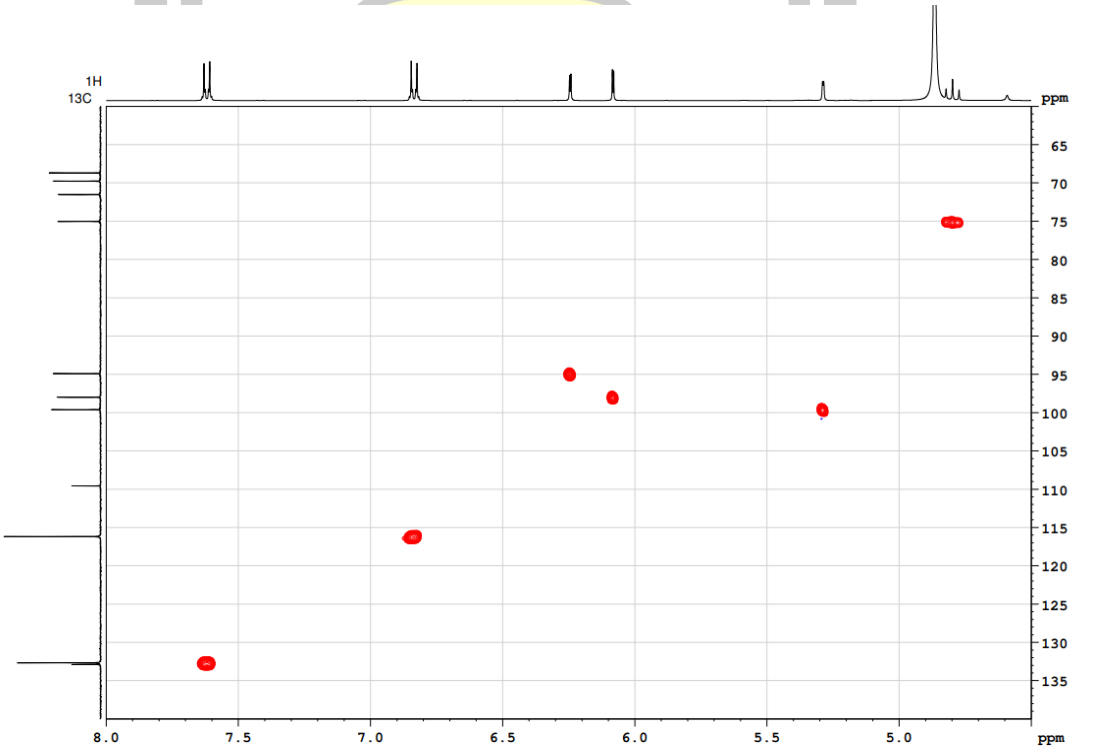

Figure A40. HSQC spectrum (expansion 1) of **40** in CD_3OD.

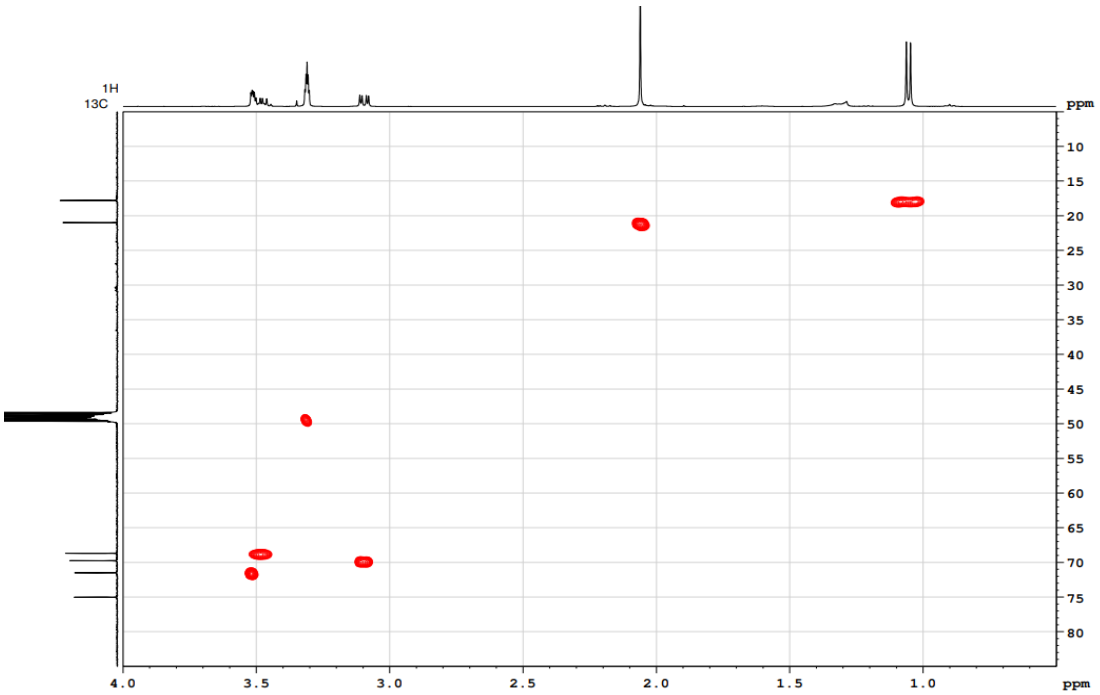

Figure A41. HSQC spectrum (expansion 2) of **40** in CD_3OD.

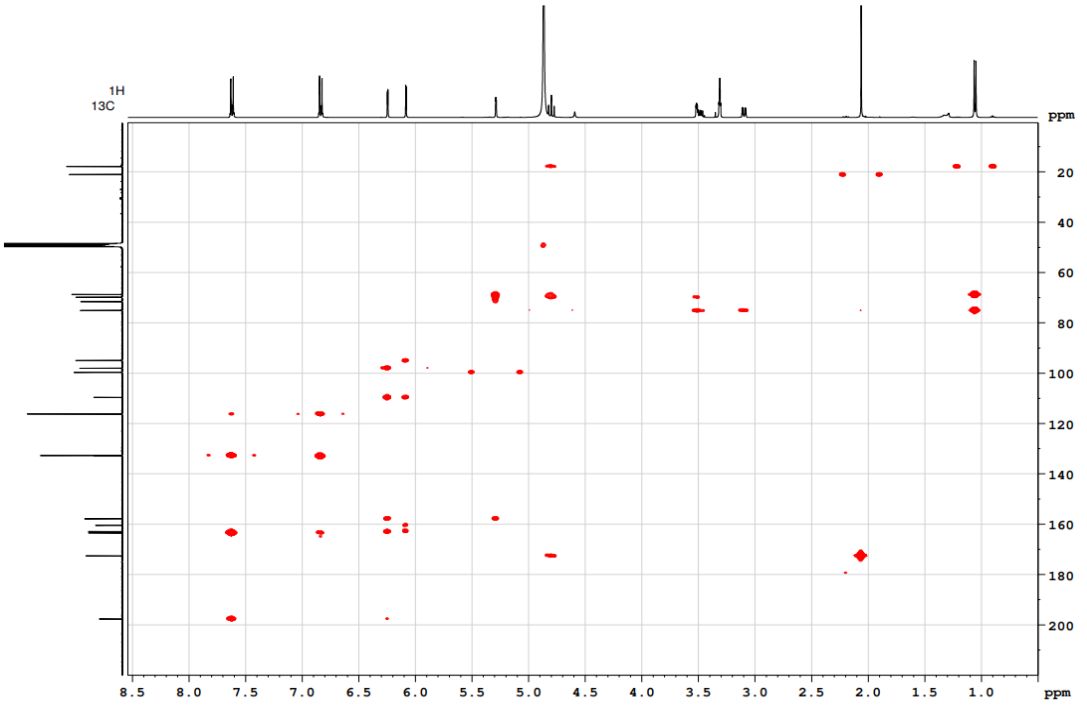

Figure A42. HMBC spectrum of **40** in CD_3OD.

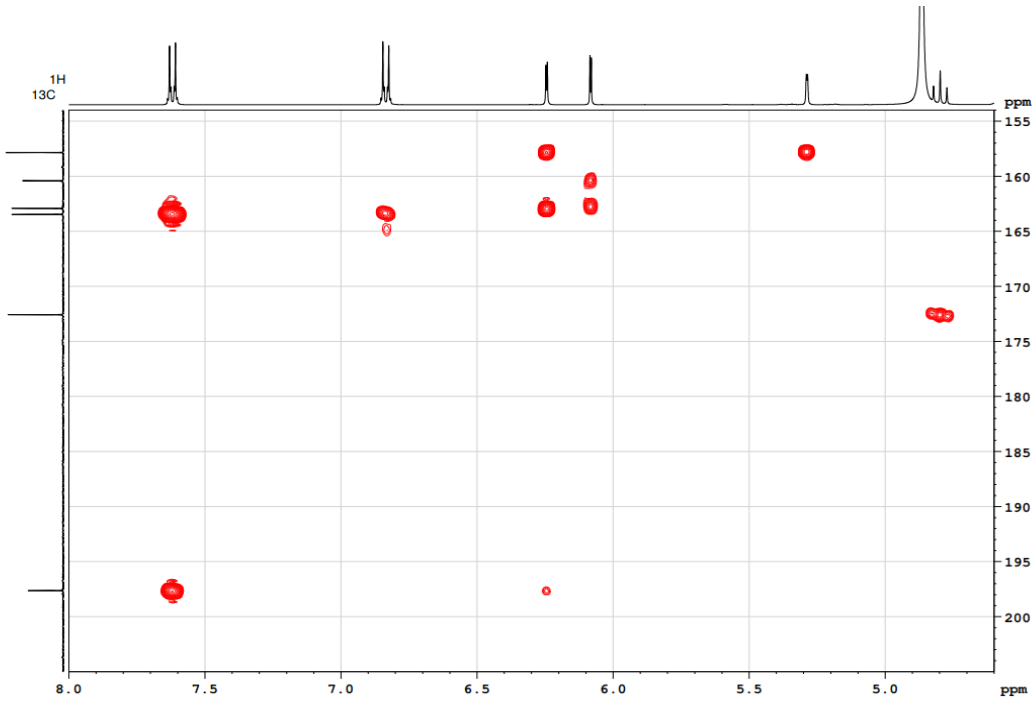

Figure A43. HMBC spectrum (expansion 1) of **40** in CD_3OD.

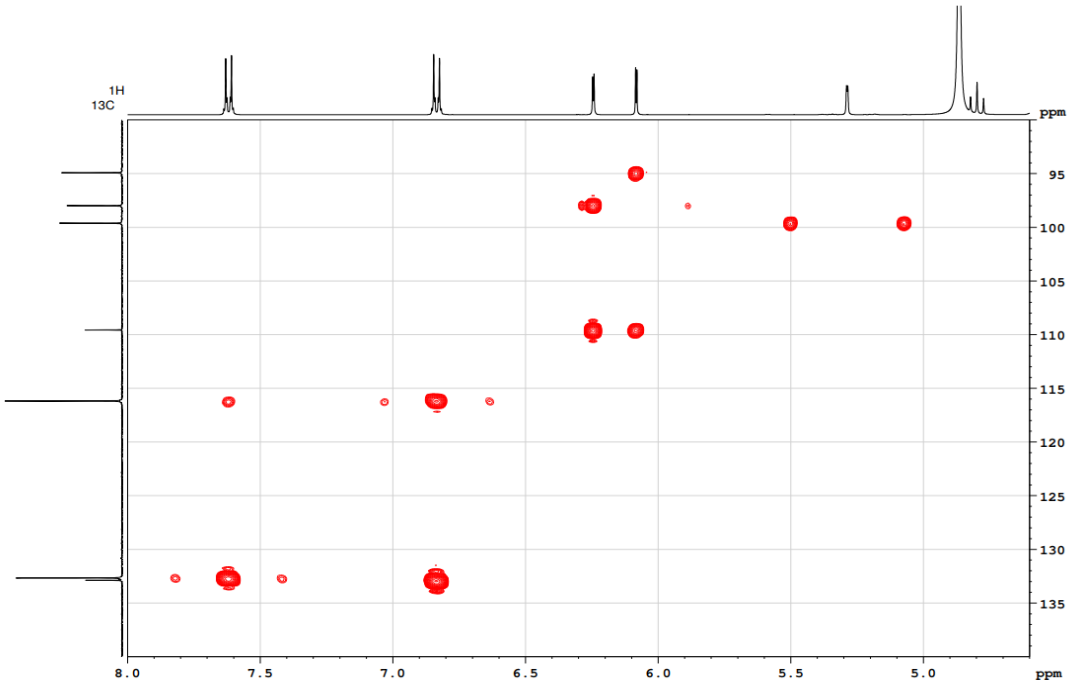

Figure A44. HMBC spectrum (expansion 2) of **40** in CD_3OD.

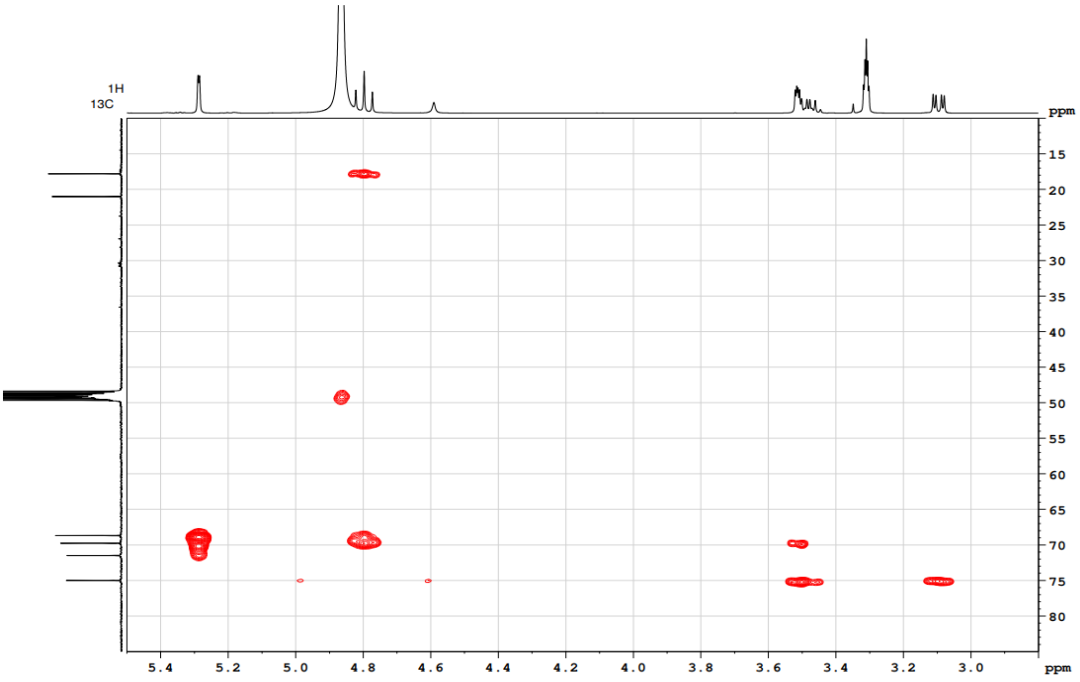

Figure A45. HMBC spectrum (expansion 3) of **40** in CD_3OD.

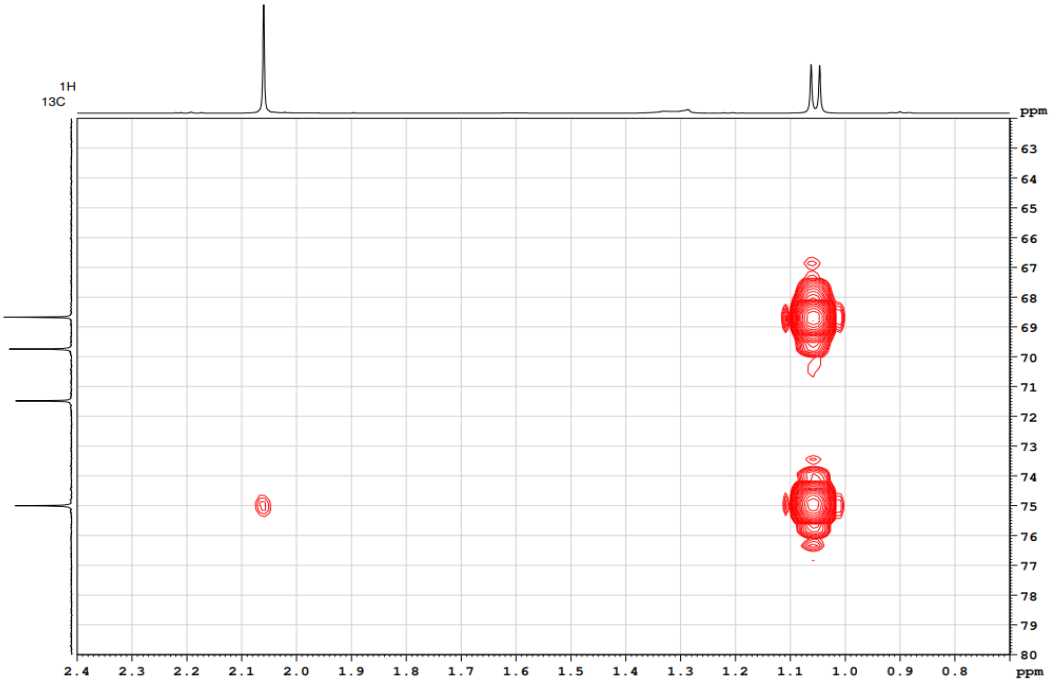

Figure A46. HMBC spectrum (expansion 4) of **40** in CD_3OD.

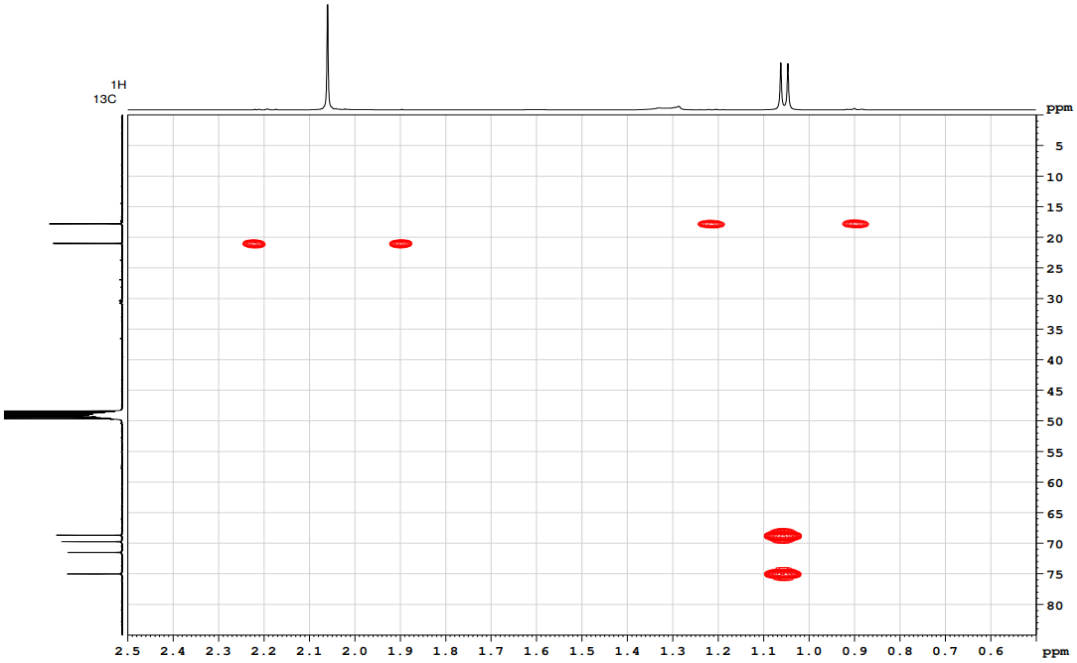

Figure A47. HMBC spectrum (expansion 5) of **40** in CD_3OD.

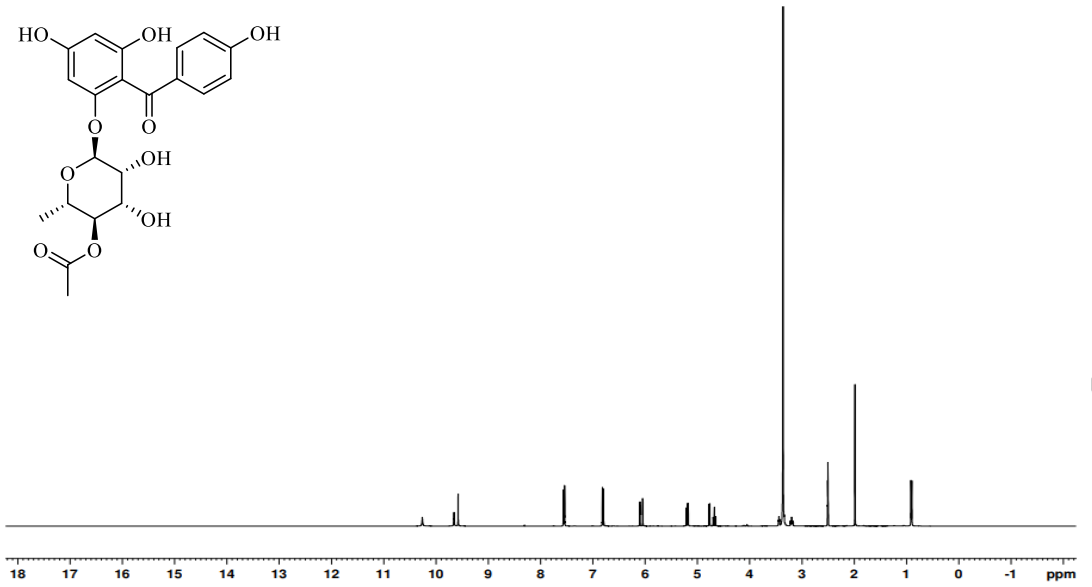

Figure A48. ^{1}H NMR spectrum of **40** (DMSO-d_6, 400 MHz).

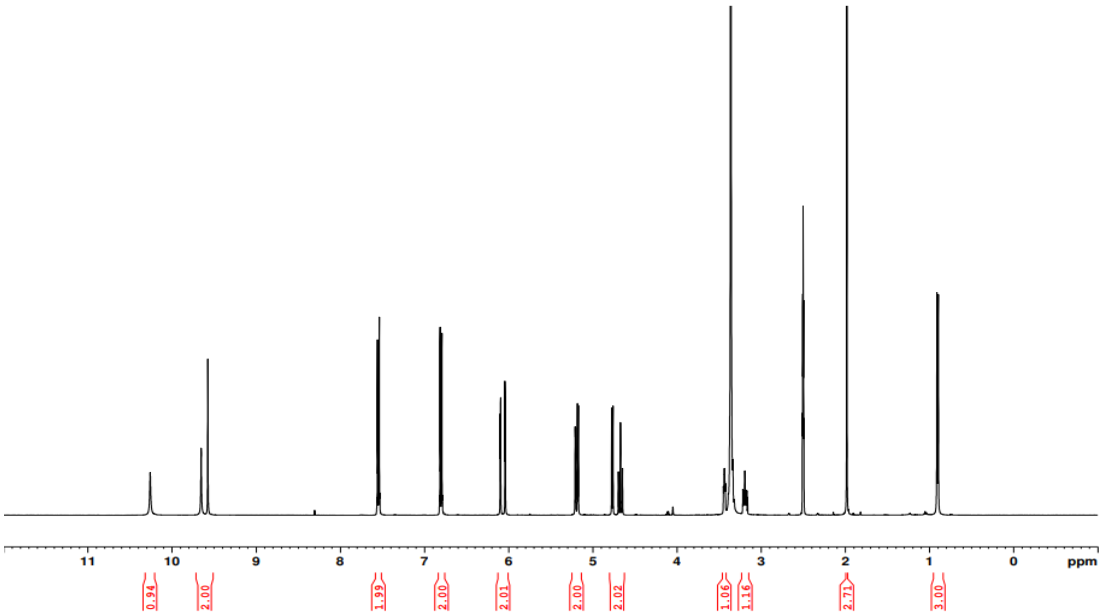

Figure A49. ^{1}H NMR spectrum (expansion 1) of **40** (DMSO-d_6, 400 MHz).

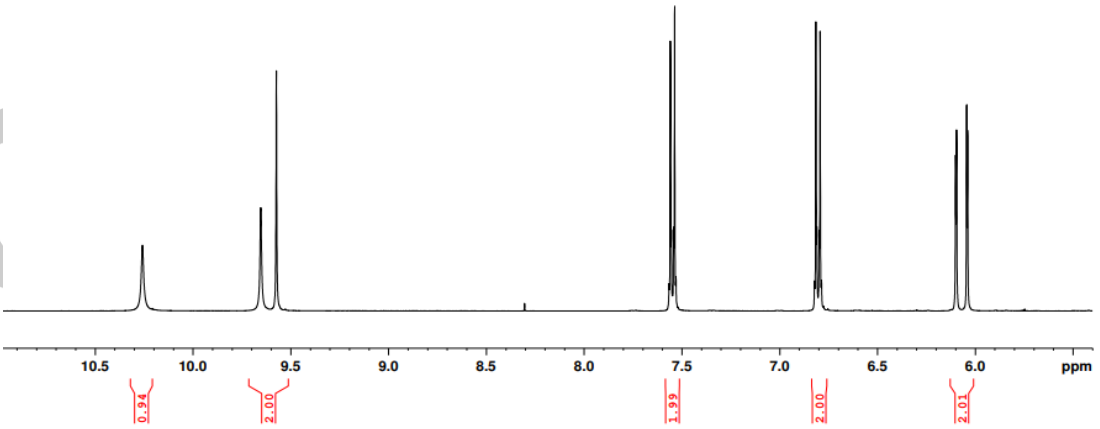

Figure A50. ^{1}H NMR spectrum (expansion 2) of **40** (DMSO-d_6, 400 MHz).

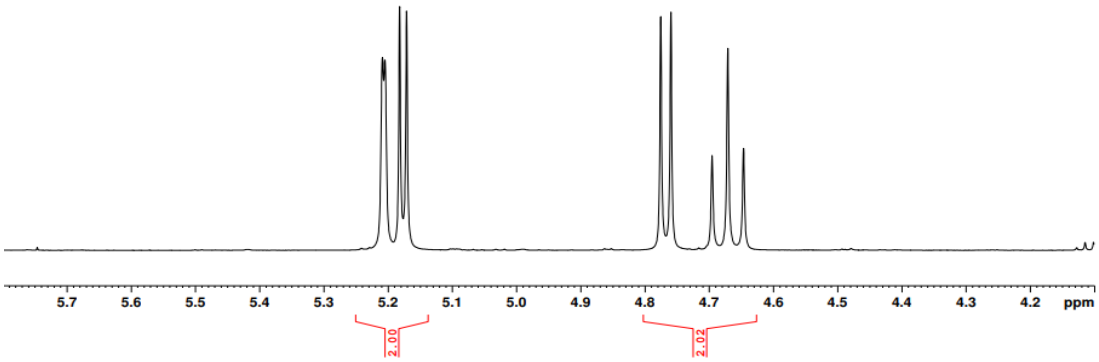

Figure A51. ^{1}H NMR spectrum (expansion 3) of **40** (DMSO-d_6, 400 MHz).

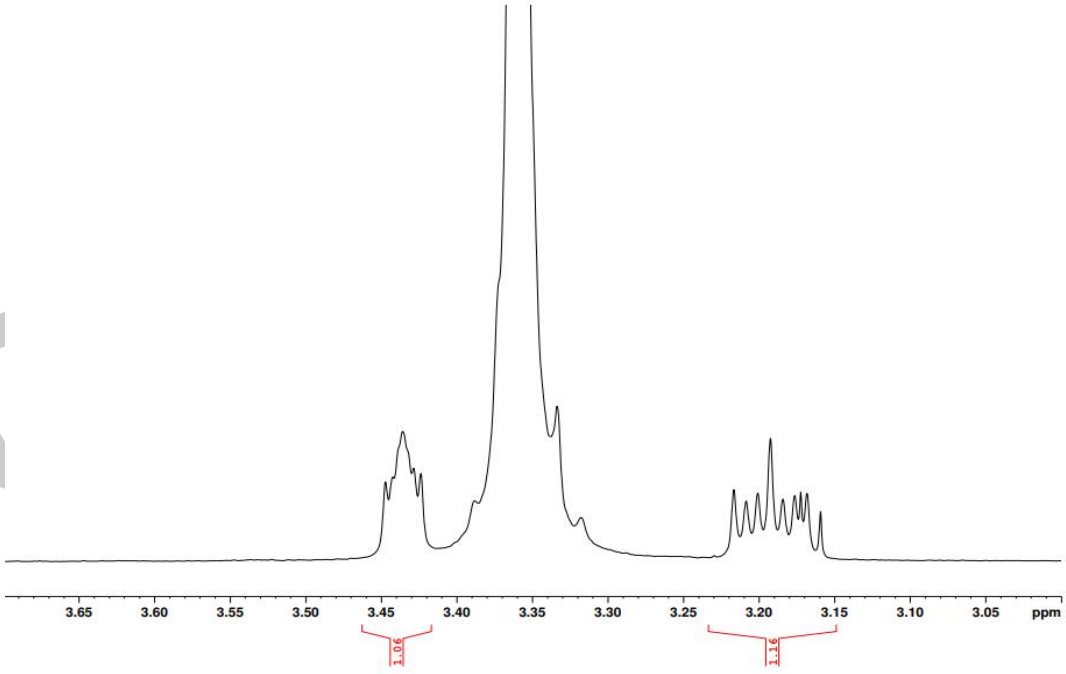

Figure A52. ^{1}H NMR spectrum (expansion 4) of **40** (DMSO-d_6, 400 MHz).

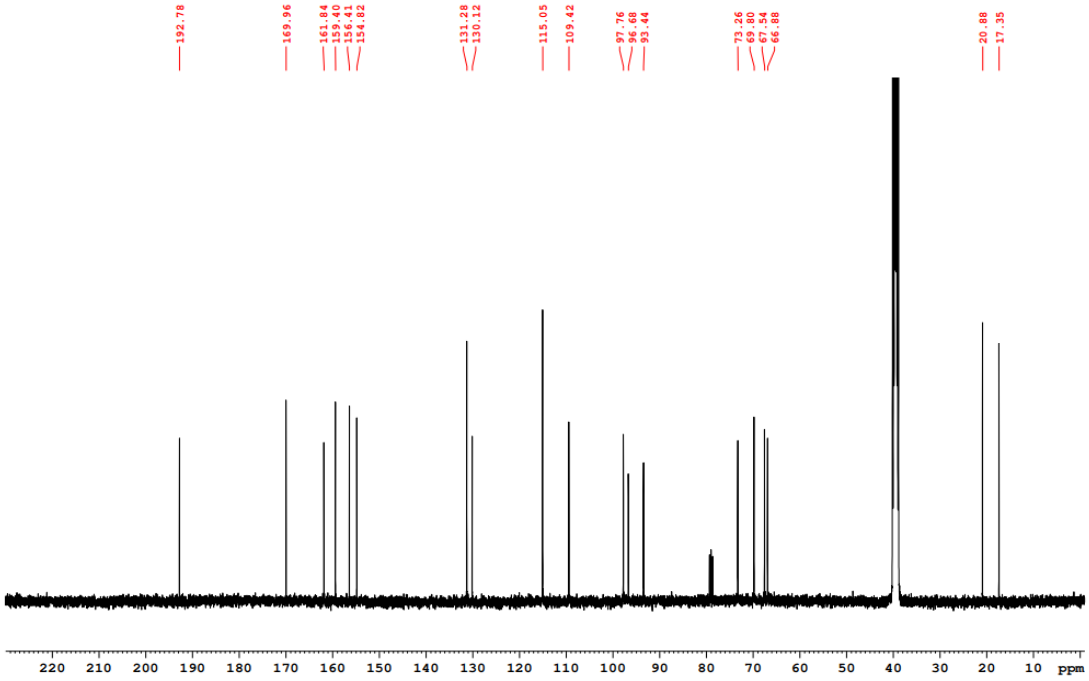

Figure A53. ^{13}C NMR spectrum of **40** (DMSO-d_6, 100 MHz).

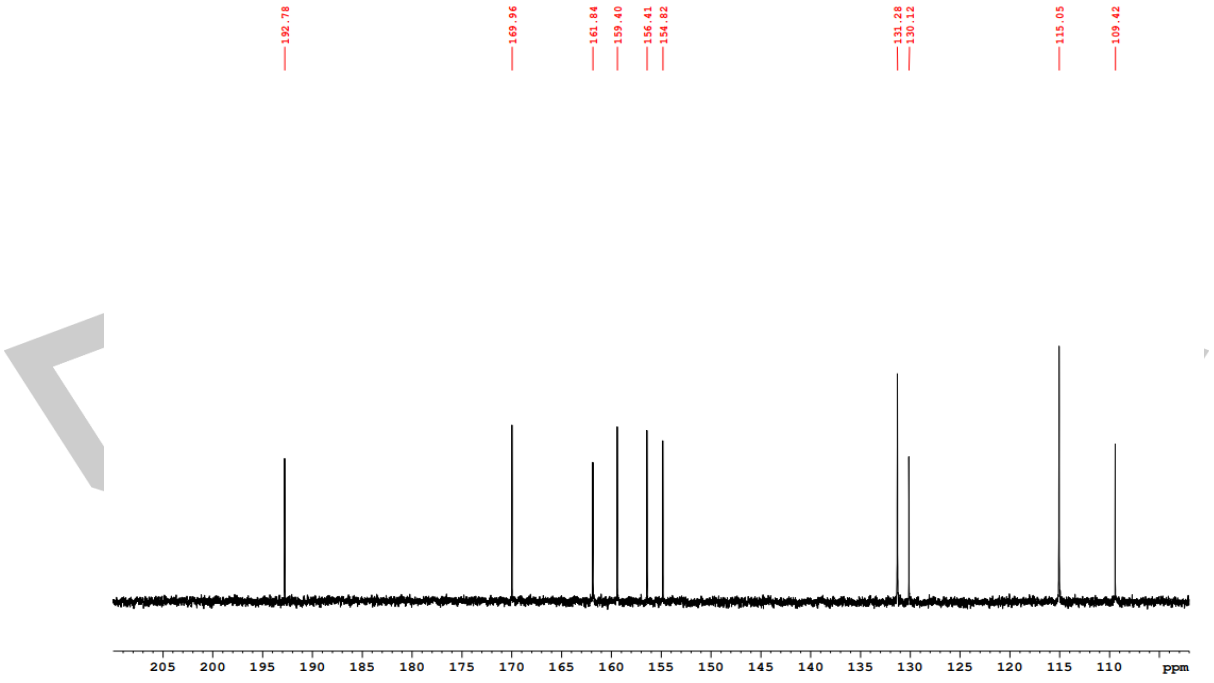

Figure A54. ^{13}C NMR spectrum (expansion 1) of **40** (DMSO-d_6, 100 MHz).

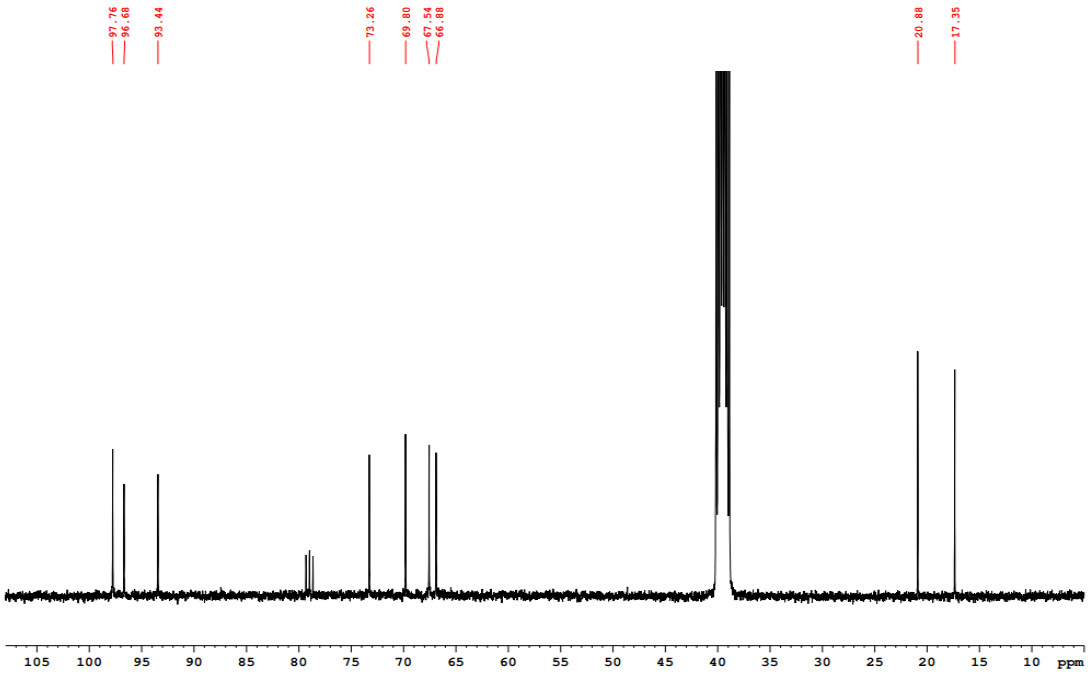

Figure A55. ^{13}C NMR spectrum (expansion 2) of **40** (DMSO-d_6, 100 MHz).

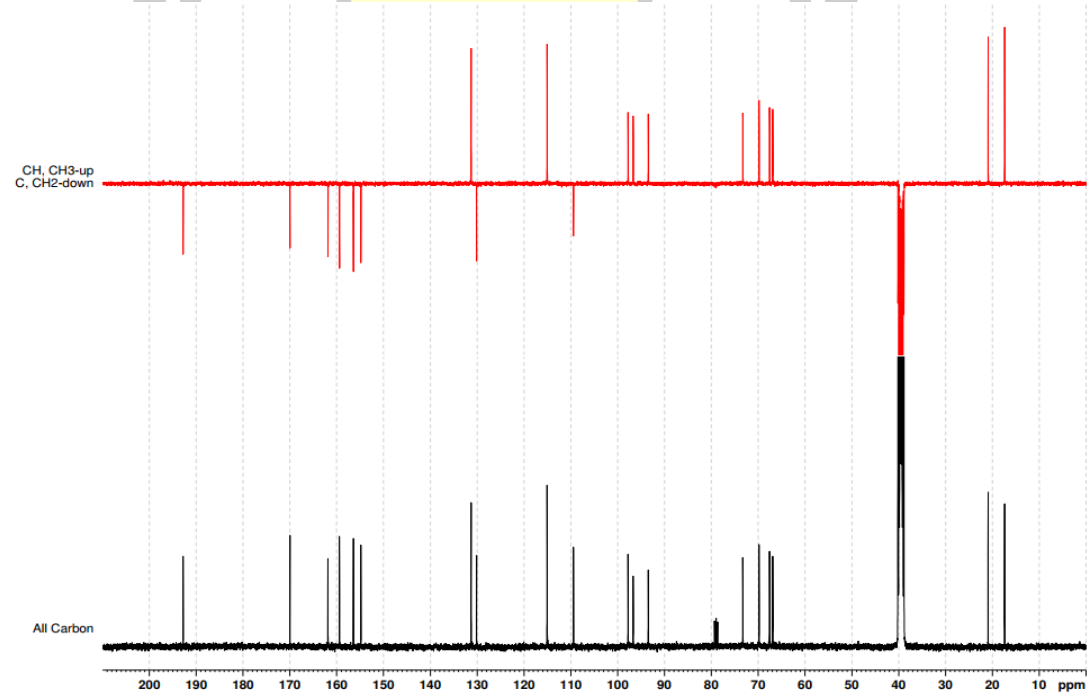

Figure A56. DEPT-135 spectrum of **40** in DMSO-d_6.

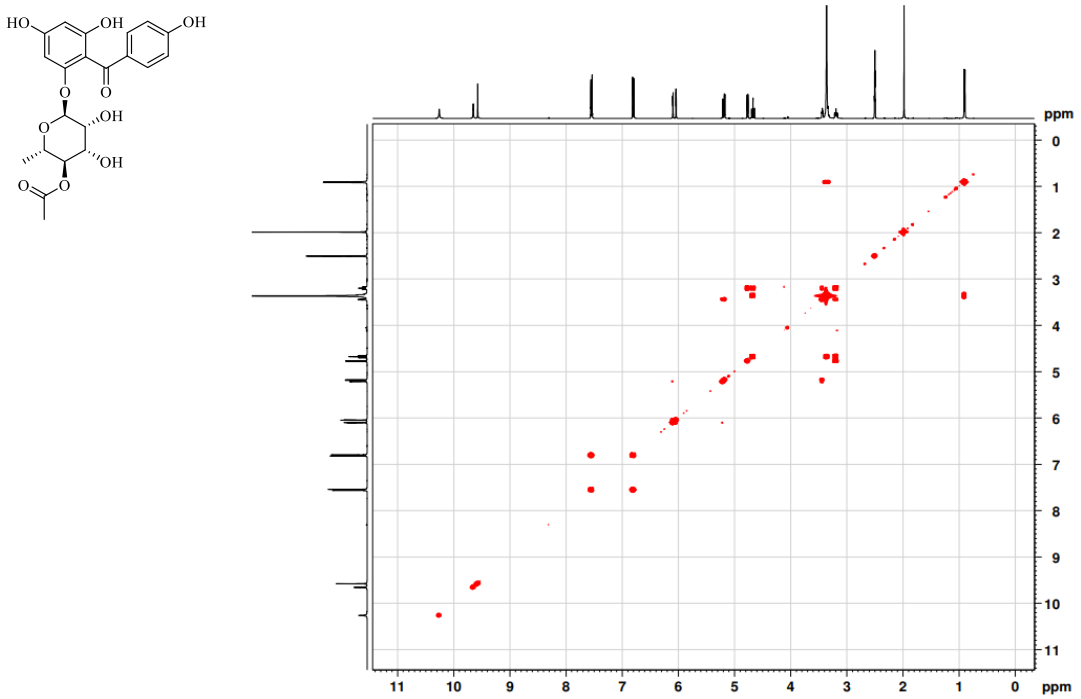

Figure A57. COSY spectrum of **40** in DMSO-d_6.

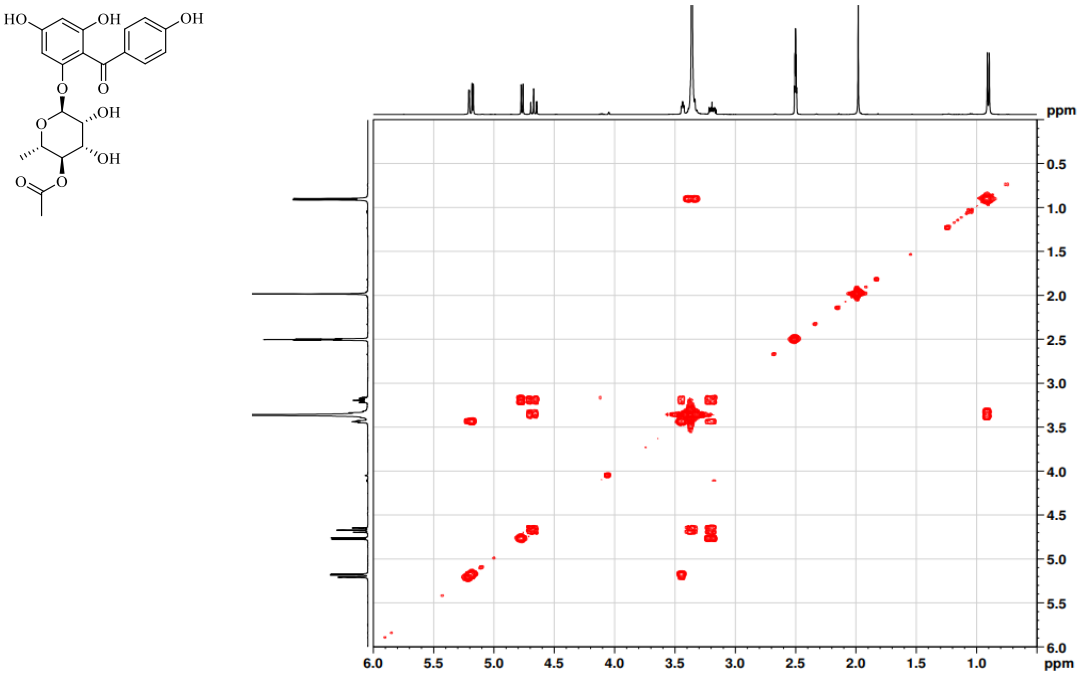

Figure A58. COSY spectrum (expansion 1) of **40** in DMSO-d_6.

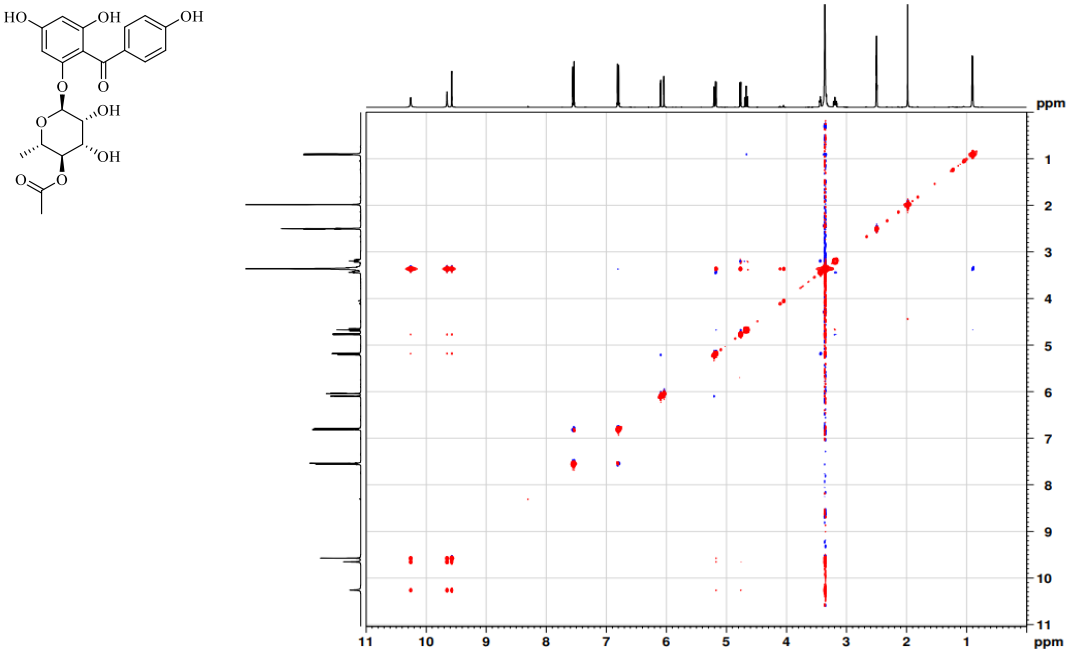

Figure A59. NOESY spectrum of **40** in DMSO-d_6.

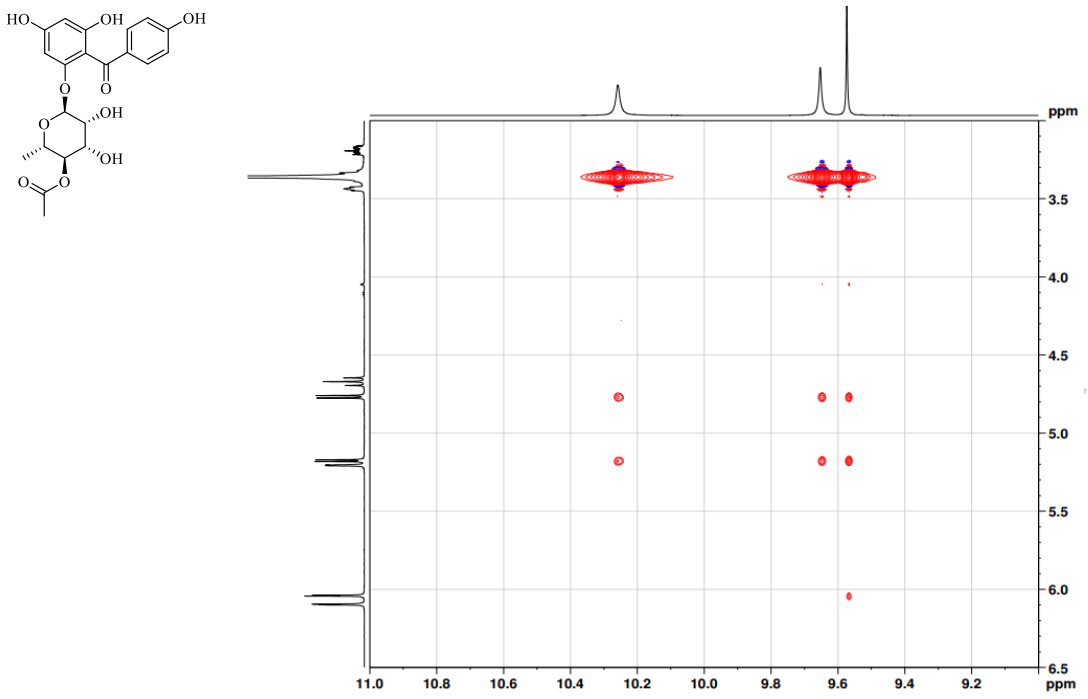

Figure A60. NOESY spectrum (expansion 1) of **40** in DMSO-d_6.

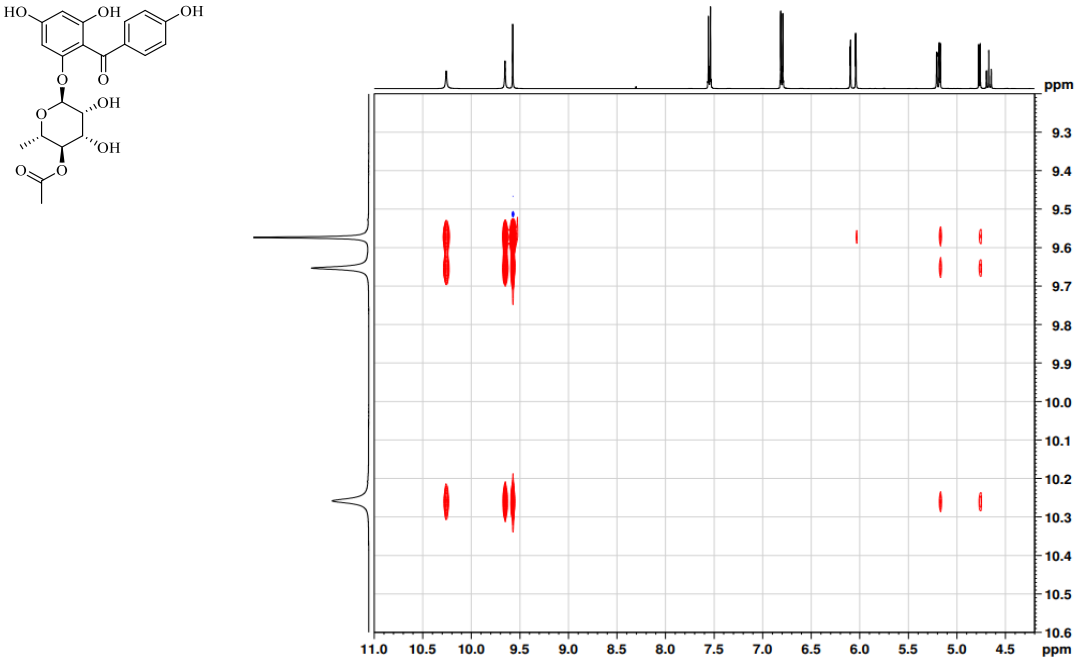

Figure A61. NOESY spectrum (expansion 2) of **40** in DMSO-d_6.

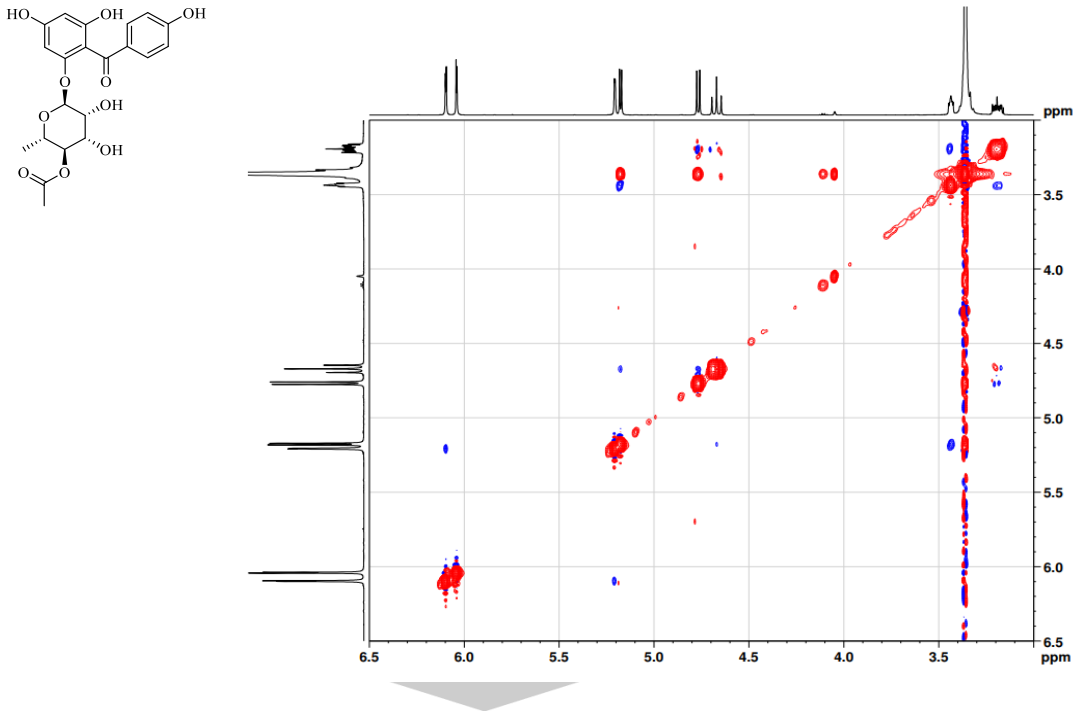

Figure A62. NOESY spectrum (expansion 3) of **40** in DMSO-d_6.

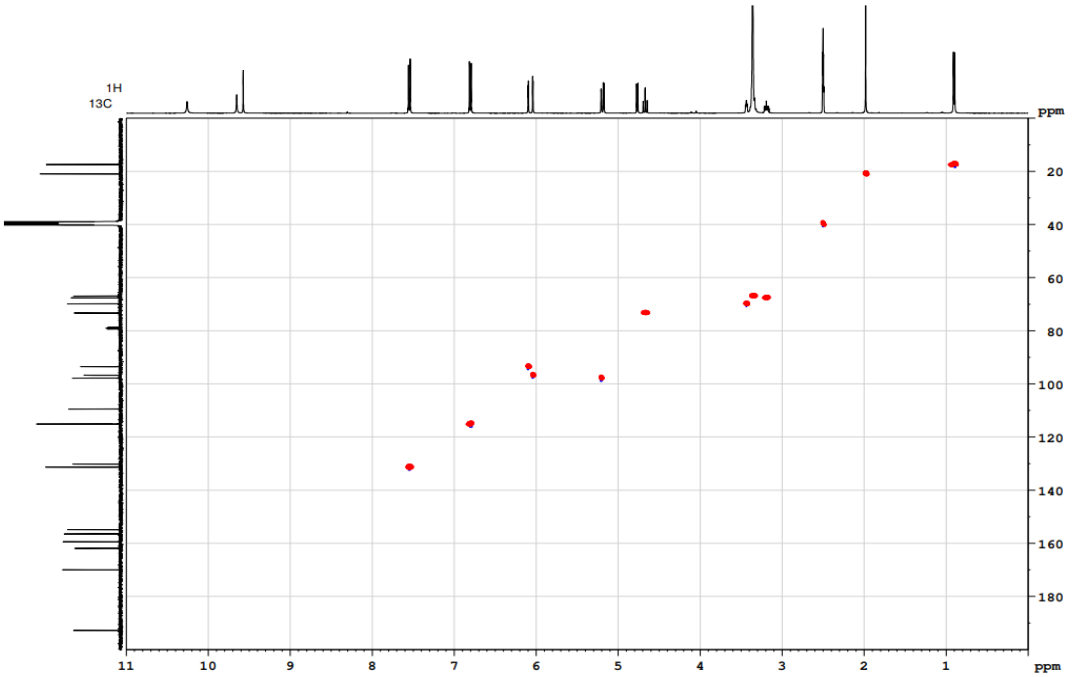

Figure A63. HSQC spectrum of **40** in DMSO-d_6.

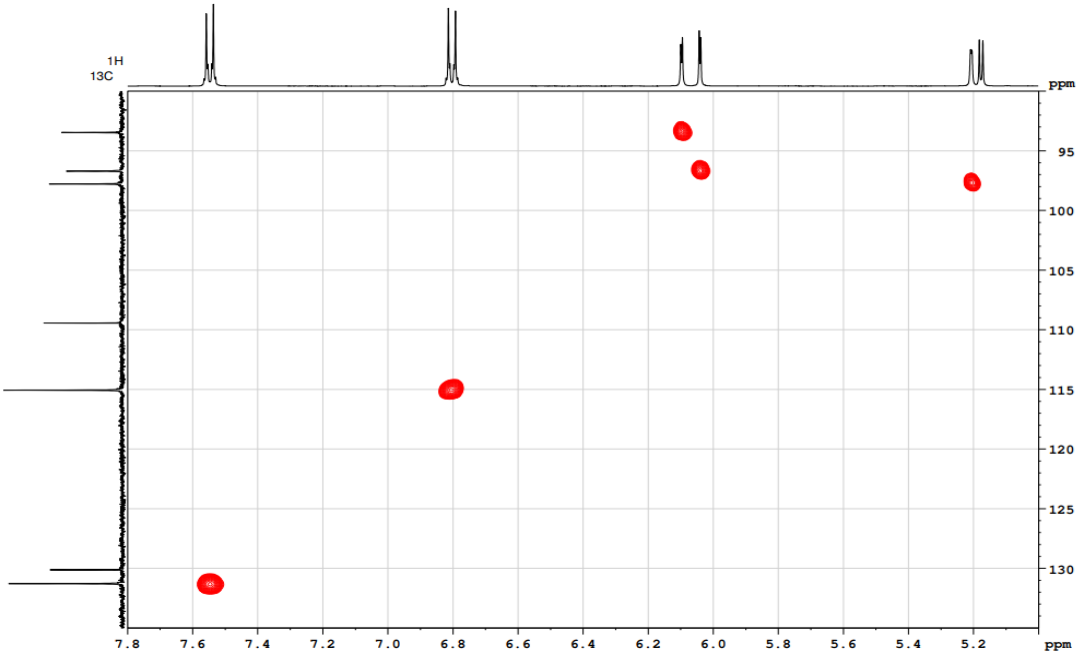

Figure A64. HSQC spectrum (expansion 1) of **40** in DMSO-d_6.

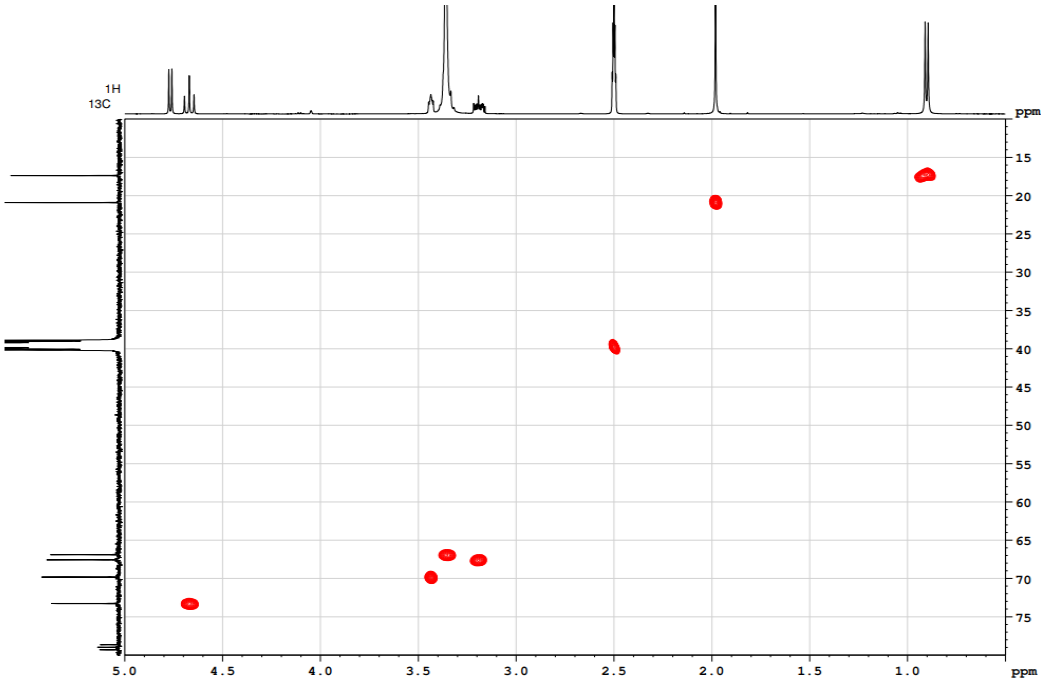

Figure A65. HSQC spectrum (expansion 2) of **40** in DMSO-d_6.

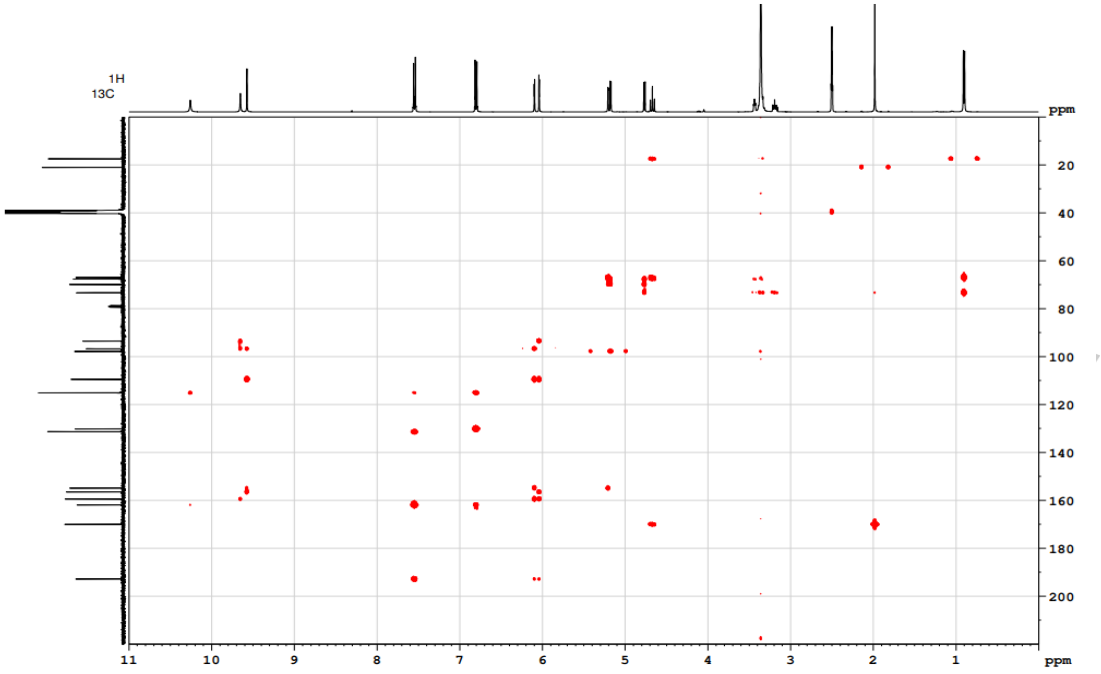

Figure A66. HMBC spectrum of **40** in DMSO-d_6.

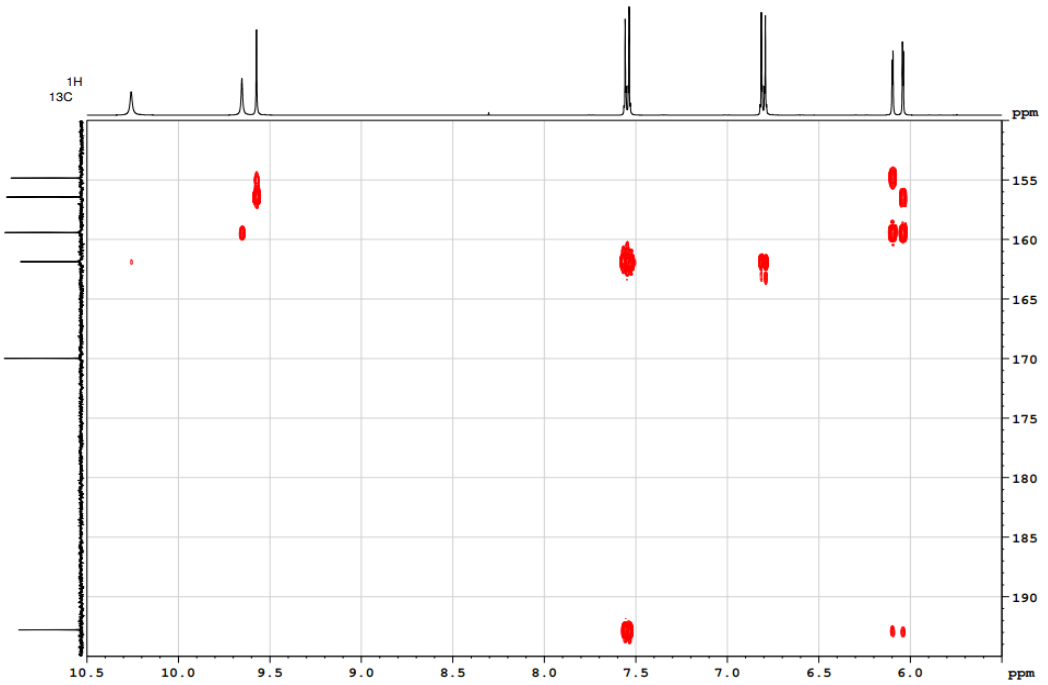

Figure A67. HMBC spectrum (expansion 1) of **40** in DMSO-d_6.

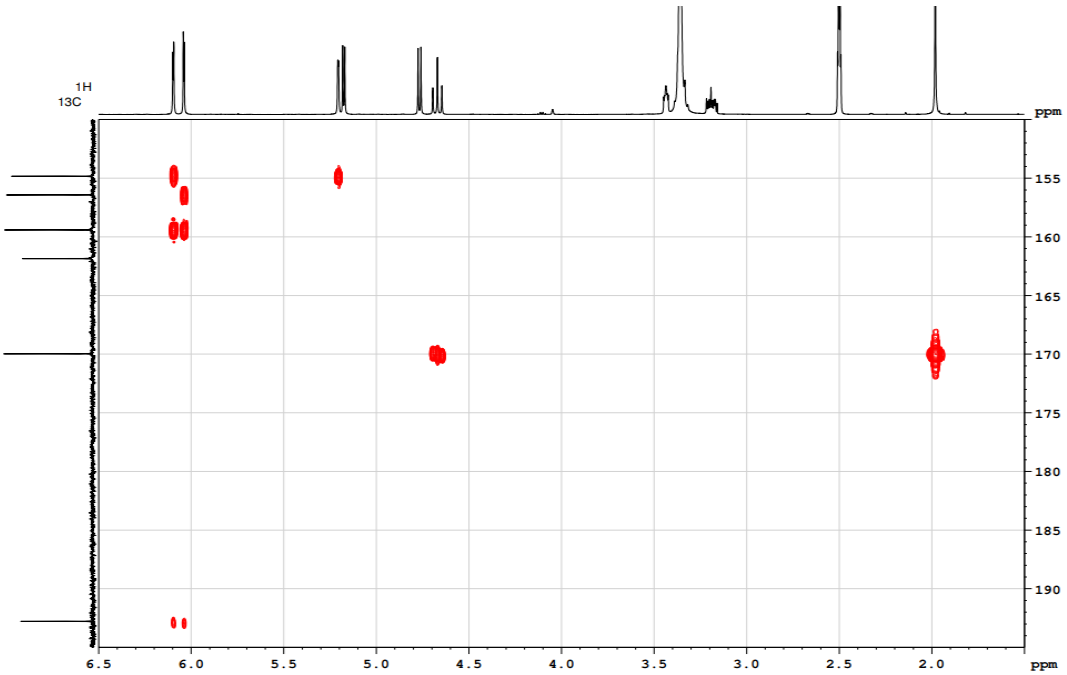

Figure A68. HMBC spectrum (expansion 2) of **40** in DMSO-d_6.

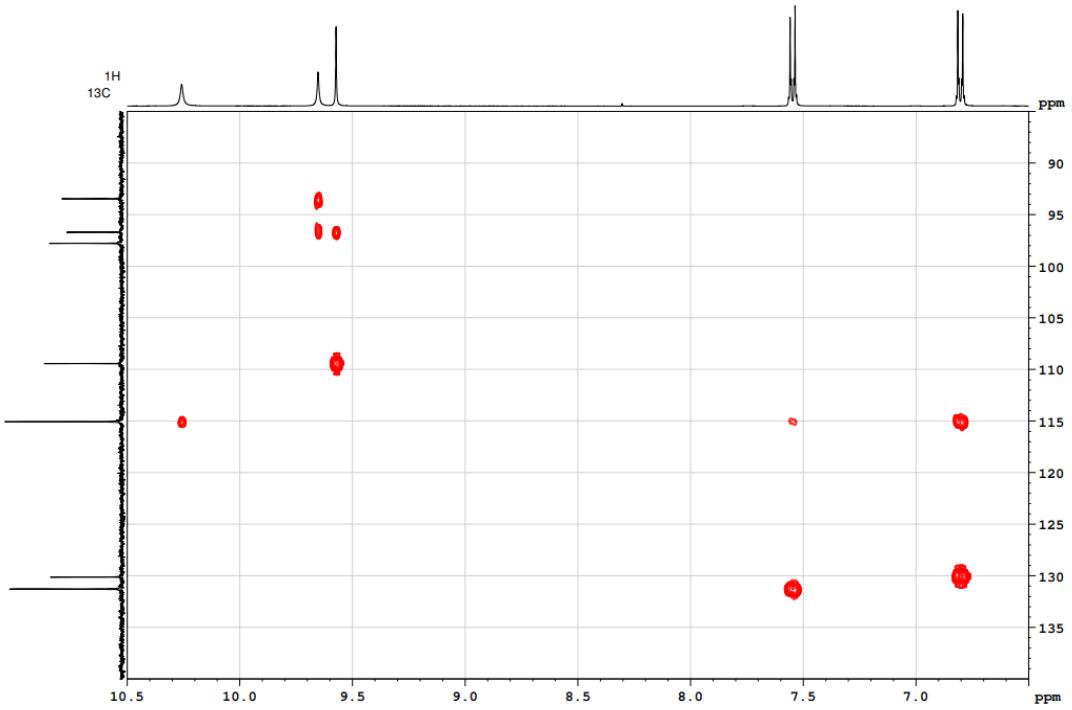

Figure A69. HMBC spectrum (expansion 3) of **40** in DMSO-d_6.

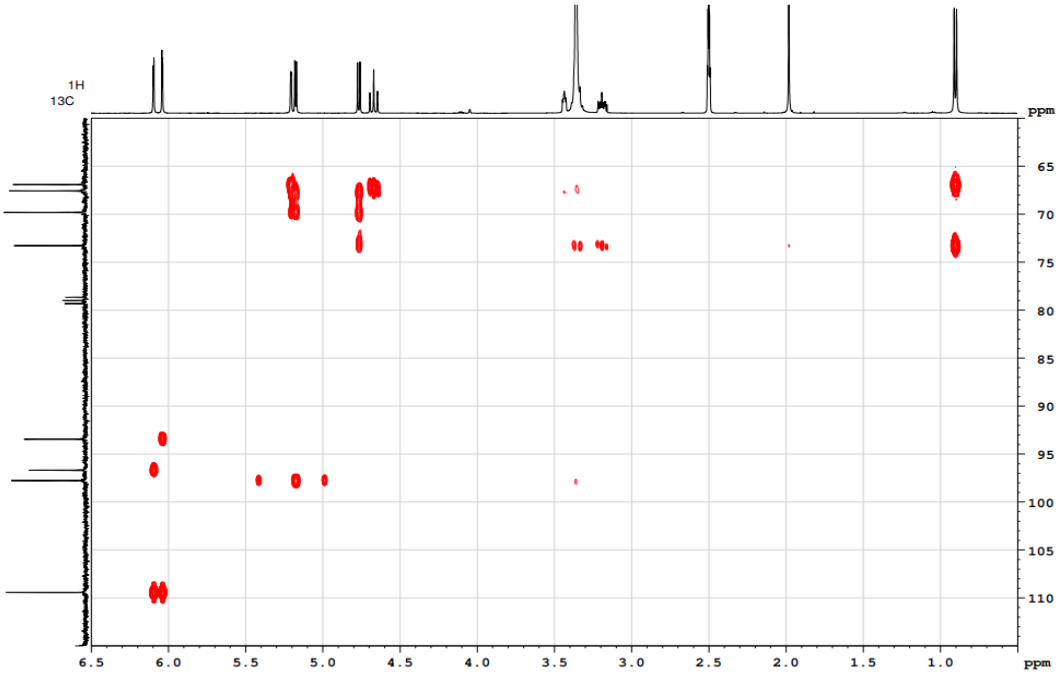

Figure A70. HMBC spectrum (expansion 4) of **40** in DMSO-d_6.

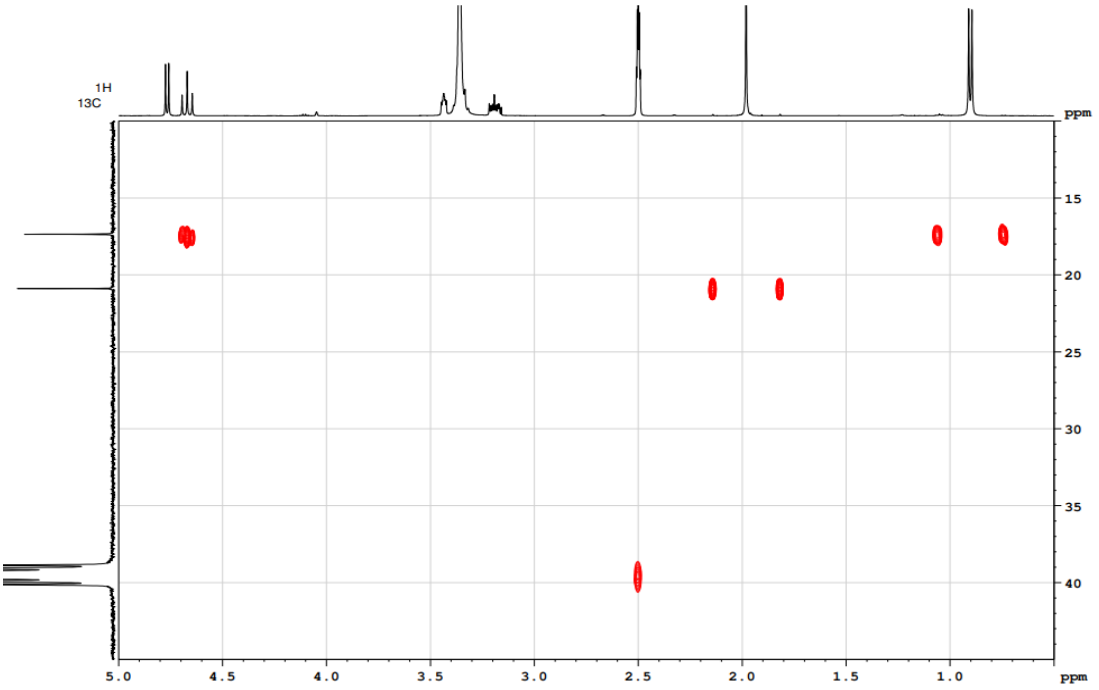

Figure A71. HMBC spectrum (expansion 5) of **40** in DMSO-d_6.

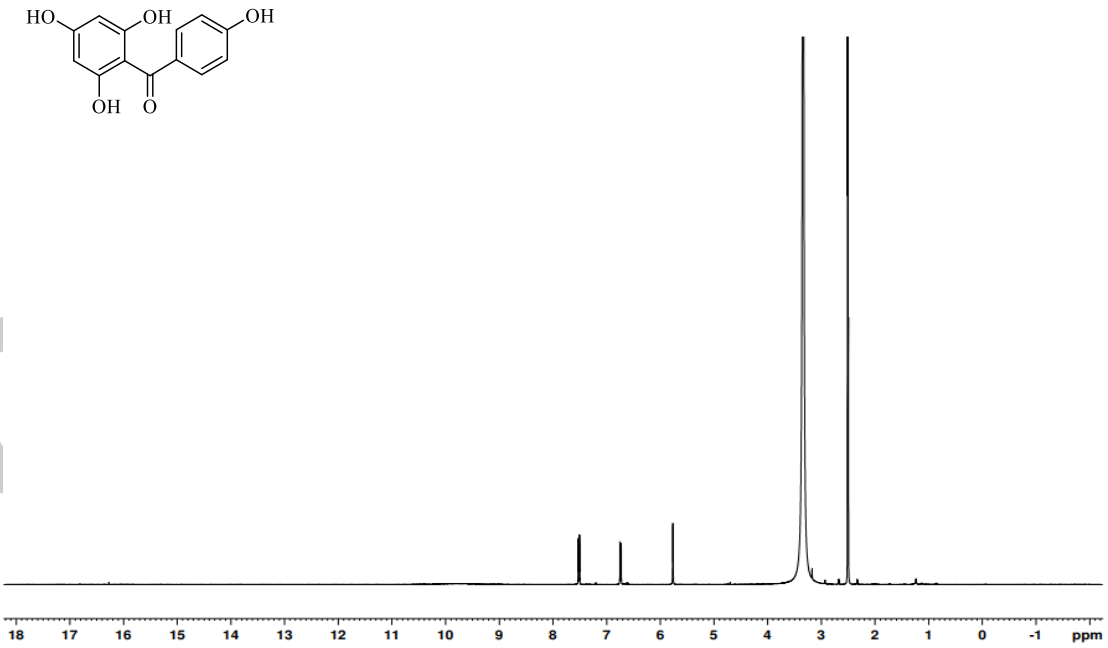

Figure A72. ^{1}H NMR spectrum of **40a** (DMSO-d_6, 400 MHz

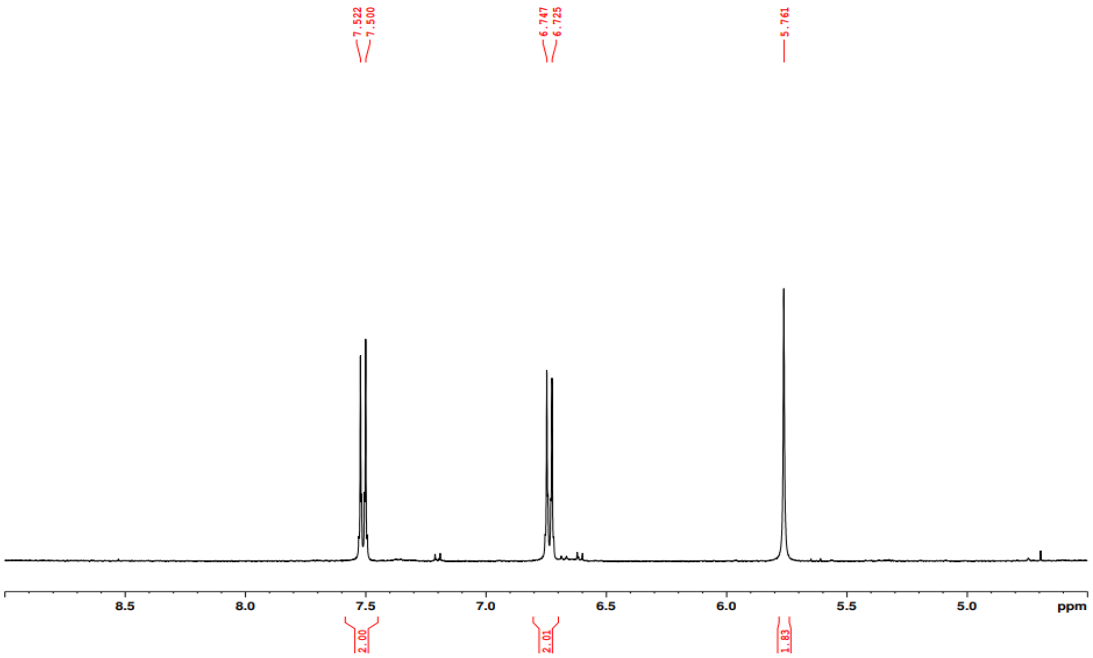

Figure A73. ^{1}H NMR spectrum (expansion 1) of **40a** (DMSO-d_6, 400 MHz).

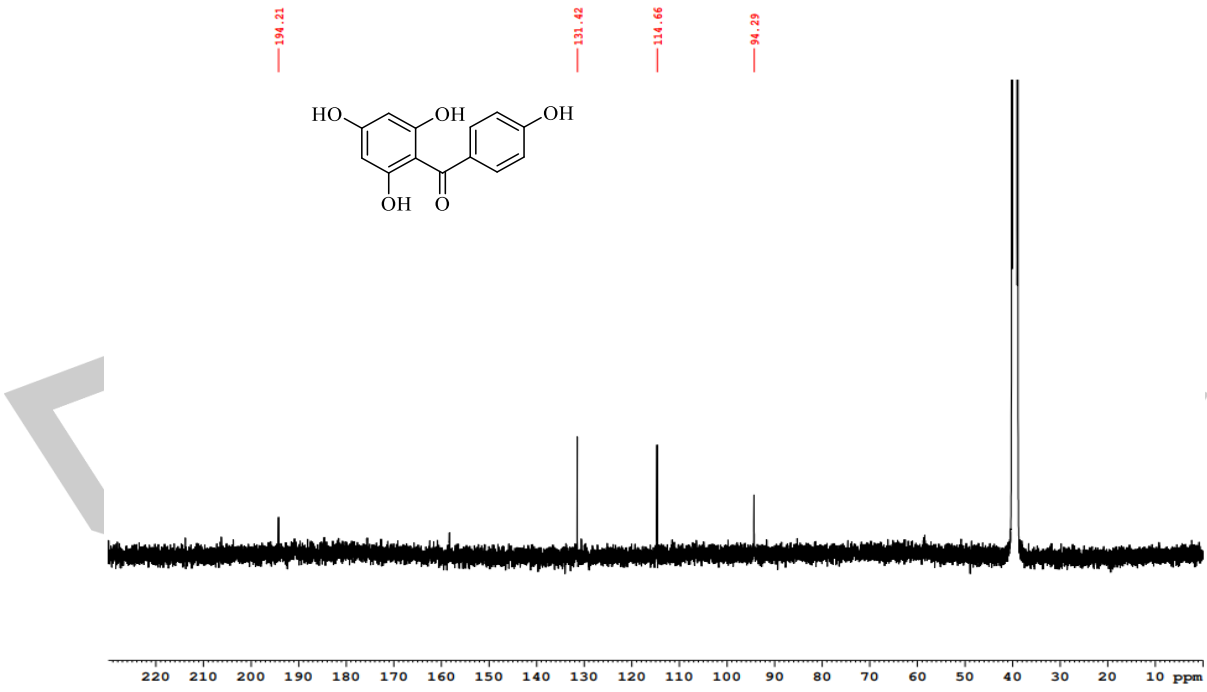

Figure A74. ^{13}C NMR spectrum of **40a** (DMSO-d_6, 100 MHz).

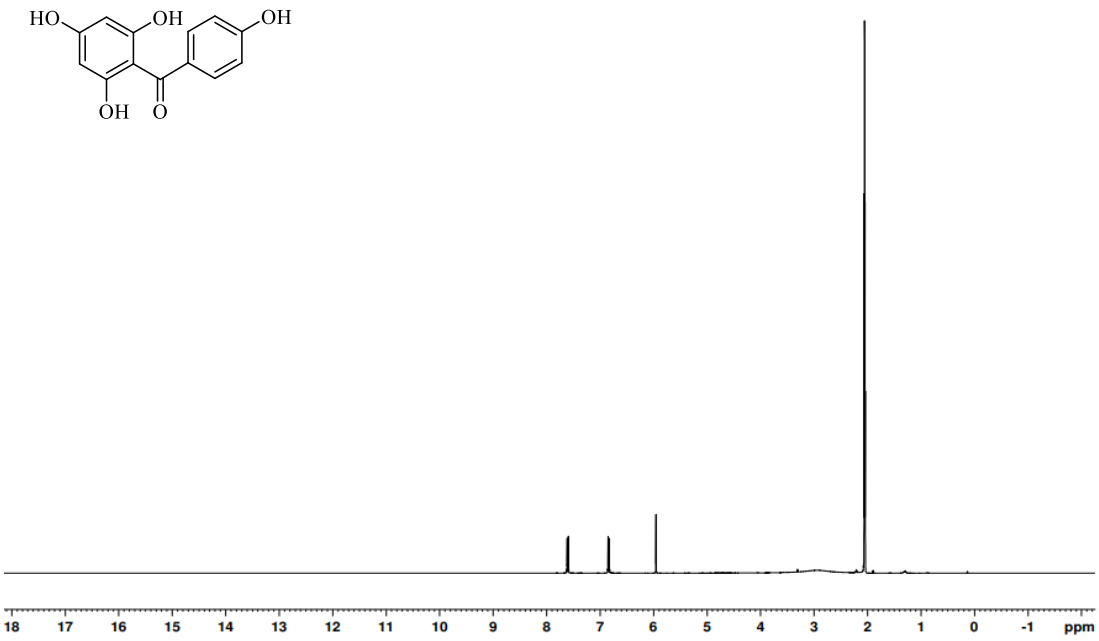

Figure A75. ^{1}H NMR spectrum of **40a** (acetone-d_6, 400 MHz).

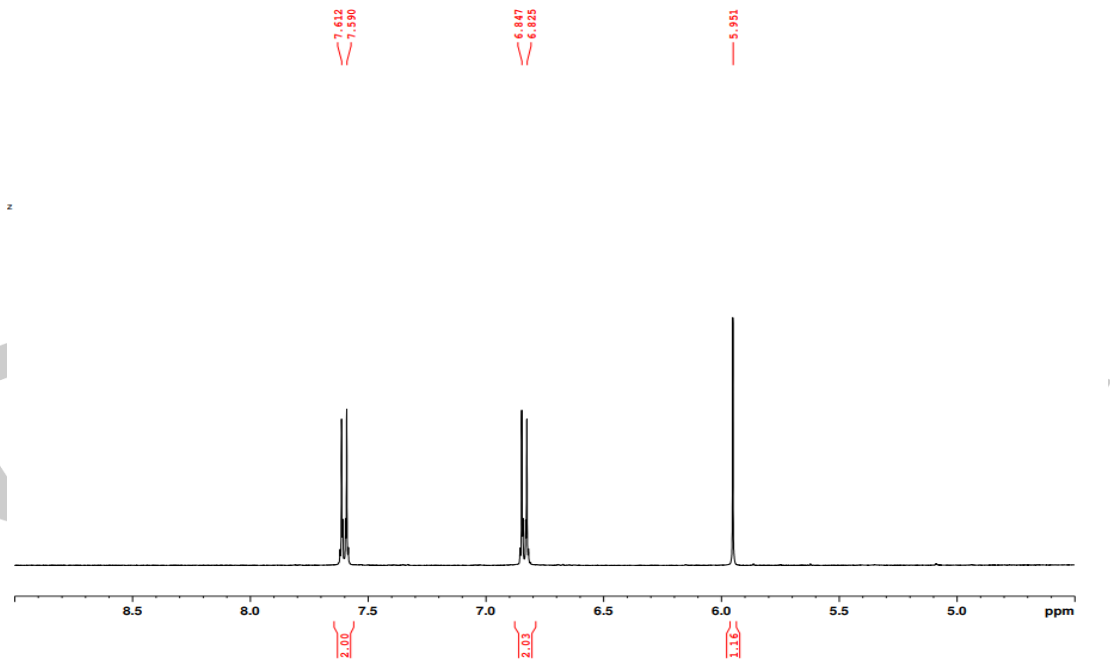

Figure A76. ^{1}H NMR spectrum (expansion 1) of **40a** (acetone-d_6, 400 MHz).

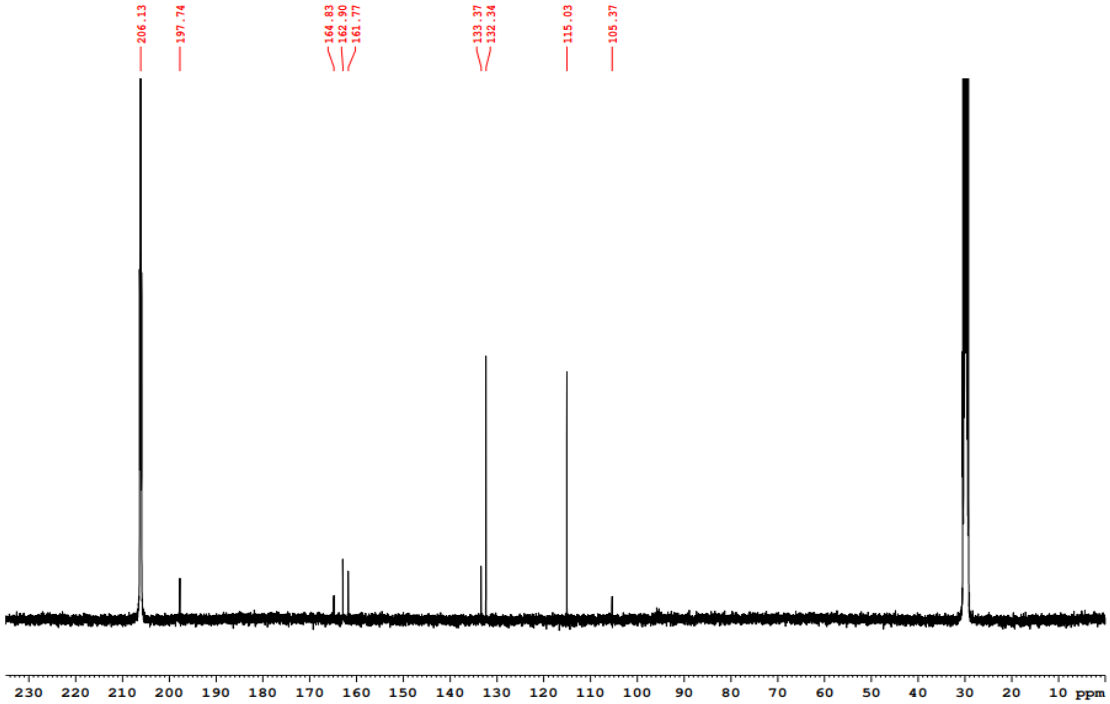

Figure A77. ^{13}C NMR spectrum of **40a** (acetone-d_6, 100 MHz).

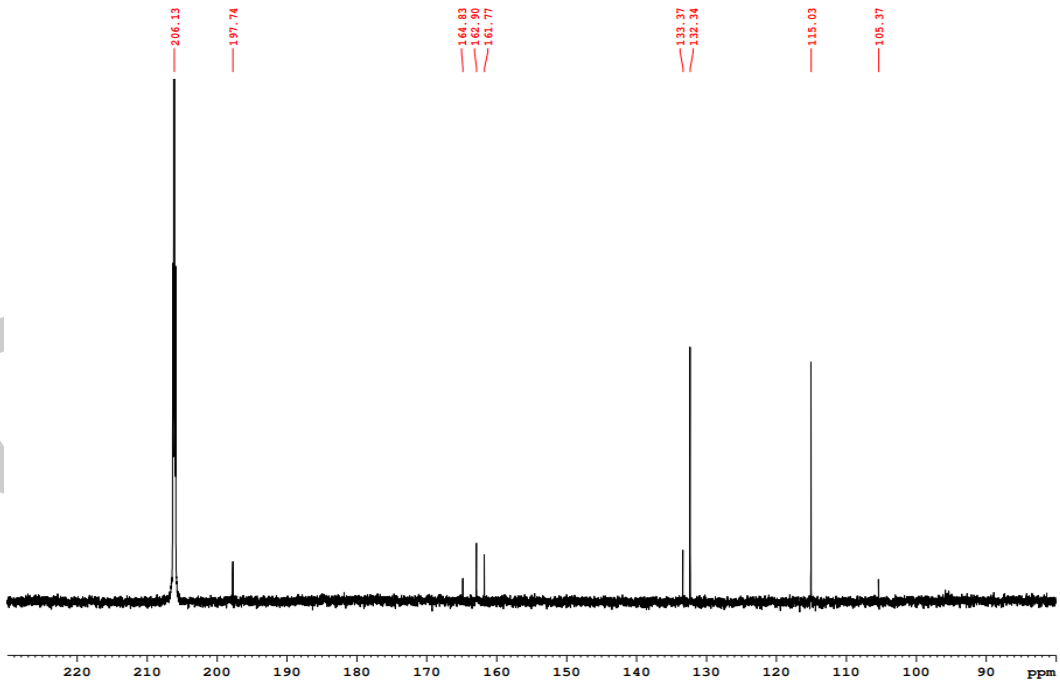

Figure A78. ^{13}C NMR spectrum (expansion 1) of **40a** (acetone-d_6, 100 MHz).

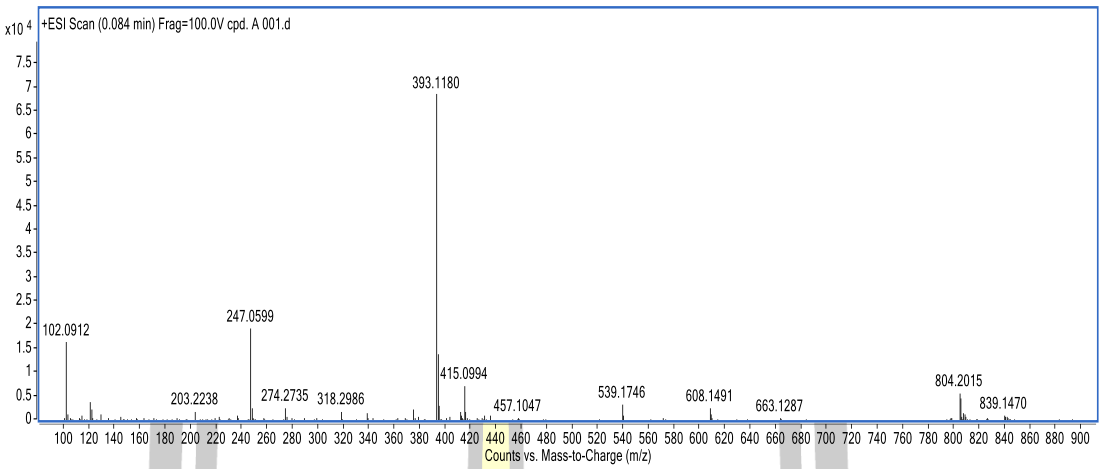

Figure A79. MS spectrum (positive mode) of compound **41**.

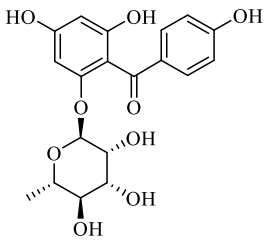

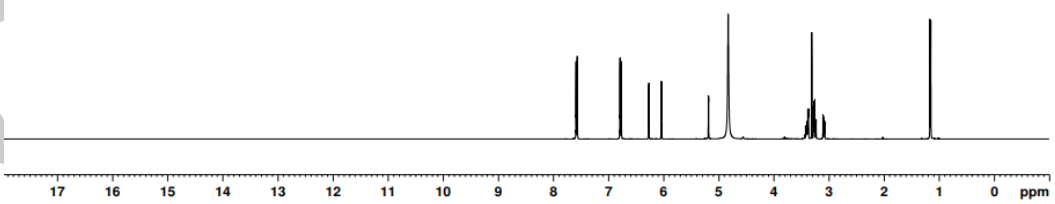

Figure A80. ^{1}H NMR spectrum of **41** (CD_3OD, 400 MHz).

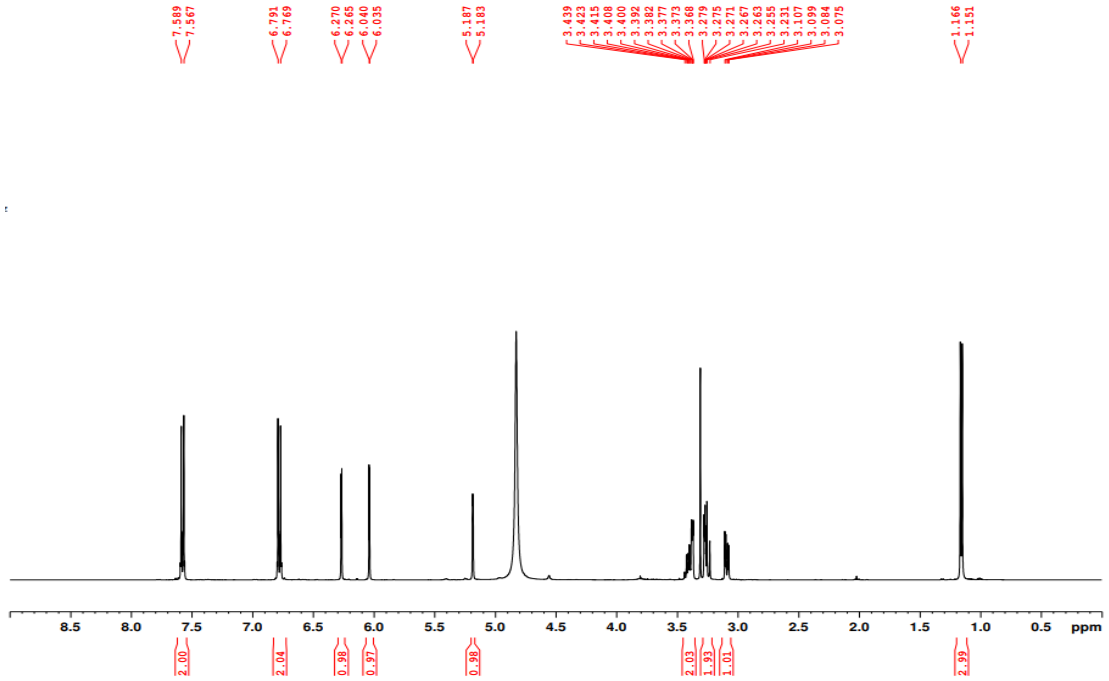

Figure A81. ^{1}H NMR spectrum (expansion 1) of **41** (CD_3OD, 400 MHz).

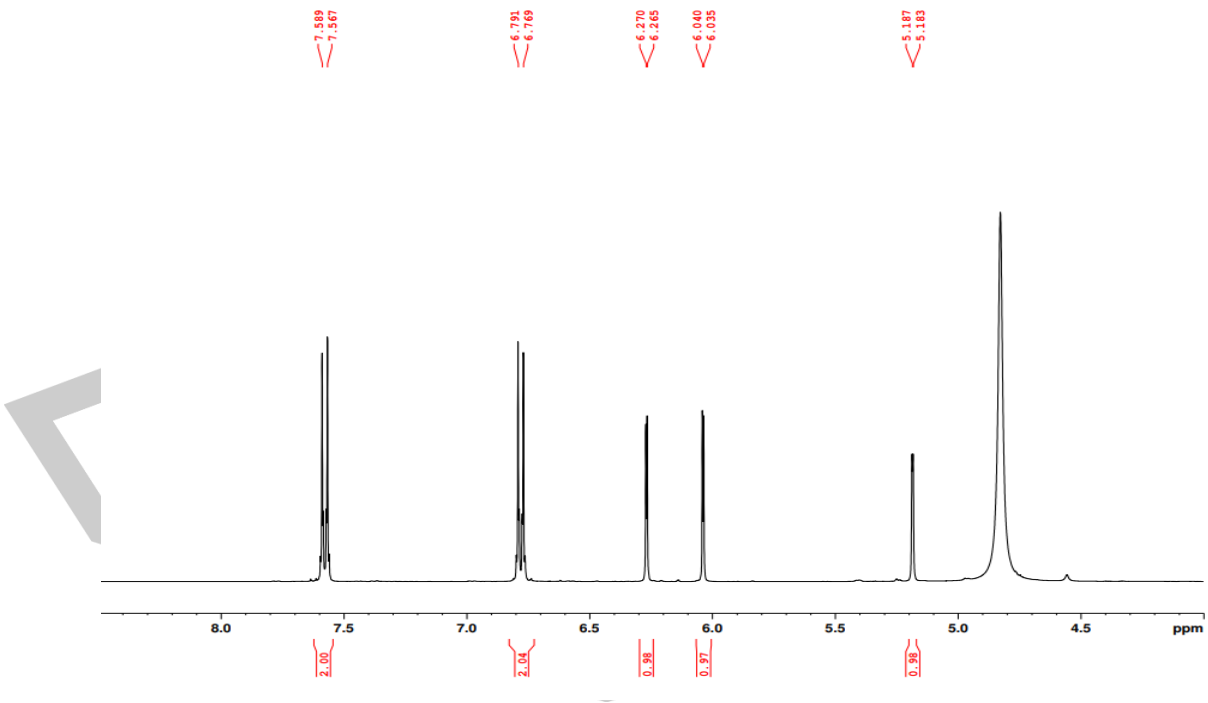

Figure A82. ^{1}H NMR spectrum (expansion 2) of **41** (CD_3OD, 400 MHz).

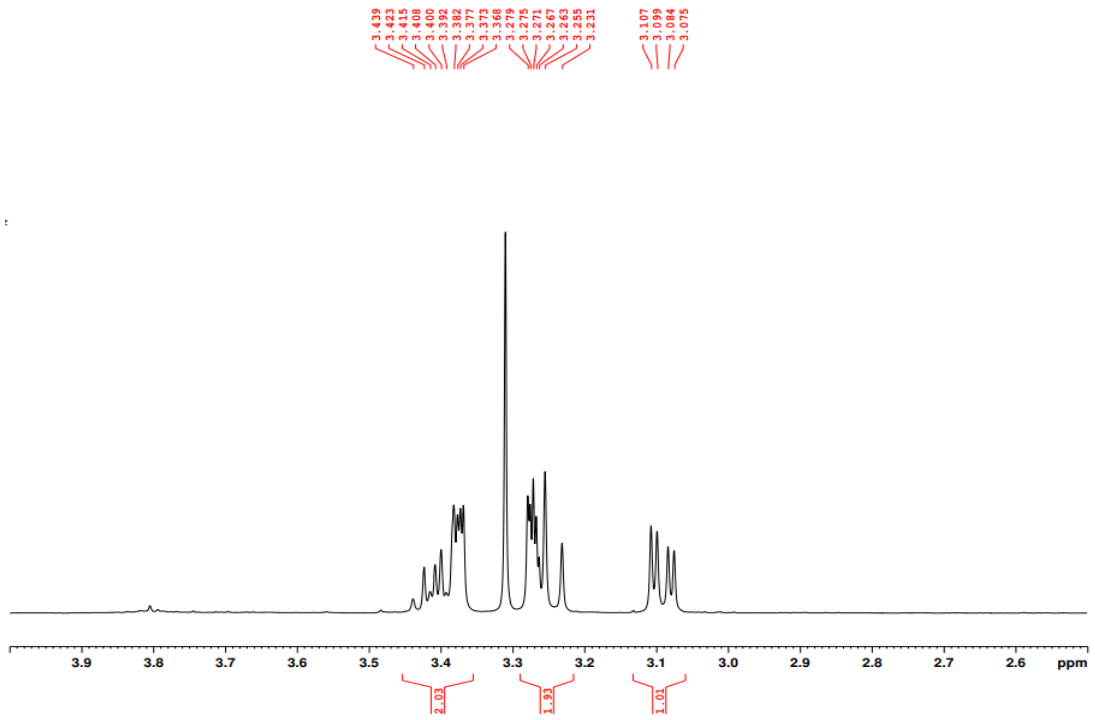

Figure A83. ^{1}H NMR spectrum (expansion 3) of **41** (CD_3OD, 400 MHz).

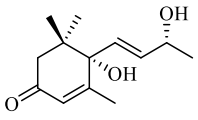

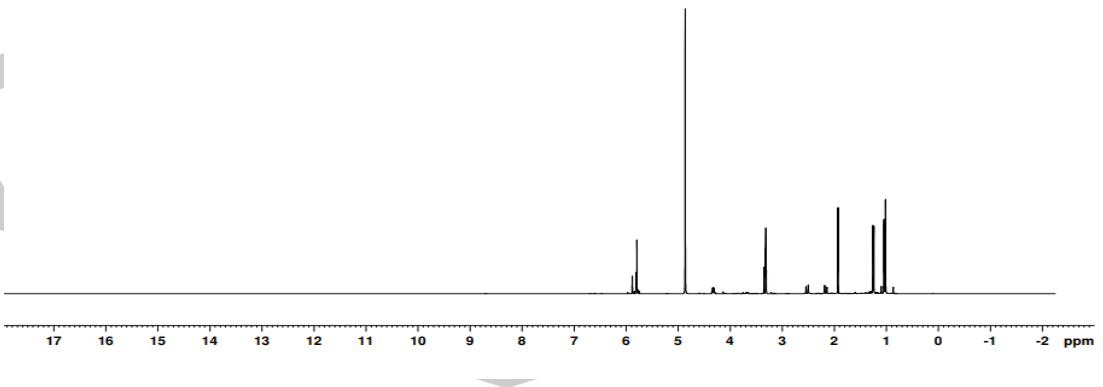

Figure A84. ^{1}H NMR spectrum of **42** (CD_3OD, 400 MHz).

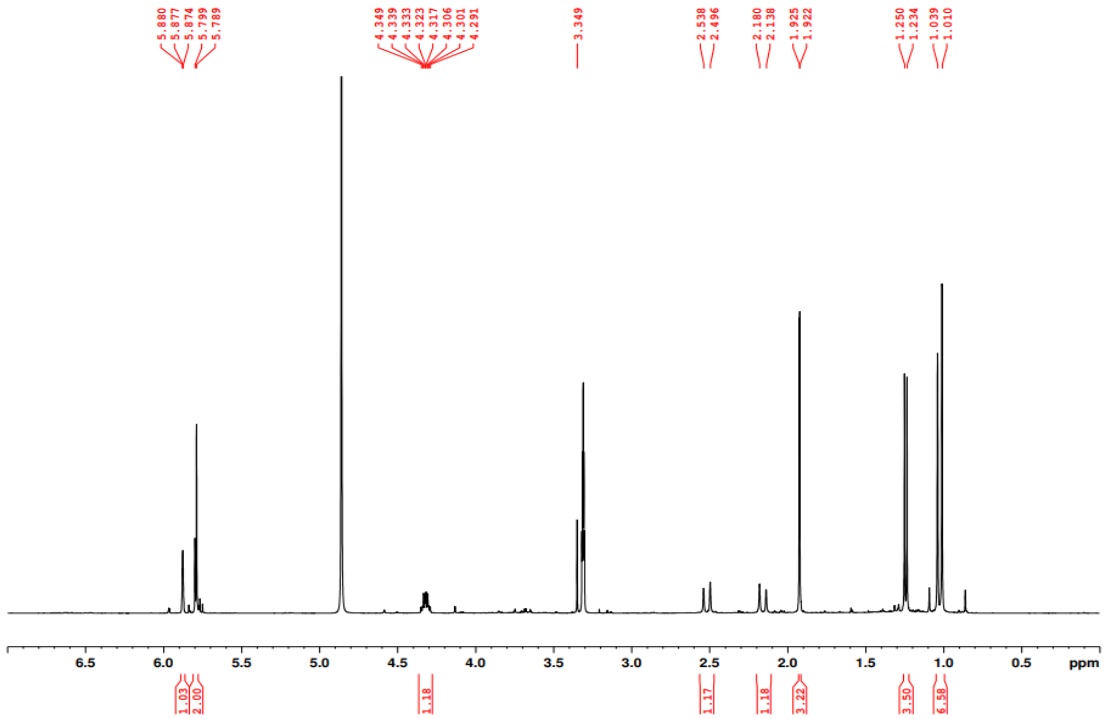

Figure A85. ^{1}H NMR spectrum (expansion 1) of **42** (CD_3OD, 400 MHz).

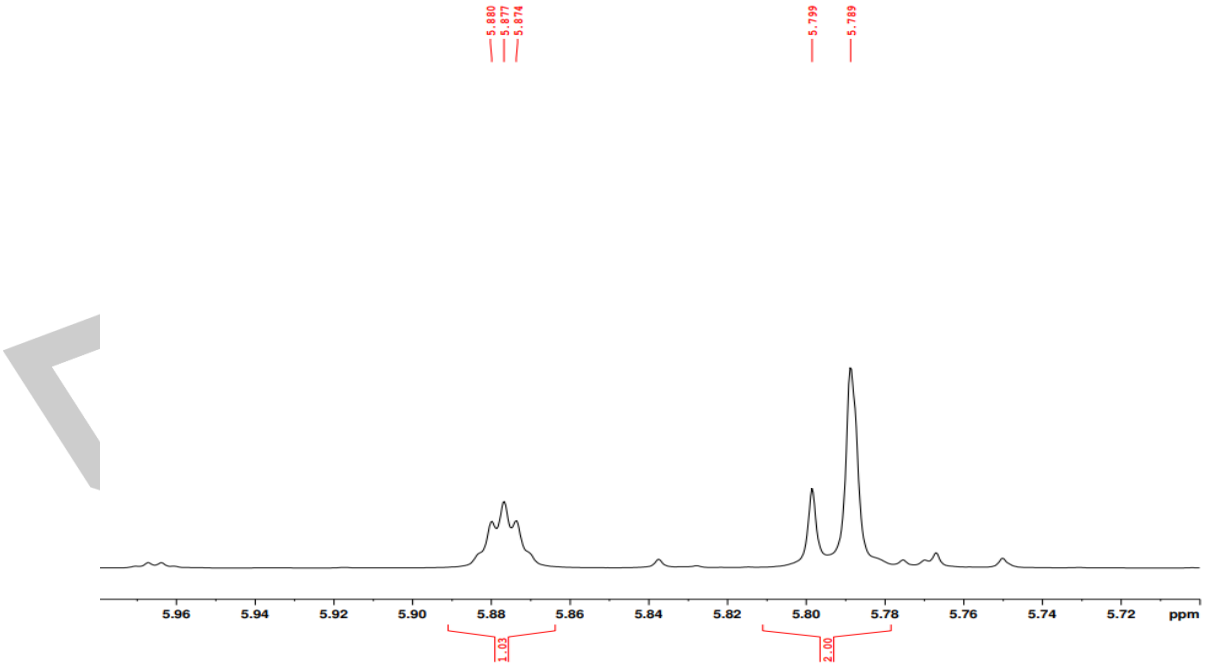

Figure A86. ^{1}H NMR spectrum (expansion 2) of **42** (CD_3OD, 400 MHz).

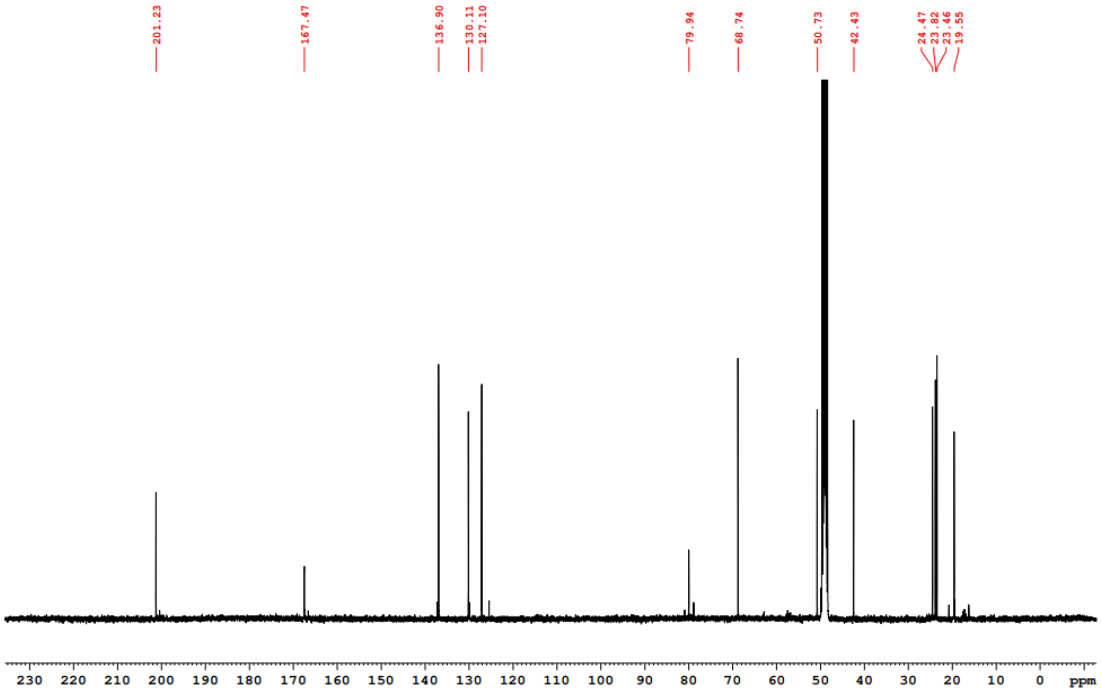

Figure A87. ^{13}C NMR spectrum of **42** (CD_3OD, 100 MHz).

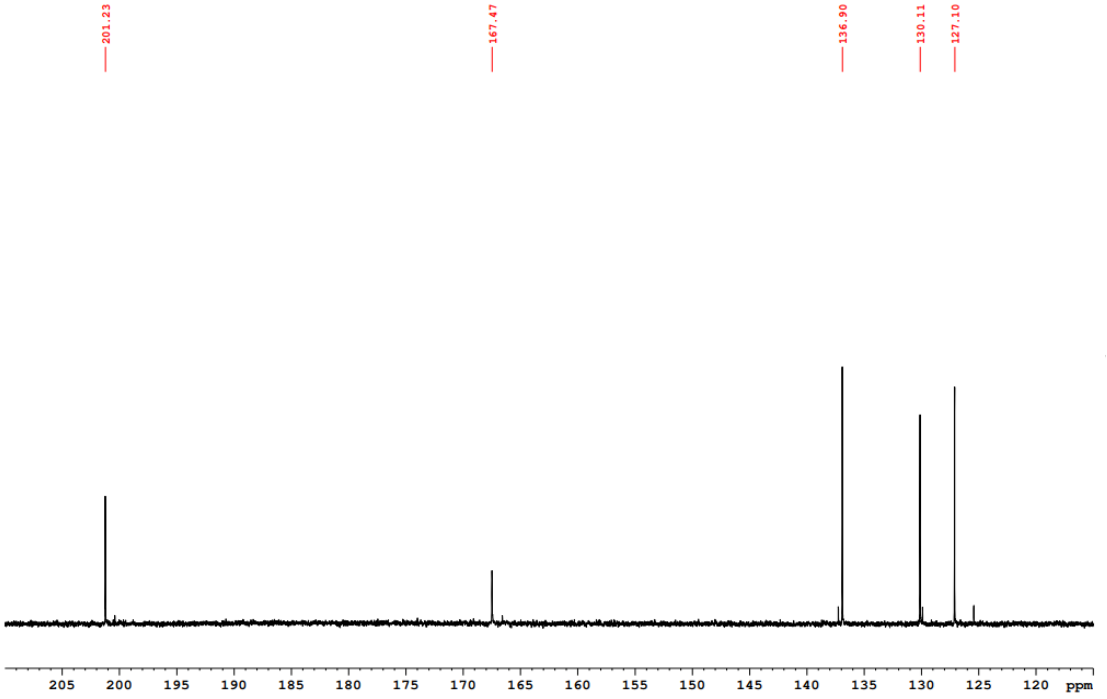

Figure A88. ^{13}C NMR spectrum (expansion 1) of **42** (CD_3OD, 100 MHz).

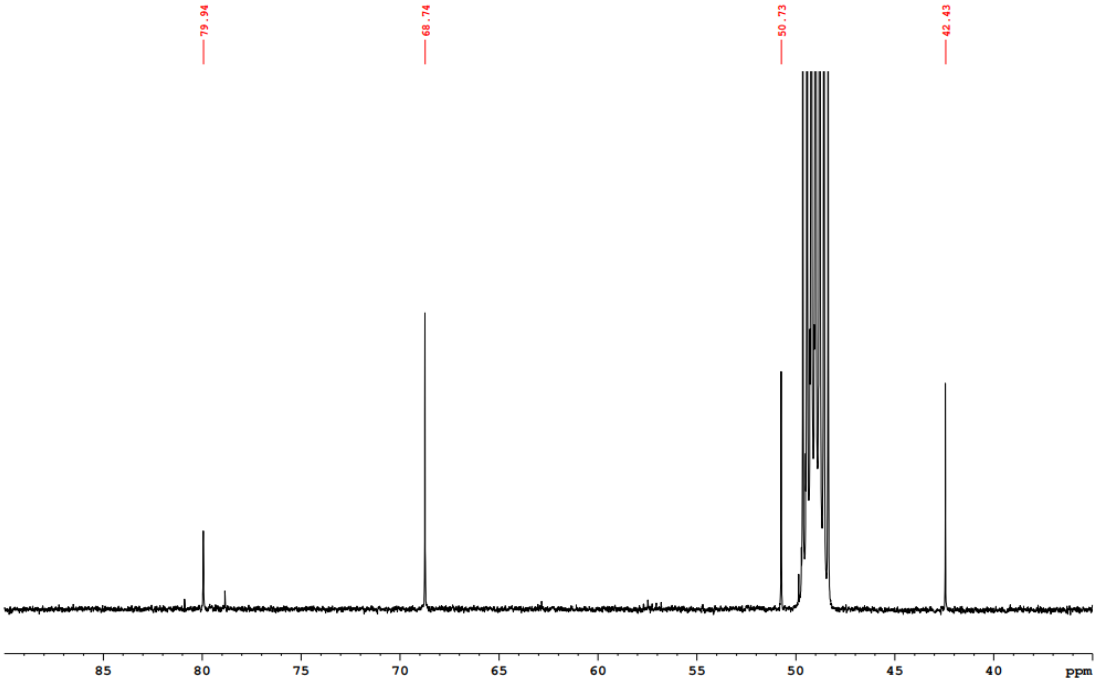

Figure A89. ^{13}C NMR spectrum (expansion 2) of **42** (CD_3OD, 100 MHz).

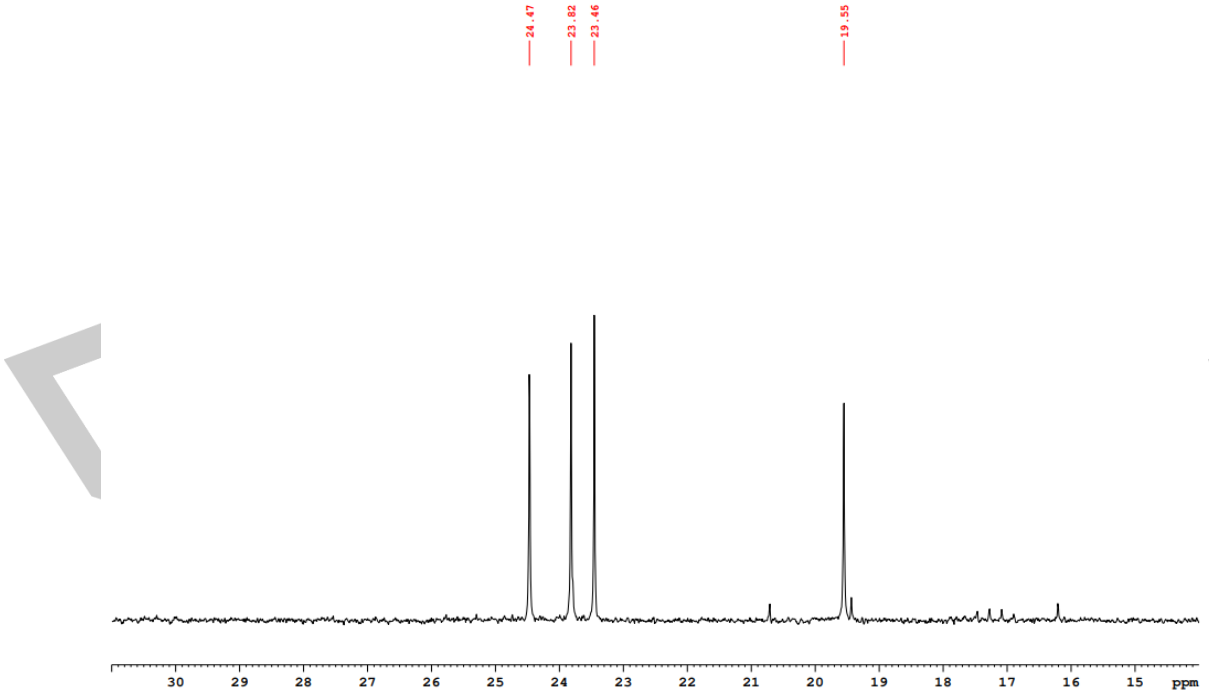

Figure A90. ^{13}C NMR spectrum (expansion 3) of **42** (CD_3OD, 100 MHz).

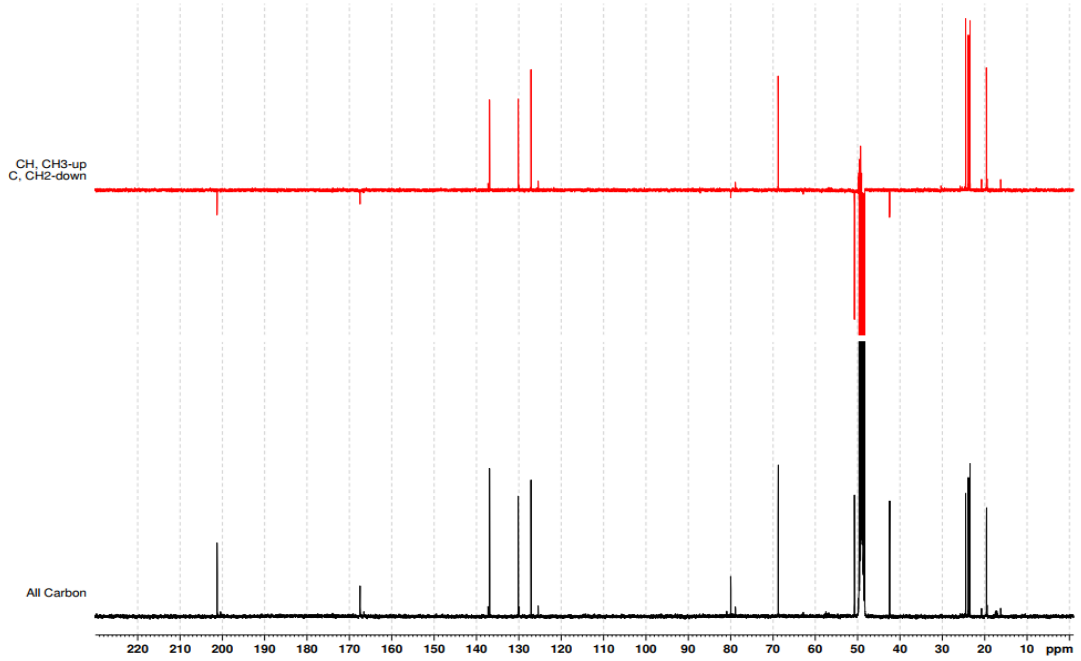

Figure A91. DEPT-135 spectrum of **42** in CD_3OD.

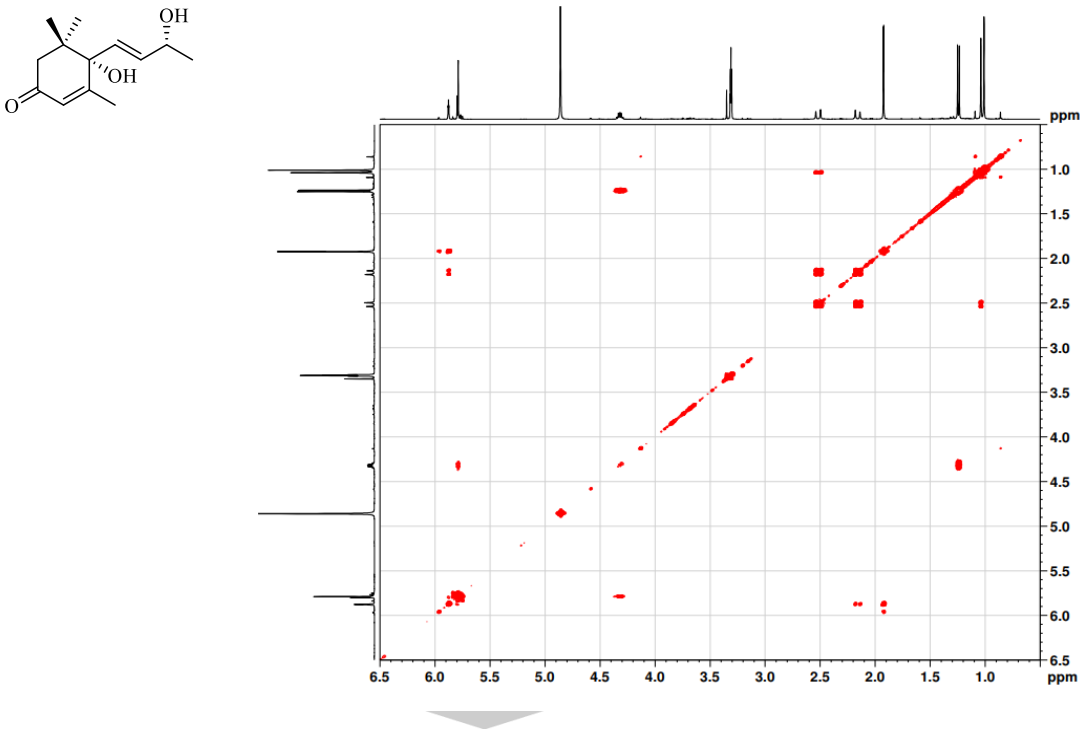

Figure A92. COSY spectrum of **42** in CD_3OD.

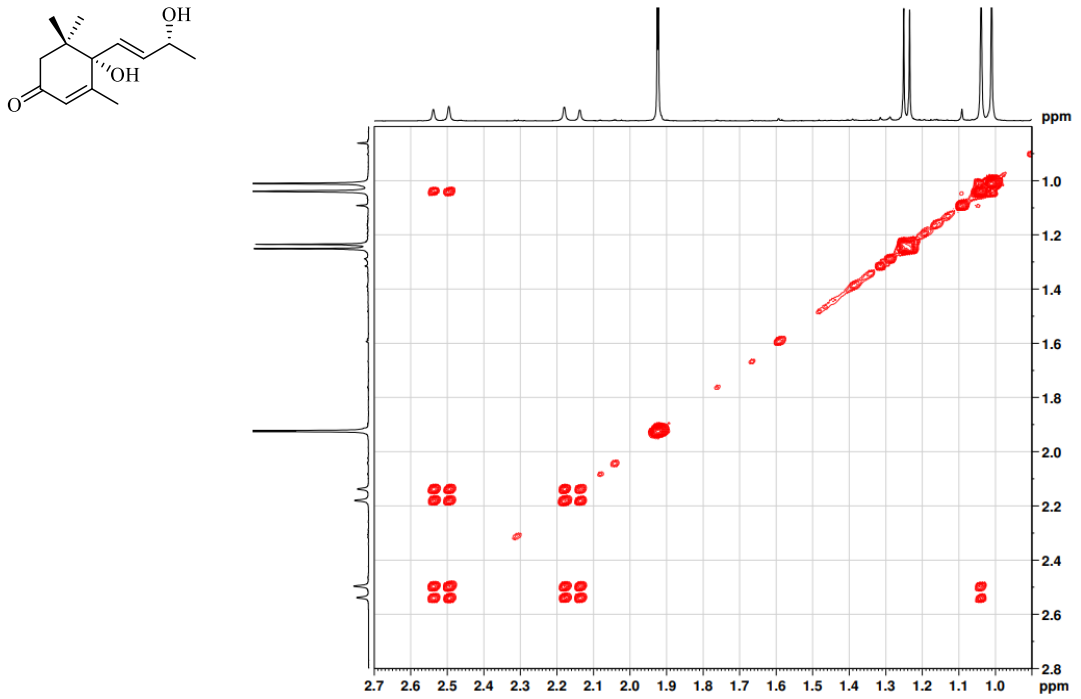

Figure A93. COSY spectrum (expansion 1) of **42** in CD_3OD.

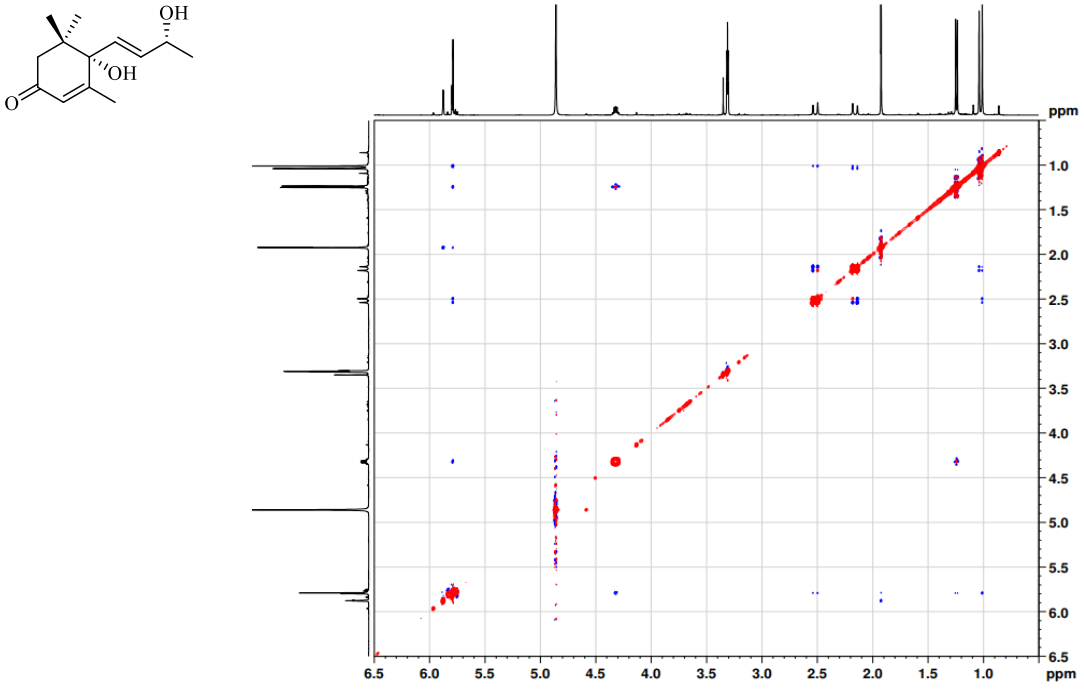

Figure A94. NOESY spectrum of **42** in CD_3OD.

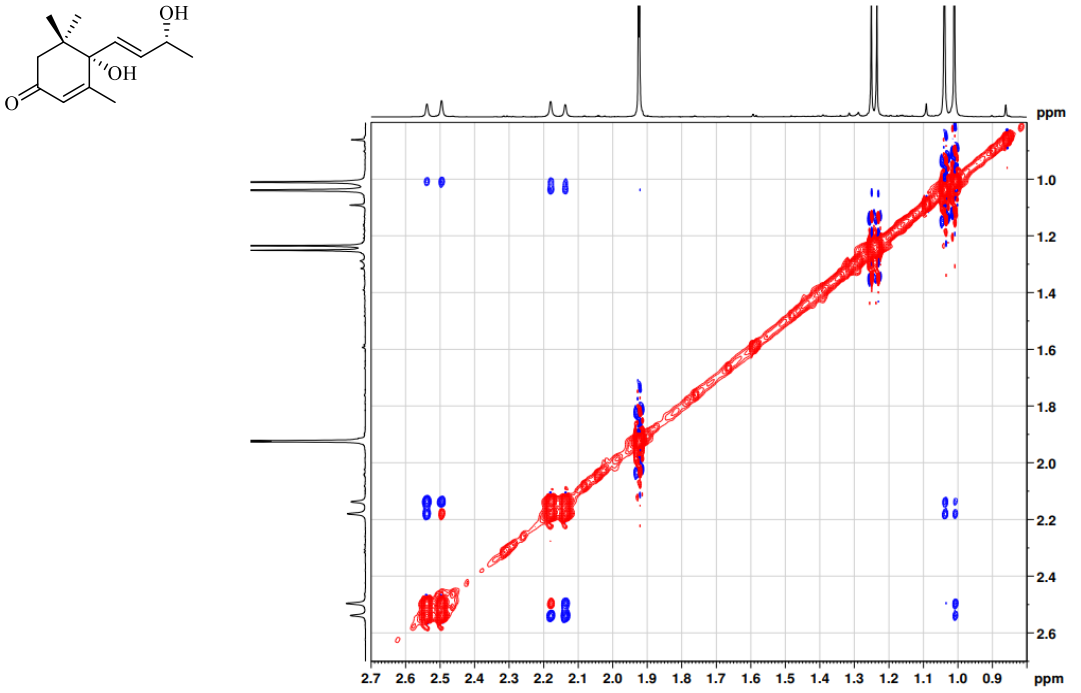

Figure A95. NOESY spectrum (expansion 1) of **42** in CD_3OD.

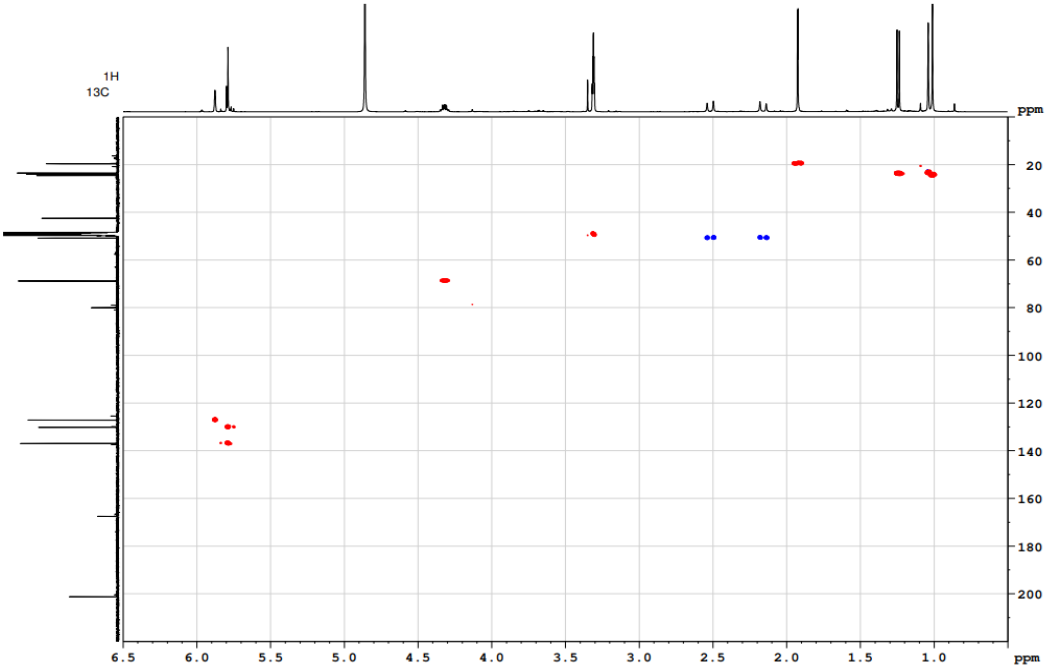

Figure A96. HSQC spectrum of **42** in CD_3OD.

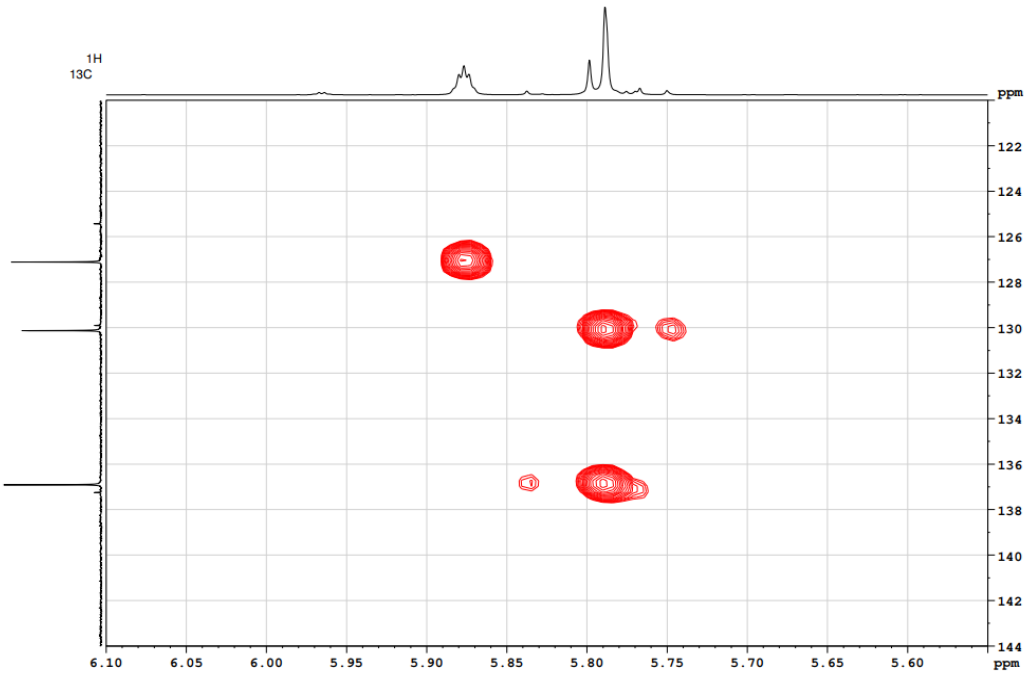

Figure A97. HSQC spectrum (expansion 1) of **42** in CD_3OD.

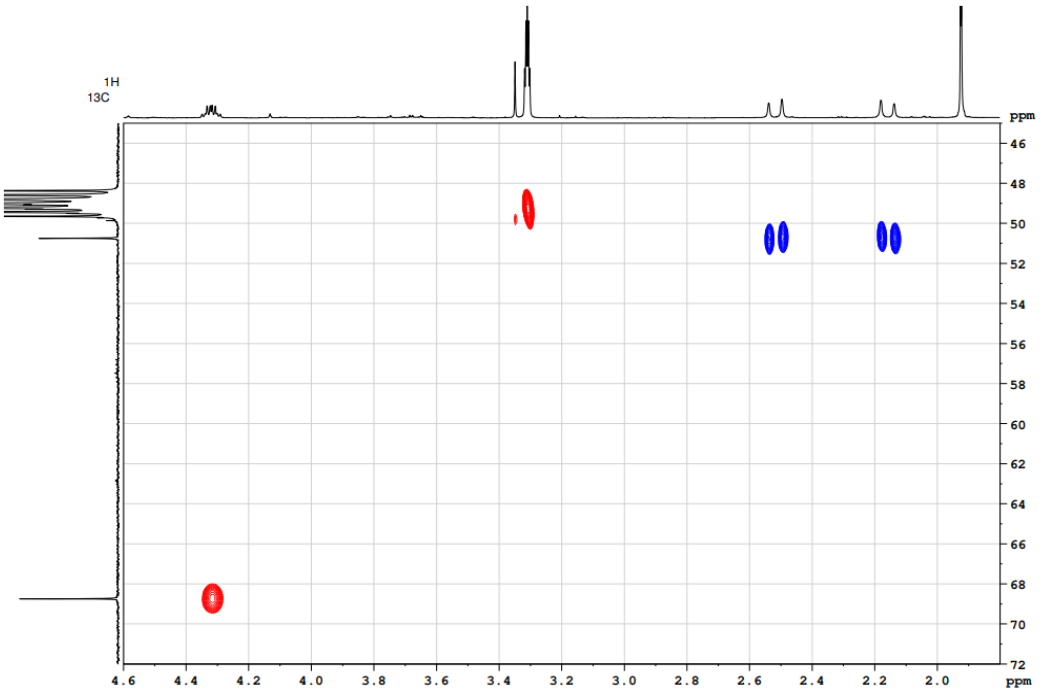

Figure A98. HSQC spectrum (expansion 2) of **42** in CD_3OD.

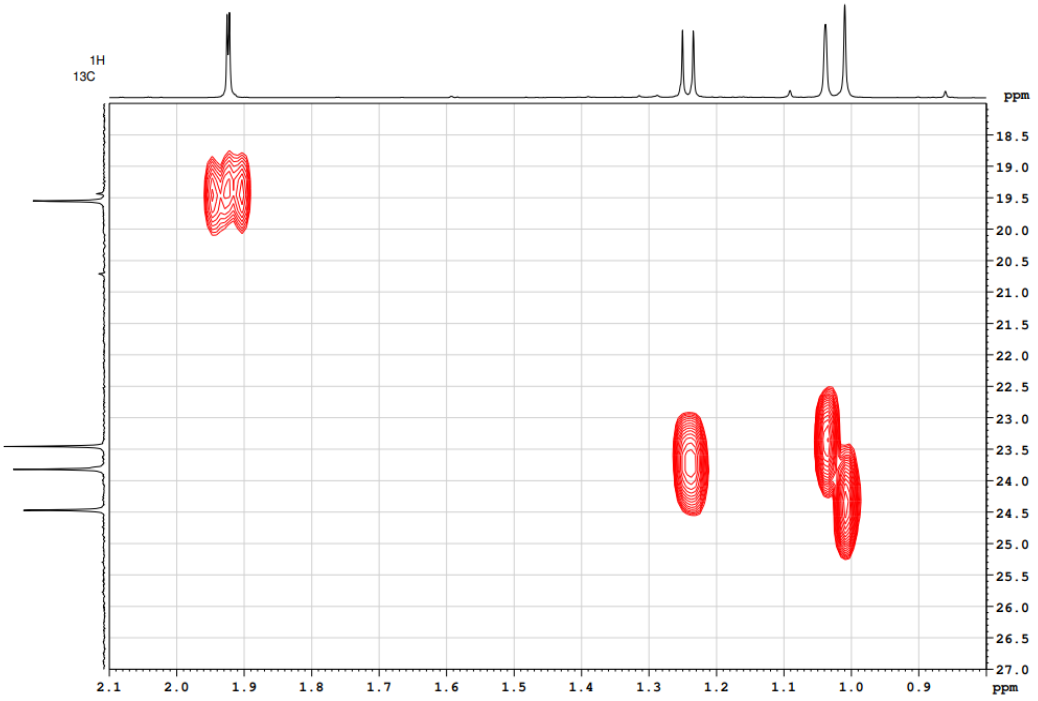

Figure A99. HSQC spectrum (expansion 3) of **42** in CD_3OD.

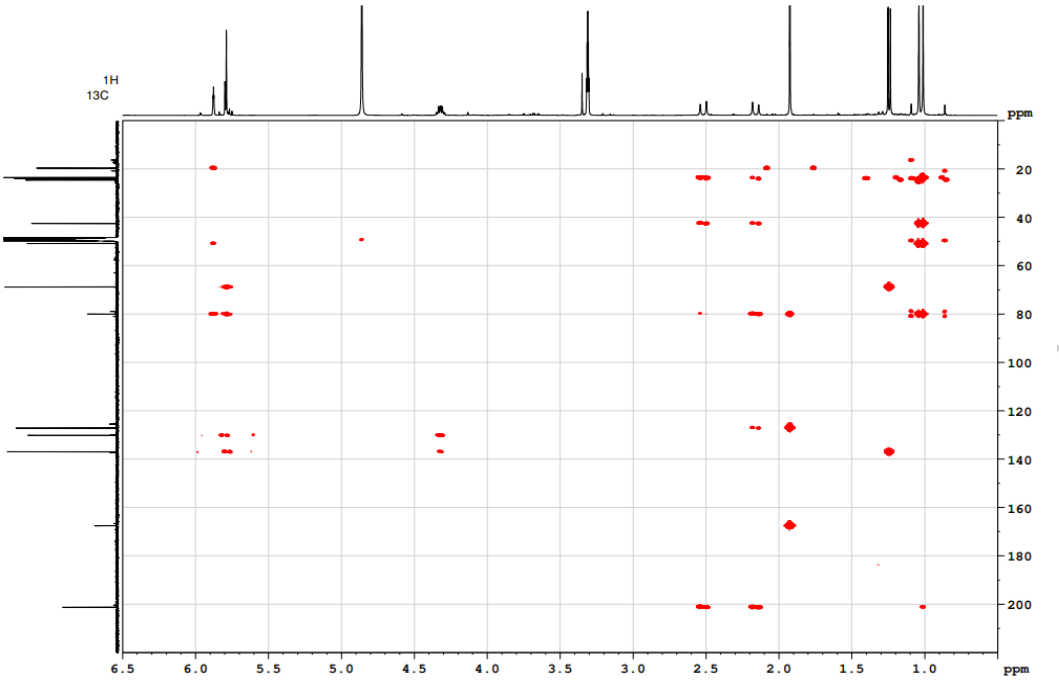

Figure A100. HMBC spectrum of **42** in CD_3OD.

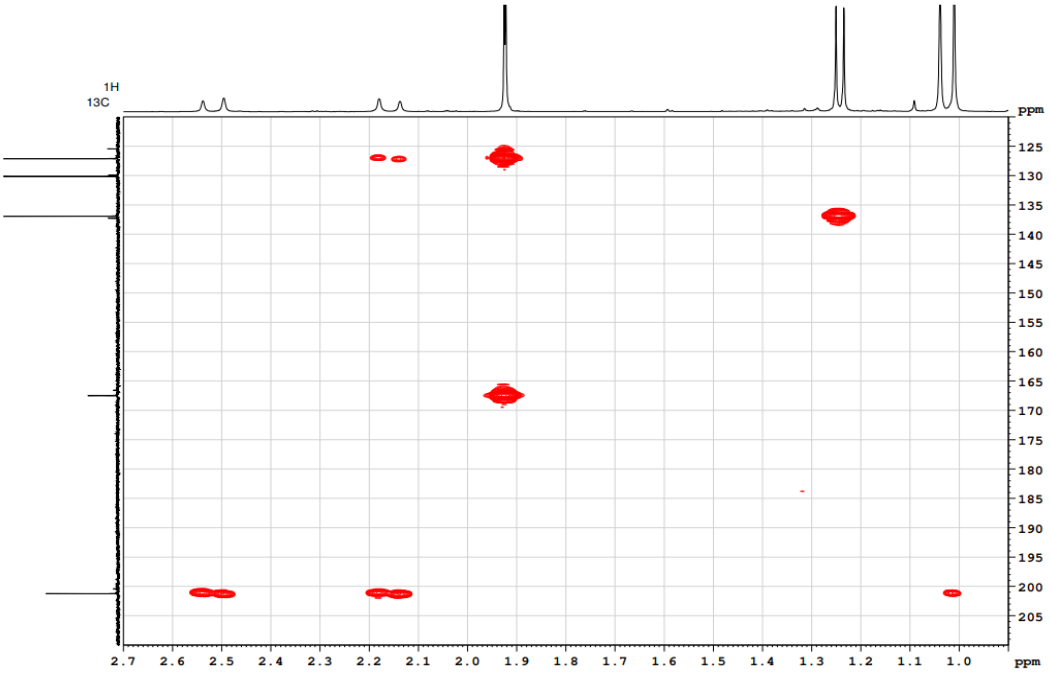

Figure A101. HMBC spectrum (expansion 1) of **42** in CD_3OD.

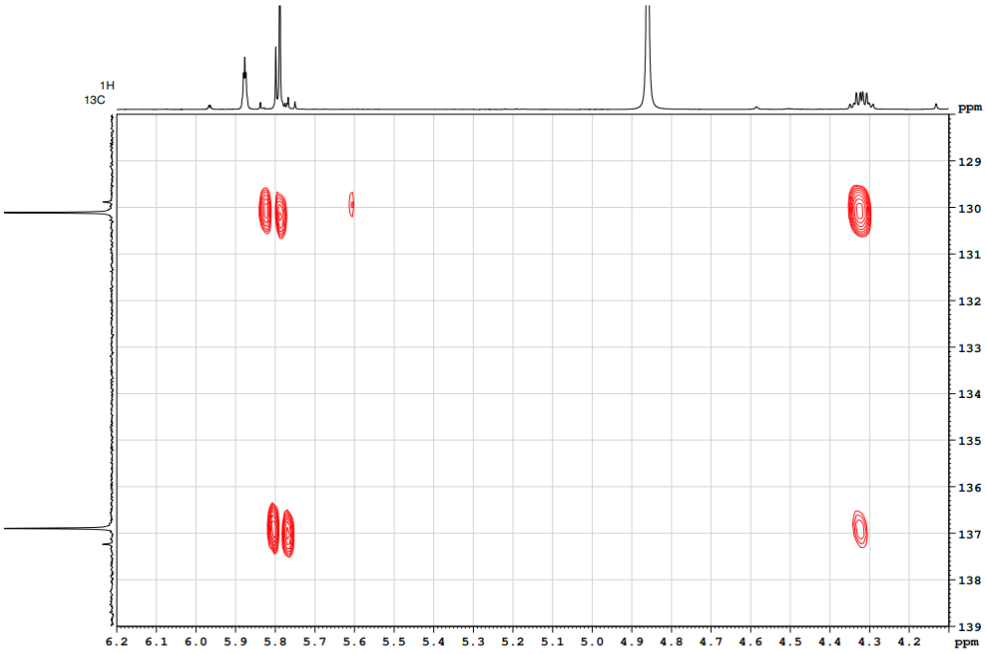

Figure A102. HMBC spectrum (expansion 2) of **42** in CD_3OD.

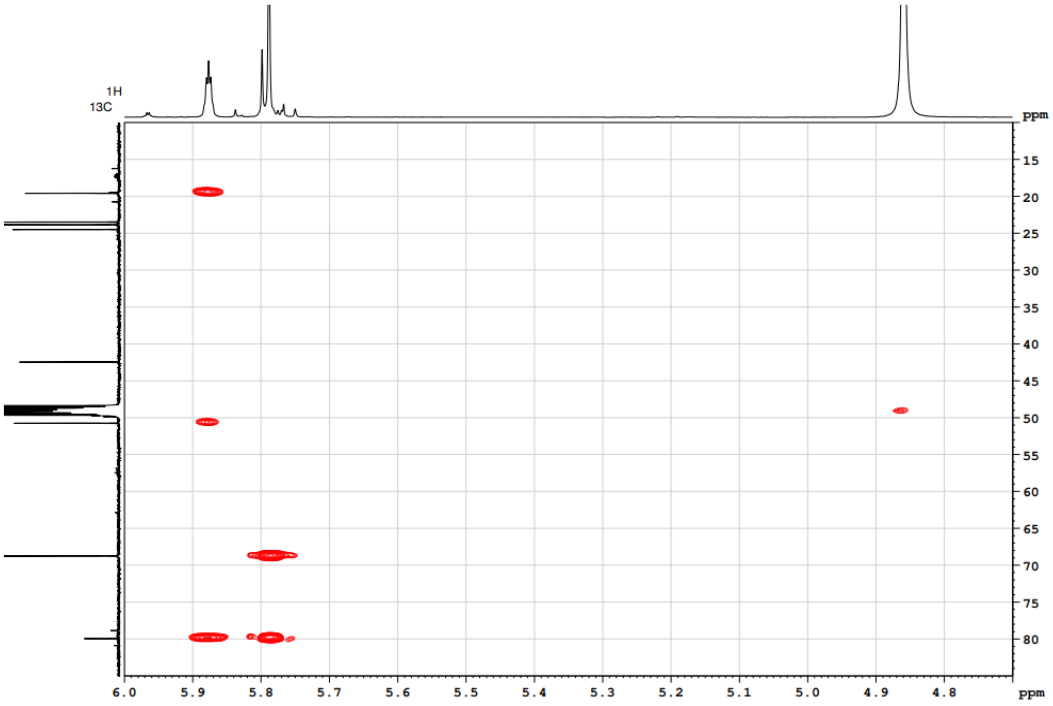

Figure A103. HMBC spectrum (expansion 3) of **42** in CD_3OD.

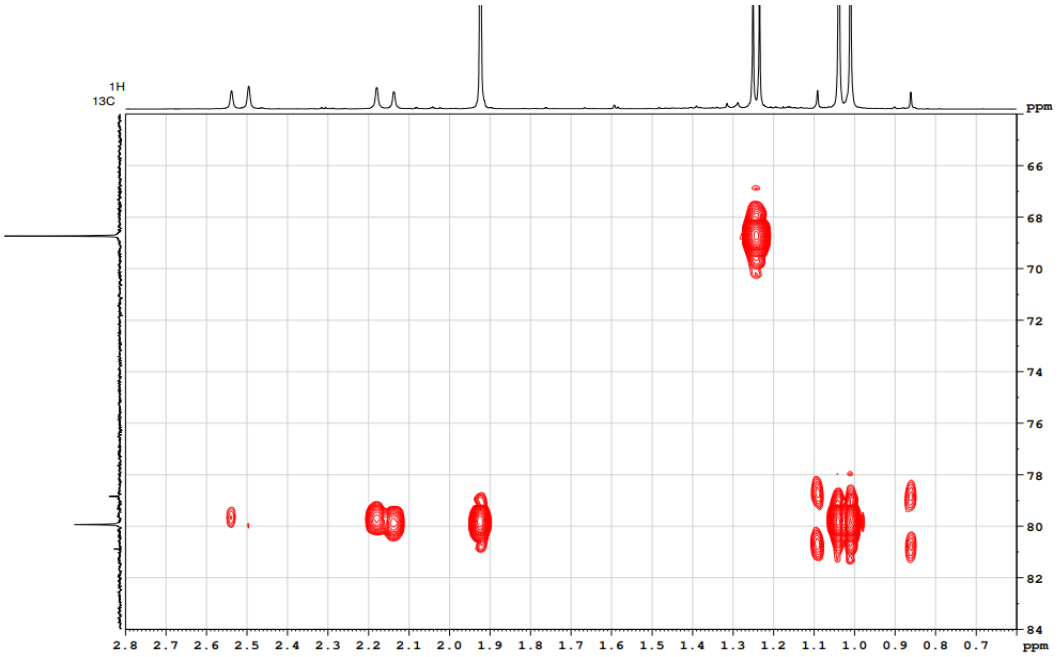

Figure A104. HMBC spectrum (expansion 4) of **42** in CD_3OD.

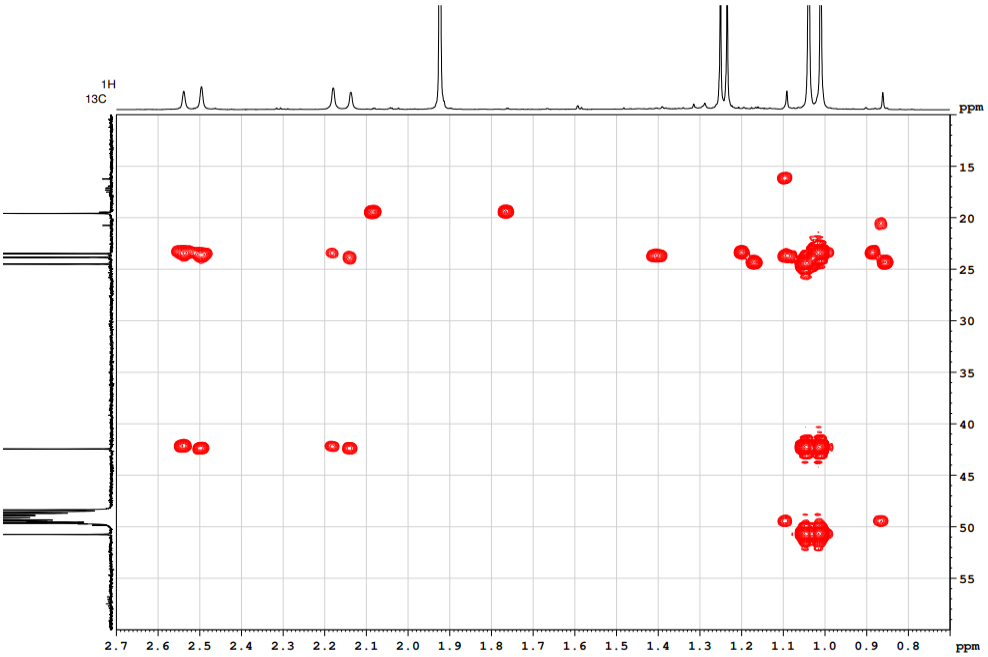

Figure A105. HMBC spectrum (expansion 5) of **42** in CD_3OD.

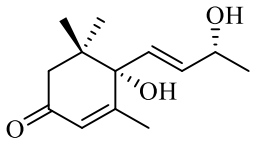

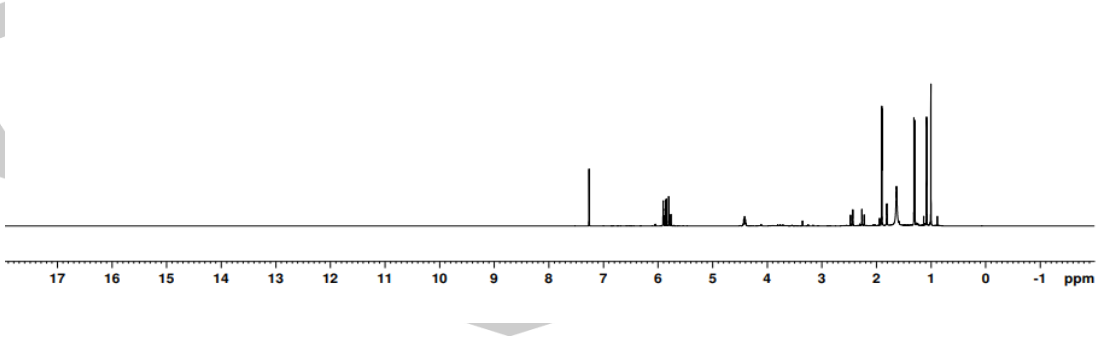

Figure A106. ^1H NMR spectrum of **42** ($CDCl_3$, 400 MHz).

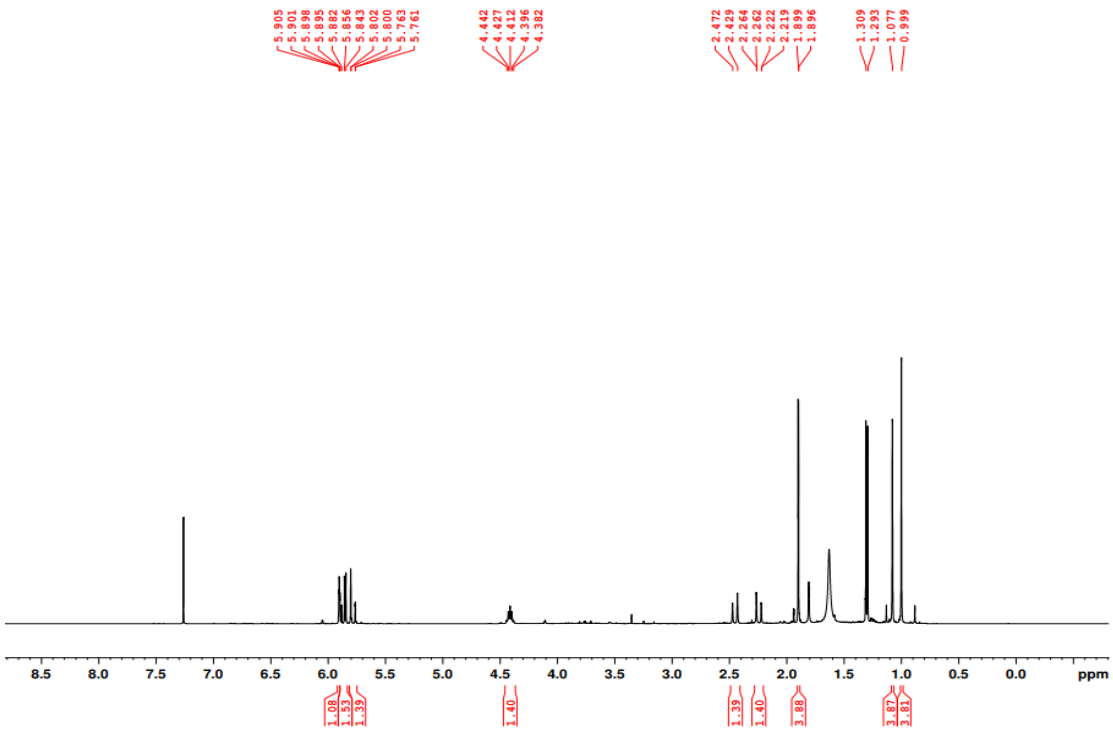

Figure A107. ^{1}H NMR spectrum (expansion 1) of **42** ($CDCl_3$, 400 MHz).

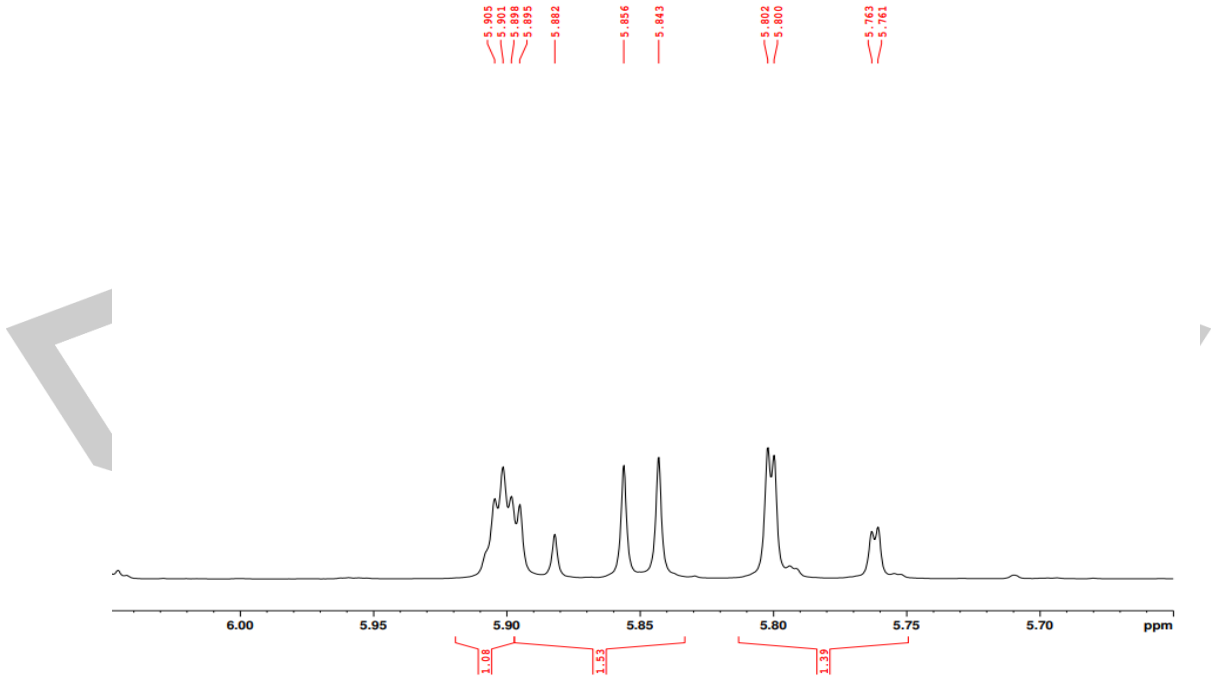

Figure A108. ^{1}H NMR spectrum (expansion 2) of **42** ($CDCl_3$, 400 MHz).

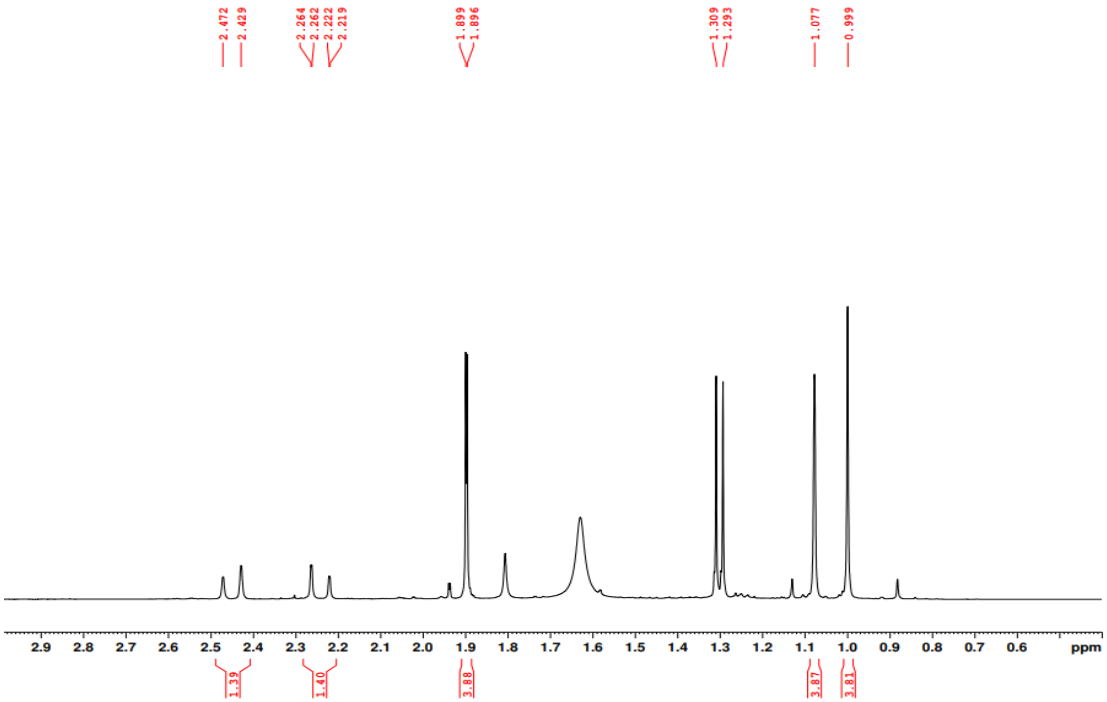

Figure A109. ^{1}H NMR spectrum (expansion 3) of **42** ($CDCl_3$, 400 MHz).

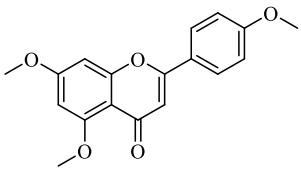

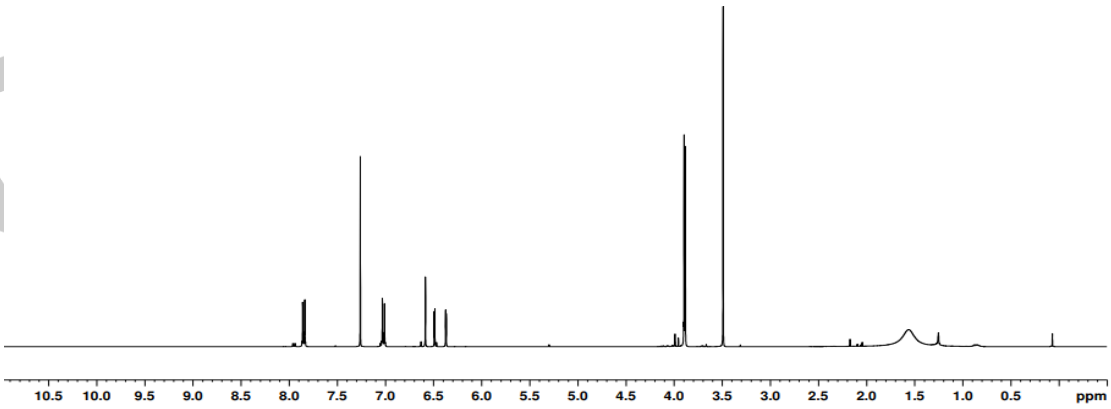

Figure A110. ^{1}H NMR spectrum of **43** ($CDCl_3$, 400 MHz).

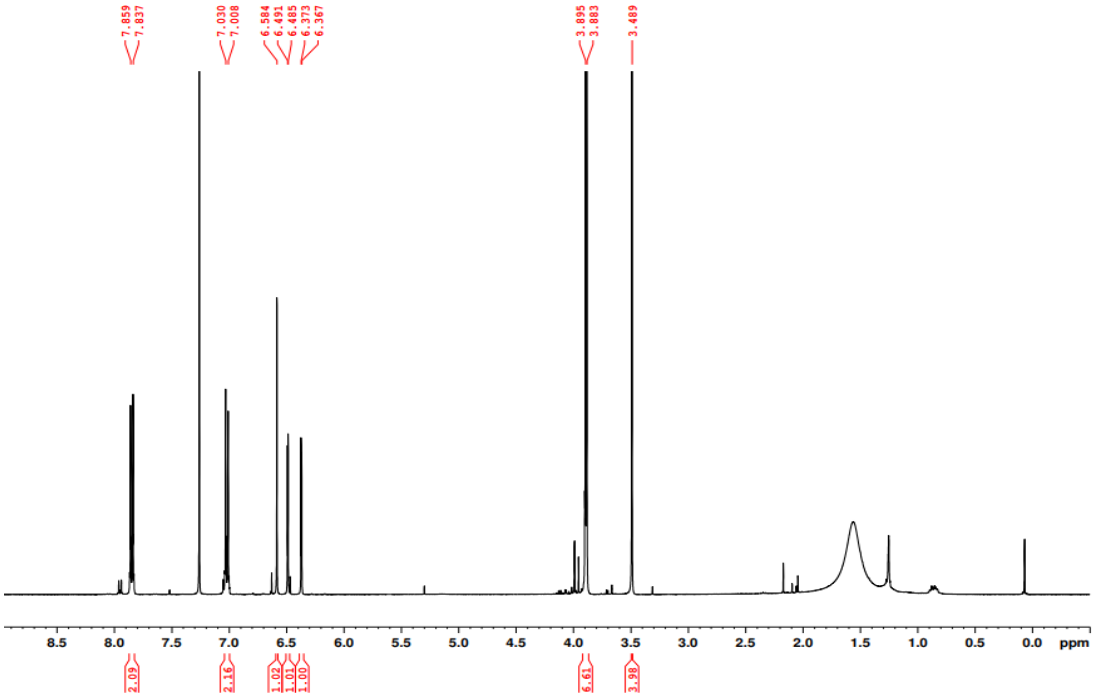

Figure A111. ^{1}H NMR spectrum (expansion 1) of **43** ($CDCl_3$, 400 MHz).

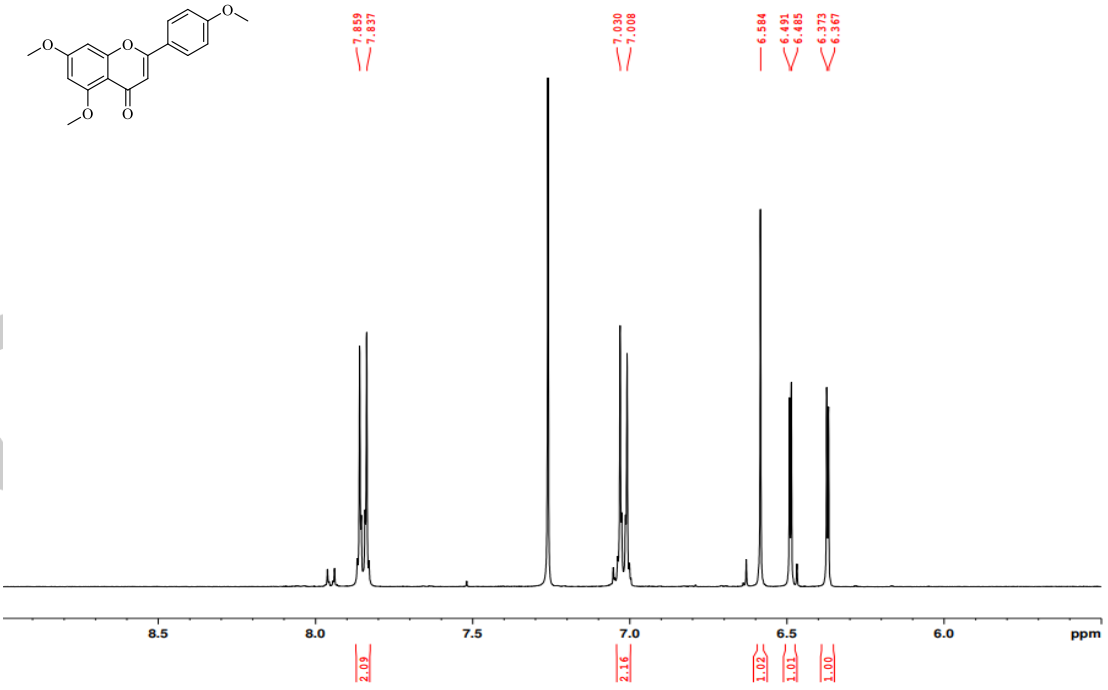

Figure A112. ^{1}H NMR spectrum (expansion 2) of **43** ($CDCl_3$, 400 MHz).

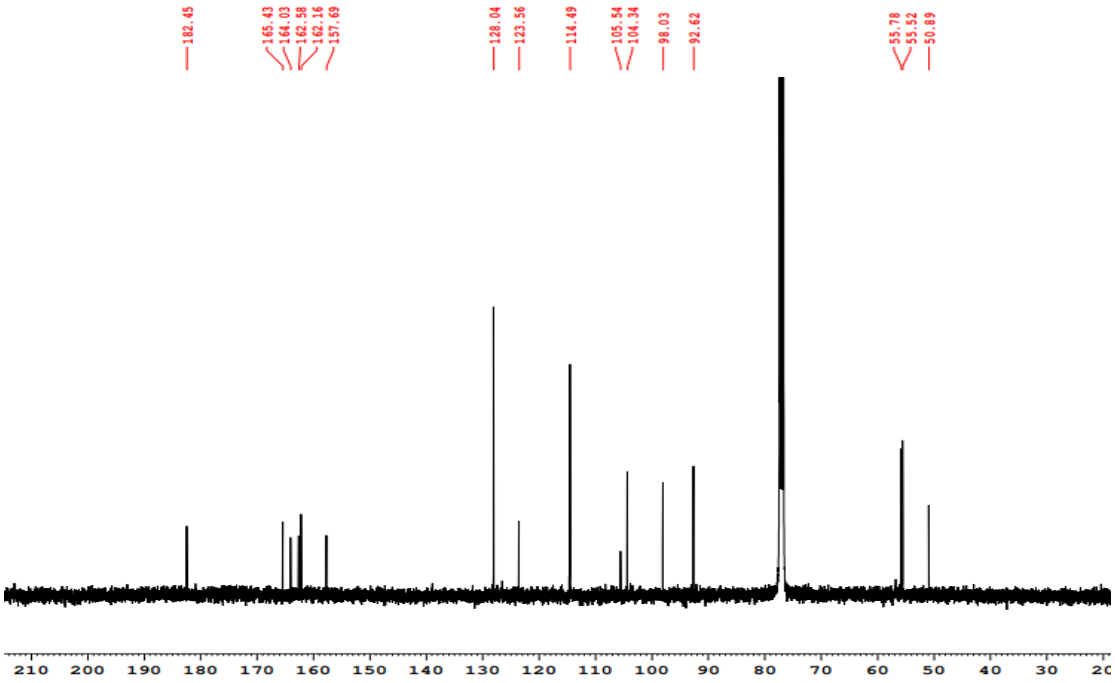

Figure A113. ^{13}C NMR spectrum of **43** ($CDCl_3$, 100 MHz).

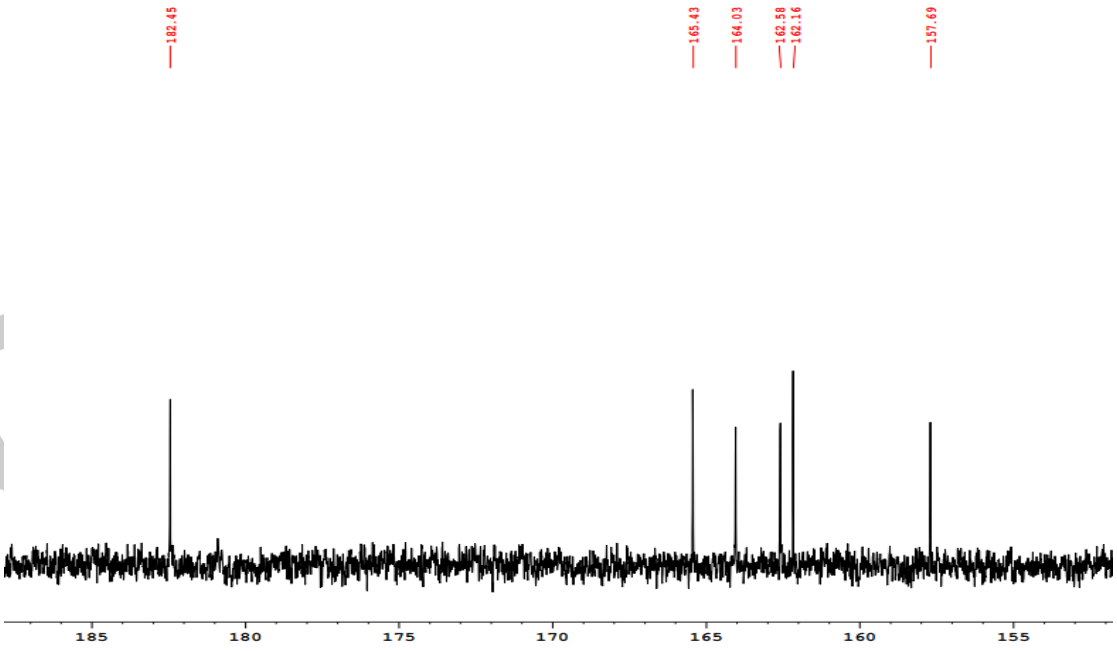

Figure A114. ^{13}C NMR spectrum (expansion 1) of **43** ($CDCl_3$, 100 MHz).

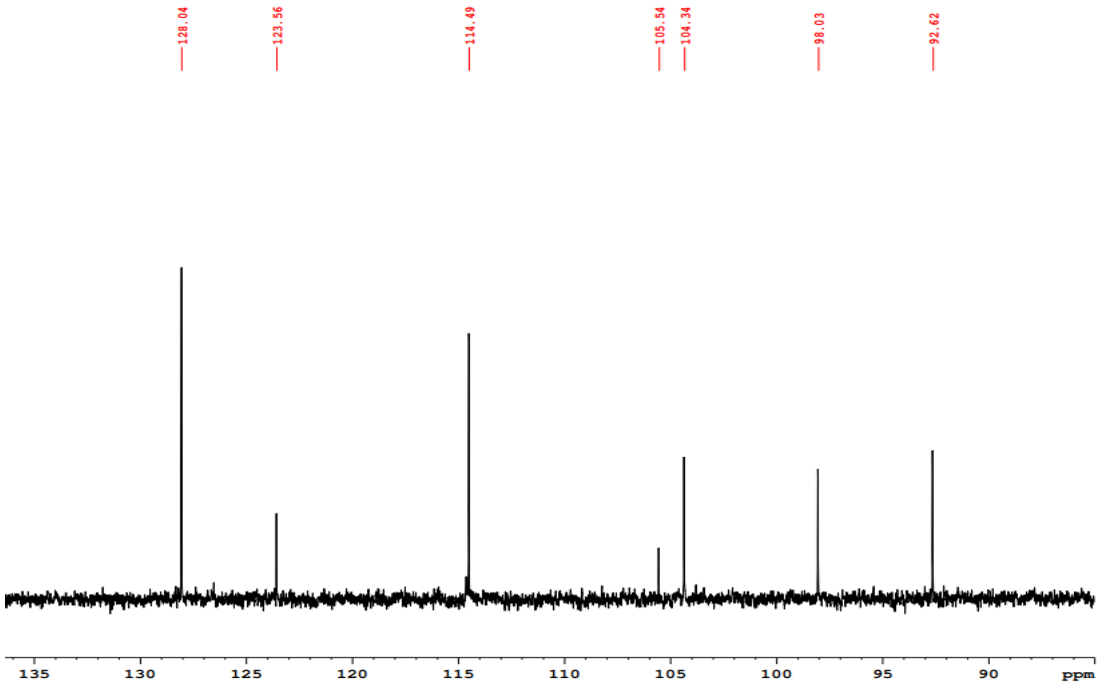

Figure A115. ^{13}C NMR spectrum (expansion 2) of **43** ($CDCl_3$, 100 MHz).

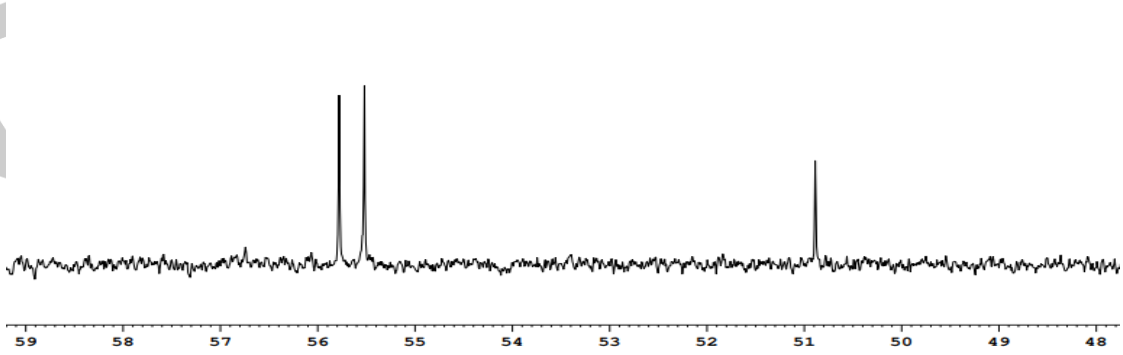

Figure A116. ^{13}C NMR spectrum (expansion 3) of **43** ($CDCl_3$, 100 MHz).

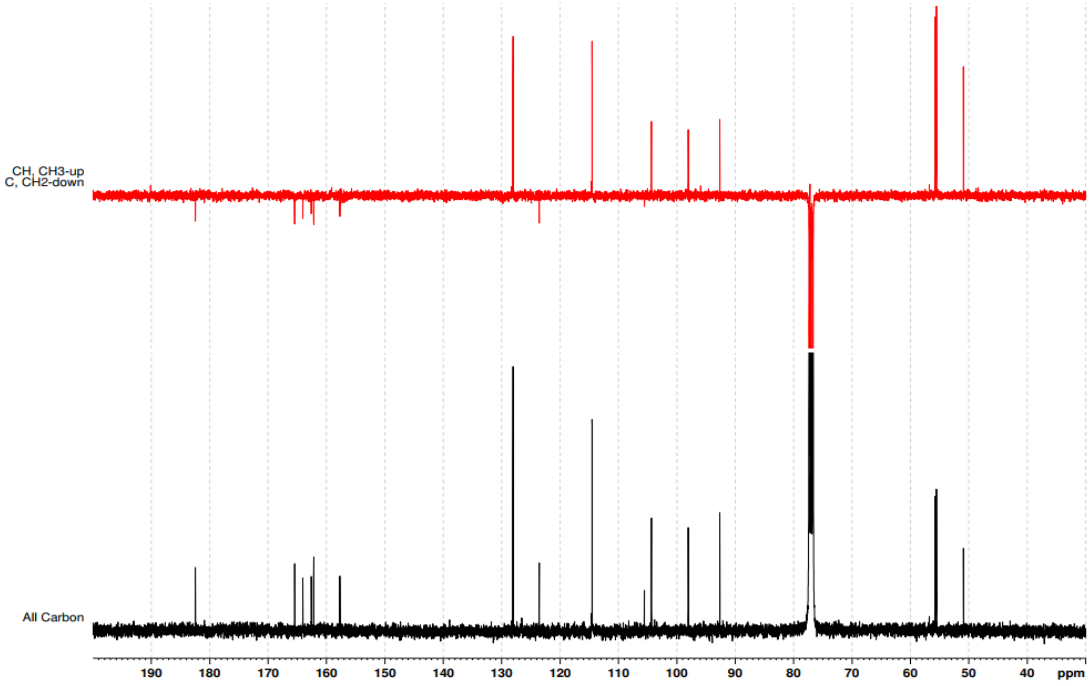

Figure A117. DEPT-135 spectrum of **43** in $CDCl_3$.

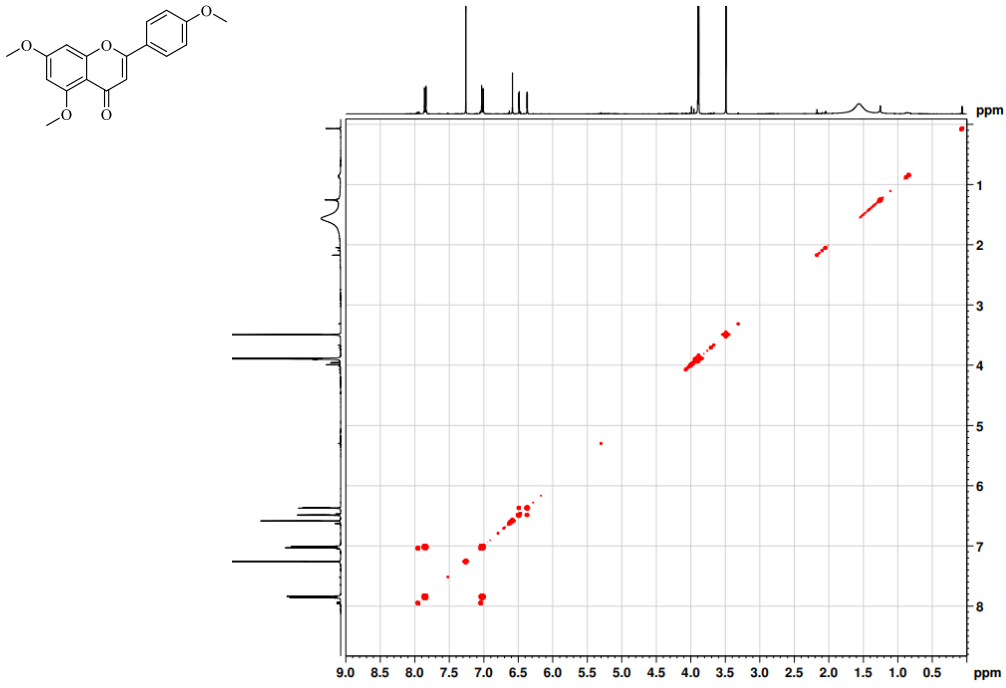

Figure A118. COSY spectrum of **43** in $CDCl_3$.

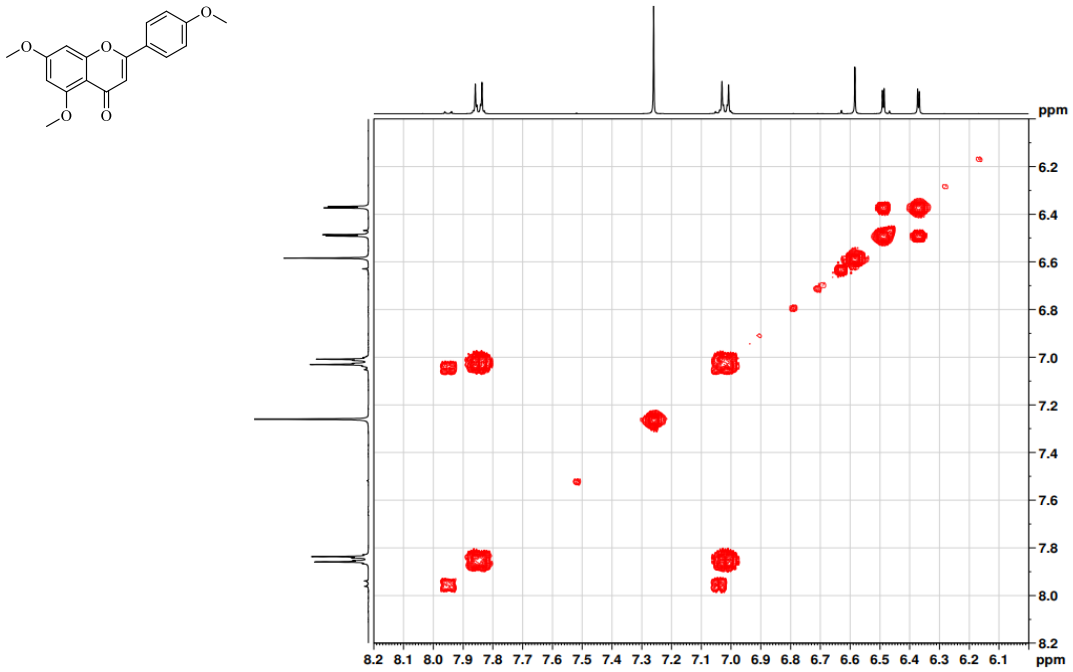

Figure A119. COSY spectrum (expansion 1) of **43** in $CDCl_3$.

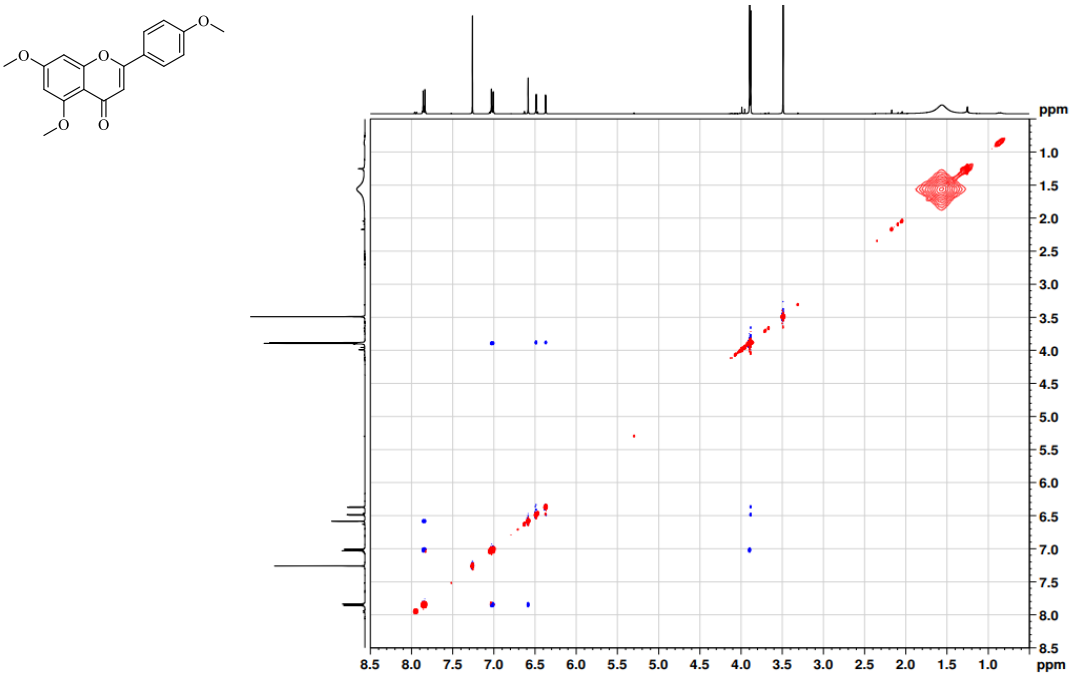

Figure A120. NOESY spectrum of **43** in $CDCl_3$.

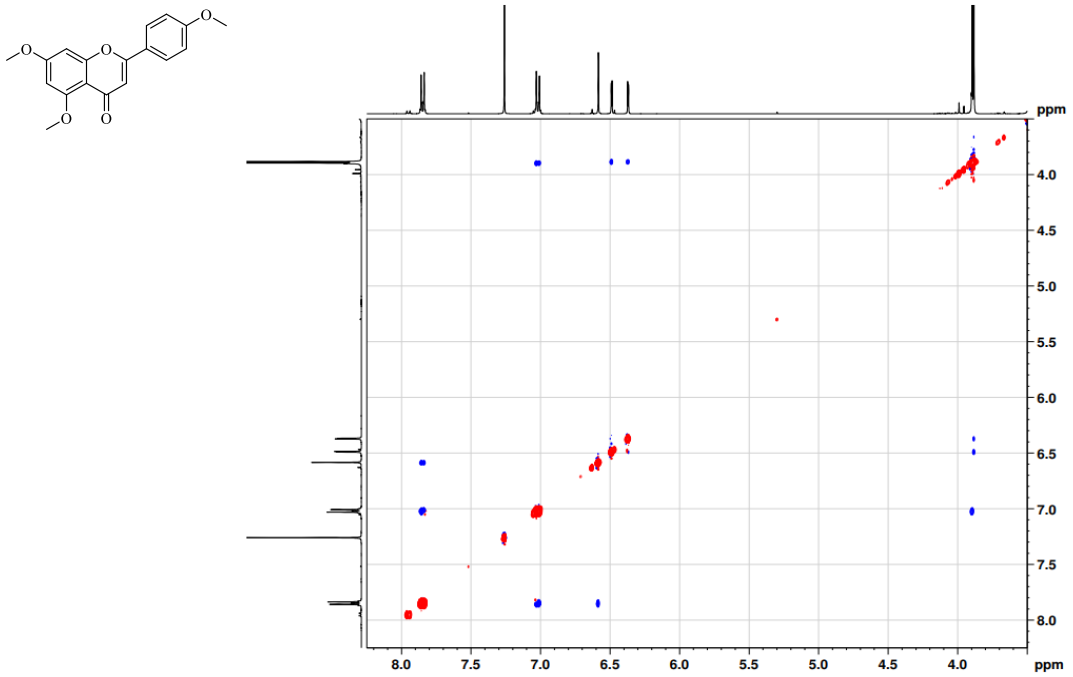

Figure A121. NOESY spectrum (expansion 1) of **43** in $CDCl_3$.

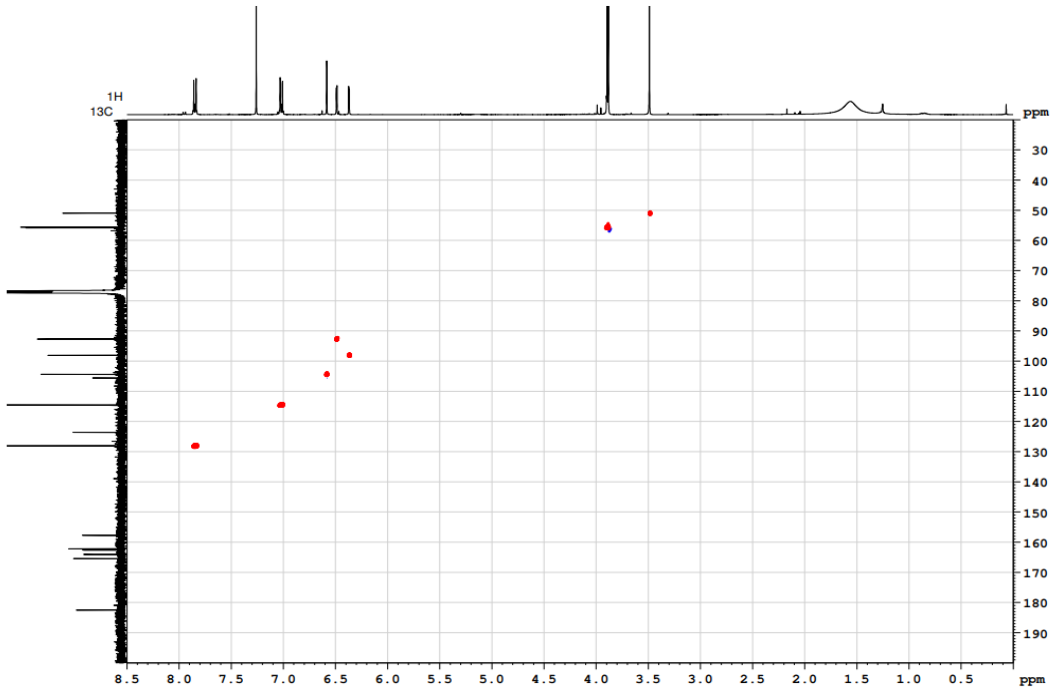

Figure A122. HSQC spectrum of **43** in $CDCl_3$.

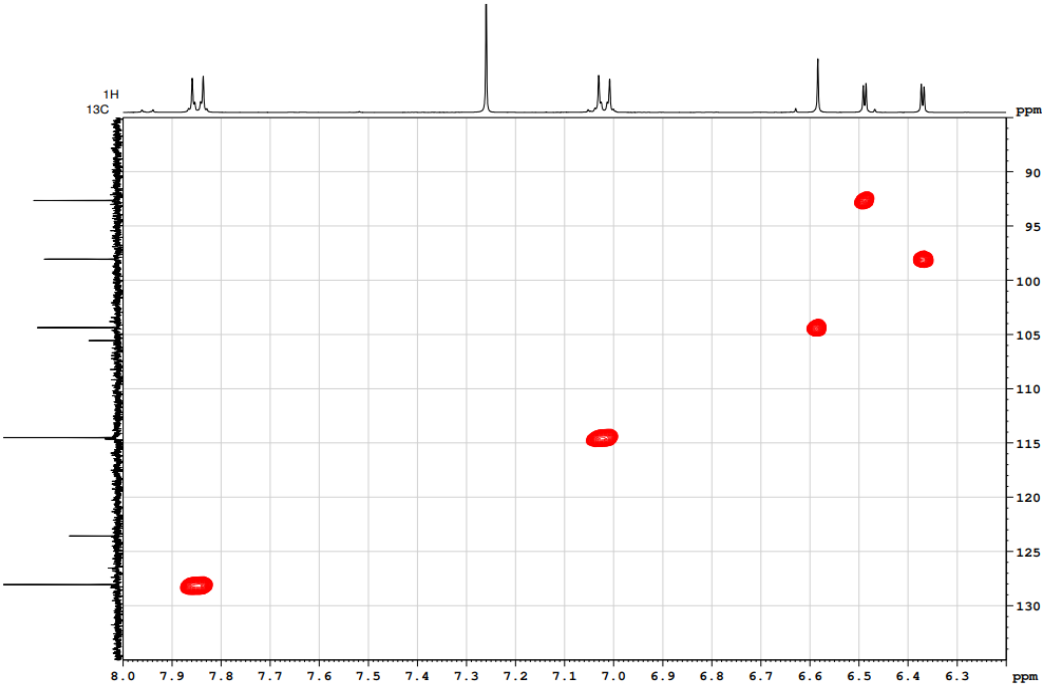

Figure A123. HSQC spectrum (expansion 1) of **43** in $CDCl_3$.

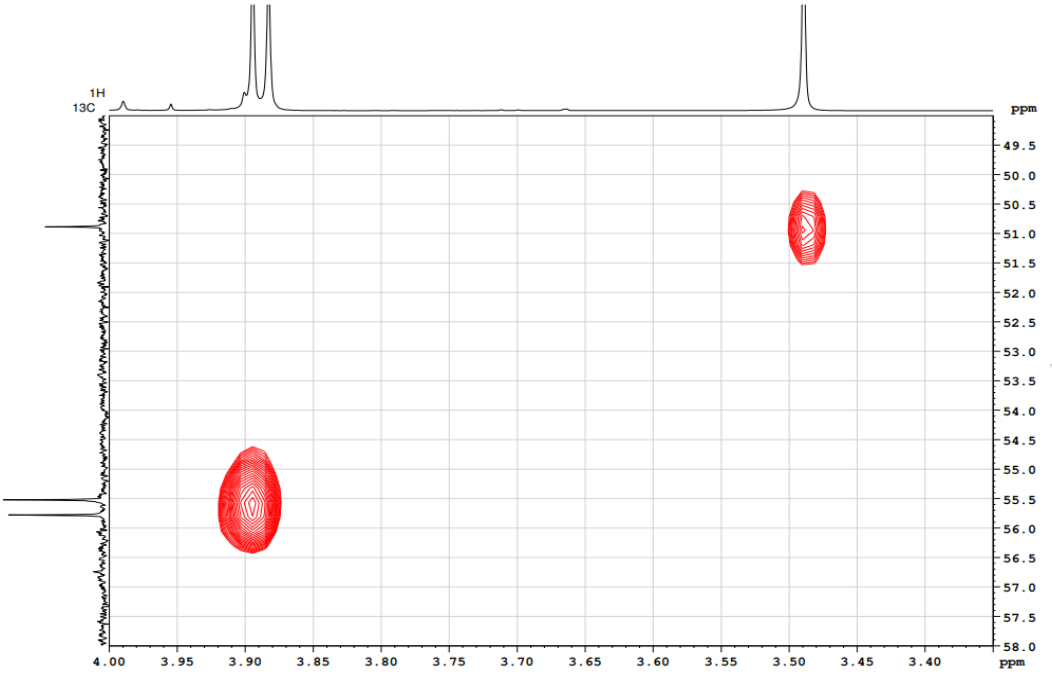

Figure A124. HSQC spectrum (expansion 2) of **43** in $CDCl_3$.

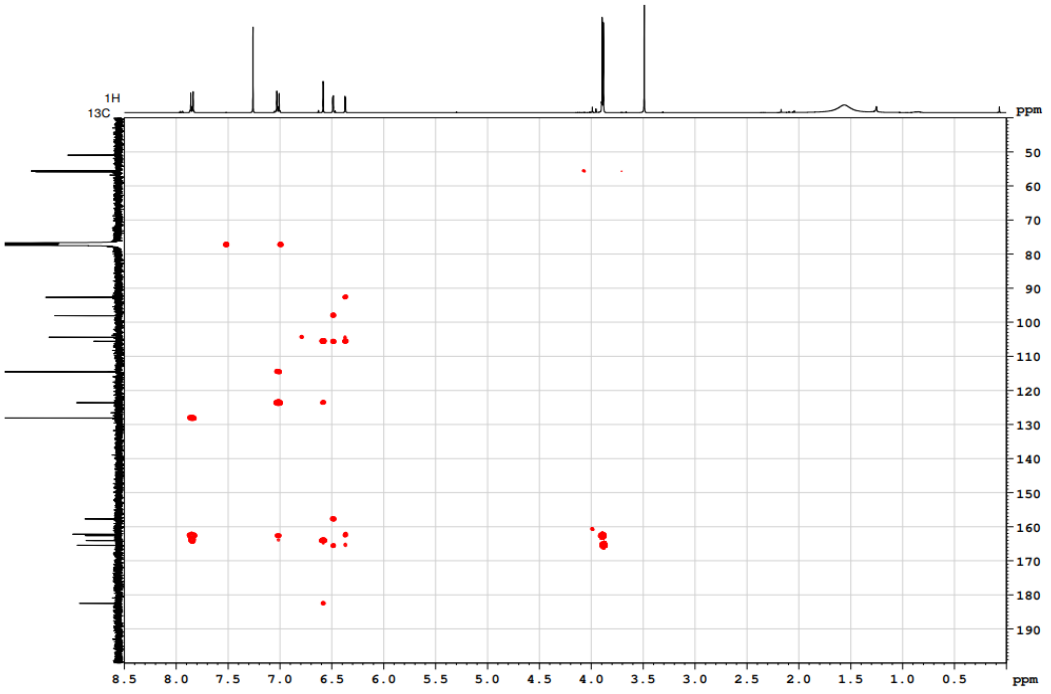

Figure A125. HMBC spectrum of **43** in $CDCl_3$.

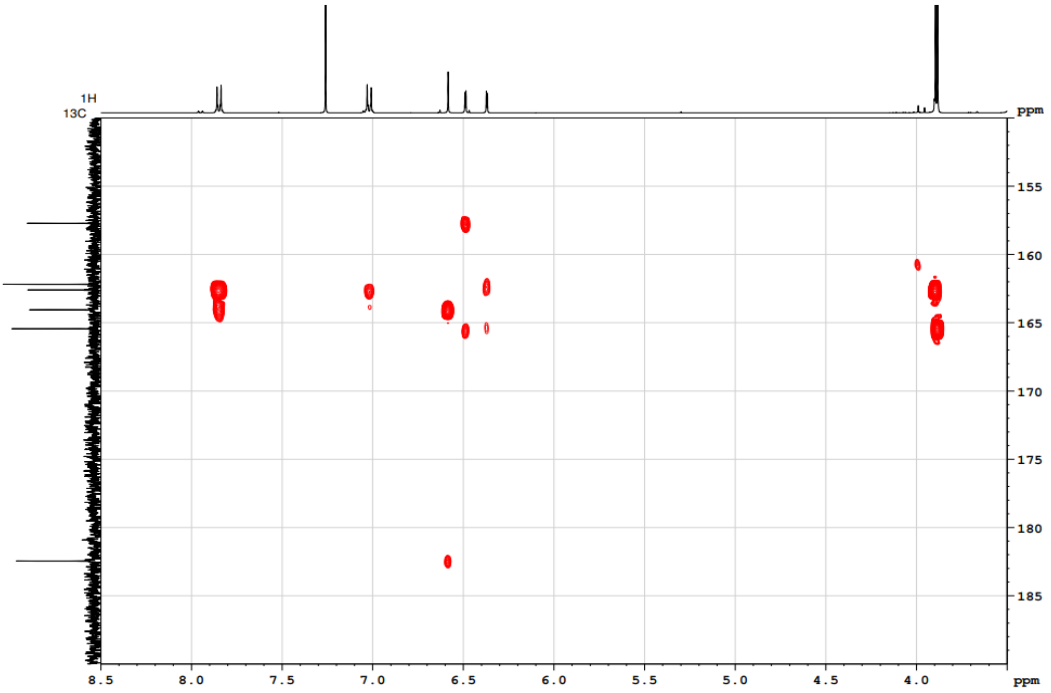

Figure A126. HMBC spectrum (expansion 1) of **43** in $CDCl_3$.

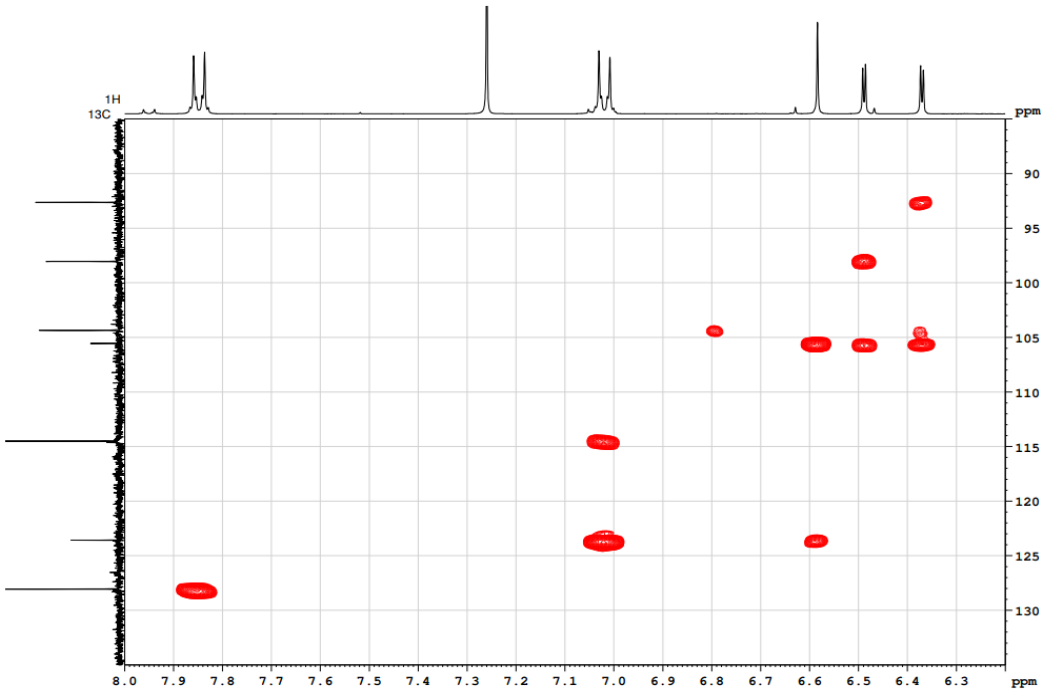

Figure A127. HMBC spectrum (expansion 2) of **43** in $CDCl_3$.

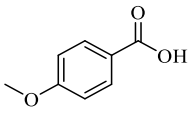

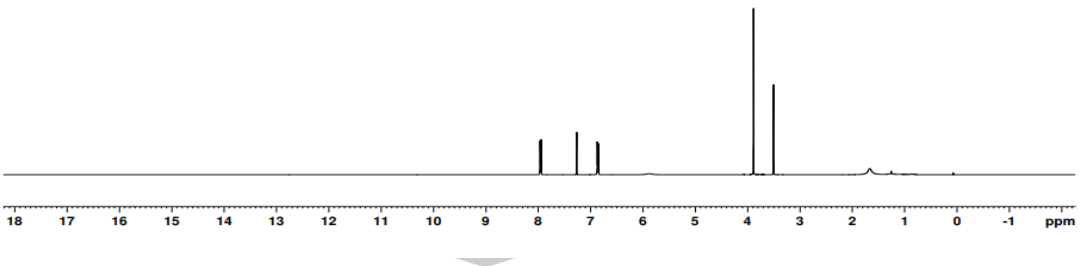

Figure A128. ^{1}H NMR spectrum of **44** ($CDCl_3$, 400 MHz).

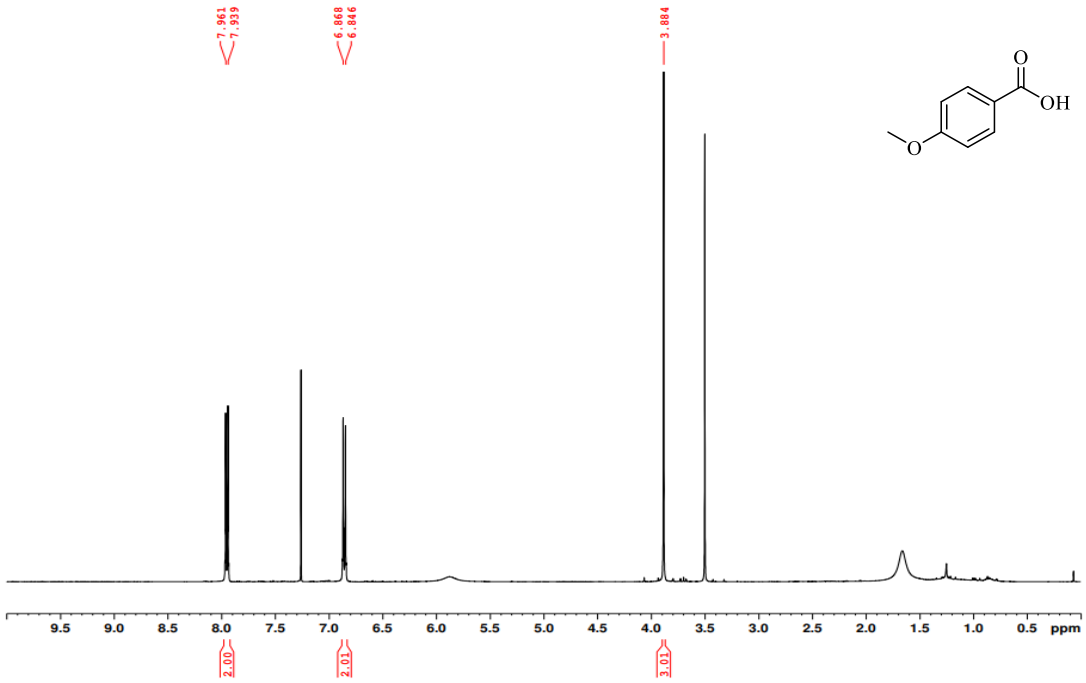

Figure A129. ^{1}H NMR spectrum (expansion 1) of **44** ($CDCl_3$, 400 MHz).

BIOGRAPHY

NAME	Miss Siriwan Srisit
DATE OF BIRTH	February 17, 1999
PLACE OF BIRTH	SaKhon Nakhon
ADDRESS	House No. 39 Moo 12, Ban Siri Charoen, Tha Kok Daeng Sub-district, Seka District, Bueng Kan Province, 38150
EDUCATION	2017 High School, Nonghingpittaya School 2022 Bachelor of Science (B.Sc.) in Chemistry, Mahasarakham University 2025 Master of Science (M.Sc.) in Chemistry, Mahasarakham University
Research grants & awards	- Mahasarakham University (Postgraduate Research Scholarship) - National Research Council of Thailand (NRCT) - Center of Excellence for Innovation in Chemistry (PERCH-CIC)
Research output	- Srisit, S.; Seephonkai, P. Terpenoids isolated from Siphonodon celastrineus Griff. Burapha Science journal. 2023; 28(3): 2087−2100. - Srisit, S,: Bunloed, C.; Soma, W.; Panchompoo, J.; Takpho, C.; Rattarom, R.; Sangdee, A.; Seephonkai, P. The Isolation of 5-hydroxymethylfuran metabolites from the broth extract of Fomitopsis meliae (Agaricomycetes). International Journal of Medicinal Mushrooms. 2024; 26(12): 21−31.